City Research Online

City, University of London Institutional Repository

The Use of Compound Options for Credit Risk Modelling

Federico Maglione

Faculty of Finance

Cass Business School, City, University of London

This dissertation is submitted for the degree of

Doctor of Philosophy

June 2020

Acknowledgements

I owe my deepest gratitude to my supervisor, Dr. Laura Ballotta and Prof. Gianluca Fusai, for their skilful guidance and relentless support through every step of the process. It has been a real privilege to learn from them during these years. Their knowledge, passion for research and work ethic have been truly inspirational for me to become a better researcher.

Besides my supervisors, I also want to express my gratitude of to Prof. Giovanni Cespa, Director of the PhD Program, for his advice, patient and continuous encouragement. I am also deeply grateful to Prof. Peter Carr, Prof. Darrell Duffie, and Prof. Raman Uppal for their invaluable comments and suggestions. I also want to express my gratitude to the academics affiliated with the London Graduate School of Mathematical Finance who I had the privilege to meet and learn from, in particular Prof. Damiano Brigo, Prof. Rama Cont, Prof. Helyette Geman, Dr. Marcello Minenna and Prof. Johannes Ruf.

I want to thank Dr. Sonia Falconeri for her continuous support throughout these years. I also want to thank Prof. David Blake, Prof. Aleš Černý, Prof. Keith Cuthbertson, Dr. Ioannis Kyriakou, Prof. Ian Marsh and Prof. Giovanni Urga for the helpful comments and discussions. Moreover, I would like to deeply thank my examiners, Prof. Santiago Forte and Prof. Anthony Neuberger.

Finally, I will always be grateful to Elisa Pazaj for the daily discussions and companionship during these years, as well all my other fellow PhD colleagues at Cass Business School. Last, but not least I would like to thank my family and close friends for the patience, understanding and unconditional support.

Declaration

I hereby declare that except where specific reference is made to the work of others, the contents of this dissertation are original and have not been submitted in whole or in part for consideration for any other degree or qualification in this, or any other university. This dissertation is my own work and contains nothing which is the outcome of work done in collaboration with others, except as specified in the text and Acknowledgements.

I also grant the permission to the University Librarian to allow the thesis to be copied in whole or in part without further reference to the author. The permission is intended for single copies made for study purposes only, subject to normal conditions of acknowledgement.

<div align="right">

Federico Maglione

June 2020

</div>

Abstract

When a company experiences credit-rating downgrades, its equity inevitably drops by a sizable amount as well as the prices of the derivative contracts written on the company's equity and debt react accordingly. Stemming from the works of Merton (1974), Geske (1977) and Geske (1979), a new structural model of default is introduced. As the reference firm is assumed to have issued n bonds maturating at different future dates, the firm's equity is modelled as an n-fold compound option written on the firm's assets and struck at the face values of the bonds outstanding. This framework is used across the chapters of the thesis, each constituting a different and original piece of research.

The first paper, '*The Impact of Credit Risk on Equity Options*' analyses the effect of credit risk on equity options. In order to conduct the analysis, a measure of impact of credit risk option contracts is introduced. Consistently with the theory and economic intuition, the option contracts which are mostly affected by changes in the underlying default risk are put options. I further document that their pricing is consistent with the probability of default embedded in the credit default swaps written on the same reference entity. It is also shown that the implied volatilities estimated á la Black-Scholes tend to average out the effect of credit risk over the moneyness space, leading to potential biases when applied for risk management purposes.

The second paper, '*Credit Spreads, Leverage and Volatility: A Cointegration Approach*' documents the existence of a cointegration relationship between credit spreads, leverage and equity volatility for a large set of US companies. It is shown that accounting for the long-run equilibrium dynamic is essential to correctly explain credit spread changes. Once credit these variables are correctly modelled, the fit of the regressions sensibly increases if compared to the results of previous research.

The third paper, '*The Option-implied Asset Volatility Surface*' provides a simple way to estimate the option-implied asset volatility surface. To describe the properties of the surfaces, principal component analysis is conducted both across the moneyness and the time-to-maturity dimension, as well as on the overall surface. Finally, the joint evolution of the smirk and the slope of the surface is modelled as a Vector Autoregressive model with exogenous variables. Both slope and smirk appear to be jointly autocorrelated.

Table of contents

Chapter 1

The Impact of Credit Risk on Equity Options

Abstract

The aim of this work is to understand and measure to what extent equity options price credit risk. In addressing this question and, subsequently, to what extent the credit default swap and equity option markets are integrated, the literature has focused on reduced-form models (Carr and Linetsky 2006, Carr and Wu 2010, Carr et al. 2010). Here, instead, a novel structural model is used, thus allowing to investigate and model the connection between the firm's fundamentals and the pricing of these derivative contracts. The proposed model stems from Geske (1977, 1979) in which equity is priced as a compound call option written on the firm's asset. Then, the model allows to decompose the price of equity options in order to construct a measure of impact of credit risk on the the contract. In terms of relative impact across different options, empirical test confirm the economic intuition of put options being sensitive to changes in the default risk in the underlying company. Contrarily, call options do not appear to price credit risk. Furthermore, the same measure is shown to have some predictive power in forecasting future changes of the negative skew of long-term maturity options. Finally, it is shown that the implied volatilities estimated á la Black-Scholes tend to average out the effect of credit risk over the moneyness space, leading to potential biases when applied for risk management purposes.

1.1 Introduction

Markets for both stock options and credit derivatives have experienced a significant growth in the last decades. Along with the rapid growth, academics have started investigating a possible link between stock option implied volatilities and credit default swaps (CDS) spreads: when a company experiences credit-rating downgrades, its equity inevitably drops by a sizable amount and, therefore, the prices of the options written on the company's equity react as well. As a result, the possibility of default induces negative skewness in the probability distribution of stock returns. This negative skewness is manifested in the relative pricing of stock options across different strikes: when the Black and Scholes (1973) implied volatility is plotted against moneyness at fixed maturities, the slope of the graph is positively related to the risk-neutral skewness of the stock return distribution. This phenomenon is commonly referred in the literature as the leverage effect.

The aim of this work is to exploit this overlapping information on the market risk and the credit risk of a company to provide better identification of the dynamics of the stock return variance and default events, and how these impact equity option prices. Ultimately, this allows to measure the impact of credit risk on each equity option contract and shed light on the mechanism leading to future movements of the option skew due to credit-related events.

The first works to point out a possible effect of leverage and credit risk on equity option are Black (1976) and Christie (1982). They both argue that the possibility by the company of defaulting on its obligations can induce negative skewness in the company's return distribution. This manifests when the implied volatility is plotted against a measure of moneyness and exhibits a decreasing pattern for increasing strike prices (the so-called negative volatility skew) rather than a flat line. The skew is often observed in the region where the implied volatility is estimated using out-of-the-money put options, being the latter intrinsically affected the most by credit risk. More recent empirical works, such as Collin-Dufresne et al. (2001), Elton et al. (2001), Cremers, Driessen and Meanhout (2008), Cremers, Driessen, Meanhout and Weinbaum (2008), and Cao et al. (2010), show that CDS and bond spreads are positively correlated with both stock option implied volatility levels and the skew of the implied volatility plotted against moneyness. Also, Campbell and Taksler (2003), and Ericsson et al. (2009) document a link between bond spreads and equity historical volatility. At the aggregate level, similar results hold for sovereign CDS spreads (Carr and Wu 2007), and credit default swap index (CDX) spreads and synthetic collateralised debt obligations (CDOs) on the same index (Collin-Dufresne et al. 2012).

The relative pricing of equity and debt related derivatives instruments has been mainly explored using reduced-form models of default in the literature. Carr and Linetsky (2006), Carr et al. (2010) and Carr and Wu (2010) develop joint frameworks of valuation for credit-sensitive derivatives contracts and equity options. Their estimations highlight the interaction between market risk (return variance) and credit risk (default arrival) in pricing stock options and credit default swaps. They also point out the need of developing future models that integrate both markets, rather than having separate valuation models. This work tries to bridge this gap providing a unique structural valuation framework where both the price of CDSs and options written on the same reference entity are driven by a unique state variable, namely the firm's asset value, which ultimately determines the default event properties.

On the other side of the spectrum, the use of structural model for jointly modelling credit and equity derivative contracts has not been exhaustively explored. With the exception of Toft and Prucyk (1997), which built on the Leland (1994) model to document the effect of leverage on the pricing of options, and Hull et al. (2004), which develop a new calibration methodology based on options to implement the Merton (1974) model, there have not been significant attempts to develop structural models of default able to transmit the company's credit risk to the pricing of equity options. In this work instead, the firm is allowed to issue multiple bonds with different maturities, thus removing the restriction on perpetual debt (as in Leland 1994) or a unique zero-coupon bond (as in Merton 1974). The work of Geske et al. (2016) moves towards this direction whilst investigating capital structure effects on the pricing of equity options. However, their work does not measure the extent to which leverage and credit risk impact the pricing of options which is assessed in this paper. Also, they focus on call options only, which intuitively should be affected by credit risk the least, whilst here both call and put options are taken into consideration.

Regarding the selection of data to infer default probabilities, CDS spreads are used rather than bond prices. This is motivated by the fact that CDS spreads constitute a more direct and clean signal for the underlying default risk. In fact, CDS spreads provide relatively pure pricing of the default event of the underlying entity as they are typically traded on standardised terms: unlike bonds, CDSs have a constant maturity, the underlying instrument is always par valued, they concentrate liquidity in one instrument, and are not affected by different taxation regimes. Moreover, many corporate bonds are bought by investors who simply hold them to maturity, and the secondary market liquidity is therefore often poor[1]. CDS contracts instead allow investors to implement trading strategies to hedge credit risk

---

[1]Shorting bonds is even more difficult in the cash market as the repo market for corporate bond is often illiquid, and the tenor of the agreement is usually very short.

over a longer period of time at a known cost. In addition, as shown by Blanco et al. (2005), CDS spreads tend to respond more quickly than bond spreads to changes in credit conditions in the short run.

This work also connects with the findings in Carr and Wu (2011, 2017). More specifically, Carr and Wu (2011) show that under suitable assumptions the price of equity put options struck deepest out-of-the-money (DOOM) is entirely driven by the default possibility of the reference entity. Also, they show that the contract values of credit-sensitive instruments and put options share similar magnitudes and show strong co-movements. On the other hand, Carr and Wu (2017) is a crucial piece of research in interpreting and assessing the extent to which results on the volatility skew obtained herein could be driven by factors other than the leverage effect. In their article, the authors identify three different channels able to generate the negative volatility skew documented in equity options. They show that the option skew can be driven, as expected, by increasing leverage but also by volatility feedback and self-exciting market disruptions. They also find that, contrary to conventional wisdom, financial leverage does not always decline with increased business risk: financial leverage can be positively correlated with business risk when the increase in risk is due to small, diffusive market movements. The model I propose is able to explain this apparently counterintuitive finding.

In terms of the modelling of equity options, the theory employed is based on Merton (1974), Geske (1977), and Geske (1979) where the equity is considered as a contingent claim on the firm's value. Here, as the reference firm has issued more than one bond, equity turns into a n-fold compound option (where n is the number of bond outstanding). To the best of my knowledge, this is the first work that uses the theory of n-fold compound options for pricing vanilla equity options. Based on the model prediction and using a novel calibration technique, a measure of impact of credit risk is introduced. The effect of credit-related event is further investigated in the relative pricing of call and put option, and it is shown as put options reflect the credit risk implied by the credit spread. The ability of this new measure to forecast future movement in the option skew is then tested. Finally, the model allows to show how the estimation of the implied volatility á la Black-Scholes tend to average out the effect of credit risk over the moneyness space, leading to potential biases when applied for risk management purposes.

The rest of the paper is structured as follows: Section 1.2 introduces the value of the equity as a n-fold compound option and extend the pricing to equity options; Section 1.3 gives a description of the data and the calibration methodology; in Section 1.4 the Average Information Content Ration (*AICR*) measure of credit risk is introduced, and the different

impact of credit risk on calls and puts is investigated. Some robustness test are also conducted, allowing to also investigate the integration of the CDS and option markets. Finally, Section 1.5 concludes.

1.2 Firm's Claims as Compound Options

The given structural model of default allows to price equity, debt and options written on equity and is inspired by Merton (1974) and Geske (1977). It extends the Merton model as it allows the firm to have issued a sequence of bonds, with different face values and maturities. It also borrows the intuition of Geske (1977) to construct and modify the definition of the default events. In Geske (1977), default can occur at every coupon-payment date given one bond outstanding. In this work instead there are several bonds (due at different point in time) which the firm can default on.

Thereafter, the pricing of equity is addressed first, and eventually the same mechanism is extended to the pricing of equity options.

1.2.1 Equity as a n – fold Compound Option on Asset Value

Consider a firm which has issued n bonds and equity, both receiving payments in the form of coupons and dividends. According to the indenture of the bonds: (1) the firm promises to repay each bond, with face value F_i, to the bondholders at known times $t_i \in (t_0, t_n]$, $i \in I := \{1, \ldots, n\}$; (2) in case of default, the bondholders immediately take over the company and the shareholders receive nothing; (3) the firm cannot issue any senior or equivalent rank claims on the firm nor do share repurchases before t_n. Usual assumptions in terms of transaction cost, taxes, bid/ask spreads, short-selling and indivisibility of assets apply.

For convenience of notation, set $t_0 := 0$ and denote the generic payoff at time t_i as $X_{t_i} := X_i$. Let V, S and D represent the firm's assets, equity and debt respectively. According to the structural approach and the Modigliani-Miller theorem, both equity and debt are function of the firm's assets and not vice versa (Merton 1977). Also, I fix a filtered probability space $(\Omega, \mathscr{F}, \mathbb{F}, \mathbb{P})$ and assume no-arbitrage conditions in the economy. Under certain technical conditions, there exist a risk-neutral probability measure $\mathbb{Q}$, equivalent to $\mathbb{P}$, such that the gain process associated with any admissible trading strategy deflated by the risk-free rate is a

martingale[2]. Furthermore, the following notation for the (risk-free) discount factor

$$DF(t_i, t_j) = \frac{B_i}{B_j} = \exp\left(-\int_{t_i}^{t_j} r_s \, ds\right),$$

is used, being $B_t = \exp\left(\int_0^t r_s \, ds\right)$ the value of the money-market account at time t and r_t a (possibly stochastic) positive function of time.

Similarly to Geske (1977), the firm refinances each bond payment with equity. In this setting, bankruptcy occurs when the firm fails to make the reimbursement payment because it is unable to issue new equity. Black and Cox (1976) have argued that the firm will find no takers for its stock whenever the value of the equity, if the payment is made, is less than the value of the payment due. If all the firm debt is finally repaid, the firm is liquidated and the shareholders receive any remaining value as lump-sum liquidating dividend.

More specifically, if at time t_i the value of equity prior to making the payment is larger than payment due, the bond is paid off and the firm is kept alive; otherwise bondholders declare bankruptcy. In the case the bond is repaid, the same mechanism occurs at the next payment date, t_{i+1}, and so on until the last payment date, t_n. This mechanism can also be interpreted as the the firm defaulting on its debt because is unable to issue new equity (Geske 1977).

Hence, the default time is defined as

$$\tau := \inf_{i \in I} \{t_i : S_i^\star(V) < F_i\} \tag{1.1}$$

where $S_i^\star(V)$ is the continuation value of equity[3]. The eventuality that shareholders may have an incentive to raise new equity to keep receiving dividends in the future, thus postponing default, is not possible within this model. First, as shown in Section 1.2.2, the effect of dividends and coupons cannot be disentangled from the firm's overall payout[4]. Second, larger

---

[2]Without further assumptions, the market is incomplete as both the firm's equity and debt are contingent claims on the firm's asset which is a non-tradable asset (therefore, the replicating portfolio cannot be constructed). In order to implement the model, as described in Section 1.3, a calibration on the equity and options is in fact required (options are not redundant assets). However, as shown in Ericsson and Reneby (2002), if the interest rate market is complete and the firm's equity is traded, completeness can be achieved (thus leading to a unique measure $\mathbb{Q}$). In fact, considering a Black and Scholes (1973) economy, as the value of equity options can be replicated by trading the stock and a riskless bond, the converse il also true: the payoff of the stock can be replicated by trading the option and the bond. Similarly, as in the structural approach of default equity is an option on the firm value, the payoff of the latter can be replicated by trading the firm's equity and the risk-free bond.

[3]That is the value of equity before paying the bond. E.g. if the continuation value of the equity $S^\star$ is 20 and the face value of debt is 30, then equity is worthless ($S = 0$).

[4]This is a clear limitation of the model.

payouts tend to reduce the value of the equity as shown in the same Section. Finally, the dilution effect driven by the issuance on new equity have the effect of reducing the dividend per shares and therefore this incentive.

As equity is a function of the firm value, default times can be re-expressed as events in the asset value space: for each value of equity which triggers default corresponds only one value of the firm assets, namely $\bar{V}_i$ at time t_i, which implies (1.1), that is

$$\tau = \inf_{i \in I} \left\{ t_i : V_i < \bar{V}_i \right\}.$$

The default barrier $(\bar{V}_i)_{i \in I}$ can be interpreted as a latent sequence of thresholds embedded into the firm's capital structure and riskiness. Operationally, the default thresholds are found recursively starting from the default threshold in t_n which coincides with F_n as in the Merton model. The other values of the barrier are calculated as the solution of an integral equation, where the dimension of the integrals increases alongside with the number of bond outstanding (i.e., given n bond outstanding, $n-1$ integral equation must be solved, being the last integral to be solved an $(n-1)$-dimensional integral). For further details on the estimation of the default barrier, see Appendix E.

Within this framework, both the present and the continuation value of the equity can be calculated as the risk-neutral expectation of their terminal payoffs. At any time $t_i \in [0, t_n]$, the terminal payoff of the the firm's equity can be expressed as

$$S_n(V) = V_n \mathbb{1}_{\tau > t_n} - \sum_{k=i+1}^{n} \frac{F_k}{DF(t_k, t_n)} \mathbb{1}_{\tau > t_k}. \tag{1.2}$$

The interpretation of the payoff function is straightforward: equity holders receive the asset value in t_n (if the firm has been able to repay all its outstanding debt), net of all the future reimbursements (if the firm has survived at each default point).

The continuation value of the equity is given by the present value of the expected payoff of the equity before having checked for the potential default occurring at t_i, that is

$$S_i^\star(V) = \mathbb{E}_i^{\mathbb{Q}} \left[DF(t_i, t_n) S_n(V) \right], \tag{1.3}$$

where the expectation is taken under the risk-neutral measure. As a consequence, the value of the equity is given by

$$S_i(V) = \max \left\{ S_i^\star(V) - F_i, 0 \right\}. \tag{1.4}$$
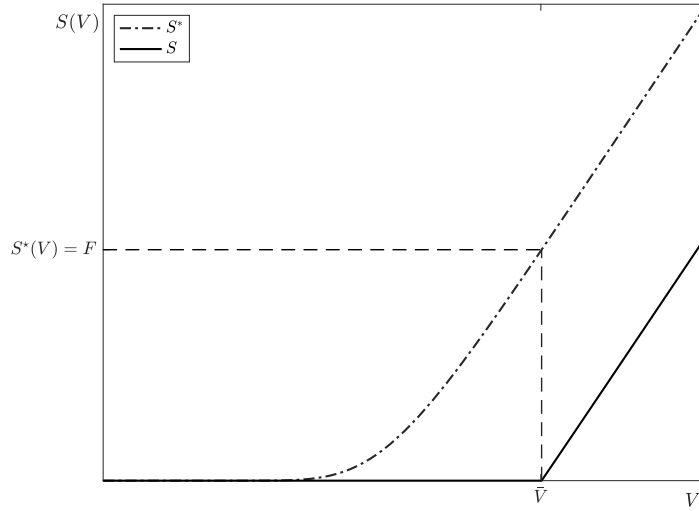
Fig. 1.1 Continuation value (dashed and dotted line) and value (solid line) of the equity. Checking whether the continuation value of the equity $S^\star$ is greater than the face value of the bond F is equivalent to finding the value of the assets V greater than the default threshold $\bar{V}$.

See Figure 1.1 for a visual representation of the continuation and actual value of the equity. Under (1.1), (1.3) can be further expressed in terms of events in equity space and, ultimately, in the asset value space. Therefore

$$
\begin{aligned}
S_i^\star(V) &= \mathbb{E}_i^{\mathbb{Q}}\left(DF\left(t_i,t_n\right)V_n\mathbb{1}_{\cap_{h=i+1}^n\left\{S_h^\star(V)\geq F_h\right\}}\right) - \sum_{k=i+1}^n F_k\mathbb{E}_i^{\mathbb{Q}}\left(DF\left(t_i,t_k\right)\mathbb{1}_{\cap_{h=i+1}^k\left\{S_h^\star(V)\geq F_h\right\}}\right)\\
&= \mathbb{E}_i^{\mathbb{Q}}\left(DF\left(t_i,t_n\right)V_n\mathbb{1}_{\cap_{h=i+1}^n\{V_h\geq\bar{V}_h\}}\right) - \sum_{k=i+1}^n F_k\mathbb{E}_i^{\mathbb{Q}}\left(DF\left(t_i,t_k\right)\mathbb{1}_{\cap_{h=i+1}^k\{V_h\geq\bar{V}_h\}}\right).
\end{aligned}
$$

(1.5)

Notice that (1.5) is the most general expression for the continuation value of the equity. So far, no distributional assumptions have been made on the process driving the asset value nor on the form of the discount factor. The asset value process could be a Lévy process, as well as a process with continuous paths and stochastic volatility; similarly, the discount factor could be assumed stochastic. However, Frey and Sommer (1998) showed that compound option problems such as in Geske (1977), Geske (1979) and Geman et al. (1995) can neither be solved in a semi-closed form under stochastic interest rates nor stochastic volatility. Consequently, in order to preserve analytical tractability, a positive constant continuously compounded risk-free rate r is assumed throughout. Also, a geometric Brownian motion is

considered for the asset value process, that is

$$dV_t = (r - \varpi) V_t \, dt + \sigma_V V_t \, dW_t^{\mathbb{Q}}, \tag{1.6}$$

where ϖ is the continuously compounded payout rate, σ_V the instantaneous volatility of the assets, and $W_t^{\mathbb{Q}}$ a $\mathbb{Q}$-standard Brownian motion. The asset value is modelled as a geometric Brownian motion as it allows to obtain semi-closed formulas for the compound option problem.

Defining the events $\mathscr{V}_{i,k} := \bigcap_{h=i+1}^{k} \{V_h \geq \bar{V}_h\}$, the t_i-continuation value of the equity can be written as

$$S_i^{\star}(V) = e^{-r(t_n - t_i)} \mathbb{E}_i^{\mathbb{Q}} \left(V_n \mathbb{1}_{\mathscr{V}_{i,n}} \right) - \sum_{k=i+1}^{n} e^{-r(t_k - t_i)} F_k \mathbb{E}_i^{\mathbb{Q}} \left(\mathbb{1}_{\mathscr{V}_{i,k}} \right), \tag{1.7}$$

and for $t_i = t_0$, it follows

$$S_0(V) = e^{-r t_n} \mathbb{E}^{\mathbb{Q}} \left(V_n \mathbb{1}_{\mathscr{V}_n} \right) - \sum_{k=1}^{n} e^{-r t_k} F_k \mathbb{Q} \left(\mathscr{V}_k \right), \tag{1.8}$$

where $\mathscr{V}_k \equiv \mathscr{V}_{0,k}$, for $k \in I$. Notice that the t_0-continuation value of the equity and the contemporaneous value of the equity coincide as no debt is due in t_0 (i.e. $F_0 = 0$). In order to derive an analytical solution, a change of measure as in Geman et al. (1995) is performed, such that $\mathbb{M} \sim \mathbb{Q}$, with

$$\left. \frac{d\mathbb{M}}{d\mathbb{Q}} \right|_{\mathscr{F}_t} = \frac{V_t e^{\varpi t}}{V_0 B_t} = \exp \left(\sigma_V W_t^{\mathbb{Q}} - \frac{\sigma_V^2}{2} t \right).$$

The measure $\mathbb{M}$ is referred as the firm-value fund measure thereafter. Setting $t = t_n$, it follows

$$S_0(V) = e^{-\varpi t_n} V_0 \mathbb{M} \left(\mathscr{V}_n \right) - \sum_{k=1}^{n} e^{-r t_k} F_k \mathbb{Q} \left(\mathscr{V}_k \right).$$

In order to compute the probabilities under $\mathbb{M}$ and $\mathbb{Q}$, the result in Theorem 1 in Appendix C is needed. Notice that the proposed change of measure is not strictly necessary to derive the value of the equity; it is only used as a useful mean to solve the model more easily[5]. Using those results, the two probabilities can expressed as the following multivariate Gaussian integrals

---

[5]Alternatively, the first expectation in (1.8) can be expressed in terms of truncated log-normal integrals using Theorem 2 in Appendix C.

(a) Asset value (b) Asset volatility
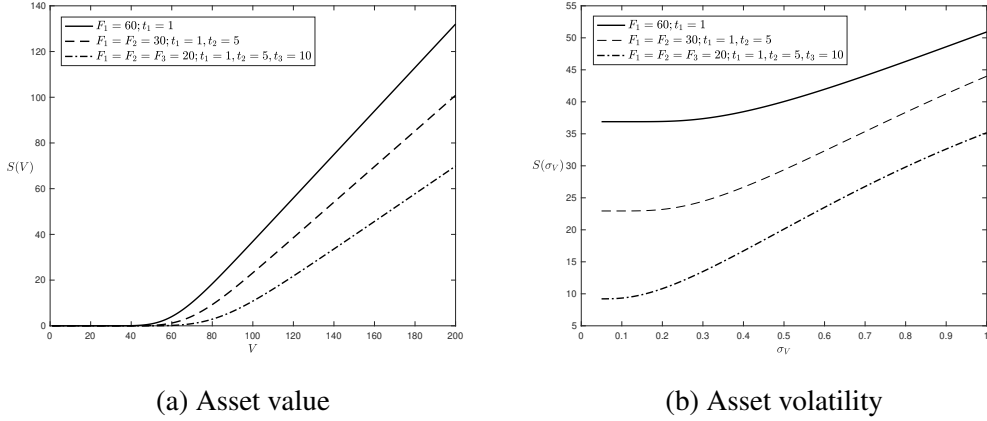
Fig. 1.2 The Figures show how clustering the whole firm debt at different maturities affect the value of equity (as a function of the asset value, as in Panel (a), and as a function of the asset volatility, as in Panel (b). Spreading the same debt level over longer maturities lowers the value of the equity given the greater uncertainty on the firm being able to repay the bonds at farther dates away in the future.

$$S_0(V) = e^{-\varpi t_n} V_0 \Phi_n\big(\mathbf{d}^{\mathbb{M}}; \mathbf{\Gamma}_n\big) - \sum_{k=1}^{n} e^{-rt_k} F_k \Phi_k\big(\mathbf{d}_k^{\mathbb{Q}}; \mathbf{\Gamma}_k\big) \tag{1.9}$$

where $\mathbf{d}^{\mathbb{M}} := \big(d_i^{\mathbb{M}}\big)_{1 \le i \le n}$ and $\mathbf{d}_k^{\mathbb{Q}} = \big(d_i^{\mathbb{M}} - \sigma_V \sqrt{t_i}\big)_{1 \le i \le k}$ with

$$d_i^{\mathbb{M}} = \frac{\ln\left(V_0/\bar{V}_i\right) + \left(r - \varpi + \sigma_V^2/2\right) t_i}{\sigma_V \sqrt{t_i}}, \qquad \mathbf{\Gamma}_k = \begin{pmatrix} 1 & \sqrt{\frac{t_1}{t_2}} & \sqrt{\frac{t_1}{t_3}} & \cdots & \sqrt{\frac{t_1}{t_k}} \\ & 1 & \sqrt{\frac{t_2}{t_3}} & \cdots & \sqrt{\frac{t_2}{t_k}} \\ \cdots & \cdots & \cdots & \cdots & \cdots \\ & & & 1 & \sqrt{\frac{t_{k-1}}{t_k}} \\ & & & & 1 \end{pmatrix}.$$

Notice that, if $n = 1$ and $\varpi = 0$, the model coincides with the Merton's model.

1.2.2 Dividends, coupon payments and payouts

The proposed way of modelling the asset value process is quite common in the literature on structural models of default (Toft and Prucyk 1997, Cremers, Driessen and Meanhout 2008, Collin-Dufresne et al. 2012 among others).

By model assumptions, a larger payout rate can be interpreted either as larger dividend payments or larger coupons (or both)[6]. As previously discussed, default cannot happen because on these payments, including coupons. Indeed, in the compound option model the

---

[6]Additional information on how this quantity is estimated is provided in Appendix B.

firm has already committed to pay-out at rate ϖ *ex ante*. This, together with the finite horizon assumption in the model, implies that different payout policies impact in the valuation of the firm securities.

However, the effect of payouts on default is indirectly induced by the drift in (1.6): given two firms which have identical capital structure (and riskiness) but differ in their payout ratio, the firm with larger ϖ would be more likely to default because of a smaller (and possibly negative) drift. Nonetheless, the separate effect of dividends and coupons on ϖ cannot be disentangled here. This is clearly one of the limitations of this model.

In order to understand the effect of ϖ on S, it is crucial to highlight that the risk-neutral pricing equity in (1.9) relies on the existence of a trading strategy in which equity, can be perfectly replicated using the firm's assets and a riskless bond[7]. The replication arguments are similar to those in (standard) option pricing with the key difference however that options do not pay dividends but equity does.

For simplicity consider equation (1.9) with $n = 1$. The equity is replicated via a portfolio of $e^{-\varpi t_1}\Phi(d^{\mathbb{M}})$ units of V and borrowing $e^{-rt_1}F_1\Phi(d^{\mathbb{Q}})$. As the assets pay-out at rate ϖ, these cashflow are used to buy more units of V. This ensures that the pay-off at maturity of the replicating portfolio is as that one of equity, that is $\max\{V_1 - F_1, 0\}$. The same rational applies to the term $V_0 e^{-\varpi t_n}\Phi_n(\mathbf{d}^{\mathbb{M}})$ in (1.9) with $n \geq 1$.

To investigate further the the effect of payouts on the value of equity, the latter is plotted in Figure 1.3 ($\varpi = 0.05$) and 1.4 ($\varpi = 0$). Comparing the two, it is clear that the payout rate does not influence the shape of the surfaces but does affect their level. Larger payouts, whether originating from dividends or coupon payments, have the effect of reducing the equity prices. This fact can be explained as follows.

Let us first assume that larger ϖ of the firm in Figure 1.3 is due to either the firm having larger debt (thus having to meet larger interest expenses) or lower creditworthiness (thus calling for larger credit spreads). As the payment of the firm's debt is financed via issuing new equity, having a larger payout implies either more debt to refinance or a lower risk-neutral drift in (1.6) (and hence in (1.10)). Either way, this implies larger issuances of new equity with the inevitable dilution effect which is incorporated in its price today.

Here instead let us assume that a larger ϖ is observed because the firm pays more dividends. Building on the Modigliani-Miller proposition on the irrelevance of the dividend policy (Miller and Modigliani 1961), firms that pay more dividends offer less price appreciation but must provide the same total return to stockholders, given their risk characteristics and the cash flows from their investment decisions. Although the value of equity in a firm

---

[7]About the ability to trade the asset value see Footnote 2
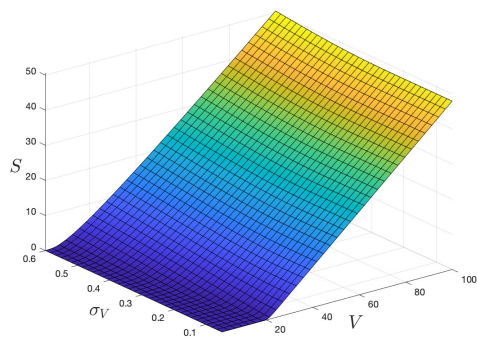
$$\text{(a)} \quad \begin{array}{lll} F_1 = 1 & F_2 = 5 & F_3 = 10 \\ t_1 = 1 & t_2 = 5 & t_3 = 10 \end{array}$$

$$\text{(b)} \quad \begin{array}{lll} F_1 = 1 & F_2 = 5 & F_3 = 10 \\ t_1 = 1 & t_2 = 10 & t_3 = 30 \end{array}$$

$$\text{(c)} \quad \begin{array}{lll} F_1 = 5 & F_2 = 10 & F_3 = 50 \\ t_1 = 1 & t_2 = 5 & t_3 = 10 \end{array}$$

$$\text{(d)} \quad \begin{array}{lll} F_1 = 5 & F_2 = 10 & F_3 = 50 \\ t_1 = 1 & t_2 = 10 & t_3 = 30 \end{array}$$
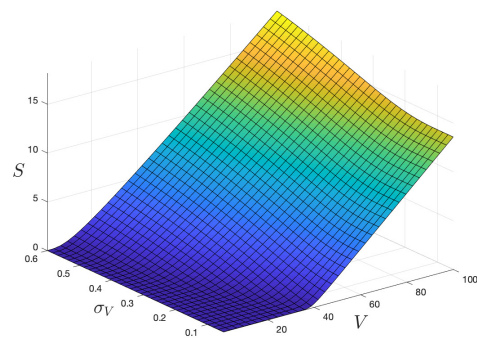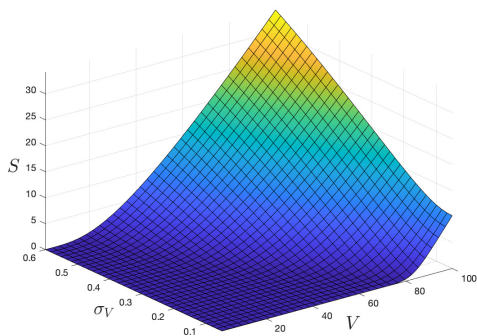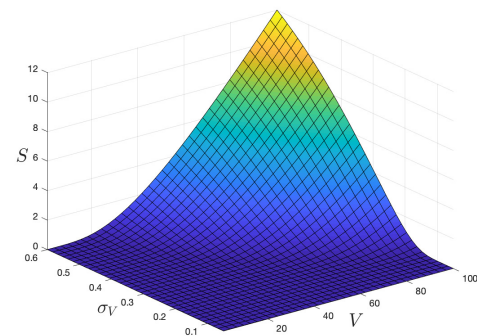
Fig. 1.3 Equity (S) as a function of the firm value (V) and asset volatility (σ_V) for different sets of parameters ($r = 0.03$, $\varpi = 0.05$). F_i denotes the face value of debt due at time t_i, for $i = \{1, 2, 3\}$. Panels (a) to (d): impact of different levels of leverage and debt maturities on value of the equity (for a given σ_V, i.e. the riskiness of the firm). Safer firms (lower debt, shorter maturities: Panel (a)) are least affected by changes in σ_V. Progressively riskier firms (lower debt, longer maturities: Panel (b); larger debt, shorted maturities: Panel (c); larger debt, longer maturities: Panel (d)) display significant differences in the value of equity for different levels of riskiness. Firms in Panel (d) are the most sensitive to changes in σ_V.

$$
\text{(a)} \quad
\begin{array}{lll}
F_1 = 1 & F_2 = 5 & F_3 = 10 \\
t_1 = 1 & t_2 = 5 & t_3 = 10
\end{array}
$$

$$
\text{(b)} \quad
\begin{array}{lll}
F_1 = 1 & F_2 = 5 & F_3 = 10 \\
t_1 = 1 & t_2 = 10 & t_3 = 30
\end{array}
$$

$$
\text{(c)} \quad
\begin{array}{lll}
F_1 = 5 & F_2 = 10 & F_3 = 50 \\
t_1 = 1 & t_2 = 5 & t_3 = 10
\end{array}
$$

$$
\text{(d)} \quad
\begin{array}{lll}
F_1 = 5 & F_2 = 10 & F_3 = 50 \\
t_1 = 1 & t_2 = 10 & t_3 = 30
\end{array}
$$
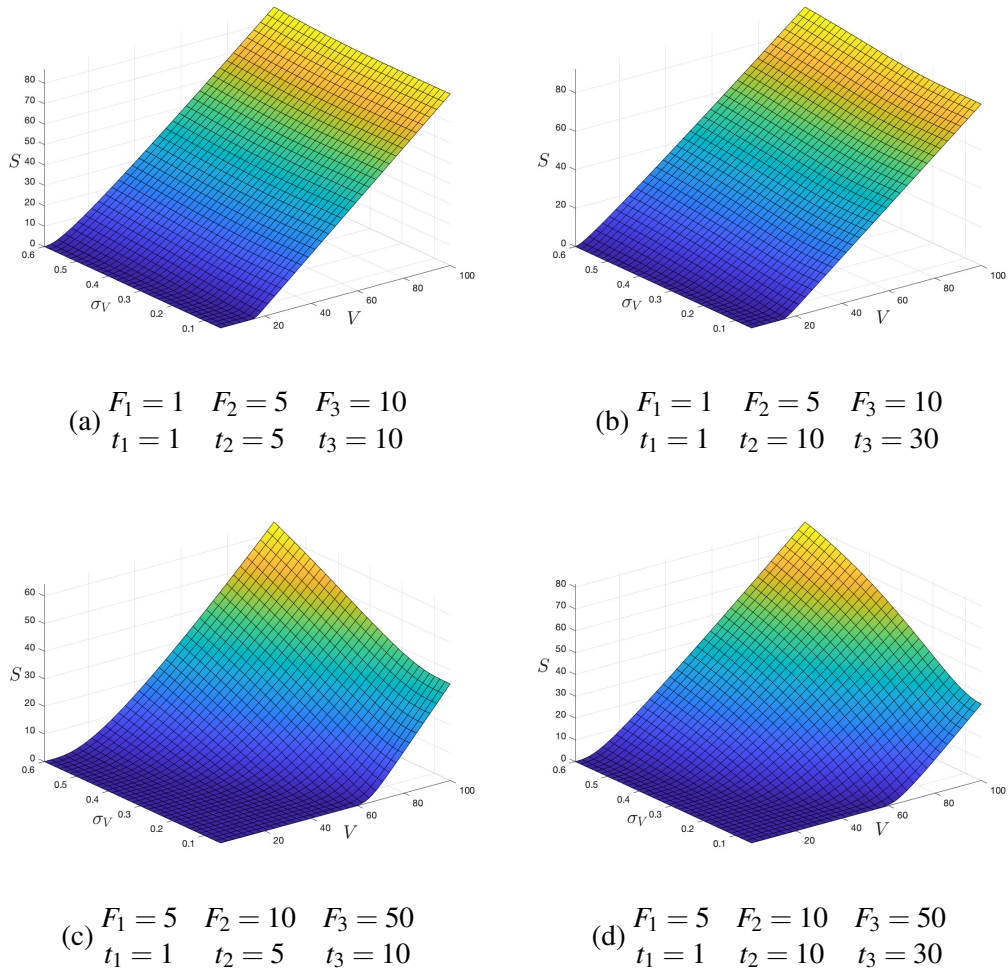
Fig. 1.4 Equity (S) as a function of the firm value (V) and asset volatility (σ_V) for different sets of parameters ($r = 0.03$, $\varpi = 0$). F_i denotes the face value of debt due at time t_i, for $i = \{1, 2, 3\}$. Similar shapes compared to the surfaces in Figure 1.3 are obtained when dividends and coupons are excluded; the levels are however sensibly different: as expected, larger payout rates induce lower risk-neutral drifts in (1.6) and hence lower equity values.

should not change as its dividend policy changes, this does not imply that the price per share will be unaffected, since larger dividends should result in lower stock prices and more shares outstanding (and the subsequent dilution effect).

Nonetheless, one limitation of the model is its inability to identify whether a share price reduction is to be attributed to larger dividends or larger coupons.

Finally, the pricing equation (1.9) allow also to determine the market value of the firm's debt which is given by $D_0(V) = e^{-\varpi t_n}V_0 - S_0(V)$. This quantity represents the total debt of the firm. Semiclosed-form solutions for the market value of each bond outstanding with face value F_i and maturity t_i, say $D_{0,i}(V)$ with $\sum_{i \in I} D_{0,i}(V) = D_0(V)$, can also be obtained (see Chen 2013).

The relationship

$$e^{-\varpi t_n}V_0 = S_0(V) + D_0(V)$$

can also be expressed as

$$V_0 = S_0(V) + D_0(V) + X_0(V)$$

with $X_0(V) = V_0(1 - e^{-\varpi t_n})$. The quantity $X_0(V)$ can be interpreted as the cash-flow already promised to the firm's stakeholders which are kept in a separate item of the firm's balance sheet such as committed funds (which are not tradable). As a matter of fact, the compound option model is a structural model of default with commitment and known liquidation horizon: being the firm's payouts deterministic, the amount $X_0(V)$ accounts for the amount, as of today, that will be paid to the firm's stakeholders. As the firm approaches to the liquidation time t_n, X declines.

1.2.3 Other properties of a compound option model of default

Figure 1.3 shows also how the value of the equity changes for different sets of parameters, when equity is a compound option: the model is the 3–fold compound option which is also used throughout the empirical investigation. The motivations for selecting $n = 3$ are discussed in the next subsection.

Remarkably, equity is an increasing function of the asset volatility (as expected, being a compound call option). Firms with relatively lower debt and shorter maturities are the least affected by changes in the riskiness of the firms (see Panel(a)). Progressively riskier firms (lower debt, longer maturities: Panel (b); larger debt, shorted maturities: Panel (c); larger debt, longer maturities: Panel (d)) display significant differences in the value of equity for different levels of riskiness. Also, the effect of progressively larger asset volatility on equity is magnified for highly-levered firms with larger fraction of long-term debt (Panel (d)).
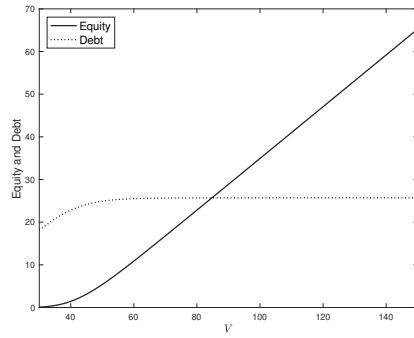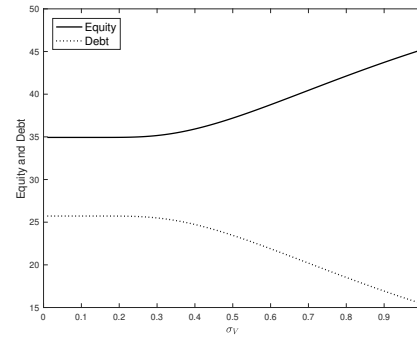
(a) S and D as functions of V

(b) S and D as functions of σ_V
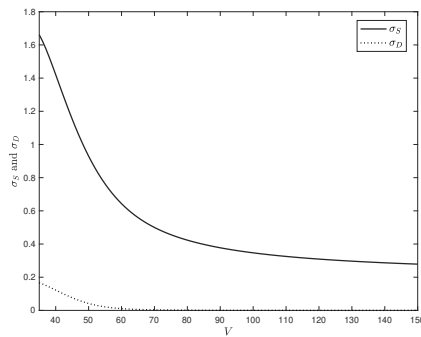
(c) σ_S and σ_D as functions of V
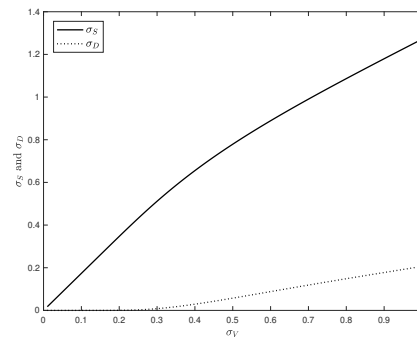
(d) σ_S and σ_D as functions of σ_V
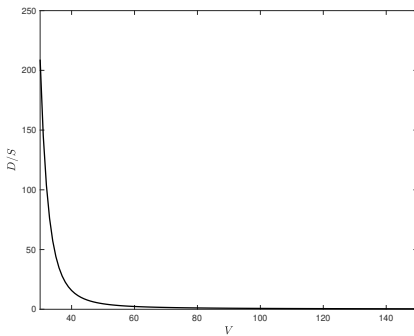
(e) D/S as function of V
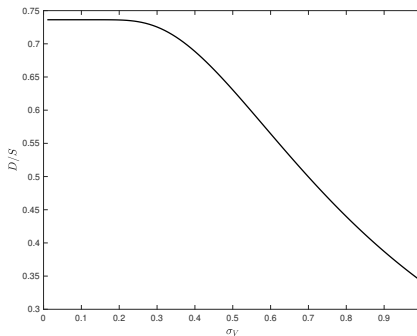
(f) D/S as function of σ_V

Fig. 1.5 $F_1 = F_2 = F_3 = 10$; $t_1 = 1, t_2 = 5, t_3 = 10$, $r = 0.03$, $\varpi = 0.05$. When leverage is fixed (Panels (a), (c), (e)) the firm's riskiness is set to $\sigma_V = 0.2$; when the firm's riskiness is fixed (Panels (b), (d), (f)), the value of the asset is set to $V = 100$. Panel (a) shows that both equity and debt are increasing functions of V, with equity being convex whilst debt being concave. Panel (b) shows both equity and debt as functions of the firm's riskiness, with equity being an increasing and convex function, whilst debt being decreasing and concave. Panel (c) displays the volatility of equity and debt as function of leverage, showing σ_D far less sensitive to leverage than σ_S, with the latter also always larger. Panel (d) analyses the same volatilities with respect to the asset volatility: both are increasing in the volatility of the assets, despite being σ_V more affected. Panel (e) shows how leverage decreases as the value of the assets increases and panel (f) shows that leverage tend to decrease with larger level of asset volatility as the the numerator of D/S tends to decrease while the denominator increases.

To investigate further the model dynamics and predictions,

Furthermore, Figure 1.2 shows how the value of the equity is affected by the maturity of the firm's debt. Given the same total face value of the bonds outstanding, firms whose debt is concentrated at the first payment date are the ones whose equity is valued the most. This result is intuitive and is due to the fact that companies whose debt is spread further into the future are more exposed to uncertainty (i.e. they have more chances of defaulting). Therefore, the today-price of the equity incorporates this future risk.

To conclude, the stochastic properties of the process driving the value of the equity are discussed. By the virtue of Itô's Lemma, the value of the equity does not follow a geometric Brownian motion but instead a process that I refer as Stochastic Elasticity of Variance (SEV). As a matter of fact, it can be shown that

$$dS_t = \alpha_S^{\mathbb{Q}}(V_t,t)S_t\,dt + \sigma_V S_t^{\beta(V_t,t)}\,dW_t^{\mathbb{Q}}, \tag{1.10}$$

with

$$\alpha_S^{\mathbb{Q}}(V_t,t) := \frac{1}{S_t}\left(\frac{\partial S}{\partial t} + \frac{\partial S}{\partial V}(r-\varpi)V_t + \frac{1}{2}\frac{\partial^2 S}{\partial V^2}\sigma_V^2 V_t^2\right) \quad \text{and} \quad \beta(V_t,t) := 1 + \frac{\ln \mathrm{El}_V(S_t)}{\ln S_t}$$

where $\mathrm{El}_V(S_t) := \frac{\partial S}{S_t}/\frac{\partial V}{V_t}$ is the elasticity of the firm's equity with respect to the asset value. This model closely resembles the Cox (1996) Constant Elasticity of Variance (CEV) in which the parameter β is assumed constant. Here, the volatility of equity is stochastic and given by

$$\sigma_{S,t} = \sigma_V \Delta_S^{(n)} \frac{V_t}{S_t}, \tag{1.11}$$

where $\Delta_S^{(n)}$ is the sensitivity of the equity with respect to changes of the asset value (as equity is an option, it is the 'Delta' of the equity). Analytical expressions of $\Delta_S^{(n)}$ – which depends on the number of bond outstanding n – are available in Appendix F. It is worth highlighting that the process does not only have stochastic volatility, but it is also a model of local volatility in the sense of Dupire (1994) as it depends on the current level of the equity. Therefore, the model driving equity returns is a local-stochastic volatility model (for further details on this class of models, see Henry-Labordère 2009).

To some extent the process in (1.10) produces similar trajectories to the reduced-form default-extended CEV process in Carr and Linetsky (2006). The main difference between the two approaches is that their process is only able to statistically reproduce the patterns caused

(a) Merton's model　　　　　　　(b) 3–fold compound option model
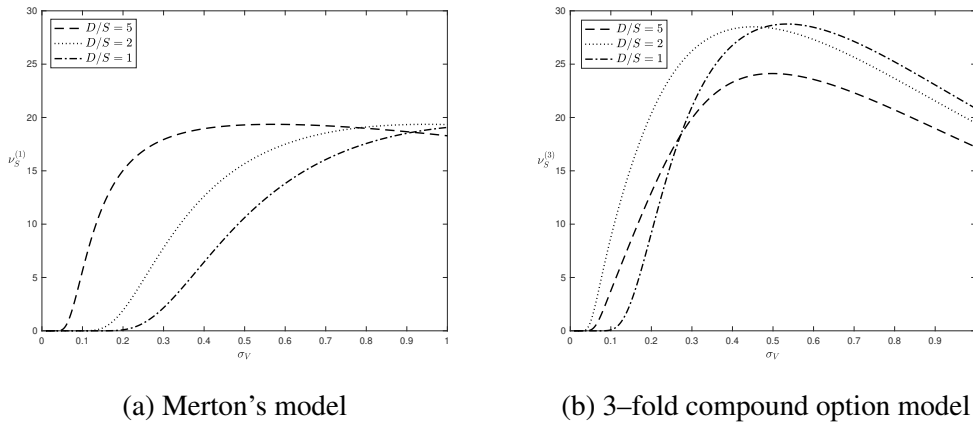
Fig. 1.6 Sensitivity of equity with respect to asset volatility under the Merton (panel (a)) and a compound option model (panel (b)) ($r = 0.03$, $\varpi = 0.05$). In panel (a): $F_1 = 50$, $t_1 = 1$; in panel (b): $F_1 = F_2 = F_3 = 50/3$; $t_1 = 1$, $t_2 = 5$, $t_3 = 10$. Panel (a) shows how $v_S^{(1)}$ reacts to changes in the riskiness of the firm: it is optima for equity holders to increase leverage, as this makes equity more sensitive to further changes in volatility. Panel (b) shows how $v_S^{(3)}$ reacts to increasing business risk: pushing leverage is optimal as long as the sensitivity of equity starts decreasing. The sensitivity of a highly-levered (dashed) company falls between the sensitivities of the medium-levered (dotted) and low-levered (dotted-dashed) companies for plausible value of $\sigma_V \in (0, 0.3)$ p.a..

by the leverage effect, while here the statistical properties of the SEV are directly attributable to the firm's capital structure.

1.2.4　Why a 3–fold compound option?

On a different note, a compound option default model is also able to explain some of the 'puzzling' findings in Carr and Wu (2017). The authors document that, contrary to conventional wisdom, financial leverage does not always decline with increased business risk. Instead, financial leverage can increase if the risk increase is due to small, diffusive market movements. Also Cremers, Driessen, Meanhout and Weinbaum (2008) document a negative correlation between market volatilities and credit spread (and, therefore, default probabilities) performing panel regressions. Given some suitable and reasonable assumptions, these findings can be reconciled with the predictions of my model, and are discussed below.

If the volatility of the company increases, every structural model à la Merton would predict that the value of its equity increases too as displayed in Figure 1.5 (b). Also, in line with common sense, Figure 1.5 (a), (c) and (e) shows that the firm equity and debt are increasing in the asset value (but they display opposite concavity), and that the volatility of equity and debt both tend to decline as the firm becomes safer due to a larger asset value.

The same applies for the debt to equity ratio. On the other hand, panels (d) and (f) can help shedding some light on the counter-intuitive findings in Carr and Wu (2017).

In a model in which the capital structure is insensitive to changes in the business risk (as in Merton 1974, Geske 1977 and here), the company's financial leverage drops with increasing business risk (panel (f)). Instead, in a more sophisticated compound option model in which the firm can react to changes in its business risk and adjust its capital structure accordingly, as the riskiness of the firm increases, it would be optimal to take on more debt given the rise in equity so that the leverage ratio remains constant. Also, it would be more beneficial for equityholders to take in a larger fraction of debt than the percentage increase of the value of equity, being debt less volatile than equity (panel (d)). Thus, the findings in Carr and Wu (2017) of increasing leverage for increasing diffusive volatility can be easily reconciled with a model in which shareholders maximise the firm value, based on a targeted leverage ratio, and where equity is seen as a compound option.

Finally, to illustrate why a 3–fold compound option model is used, the sensitivity of the equity with respect to asset volatility, $v_S^{(n)}$ (i.e. the 'Vega' of the equity), can be looked at. Analytical expressions for $v_S^{(n)}$ are available in Appendix G. Figure 1.6 shows how equity reacts to volatility changes over different capital structures and aggregation schemes. Panel (a) shows the sensitivity of the equity under the Merton model (where the whole firm's debt is clustered at unique date in the future). Panel (b) shows how the same sensitivity displays a different behaviour by having allowed for a more realistic aggregation scheme of the company's capital structure: short, medium and long-term debt.

Comparing the two panels, it is evident that the effect of leverage is exacerbated in a compound option model: the equity of moderately-levered firms changes more severely in panel (b). For reasonable combinations of asset volatility and leverage, there is an incentive by the shareholders to increase the leverage. Considering plausible values of the asset volatility (say between 5% and 40% p.a.), panel (b) in Figure 1.6 shows that equityholders of the 'dashed company' would be better off increasing leverage to become the 'dotted company'. However, increasing leverage further, that is turning into the 'dotted-dashed company', would reflect into a reduction on the sensitivity of the equity. On the other hand, the Merton's model is not able to reproduce this pattern: it is always optimal for shareholders to increase leverage further.

This findings should not considered in contrast with the literature on optimal capital structure and the trade-off theory. As this model does neither account for taxes nor for bankruptcy costs, the implications in terms of optimal capital structures above described relates to the sensitivity of the equity with respect to the firm riskiness (intended as volatility

of its cashflow) not to the value of the equity itself. Being equity a compound call option, its value is increasing with σ_V.

However, for a given leverage ratio, a maximum is observed in $\nu_S^{(3)}$: if equity holders are able to change the riskiness of the firm σ_V, then a 3–fold option model is able to determine the optimal riskiness which maximises the Vega of the equity. In addition, if equityholders can modify the composition of the capital structure (which is not taken into account thereafter), it is arguable that there exist a leverage ratio for which $\nu_S^{(3)}\left(\frac{D}{S}\right)$ is maximised regardless of value of σ_V (though still considering reasonable values, say between 5% and 40% p.a.). Nonetheless, optimal capital structure is not investigated in the following sections and left for future research[8].

1.2.5 Call and Put Equity Options as a $(n+1)$ – fold Compound Options on Asset Value

Intuitively, as equity is an n–fold compound option, vanilla options are $(n+1)$–fold compound options on the firm's assets. Consider an European option with maturity $T \in (t_i, t_{i+1})$, with $0 \leq t_i < t_{i+1} \leq t_n$, and strike price K written on the firm's equity. If the company is allowed to default at any t_i, the generic terminal payoff of the option is

$$P_{T,\xi} = \xi \left(S_T(V)\mathbb{1}_{\{\tau>T\}} - K \right) \mathbb{1}_{\{\xi S_T(V) \geq \xi K\}} \tag{1.12}$$

where ξ is a binary variable taking values $+1$ (respectively -1) in the case in which the option is a call (respectively a put), $\mathbb{1}_{\{\xi S_T(V) \geq \xi K\}}$ determines the condition for the option to expire in-the-money, and $\mathbb{1}_{\{\tau>T\}} \equiv \mathbb{1}_{\{\tau>t_i\}}$ is the condition to ensure that the firm has not defaulted before the maturity of the option. Notice that the possibility for the company to default after the maturity of the option is already accounted in the value of $S_T(V)$. In case the company defaults before the option maturity (that is the first indicator function is zero) the firm's equity drops to zero[9].

---

[8]It may be the case that this concavity is induced by "hidden" bankruptcy costs in the model: if the firm defaults, bondholders receive less than their claim, namely $S_i^\star$ instead of F_i (and equitholders receive nothing).

[9]To be precise, the option's payoff consistent with the compound option model of equity should be

$$P_{T,\xi} = \xi \left(S_T(V)\mathbb{1}_{\{\tau>T\}} + S_i^\star\mathbb{1}_{\{\tau\leq T\}} - K \right) \mathbb{1}_{\{\xi S_T(V) \geq \xi K\}},$$

where $S_i^\star$ is the value of the equity for which the firm defaulted at t_i (which is the payment date before the maturity of the option). As $S_i^\star$ depends on the model's assumptions and needs to be estimated, it is more likely that market participants trading option assume zero value for the equity at default (also for precautionary reasons), and is therefore ignored. Also, for the vast majority of the options in the sample, the option's maturity is before the maturity of the first debt (that is $T < t_1$), thus implying (1.12) to be the exact payoff function.

Under risk-neutral valuation, the present value of the option is given by

$$P_{0,\xi} = e^{-rT} \mathbb{E}^{\mathbb{Q}} \left(P_{T,\xi} \right).$$

In the same fashion as Section 1.2.1, the event of the option expiring in-the-money, $\{\xi S_T(V) \geq \xi K\}$, can be redefined as the event $\{\xi V_T \geq \xi \bar{V}_K\}$, where $\bar{V}_K$ is nothing but the value of the assets corresponding to the equity value that makes the option expire in-the-money. Letting $\mathscr{V}_T^{\xi} := \{\xi V_T \geq \xi \bar{V}_K\}$ and rearranging, the value of the option can be written as

$$P_{0,\xi} = \xi e^{-rT} \left[\mathbb{E}^{\mathbb{Q}} \left(S_T(V) \mathbb{1}_{\mathscr{V}_i \cap \mathscr{V}_T^{\xi}} \right) - K \mathbb{Q} \left(\mathscr{V}_T^{\xi} \right) \right],$$

where, using (1.7), the value of the equity at the maturity of the option is given by

$$S_T(V) = e^{-r(t_n - T)} \mathbb{E}_T^{\mathbb{Q}} \left(V_n \mathbb{1}_{\mathscr{V}_{i,n}} \right) - \sum_{k=i+1}^{n} e^{-r(t_k - T)} F_k \mathbb{E}_T^{\mathbb{Q}} \left(\mathbb{1}_{\mathscr{V}_{i,k}} \right).$$

Being $\mathbb{1}_{\mathscr{V}_i \cap \mathscr{V}_T^{\xi}}$ $\mathscr{F}_T$-measurable, and applying the law of iterated expectations, it follows

$$P_{0,\xi} = \xi \left[e^{-rt_n} \mathbb{E}^{\mathbb{Q}} \left(V_n \mathbb{1}_{\mathscr{V}_n \cap \mathscr{V}_T^{\xi}} \right) - \sum_{k=i+1}^{n} e^{-rt_k} F_k \mathbb{Q} \left(\mathscr{V}_k \cap \mathscr{V}_T^{\xi} \right) - e^{rT} K \mathbb{Q} \left(\mathscr{V}_T^{\xi} \right) \right].$$

Operating the same change of measure of Section 1.2.1, the price of the option can be expressed as

$$P_{0,\xi} = \xi \left[e^{-\varpi t_n} V_0 \mathbb{M} \left(\mathscr{V}_n \cap \mathscr{V}_T^{\xi} \right) - \sum_{k=i+1}^{n} e^{-rt_k} F_k \mathbb{Q} \left(\mathscr{V}_k \cap \mathscr{V}_T^{\xi} \right) - e^{-rT} K \mathbb{Q} \left(\mathscr{V}_T^{\xi} \right) \right].$$

Furthermore, the probabilities under $\mathbb{M}$ and $\mathbb{Q}$ can be computed using the result in Theorem 1 in Appendix C, and the price can be expressed in terms of multivariate Gaussian integral as

$$
\begin{aligned}
P_{0,\xi} = \xi \Big[& e^{-\varpi t_n} V_0 \Phi_{n+1} \left(\mathbf{d}_{\xi}^{\mathbb{M}}; \boldsymbol{\Gamma}_{n+1,\xi} \right) - \sum_{k=i+1}^{n} e^{-rt_k} F_k \Phi_{k+1} \left(\mathbf{d}_{\xi,k+1}^{\mathbb{Q}}; \boldsymbol{\Gamma}_{k+1,\xi} \right) \\
& - e^{-rT} K \Phi \left(\xi d_T^{\mathbb{Q}} \right) \Big]
\end{aligned}
\tag{1.13}
$$

with $\mathbf{d}_\xi^{\mathbb{M}} = \left(\left(d_i^{\mathbb{M}} \right)_{i=1}^{k}, \xi d_T^{\mathbb{M}}, \left(d_i^{\mathbb{M}} \right)_{i=k+1}^{n} \right)$, $\mathbf{d}_{\xi,k+1}^{\mathbb{Q}} = \left(d_{\xi,i}^{\mathbb{M}} - \sigma_V \sqrt{t_i} \right)_{1 \leq i \leq k+1}$, where $d_i^{\mathbb{M}/\mathbb{Q}}$ are defined as in Section 1.2.1 and

$$d_T^{\mathbb{M}} = \frac{\ln\left(V_0/\bar{V}_K\right) + \left(r - \varpi + \sigma_V^2/2\right) T}{\sigma_V \sqrt{T}}, \qquad \mathbf{\Gamma}_{k+1,\xi} = \begin{pmatrix} 1 & \sqrt{\frac{t_1}{t_2}} & \cdots & \xi\sqrt{\frac{t_1}{T}} & \cdots & \sqrt{\frac{t_1}{t_k}} \\ & 1 & \cdots & \xi\sqrt{\frac{t_2}{T}} & \cdots & \sqrt{\frac{t_2}{t_k}} \\ \cdots & \cdots & \cdots & \cdots & \cdots & \cdots \\ & & & & 1 & \sqrt{\frac{t_{k-1}}{t_k}} \\ & & & & & 1 \end{pmatrix},$$

and $d_T^{\mathbb{Q}} = d_T^{\mathbb{M}} - \sigma_V \sqrt{T}$. For $\varpi = 0$, $n = 1$ and $t_1 > T$, the pricing formula coincides with that in Geske (1979). The probabilities which appear in (1.8) and (1.13) are used in Section 1.4 in order to construct a novel measure of impact of credit risk based on option prices.

1.3 Data and Estimation Methodology

The dataset under investigation is composed by US companies, constituents of the S&P100 during the period January 2013 – December 2017. Companies with either preferred equity or subject to merges or acquisitions are excluded. Also, only companies for which both CDS spreads and option quotes available are included. The final sample is formed by 66 companies. Previous studies investigating the relative pricing of options and CDSs rely on much smaller samples (see for instance Hull et al. 2004, Carr and Wu 2010, and Carr and Wu 2017). Table B.1 displays the complete name list, alongside the SIC code of the companies.

In the same spirit of Carr and Wu (2017), the sample is further divided into four categories based on the industry/type or business: (a) Financial companies; (b) Mining, Energy and Utilities companies; (c) Manufacturing; (d) Retail, Wholesale and Services. See Figure 1.7 for the relative frequencies of the different industries/sectors. A sub-sample analysis based on these groups is carried out in Section 1.4.2.

Data on stock prices, number of shares outstanding, dividends and the risk-free yield curve are obtained from Bloomberg. Option quotes are collected from Optionmetrics. CDS spreads are from Thompson Reuters Datastream. Information relative to the firms' capital structures and cost of debt is gathered from Compustat and the 10-K documents. It is worth mentioning that, with the exception of Vassalou and Xing (2004), Forte and Lovreta (2012) and Ericsson et al. (2015), none of the contributions on structural models of default use calibrations on stock prices, as they mostly rely on bond quotes or option-implied volatilities (which are usually model-dependent).
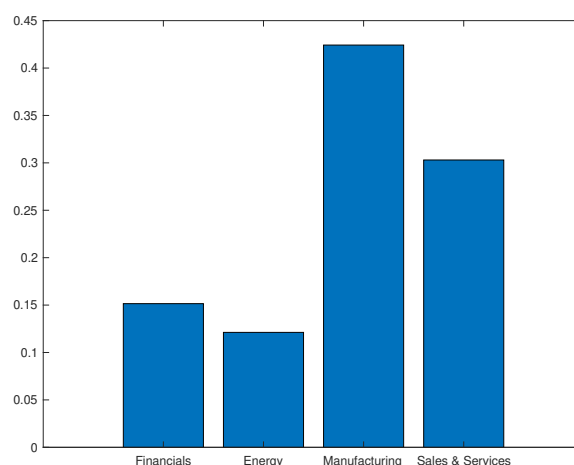
Fig. 1.7 Industry/sector composition of the whole sample: (a) Financial companies (15%); (b) Mining, Energy and Utilities companies (12%); (c) Manufacturing (42%); (d) Retail, Wholesales and Services (30%).

Option quotes, CDS spreads and equity prices are observed at daily frequency. The data from Compustat on the firms' debt is available only at quarterly frequency though. Therefore, it is assumed that the capital structure remains fixed within quarters, having only adjusted the time to maturity of the firm's debt due to the passage of time. It appears a reasonable assumption given the empirical evidence on how often US firms decide to rebalance their capital structures (see Strebulaev and Whited 2012).

Given the large amount of option data, only the most liquid OTM call and put options traded every Wednesdays with time-to-maturity greater than six months are taken into consideration. To determine the most liquid traded options, those prices whose moneyness is outside the 5th to 95th percentile range are firstly removed. Secondly, only those options with volume above their annual median are kept.

As one of the aims of this work is to study the interplay between market and credit risk, and how this is reflected into the relative pricing of derivatives contracts (options and CDSs) written on the same company, I opt for focusing on those option for which the impact of credit risk is presumably not negligible. In fact, as the database is composed by firms members of the S&P100 – which should be considered as 'safe' companies in the short-term – it seems very unlikely that options with maturities lesser than six months would price any credit risk. This intuition is also confirmed by Cremers, Driessen, Meanhout and Weinbaum (2008).

The price of the option is defined as the average of the bid and ask price when both are available; the observation is removed otherwise. Finally, options with zero trading volume and negative bid-ask spread are also excluded. The final sample counts 92,879 valid call and
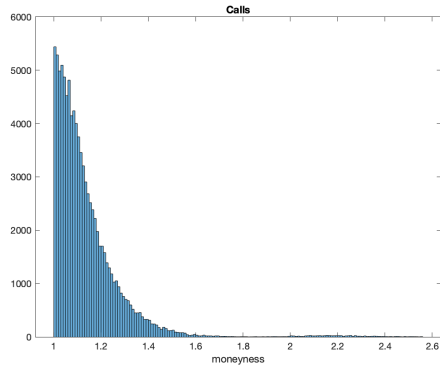
(a) OTM Calls' moneyness
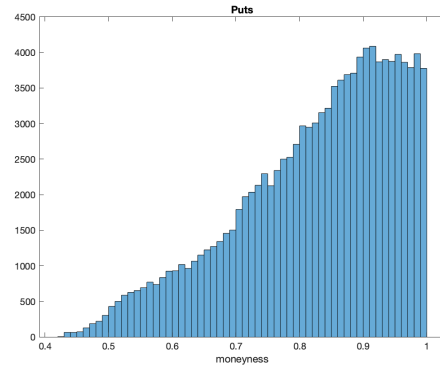
(b) OTM Puts' moneyness
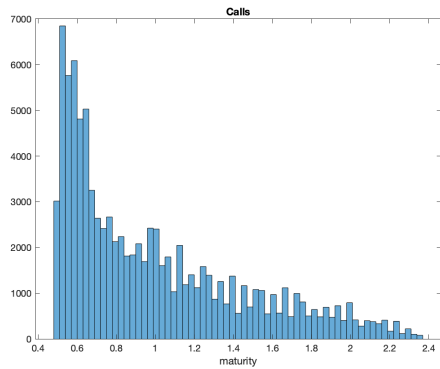
(c) OTM Calls' maturity
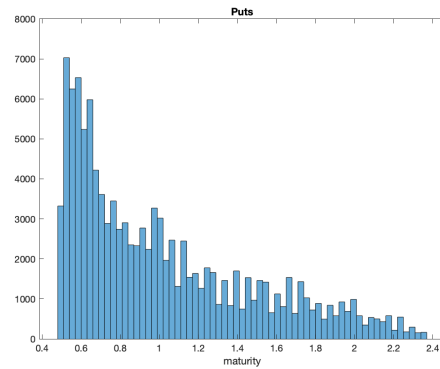
(d) OTM Puts' maturity

Fig. 1.8 Empirical distributions of moneyness (K/S) and maturity (T) of option data. Panel (a) shows that most of the valid call option observations have moneyness in $(1, 1.8)$, whilst for put options, displayed in panel (b), the moneyness is in $(0.6, 1)$. The distribution of put options is less peaked than the one of calls. Panels (c) and (d) takes into account the maturities of the options which range from 0.5 to 2.4 years form both call and put quotes, being the distributions very similar.

112,347 put options observations over 259 weeks. Figure 1.8 shows the options' distribution in terms of moneyness and maturity.

One of the main disadvantage of working with equity options is that they are usually American-style. This is the case in the analysed dataset and, in order to test and implement the model, European quotes should be used. Hence, the de-Americanization procedure introduced by Carr and Wu (2010) and further tested in Burkovska et al. (2018) is applied. The aim of the de-Americanization is to find the corresponding European price (the so-called pseudo-European price) for a given American price. That is, the price ought to be observed if the contract would not allow to exercise the option before maturity. In a nutshell, a binomial tree is used to price the American option. The volatility parameter such that the squared

difference between the market price and the price generated by the tree is minimised is set as the option implied volatility. Once estimated, the pseudo-European price is found by applying the Black-Scholes formula for European options.

In order to estimate the impact of credit risk on equity options, and verify whether the option market participants price credit risk consistently with the swap market, a calibration based on equity prices, CDS spreads and option quotes is carried out. In addition, the term-structure of the firm's debt must be known or approximated somehow. I opt for clustering the firm's debt at three fixed point, $t_i = \{1, 5, 10\}$ years, $i = 1, 2, 3$. The face values of the bond due in $t_1 = 1$ represents the company's short-term debt and is computed as the Compustat variable DD1Q (Long-Term Debt Due in One Year). The remaining two bonds clustered at $t_2 = 5$ and $t_3 = 10$ are obtained as half of DLTQ (Long-Term Debt Total) each.

The choice of setting $n = 3$ appears again optimal as it is also the smallest number of maturity dates needed in order to match both the level, slope and curvature of the term structure of the survival probabilities extracted from the CDSs. As a matter of fact, an effective calibration of the model should aim at reproducing the aforementioned term structure as accurately as possible. For a more in-depth description of the construction of F_i and the payout rate see Appendix B. Furthermore, as shown in the previous Section, a 3–fold compound option model displays some desirable properties.

The unknown parameters of the model are the value of the company's asset, V_0, and its volatility, σ_V. In order to estimate their values, (1.9) and (1.13) are used (the two pricing equations constitute a non-linear system of equations in two unknowns). In the same spirit of estimating the implied volatility à la Black-Scholes, the value of the asset volatility, $\sigma_V^\star$, and corresponding asset value, $V_0^\star$, are found such that both the market price of equity and the option quote are matched.

Notice that the calibration can be implemented without using the risk-neutral probability of survival estimated from the CDS spreads (to solve for two unknowns, only two equations are needed, namely (1.9) and (1.13)). However the risk-neutral probabilities in (1.9), $\mathbb{Q}(\tau > t_i)$, can be replaced by those estimated from the CDS spreads. Nonetheless, the price of the firm's equity is still represented by an equation unknown in σ_V and V_0 as the probability under the firm-value fund measure, $\mathbb{M}(\tau > t_n)$, cannot be determined from CDS quotes. Thus, comparing the model estimates with and without the inclusion of CDS data should constitute a test of relative pricing between the option and CDS markets. If the default probabilities generated by the model – based on the calibration on the option and stock prices only – is able to reproduce those estimated form the CDS spreads, it could be inferred that the two markets are well integrated. For a further discussion on this topic and on how compute the

implied default barrier (which determines the model-implied probabilities of survival), see Appendix E.

This calibration on the equity and option prices also allows to construct the asset volatility surface. Moreover, the equity volatility surface calculated as in (1.11) can be estimated. This allows to make a direct comparison with the equity volatility surface obtained from the inversion of the Black-Scholes formula, and it is addressed in the next section. Also, the ability of the model to price option based on the previous asset volatility surface is tested also in Section 1.4.5.

1.4 Empirical Results

In this section, a new measure of impact of credit risk on options is first introduced. Using this measure I later test whether call and put options display different price impacts in terms of credit risk, and I further look at differences among industries in terms of credit risk pricing. Finally, it is shown that the same measure is able to forecast future movements of the options' negative skew. In the robustness section, evidence for the integration of the option and CDS markets is also discussed.

1.4.1 Information Content Ratios as Measure of Impact of Credit Risk

After having estimated the asset volatility and value such that (1.9) and (1.13) are met, a measure of impact of credit risk on option prices can be constructed based on the pricing equation (1.13). In the model, the option price depends on the risk-neutral probabilities

$$\mathbb{Q}\left(\tau > t_i \cap \xi S_T > \xi K\right) \tag{1.14}$$

with $i \in I$ and μ intended as the risk-neutral measure (when it multiplies the discounted face values) and the firm-value fund measure (when it multiplies the asset value). These are the risk-neutral probabilities of the event for which the firm survives (up to t_i) and the option expires in-the-money. They can be factorised as

$$\mathbb{Q}\left(\tau > t_i\right)\mathbb{Q}\left(\xi S_T > \xi K | \tau > t_i\right), \tag{1.15}$$

and can be interpreted as follows. The first factor is the probability of the firm surviving until t_i, whilst the second is the probability of the option expiring in-the-money conditional on the firm having survived. Therefore, this decomposition rigorously disentangles the source of

25

	Calls		Puts	
	K	T	K	T
Correlation (w/o CDS)	-0.0963	0.2209	-0.2573	0.2902
p-value	0.000***	0.000***	0.000***	0.000***
Correlation (with CDS)	-0.1078	0.2199	-0.2611	0.2876
p-value	0.000***	0.000***	0.000***	0.000***

Table 1.1 Average sample correlation of *AICR* (calls and puts, with and without having used the CDS to calibrate) with strike price (K) and maturity (T) of the options. As expected, for both calls and puts, the *AICR* is negatively correlated with the strike price, as lower strikes proxies for default thresholds, and positively correlated with the time-to-maturity of the option, as the probability of defaulting is increasing with the time horizon. The estimates are carried out both having calculated the *AICR*s with and without the extra calibration of the risk-neutral probabilities extracted from CDSs (and are statistically equivalent).

credit and market risk and how these reflect into option prices. Notice that the estimation of $\sigma_V^\star$ and $V_0^\star$ as in Section 1.3 allows to compute the probabilities in (1.14) as well as the risk neutral probabilities of survival in (1.15). Hence, the probability of the option expiring in-the-money conditional on surviving can be computed as well.

Alternatively, the risk-neutral probabilities of survival can be directly estimated in a model-free fashion using the CDSs spreads (see Appendix D). The comparison of the latter with those produced by the model allows to investigate the its ability to replicate the observed term-structure of default probabilities and, indirectly, to test for the integration of the two markets. In fact, if the model is calibrated on option quotes only and the generated probabilities are close those estimated via the CDSs, this would point towards a similar and consistent pricing of the two derivatives contracts by the economic agents trading in the two markets.

In order to turn the multiplicative link into an additive one, instead of looking at raw probabilities, their information content[10] is instead considered. Thus, the Information Content Ratio (*ICR*) for each probability is defined as

$$ICR_{i,\xi}(K,T) = \frac{\log \mathbb{Q}(\tau > t_i)}{\log \mathbb{Q}(\tau > t_i \cap \xi S_T > \xi K)}. \tag{1.16}$$

This represents the percentage of credit risk over the whole event of the firm surviving and the option expiring in-the-money, expressed in terms of the information content of the two events.

---

[10]In Information Theory, information content (or surprisal) of a signal is the amount of information gained when it is sampled. It is defined as minus the log-probability of the event: the less likely the event, the greater is the "surprise" associated if it happens. See Cover and Thomas (2006) for further details.

Once these ratios are computed for all the probabilities contributing to the price of the option, they can be then aggregated in order to measure the impact of credit risk on each option contract. The Average Information Content Ratio (*AICR*) is thus defined as a weighted average of the information content ratios, that is

$$AICR_\xi(K,T) = \frac{\sum_i w_i \cdot ICR_{i,\xi}(K,T)}{\sum_i w_i}. \tag{1.17}$$

The weights w_i are just the present values of the bond expiring in t_i. Notice that if $\tau > t_i$ a.s. for all $i \in I$, then $AICR_\xi(K,T) = 0$ (i.e. no impact of credit risk). For each option contract *AICR* is computed. Given that every day several contracts are traded, the daily average *AICR* is further calculated over all valid option prices. This allows us to construct a time series of a measure of the company's credit risk which is based on option quotes.

Moreover, the proposed measure is linked to the entropy of the default time. In fact, changing the base of the logarithm, (1.16) can be written as

$$ICR_{i,\xi}(K,T) = \log_{b_i} \mathbb{Q}(\tau > t_i)$$

with $b_i = \mathbb{Q}(\tau > t_i \cap \xi S_T > \xi K)$. Therefore,

$$AICR_\xi(K,T) = \sum_i \tilde{w}_i \cdot \log_{b_i} \mathbb{Q}(\tau > t_i)$$

and $\tilde{w}_i = w_i/\sum_i w_i$. On the other hand, the risk-neutral entrotropy in base $b \in (0,1)$ of the default time is defined as[11]

$$H_b^{\mathbb{Q}}(\text{default}) = \sum_i \mathbb{Q}(\tau = t_i)\log_b \mathbb{Q}(\tau = t_i),$$

and similarly

$$H_b^{\mathbb{Q}}(\text{survival}) = \sum_i \mathbb{Q}(\tau > t_i)\log_b \mathbb{Q}(\tau > t_i).$$

---

[11]Usually, the $\mathbb{P}$-entropy of a discrete random variable X is defined as $H_b^{\mathbb{P}}(X) = -\sum_i \mathbb{P}(X = x_i)\log_b \mathbb{P}(X = x_i)$ as the chosen base is usually $b = \{2, e, 10\}$. Here, instead, the base is $b \in (0,1)$, that is the minus is not necessary as the $\log_b$ function is already positive.

As long as b_i is approximately constant[12] and the $\mathbb{Q}\left(\tau > t_i\right) \propto \tilde{w}_i$ (i.e. they are proportional to the fraction of debt due at t_i), then $AICR \propto H_b^{\mathbb{Q}}(\text{survival})$.

As expected, Figure 1.9 shows that the daily average *AICR* calculated over calls is substantially smaller than those computed using put quotes. In addition, it appears that financial companies (panel (a)) display the greatest variability (both in terms of calls and puts) in the average daily *AICR*, thus suggesting a prompt reaction in option prices to changes in the company's credit risk and leverage.

Also, a correlation analysis shows that *AICR*s display a statistically significant negative correlation with the strike price: the lower the strike price, the higher the price of credit risk embedded in the option. In fact, the probability of the option expiring in-the-money for put options with progressively lower strikes should mostly reflect default events. In addition, *AICR*s is positively correlated with the maturity of the option: given the probability of survival being a decreasing function of the time horizon, long-maturity options display a larger impact of credit risk. Table 1.1 reports these estimates. These sample correlations highlight a much stronger link between credit risk and put options.

The same calculations can be done by computing the *AICR* of each option contract using either the model-implied probabilities or those extracted from the CDSs as described in Appendix D. As *AICR* is a linear functions of information contents in (1.16), the discrepancies between the *AICR*s computed using the two different sets of probabilities can shed light on the level of integration of the two markets. The next section addresses the link between the two constructions as well as the difference behaviour of put and call options in term of pricing of credit risk. A more formal test of integration is conducted in Section 1.4.5.

Notice that the risk-neutral probabilities estimated as in Appendix D are model-free and the estimation technique makes use of the whole term-structure of credit spreads (usually available for several tenors between 6 months and 30 years). On the other hand, the implementation of the compound option model assumes that default can happen at three points in time only. Regardless the compound option model is applied to a subset of the traded tenors, if it is able to produce similar default probabilities (for 1, 5 and 10 years) to those estimated directly from the spread (which are model-free), it could be argued that the option market participants price default risk (via the compound option model) in a similar fashion to the actual pricing observed in the market.

---

[12]Unreported empirical tests show that b_i are indeed approximately constant for the sample. In fact b_i is already bounded in $(0,1)$; moreover it is the probability of the intersection of the option expiring ITM and the firm surviving up to t_i. Therefore as the probability of the intersection is smaller of the probabilities of the single events, it should not surprise that b_i is quite small and stable.

(a) Financials

(b) Mining, Energy and Utilities

(c) Manufacturing

(d) Retail, Wholesale and Services
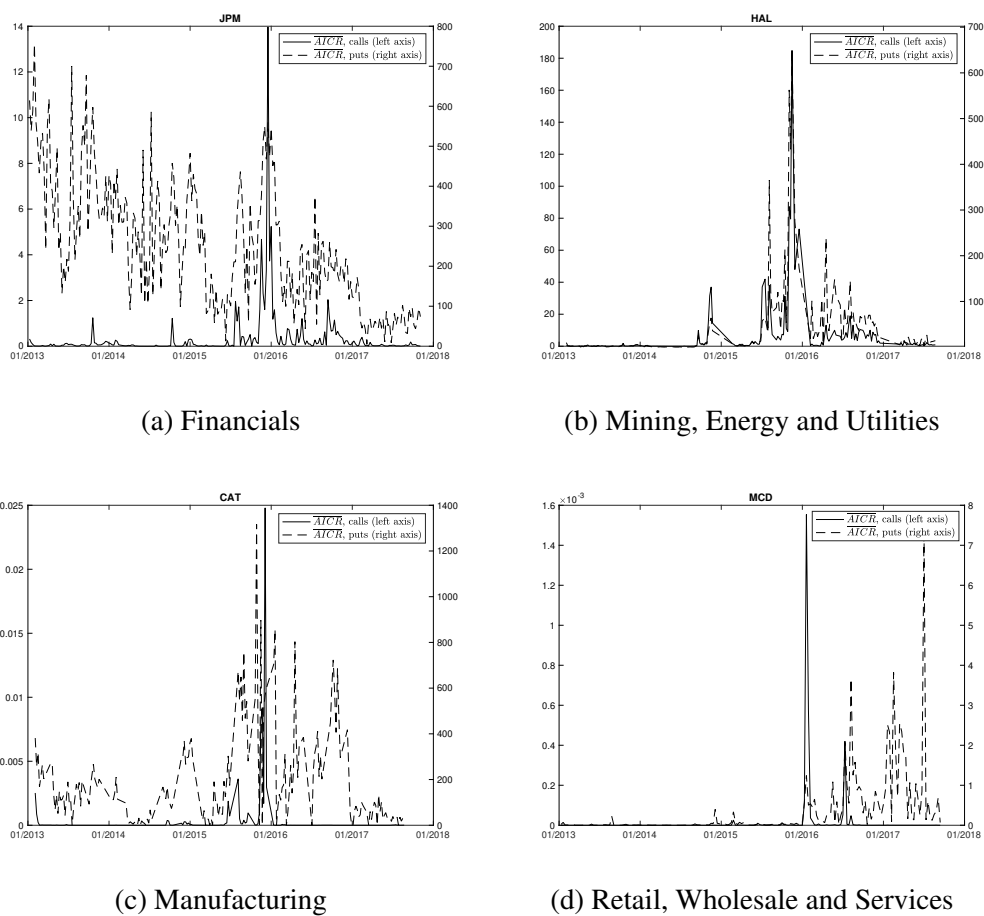
Fig. 1.9 Comparison of daily average *AICR* calculated over call and put options for four companies representing the four selected industries/sectors. As expected, $\overline{AICR}$ calculated using call (solid lines) options is much smaller than those obtained from put (dashed lines) options. $\overline{AICR}$s are expressed in basis points.
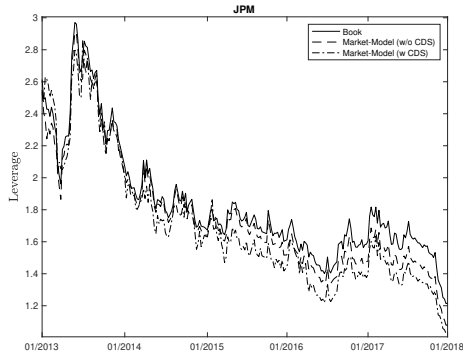
(a) Financials
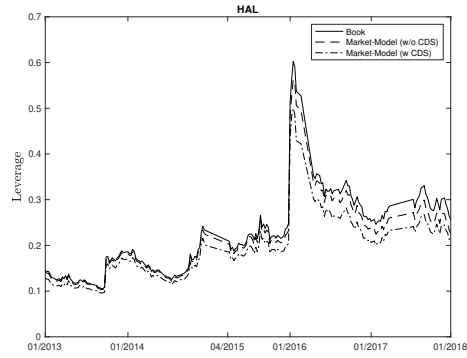
(b) Mining, Energy and Utilities
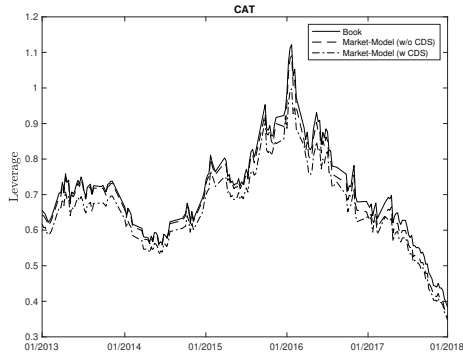
(c) Manufacturing
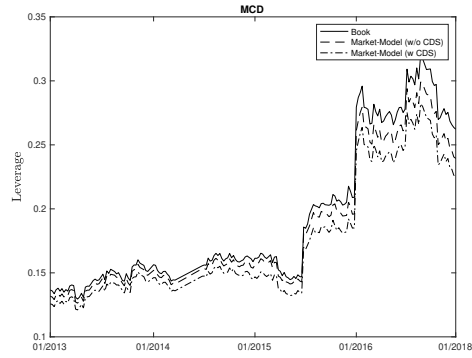
(d) Retail, Wholesale and Services

Fig. 1.10 Measures of leverage for four companies representing the four selected industries/sectors. The solid line is a measure of leverage calculated as book value of debt over market value of equity. The dashed line is a measure of leverage calculated as model-implied market value of debt (without having used the risk-neutral probabilities of default from CDS spreads) over the market value of equity. The dashed-dotted line is a measure of leverage calculated as model-implied market value of debt (having used the risk-neutral probabilities of default from CDS spreads) over the market value of equity.

Alternatively, once $V_0^\star$ and $\sigma_V^\star$ are determined, the compound option model could be solved for the implied credit spread s^{model}. This can be done via expressing the market value of debt maturing at t_i as a function of the asset value and risk, that is $D_i = f_i(V, \sigma_V)$, and then compute the t_i-spread as $s_i^{model} = -\frac{1}{t_i} \ln\left(\frac{f_i(V, \sigma_V)}{F_i e^{-rt_i}}\right)$. As the measure in (1.17) is constructed via the probability of survival (and not the spread), it appears more appropriate to calibrate the model to obtain $V_0^\star$ and $\sigma_V^\star$ and then compute the model-implied risk-neutral probabilities of survival.

1.4.2 Cross Sectional Differences in Calls and Puts

Economic and financial intuition suggests that a different pricing behaviour of credit risk should be observed between calls and puts. As default is an event which is priced in the left side of the equity distribution, put options, which constitute insurances against price falling, should be affected more by credit-related events more than calls. As a matter of fact, Carr and Wu (2011) show that, under a general class of stock price dynamics, a portfolio of two deep out-of-the-money American-style equity put options can replicate a pure credit insurance contract that pays off if and only if the company defaults prior to the option expiry.

A preliminary test is conducted on the relationship between the two measures of impact of credit risk, either constructed using option quotes only (*AICR*) or based on the option prices and CDS spreads (*AICR'*). As these measures are option-specific, the daily average for the whole set of available call and put options is calculated each week ($\overline{AICR}$ and $\overline{AICR}'$ respectively). In order to estimate the risk-neutral probabilities from the CDSs, a 50% loss given default is assumed. A 50% recovery rate is consistent with the median value for senior unsecured bonds reported in Duffie and Singleton (1999). Other values of loss given default are investigated as a robustness test in the next section.

The following set of unbalanced panel pooled regressions are estimated

$$\overline{AICR}'_{j,t,\xi} = \alpha + \beta \overline{AICR}_{j,t,\xi} + \eta_{j,t,\xi}, \tag{1.18}$$

with $j \in J$, being J the set of 66 US companies, t the weekly observation, and ξ the binary variable that takes value $\xi = 1$ for calls and $\xi = -1$ for puts. Firstly, these regressions serve as a sanity check of the co-movements of the two measures of impact of credit risk. Secondly, the residuals $\eta_{j,t,\xi}$ summarise the pricing information carried by CDS in determining the *ICR*s which is not obtainable from option prices. Results are reported in Table 1.2. As expected, the two measures strongly co-move and the loading coefficients have the predicted sign.

The next step is assessing the different impact of credit risk on call and put options. Different measures of leverage (book leverage, market model-implied leverage obtained from the calibration on options only, market model-implied leverage using both options and CDSs) can be used as proxies of credit risk. These measures of leverage are then regressed onto $\overline{AICR}$ and $\overline{AICR}'$ of calls and puts for each set of weekly observations. By common sense and the model predictions, a higher leverage should induce a larger impact of credit risk on the company's securities. Put options are expected to show statistically significant positive

loadings. More specifically, panel regressions are implemented with year- and industry-fixed effects. These are

$$\overline{AICR}_{j,t,\xi} = \alpha_\xi + \mu_{i,\xi} + \theta_{y,\xi} + \beta LEV_{j,t} + \varepsilon_{j,t,i,y,\xi}$$
$$\overline{AICR}'_{j,t,\xi} = \alpha'_\xi + \mu'_{i,\xi} + \theta'_{y,\xi} + \beta' LEV_{j,t} + \varepsilon'_{j,t,i,y,\xi}. \tag{1.19}$$

Year-fixed effects ($\theta_{y,\xi}$ and $\theta'_{y,\xi}$, with $y = \{2013,\ldots,2017\}$) should capture the time-series variation in the volatility of the market, whilst the industry-fixed effects ($\mu_{i,\xi}$ and $\mu'_{i,\xi}$, with $i = \{$Financials; Mining, Energy and Utilities; Manufacturing; Retail, Wholesale and Services$\}$) account for possible cross-sectional heterogeneity due to the sector the company operates.

For the variable *LEV*, the market leverage defined as model-implied value of debt over market value of equity (dotted-dashed line in Figure 1.10) is used. More specifically, after estimating the asset volatility surface via a joint calibration on options and CDSs, the average value $\bar{\sigma}_V$ is used to compute the model implied asset value, that is the value of the firm such that (1.9) holds. Subsequently, the model implied market value of debt is obtained. Unreported results, available upon request, show that these findings are robust across other measures of leverage.

The results are reported in Table 1.3. Remarkably, despite the two measures of credit risk strongly co-move, in the case of call options, only $\overline{AICR}'$ – the measure obtained by adding the information carried by CDSs – is able to capture the credit risk of the company. Since the main effect of default on equity is to reduce its value by a sizable amount, it is understandable that credit risk has its minor impacts on these options. Therefore, the joint calibration on options and CDS carries extra information that, especially for call options, is relevant to capture default risk dynamics.

To stress this point further, the following regressions

$$\eta_{j,t,\xi} = \alpha_\xi + \mu_{i,\xi} + \theta_{y,\xi} + \beta LEV_{j,t} + \varepsilon_{j,t,i,y,\xi}, \tag{1.20}$$

are estimated. Here, the left-hand side is constituted by the residuals obtained from regression (1.18). These residuals indeed capture the extra information provided by the calibration on CDSs which is not accounted for by call options. As shown in Table 1.4, the residuals obtained from regression (1.19) when call options are used are still strongly correlated with leverage, even after having controlled for year-fixed and industry-fixed effects. Furthermore, the relatively high adjusted R^2 signals an undoubted explanatory power of leverage on those

Regressand				Adj–R^2:	0.8804
$\overline{AICR}'_1$					

Regressors	Coefficient	Robust Standard Error	t–stat	p–value	
$\overline{AICR}_1$	0.7813466	0.0053647	145.65	0.000	***
α_1	0.0015068	0.0000465	32.39	0.000	***

(a): $\overline{AICR}'$ regressed onto $\overline{AICR}$ (both constructed on calls).

Regressand				Adj–R^2:	0.5359
$\overline{AICR}'_{-1}$					

Regressors	Coefficient	Robust Standard Error	t–stat	p–value	
$\overline{AICR}_{-1}$	0.5577679	0.0362096	15.40	0.000	***
α_{-1}	0.0003161	0.0001010	3.13	0.002	***

(b): $\overline{AICR}'$ regressed onto $\overline{AICR}$ (both constructed on puts).

Table 1.2 Estimation of regression (1.18).
(a): Estimates of the pooled panel regression of average *AICR* obtained from call options ($\xi = 1$) and CDS regressed onto average *AICR* obtained from call options only. Number of observations: 15,470. F–stat: 21,212.88 (p–value: 0.0000).
(b): Estimates of the pooled panel regression of average *AICR* obtained from put options ($\xi = -1$) and CDS regressed onto average *AICR* obtained from put options only. Number of observations: 15,027. F–stat: 237.28 (p–value: 0.0000).
A sandwich estimator for panel data is used to obtain robust standard errors. Significance levels: 10% (*), 5% (**), 1% (***).

Regressand				Adj–R^2:	0.0336
$\overline{AICR}_1$					

Regressors	Coefficient	Robust Standard Error	t–stat	p–value	
LEV	0.0030977	0.0041647	0.74	0.511	
α_1	-0.000620	0.0024973	-0.25	0.820	
Industry-FE	✓				
Year-FE	✓				

(a): $\overline{AICR}$ (constructed on calls) regressed onto *LEV*.

Regressand				Adj–R^2:	0.1113
$\overline{AICR}'_1$					

Regressors	Coefficient	Robust Standard Error	t–stat	p–value	
LEV	0.0128021	0.0027542	4.65	0.019	**
α_1	-0.0020046	0.0014777	-1.36	0.268	
Industry-FE	✓				
Year-FE	✓				

(b): $\overline{AICR}'$ (constructed on calls and CDSs) regressed onto *LEV*.

Regressand				Adj–R^2:	0.4586
$\overline{AICR}_{-1}$					

Regressors	Coefficient	Robust Standard Error	t–stat	p–value	
LEV	0.0336547	0.0037234	9.04	0.003	***
α_{-1}	-0.0083151	0.0032709	-2.54	0.085	*
Industry-FE	✓				
Year-FE	✓				

(c): $\overline{AICR}$ (constructed on puts) regressed onto *LEV*.

Regressand				Adj–R^2:	0.5707
$\overline{AICR}'_{-1}$					

Regressors	Coefficient	Robust Standard Error	t–stat	p–value	
LEV	0.0290758	0.0095415	3.05	0.056	*
α_{-1}	-0.0085324	0.0078328	-1.09	0.356	
Industry-FE	✓				
Year-FE	✓				

(d): $\overline{AICR}'$ (constructed on puts and CDSs) regressed onto *LEV*.

Table 1.3 Estimation of regression (1.19)
(a): Estimates of the fixed-effects panel regression of market model-implied leverage *LEV* onto average *AICR* calculated over call options only. Number of observations: 15,470.
(b): Estimates of the fixed-effects panel regression of market model-implied leverage *LEV* onto average *AICR* calculated over call options and CDSs. Number of observations: 15,470.
(c): Estimates of the fixed-effects panel regression of market model-implied leverage *LEV* onto average *AICR* calculated over put options only. Number of observations: 15,027.
(d): Estimates of the fixed-effects panel regression of market model-implied leverage *LEV* onto average *AICR* calculated based on put options and CDSs. Number of observations: 15,027.
Standard errors are adjusted for four clusters based on industry. Significance levels: 10% (*), 5% (**), 1% (***).

residuals. Therefore, I conclude that CDS quotes carry extra information regarding the credit risk of the companies when compared with pricing information embedded in call options. The same conclusion does not hold for equity put options which share most of the pricing information in terms of default with the CDS written on the same reference entity.

1.4.3 Sub-samples analysis

In order to investigate further the link between options and credit risk, the same regressions in (1.19) are re-estimated over the four sub-samples based on industry (therefore, the industry-fixed effect is removed, whilst the year-fixed effect is kept). Based on the findings in Carr and Wu (2017), a cross-sectional diversity should emerge. Only put options are taken into consideration as the impact of default risk on call options was shown to be insignificant. Results are reported in Table 1.5.

As manufacturing companies usually invest in long-term assets, they tend to have the same debt for a long period of time, without actively rebalancing their capital structure. Therefore, their financial leverage varies passively with the stock price fluctuations. Also, in addition to having a relatively small average $\overline{AICR}'_{-1}$ (see Table 1.6), they also have the smallest mean leverage across the categories. This is reflected into the results of the regression: default does not play a major role in affecting the price of put options, displaying a relatively low adjusted R^2.

On the other hand, financial firms tend to actively manage their capital structures according to changes in market conditions and, for banks, to satisfy regulatory requirements. The results indeed capture the impact of credit risk to be driven by financial leverage (highest adjusted R^2 and significance). The same conclusion applies to companies operating in sales and services, despite to a mush weaker extent: given an average leverage comparable to manufacturing companies, they also show relatively small $\overline{AICR}'_{-1}$. The regression adjusted R^2 is just a third of that obtained from financial companies. Similarly, put prices of utility and energy companies seem to be influenced by credit risk as well. Operating in regulated businesses and being strongly influenced by systemic factors as the state of the economy, perhaps the regression fit could be enhanced accounting for macroeconomic factors.

Unreported results available upon request show that these findings across the four sub-samples still hold after having accounted for a firm-fixed effect.

Regressand					Adj–R^2:	0.6001
η_1						

Regressors	Coefficient	Robust Standard Error	t–stat	p–value	
LEV	0.0103818	0.0021359	4.86	0.017	**
α_1	-0.003027	0.0015659	-1.93	0.149	
Industry-FE	✓				
Year-FE	✓				

(a): Extra-information provided by CDSs when calls are used to infer credit risk.

Regressand					Adj–R^2:	0.1503
η_{-1}						

Regressors	Coefficient	Robust Standard Error	t–stat	p–value
LEV	0.0103043	0.0076949	1.34	0.273
α_{-1}	-0.0042105	0.0063554	-0.66	0.555
Industry-FE	✓			
Year-FE	✓			

(b): Extra-information provided by CDSs when puts are used to infer credit risk.

Table 1.4 Estimation of regression (1.20)
(a): Estimates of the fixed-effects panel regression of market model-implied leverage *LEV* onto the residuals obtain from regression (1.18) (calls). Number of observations: 15,470.
(b): Estimates of the fixed-effects panel regression of market model-implied leverage *LEV* onto the residuals obtain from regression (1.18) (puts). Number of observations: 15,027.
Standard errors are adjusted for four clusters based on industry. Significance levels: 10% (*), 5% (**), 1% (***).

Regressand				Adj–R^2:	0.6608
$\overline{AICR}'_{-1}$					

Regressors	Coefficient	Robust Standard Error	t–stat	p–value	
LEV	0.0391051	0.0012387	31.57	0.000	***
α_{-1}	-0.0145449	0.0011321	-12.85	0.000	***
Year-FE	✓				

(a): Financials

Regressand				Adj–R^2:	0.2128
$\overline{AICR}'_{-1}$					

Regressors	Coefficient	Robust Standard Error	t–stat	p–value	
LEV	0.0069186	0.0004261	16.24	0.000	***
α_{-1}	-0.0007640	0.0001489	-5.13	0.000	***
Year-FE	✓				

(b): Mining, Energy and Utilities

Regressand				Adj–R^2:	0.1173
$\overline{AICR}'_{-1}$					

Regressors	Coefficient	Robust Standard Error	t–stat	p–value	
LEV	0.0014455	0.0000861	16.78	0.000	***
α_{-1}	-0.0000211	0.0000163	-1.29	0.197	
Year-FE	✓				

(c): Manufacturing

Regressand				Adj–R^2:	0.2450
$\overline{AICR}'_{-1}$					

Regressors	Coefficient	Robust Standard Error	t–stat	p–value	
LEV	0.0075047	0.0009004	8.34	0.000	***
α_{-1}	-0.0007342	0.0001427	-5.14	0.000	***
Year-FE	✓				

(d): Retail, Wholesale and Services

Table 1.5 Estimation of regression (1.19) over the four sub-samples.
(a): Estimates of the year-fixed effect panel regression of market model-implied leverage LEV onto average $AICR$ calculated over put options and CDSs of Financials. Number of observations: 1,938. F–stat = 199.90 (p–value = 0.000).
(b): Estimates of the year-fixed effect panel regression of market model-implied leverage LEV onto average $AICR$ calculated over put options and CDSs of Mining, Energy and Utilities. Number of observations: 1,916. F–stat = 73.60 (p–value = 0.000).
(c): Estimates of the year-fixed effect panel regression of market model-implied leverage LEV onto average $AICR$ calculated over put options and CDSs of Manufacturing. Number of observations: 6,515. F–stat = 80.21 (p–value = 0.000).
(d): Estimates of the year-fixed effect panel regression of market model-implied leverage LEV onto average $AICR$ calculated over put options and CDSs of Retail, Wholesale and Services. Number of observations: 4,658. F–stat = 20.63 (p–value = 0.000).
A sandwich estimator for panel data is used to obtain robust standard errors. Significance levels: 10% (*), 5% (**), 1% (***).

	Financials	Energy and Utilities	Manufacturing	Sales and Services
$\overline{LEV}$	0.9090	0.3791	0.1853	0.1905
$\overline{\overline{AICR}}'_{-1}$	0.0148	0.0023	0.0003	0.0007

Table 1.6 Sub-sample averages for leverage and $\overline{AICR}$ obtained from put options and CDSs.

1.4.4 Explaining the Skew

Many attempts have been made in the literature in order to explain the shapes of the implied volatilities obtained from options. It is well-known that inverting the Black-Scholes formula to determine the value of the volatility which matches the observed price produces the so called volatility smile or smirk, instead of a flat line (which would be expected if the Black-Scholes model were correct). It is also well-documented that equity volatilities display more often a smirk, that is the volatility is a decreasing and convex function of the moneyness of the option. The negative slope of the implied volatility function is referred to as negative skew.

The first works attempting to give a explanation for the observed skew are Black (1976) and Christie (1982). Both attribute the negative slope to the possibility of the underlying to default, the so-called leverage effect: if the underlying of the option can default, the left tail of its distribution should be more sensitive to credit-related events which notoriously make the value of the firm's equity significantly drop. This increased probability of the underlying falling due to default would be then reflected in the pricing of options. Also, as put options protects the buyer against price falling, they should price both market and credit related events. As shown in Section 1.4.2, put options indeed price credit risk (and doubtlessly price market risk). However, some more recent works shed light on the drivers of the volatility skew.

Carr and Wu (2017) show that the leverage effect can be generated by other sources than leverage. As a matter of fact, the skew is also displayed by other assets, such as commodities or indexes, which cannot default. In their work, they individuate three possible channels influencing volatility: (1) return volatility increases with financial leverage; (2) positive shocks to systematic risk generate a negative correlation between the market's return and its volatility, regardless of the magnitude of financial leverage; (3) large negative market disruptions show self-exciting behaviours.

Their estimations show that the volatility feedback effect (2) reveals itself mainly in the variations of short-term options, the self-exciting behaviour (3) affects both short-term

and long-term option variations, and the financial leverage variation (1) has its largest impact on long-dated options. Finally, when the model of Carr and Wu (2017) is applied to individual companies, the three economic channels show up differently and to different degrees according to the company's specific business and capital structure. Therefore, their work constitutes a valuable ruler in order to asses my model's predictions and results.

From a different perspective, the shape of the volatility smile/smirk provides an insight on how the Black-Scholes model prices risk under the presence of both market and credit risk, and how the estimation of the implied volatility is affected by them. Figure 1.11 suggests that the Black-Scholes implied volatility is an average of the implied volatility estimated with a compound option model (which, instead, allows to account for the relative impact of credit and market risk separately).

Evidently, the Black-Scholes averages across the surface the impact of credit risk. Let $\mu \in \{\mathbb{M}, \mathbb{Q}\}$. Analytically, the probabilities involved into the calculation of the option price à la Black-Scholes[13] are such as

$$\mu \left(\xi S_T > \xi K \right)$$

whilst those of the compound option model are of the type

$$\mu \left(\xi S_T > \xi K | \tau > t_i \right).$$

By the law of total probability

$$\mu \left(\xi S_T > \xi K \right) = \mathbb{E}^{\mu} \left[\mu \left(\xi S_T > \xi K | \tau > t_i \right) \right],$$

thus showing that the probabilities involved in the Black-Scholes model are an average of the probability of the option expiring in-the-money conditional on the firm surviving at the reimbursement dates. Therefore, the volatility smirk produced by Black-Scholes should lie within the implied volatilities produced by the model. Figure 1.11 confirms it.

Inspecting Figure 1.11 , this averaging effect impacts mostly long-maturity options as the underlying probability of defaulting increases with the time horizon. Interestingly, for financial companies, despite displaying a negative slope for both short and long-term maturity options, the skew is more likely to be associated with the leverage effect for long-maturity options only (panel (b)). As a matter of fact, the compound option implied volatilities of the

---

[13]In the case of Black-Scholes, the probability measure $\mathbb{M}$ is intended as the stock-fund measure, that is $\Phi(\xi d_1)$.

short-term maturity options of financial companies (panel (a)) replicate almost perfectly the Black-Scholes implied volatility which does not accommodate for default risk explicitly.

More generally, the closer the two equity volatility estimates are, the lower the probability of default and therefore the impact of credit risk (i.e. leverage effect) on the pricing of the option. Notice also that, if $\sum_i F_i \downarrow 0$, the compound option model coincides with Black and Scholes (1973). Therefore, the larger the firm's financial leverage the farther the Black-Scholes implied volatilities surface should be with respect to those estimated via the compound option model. However, if the two models reproduce very similar volatility skews even when the company is highly levered (e.g. financials), it can be argued that 'apparent' leverage effect is not driven by leverage and, therefore, financial leverage is not a good proxy for default risk, at least in the short-term. This is exactly what Carr and Wu (2017) document.

Moreover, having defined the equity as a compound call options allows to further motivate why the skew is observed over the region constructed using put options. It is well-known that the price of a call option is an increasing function of the volatility of its underlying; similarly, it can be shown that the price of a compound call on call option is also an increasing function of the volatility. By induction, it can be shown that also the price of a *n*-fold compound call option is increasing of the underlying volatility.

Under Black and Scholes (1973), the Vega of a put option is an increasing function of the volatility of the underlying equity. However, as equity is itself a compound call option, an increase in the asset volatility causes an increase in the value of the equity which ultimately makes the put options less likely to expire in-the-money. Therefore, the Vega of in-the-money put options under the compound option model is negative. Figure 1.12 illustrates this aspect[14].

So far the volatility skew was only described as the negative slope displayed by the graph of the implied volatility plotted against moneyness. Following Carr and Wu (2017), the volatility skew is formally defined as

$$\text{Skew} = \frac{25\Delta\text{Put}\sigma_{IV} - 25\Delta\text{Call}\sigma_{IV}}{50\Delta\text{Put}\sigma_{IV}}, \tag{1.21}$$

---

[14]Figure 1.12 clearly shows $\partial\gamma^{CO}_{-1}/\partial\sigma_V < 0$, for $S_t < K$. Therefore

$$\frac{\partial\gamma^{CO}_{-1}}{\partial\sigma_V} = \frac{\partial\gamma^{CO}_{-1}}{\partial\sigma_S}\frac{\partial\sigma_S}{\partial\sigma_V}$$

implies $\partial\gamma^{CO}_{-1}/\partial\sigma_S < 0$, as $\partial\sigma_S/\partial\sigma_V > 0$ (see Figure 1.5 panel(d)).

(a) $T < 1$ (b) $T > 1$

(c) $T < 1$ (d) $T > 1$

(e) $T < 1$ (f) $T > 1$

(g) $T < 1$ (h) $T > 1$
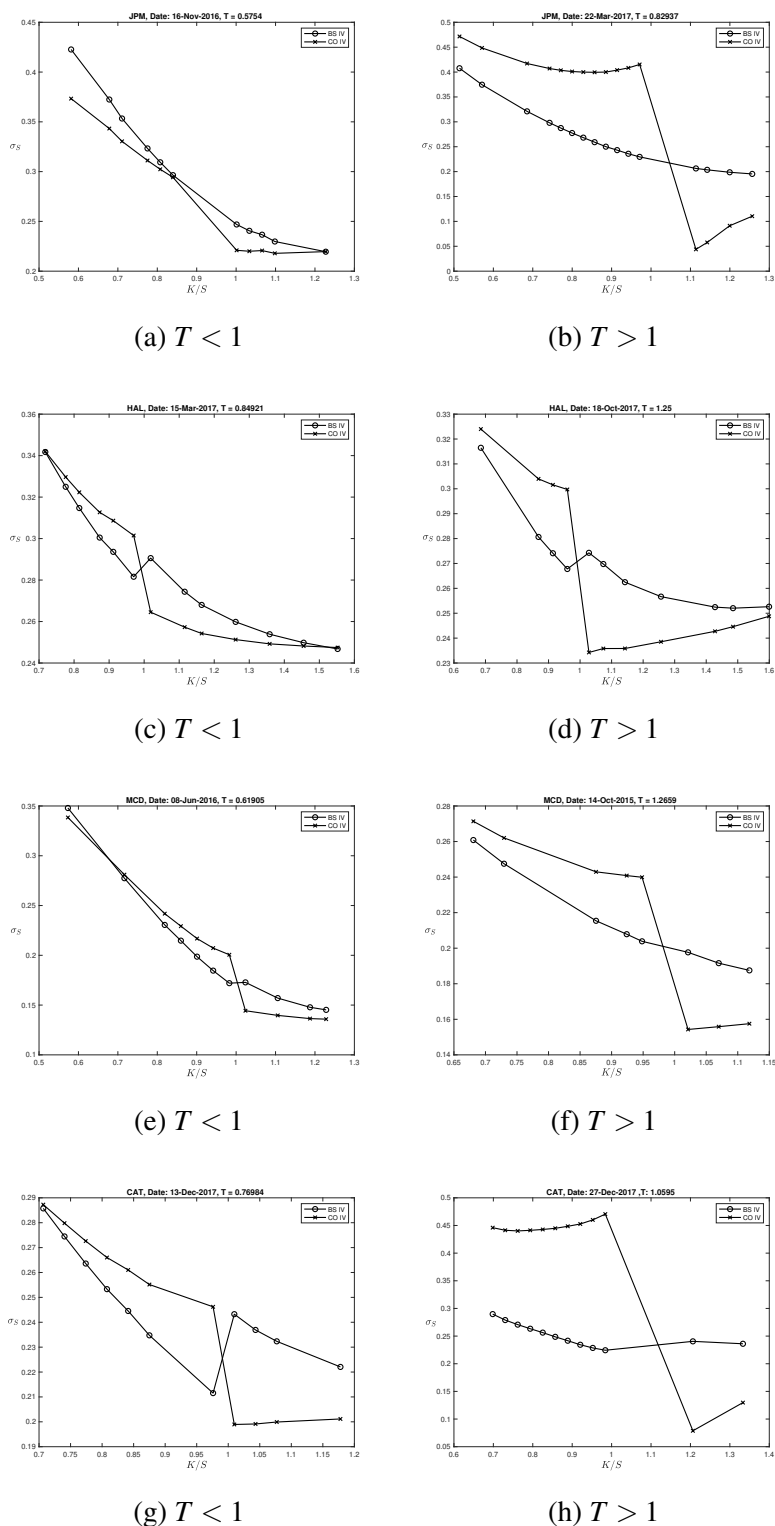
Fig. 1.11 Volatility skews for different option maturities. The lines marked with circles are the implied volatility estimates produced by the Black-Scholes model, whilst those marked with crosses are the estimates produced by the compound option model. It is evident that the Black-Scholes estimates of the implied volatility lie within the estimates produced by the model, thus suggesting the aforementioned averaging effect. This effect is more pronounced for long-term maturity options (panels (b), (d), (f), (h)) than for options with shorter maturities (panels (a), (c), (e), (g)), as the distance between the two lines is larger for $T > 1$.
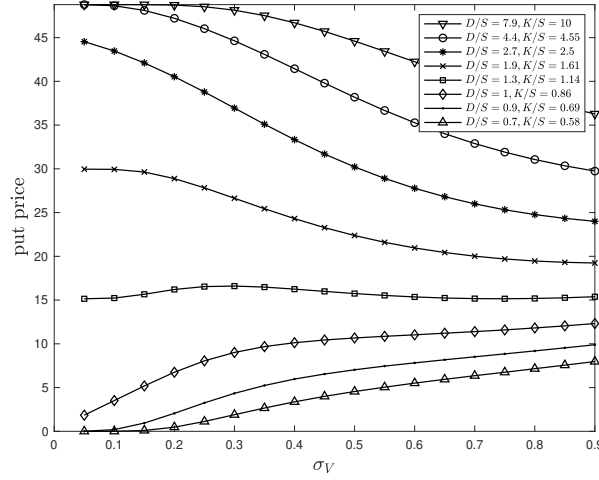
Fig. 1.12 Put price as function of asset volatility. Conversely to Black-Scholes put price, the price of compound put option on a call can be a decreasing function of the volatility. This is observed when the put option is deep into-the-money, that is when price of equity is approaching zero (therefore, default becomes more likely). Here $K = 50$, $T = 0.5$, $F_1 = F_2 = F_3 = 30$, $t_1 = 1$, $t_2 = 5$, $t_3 = 10$, $r = 0.03$ and $\varpi = 0.05$.

where $x\Delta\text{Put}\sigma_{IV}$ is the implied volatility of the put option whose delta is $-x\%$, and $y\Delta\text{Call}\sigma_{IV}$ is the implied volatility of the call with delta equal to $y\%$. The proposed measure of skewness is more positive when the risk-neutral return distribution is more negatively skewed (if the implied volatility is downward sloping, the numerator of (1.21) is positive).

In order to investigate to what extent the displayed skew is driven by leverage, the following panel regression are carried out

$$\Delta\text{Skew}_{j,t,T} = \alpha_T + \phi_{j,T} + \theta_{y,T} + \beta\overline{AICR}_{j,t-1,-1,T} + \varepsilon_{j,t,y,T}, \tag{1.22}$$

where $\overline{AICR}_{j,t-1,T,-1}$ is the average *AICR* of put options having time to maturity equal to T observed in the previous week. Rather than using industry-fixed effect, a firm-fixed effect (ϕ_j) is estimated as, ultimately, I want to show the ability of this measure to forecast future changes in the skew observed at the company level. If the skew is caused by the leverage effect, a positive and statistically significant effect should be observed.

The variable ΔSkew is calculated based on (1.21). Call options are excluded, given the results in Section 1.4.2. Also, ΔSkew is used rather than the contemporaneous level as the time-series component of the latter is non-stationary for some companies (see Figure 1.13).

In particular, based on the previous findings, two sets of regression are estimated. As for every day t, multiple maturities are observed, the skew of the shortest ($\min_T : T < 1$ year) and longest ($\max_T : T > 1$ year) maturity options is used in two separate sets of regressions.

42

(a) $T < 1$ (b) $T > 1$
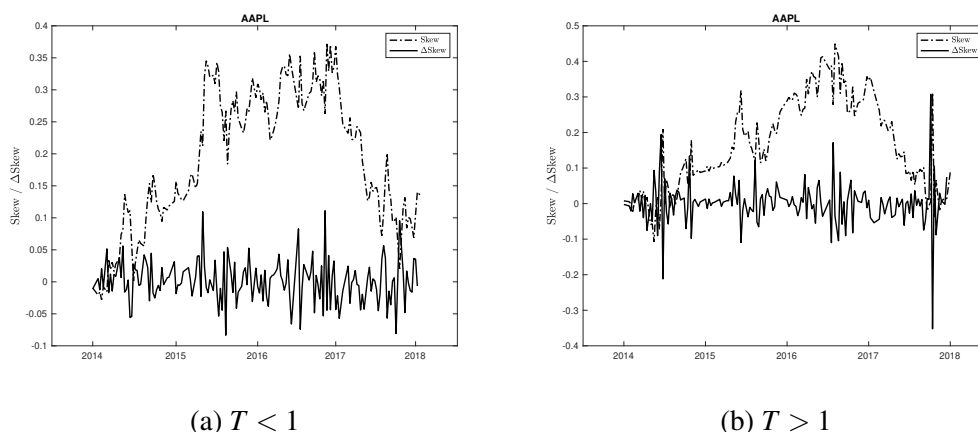
Fig. 1.13 Time-series of Skew extracted from short-term maturity options ($T < 1$, panel (a)) and from long-term maturity options ($T > 1$, panel (b)) for AAPL. Both panels show that the time series of the levels of Skew (dotted-dashed line) is non-stationary whilst the increments (solid line) are stationary.

Based on the different behaviour of the model for short and long term maturity options, the skew should be driven by credit risk (here proxied as the $\overline{ICR}$ of out-of-the-money put options) mostly for $T > 1$ rather than for $T < 1$.

The estimates are presented in Table 1.7. Consistently with economic intuition and the empirical evidence in Carr and Wu (2011) and Carr and Wu (2017), only the changes in the skew of long-maturity options are driven by the credit risk of the company. Also, the average *AICR* of put options, is able, to some extent, to predict the future changes in the skew for those options. The same variable is not able to explain the movements of the skew for options with shorter maturities. Therefore, the high significance of the average *AICR* obtained from put options, as well as the correct sign of its loading, points towards a connections between the future changes of the negative skew and the today's credit risk of the company. However, the low fit can be attributed either to the presence of other factors driving the skew or to the highly non-linear link between the movements of the skew and the impact of credit risk (or both).

In the same spirit of the tests conducted in the previous section, the sample is further split accordingly to industry classification and the regressions in (1.22) are re-estimated. As there is no effect for short-maturity options, only long dated options are taken into consideration. Results are reported in Table 1.8.

The four sets of regressions show industry differences in the ability of the measure of credit risk to predict future changes in the option skew. Mirroring the results of previous sections, a larger predictive power is associated with companies which are sensibly levered

Regressand				R^2 (between):	0.0030
$\Delta\text{Skew}_{T<1}$				R^2 (within):	0.0007

Regressors	Coefficient	Robust Standard Error	t–stat	p–value	
$\overline{AICR}'_{-1,T<1}$	0.9772085	0.714567	1.37	0.176	
$\alpha_{T<1}$	-0.0037777	0.0009448	-4.00	0.000	***
firm-FE	✓				
year-FE	✓				

(a): Predictive regression for short-term skew.

Regressand				R^2 (between):	0.1958
$\Delta\text{Skew}_{T>1}$				R^2 (within):	0.0005

Regressors	Coefficient	Robust Standard Error	t–stat	p–value	
$\overline{AICR}'_{-1,T>1}$	0.353236	0.0784575	4.50	0.000	***
$\alpha_{T>1}$	-0.0114802	0.0017093	-6.72	0.000	***
firm-FE	✓				
year-FE	✓				

(b): Predictive regression for long-term skew.

Table 1.7 Estimation of regression (1.22).
(a): Predictive regression for short-term skew based on the average *ICR* calculated over short-term put options and CDSs. Number of observations: 7,656. F–stat = 10.35 (p–value = 0.000).
(b): Predictive regression for long-term skew based on the average *ICR* calculated over long-term put options and CDSs. Number of observations: 6,818. F–stat = 11.87 (p–value = 0.000).
A sandwich estimator for panel data is used to obtain robust standard errors. Significance levels: 10% (*), 5% (**), 1% (***).

Regressand				R^2 (between):	0.0816
$\Delta\text{Skew}_{T>1}$				R^2 (within):	0.0022

Regressors	Coefficient	Robust Standard Error	t–stat	p–value	
$\overline{AICR}'_{-1,T>1}$	0.3942216	0.1693359	2.33	0.048	**
$\alpha_{T>1}$	-0.0140584	0.0116132	-1.21	0.268	
firm-FE	✓				
year-FE	✓				

(a): Financials.

Regressand				R^2 (between):	0.1803
$\Delta\text{Skew}_{T>1}$				R^2 (within):	0.0017

Regressors	Coefficient	Robust Standard Error	t–stat	p–value	
$\overline{AICR}'_{-1,T>1}$	0.2832847	0.0658556	4.30	0.004	***
$\alpha_{T>1}$	-0.0194797	0.002694	-7.23	0.000	***
firm-FE	✓				
year-FE	✓				

(b): Mining, Energy and Utilities.

Regressand				R^2 (between):	0.1266
$\Delta\text{Skew}_{T>1}$				R^2 (within):	0.0006

Regressors	Coefficient	Robust Standard Error	t–stat	p–value	
$\overline{AICR}'_{-1,T>1}$	-2.931313	2.452305	-1.20	0.247	
$\alpha_{T>1}$	-0.0078513	0.0021041	-3.73	0.001	***
firm-FE	✓				
year-FE	✓				

(c): Manufacturing.

Regressand				R^2 (between):	0.9001
$\Delta\text{Skew}_{T>1}$				R^2 (within):	0.0007

Regressors	Coefficient	Robust Standard Error	t–stat	p–value	
$\overline{AICR}'_{-1,T>1}$	0.4410598	0.0564674	7.81	0.000	***
$\alpha_{T>1}$	-0.0105209	0.0026711	-3.94	0.001	***
firm-FE	✓				
year-FE	✓				

(d): Retail, Wholesale and Services.

Table 1.8 Estimation of regression (1.22) over the four sub-samples.
(a): Predictive regression for short-term skew based on the average *ICR* calculated over long-term put options and CDSs of Financials. Number of observations: 810. F–stat = 5.18 (p–value = 0.021).
(b): Predictive regression for short-term skew based on the average *ICR* calculated over long-term put options and CDSs of Mining, Energy and Utilities. Number of observations: 791. F–stat = 32.75 (p–value = 0.000).
(c): Table 5b: Predictive regression for short-term skew based on the average *ICR* calculated over long-term put options and CDSs of Manufacturing. Number of observations: 2,305 F–stat = 4.02 (p–value = 0.012).
(d): Predictive regression for short-term skew based on the average *ICR* calculated over long-term put options and CDSs of Retail, Wholesale and Services. Number of observations: 2,912 F–stat = 38.71 (p–value = 0.000).
A sandwich estimator for panel data is used to obtain robust standard errors. Significance levels: 10% (*), 5% (**), 1% (***).

(see Table 1.8, panels (a) and (b)). Despite the average lower leverage, also the changes in the skew of retail, wholesale and services companies is partially attributable to the credit risk of the companies. On the other hand, the future changes in the negative skew of manufacturing companies (which are the least levered in the sample, see Table 1.6) are not explained by the level of credit risk and is likely to be driven by other factors. Finally, the weaker predictive power of this measure for financial companies could be explained by their relatively large probability of survival (despite being highly levered). This would mirror the graphical evidence of the implied volatility of the compound option model being very close to the implied volatility of the Black-Scholes model.

1.4.5 Robustness Tests

I first focus on how the compound option pricing model (*CO*) performs out-of-sample compared to the Black-Scholes model (*BS*). Given the option dataset, the volatility surface of equity (for *BS*) and asset (for *CO*) is estimated every week (in-sample). These estimates are used to reprice the options traded the following week (out-of-sample). Then, the pricing error is assessed as the absolute percentage error with respect to the market price, that is $|P^{market} - P^{model}|/P^{market}$. The compound option model is implemented both using stock and option price only, as well as with the triangulation stock-option-CDS, having assumed LGD = $\{50, 60, 80\}\%$. In addition to 50% assumed so far in the analysis, the loss given default parameter is also set to 60% and 80%, being these values explicitly suggested by the ISDA for the pricing of CDSs[15]. Results are reported in Tables 1.9 and 1.10.

I find that, in general, the Black-Scholes performs better out-of-sample than any compound option model, both for call and put options. The average pricing error for put options is though substantially lower than for call options, again pointing towards negligible sensitivity of the latter with respect to credit events.

More specifically, the pricing error are analysed across the leverage, time-to-maturity and moneyness dimension. The errors produced by the *CO* models are comparable in size with those of *BS* for moderately levered firms ($D/S \in (0, 0.5]$); however these tend to increase with leverage. Only for highly levered firms ($D/S \in (2, \infty)$), the pricing errors consistently reduce for both call and put options. Both the *BS* and the *CO* models show increasing pricing errors for options with longer maturities as well as for deep out-of-the-money options.

---

[15]Visit https://www.cdsmodel.com/cdsmodel/assets/cds-model/docs for the document ISDA Standard CDS Contract Converter Specification - Sept 4, 2009.pdf. A market-wide loss given default of 60% is also used by Collin-Dufresne et al. (2010).

				$LEV \in (0, 0.5]$				
T	K/S	BS	CO	CO50	CO60	CO80	N	m_C
$[0.5, 1)$	$(1, m_C)$	0.06	0.08	0.15	0.14	0.12	43,598	1.09
	$[m_C, \infty)$	0.11	0.12	0.21	0.19	0.17		
$[1, 1.5)$	$(1, m_C)$	0.05	0.10	0.13	0.13	0.11	16,634	1.12
	$[m_C, \infty)$	0.09	0.12	0.15	0.15	0.12		
$[1.5, 2)$	$(1, m_C)$	0.06	0.12	0.15	0.15	0.13	8,963	1.12
	$[m_C, \infty)$	0.10	0.12	0.15	0.15	0.13		
$[2, \infty)$	$(1, m_C)$	0.06	0.11	0.13	0.12	0.11	2,529	1.12
	$[m_C, \infty)$	0.10	0.13	0.12	0.13	0.11		

				$LEV \in (0.5, 1]$				
T	K/S	BS	CO	CO50	CO60	CO80	N	m_C
$[0.5, 1)$	$(1, m_C)$	0.08	0.14	0.69	0.57	0.49	4,239	1.08
	$[m_C, \infty)$	0.14	0.22	1.00	0.76	0.63		
$[1, 1.5)$	$(1, m_C)$	0.06	0.19	0.80	0.71	0.62	1,061	1.11
	$[m_C, \infty)$	0.14	0.32	0.94	0.78	0.65		
$[1.5, 2)$	$(1, m_C)$	0.08	0.31	0.79	0.72	0.64	653	1.11
	$[m_C, \infty)$	0.16	0.31	0.79	0.67	0.56		
$[2, \infty)$	$(1, m_C)$	0.10	0.24	0.67	0.61	0.52	225	1.09
	$[m_C, \infty)$	0.18	0.32	0.66	0.64	0.48		

				$LEV \in (1, 2]$				
T	K/S	BS	CO	CO50	CO60	CO80	N	m_C
$[0.5, 1)$	$(1, m_C)$	0.06	0.24	0.93	0.58	0.68	4,017	1.09
	$[m_C, \infty)$	0.13	0.49	1.81	0.82	1.18		
$[1, 1.5)$	$(1, m_C)$	0.06	0.33	1.06	0.95	0.84	226	1.16
	$[m_C, \infty)$	0.19	0.72	1.89	1.68	1.25		
$[1.5, 2)$	$(1, m_C)$	0.10	0.32	0.92	0.87	0.71	119	1.16
	$[m_C, \infty)$	0.20	0.55	1.38	1.01	0.97		
$[2, \infty)$	$(1, m_C)$	0.03	0.28	0.80	0.74	0.61	53	1.12
	$[m_C, \infty)$	0.12	0.35	0.85	0.78	0.63		

				$LEV \in (2, \infty)$				
T	K/S	BS	CO	CO50	CO60	CO80	N	m_C
$[0.5, 1)$	$(1, m_C)$	0.06	0.18	1.29	0.93	0.98	1,038	1.12
	$[m_C, \infty)$	0.15	0.47	2.47	1.21	1.70		
$[1, 1.5)$	$(1, m_C)$	0.34	8.38	7.32	12.76	15.58	14	1.36
	$[m_C, \infty)$	0.55	19.88	34.61	37.47	35.34		
$[1.5, 2)$	$(1, m_C)$	0.16	1.57	3.78	3.69	3.54	7	1.37
	$[m_C, \infty)$	0.40	5.98	8.93	9.05	9.05		
$[2, \infty)$	$(1, m_C)$	-	-	-	-	-	1	1.35
	$[m_C, \infty)$	0.59	7.39	16.26	17.04	17.43		

Table 1.9 Out-of-sample average absolute percentage pricing error using the Black-Scholes model versus a compound option model for call options. The compound option model is either implemented via the joint calibration stock and option price or via the triangulation stock-option-CDS spreads (having assumed LGD = $\{50, 60, 80\}\%$.) The errors are clustered based on progressively more leveraged firms ($LEV \equiv D/S$). Then, the errors are analysed based on the time-to-maturity (T) and the moneyness (K/S). The moneyness dimension is further split into OTM, $K/S \in (1, m_C)$, and deep OTM, $K/S \in [m_C, \infty)$, where m_C is the median moneyness in each cluster. N is the number of prices in each bucket. Both the Black-Scholes and the compound option pricing errors increases with T and as the option becomes more and more OTM. The pricing error of the simple compound option (CO) generally increases with leverage.

$LEV \in (0, 0.5]$

T	K/S	BS	CO	CO50	CO60	CO80	N	m_P
[0.5,1)	$[m_P,1)$	0.05	0.08	0.11	0.10	0.09	51,519	0.86
	$(0,m_P)$	0.10	0.12	0.16	0.15	0.13		
[1,1.5)	$[m_P,1)$	0.04	0.09	0.11	0.11	0.09	20,469	0.83
	$(0,m_P)$	0.08	0.11	0.13	0.13	0.11		
[1.5,2)	$[m_P,1)$	0.04	0.11	0.12	0.12	0.10	12,042	0.81
	$(0,m_P)$	0.10	0.13	0.13	0.14	0.11		
[2,∞)	$[m_P,1)$	0.06	0.14	0.13	0.14	0.13	3,554	0.79
	$(0,m_P)$	0.15	0.18	0.18	0.19	0.17		

$LEV \in (0.5, 1]$

T	K/S	BS	CO	CO50	CO60	CO80	N	m_P
[0.5,1)	$[m_P,1)$	0.05	0.12	0.41	0.41	0.28	5,373	0.88
	$(0,m_P)$	0.10	0.20	0.49	0.49	0.34		
[1,1.5)	$[m_P,1)$	0.04	0.36	0.32	0.42	0.23	1,928	0.85
	$(0,m_P)$	0.10	0.39	0.37	0.51	0.27		
[1.5,2)	$[m_P,1)$	0.05	0.36	0.33	0.42	0.26	1,280	0.83
	$(0,m_P)$	0.10	0.36	0.34	0.49	0.26		
[2,∞)	$[m_P,1)$	0.06	0.45	0.29	0.39	0.23	438	0.82
	$(0,m_P)$	0.13	0.80	0.36	0.56	0.29		

$LEV \in (1, 2]$

T	K/S	BS	CO	CO50	CO60	CO80	N	m_P
[0.5,1)	$[m_P,1)$	0.06	0.18	0.49	0.57	0.38	2,532	0.81
	$(0,m_P)$	0.20	0.44	0.68	0.73	0.60		
[1,1.5)	$[m_P,1)$	0.04	0.09	0.35	0.32	0.27	1,010	0.83
	$(0,m_P)$	0.08	0.13	0.44	0.39	0.37		
[1.5,2)	$[m_P,1)$	0.05	0.09	0.42	0.44	0.43	846	0.80
	$(0,m_P)$	0.11	0.16	0.41	0.39	0.38		
[2,∞)	$[m_P,1)$	0.05	0.43	0.29	0.56	0.21	213	0.80
	$(0,m_P)$	0.15	0.74	0.34	0.66	0.36		

$LEV \in (2, \infty]$

T	K/S	BS	CO	CO50	CO60	CO80	N	m_P
[0.5,1)	$[m_P,1)$	0.05	0.08	0.85	0.94	0.95	117	0.68
	$(0,m_P)$	0.45	0.57	2.34	1.48	1.63		
[1,1.5)	$[m_P,1)$	0.04	0.06	0.56	0.56	0.60	221	0.83
	$(0,m_P)$	0.07	0.09	0.55	0.61	0.68		
[1.5,2)	$[m_P,1)$	0.05	0.05	0.41	0.42	0.54	188	0.83
	$(0,m_P)$	0.08	0.09	0.43	0.42	0.54		
[2,∞)	$[m_P,1)$	0.06	0.50	0.87	0.88	0.99	44	0.81
	$(0,m_P)$	0.14	0.57	1.05	1.01	1.15		

Table 1.10 Out-of-sample average absolute percentage pricing error using the Black-Scholes model versus a compound option model for put options. The compound option model is either implemented via the joint calibration stock and option price or via the triangulation stock-option-CDS spreads (having assumed LGD = $\{50, 60, 80\}$%.) The errors are clustered based on progressively more leveraged firms ($LEV \equiv D/S$). Then, the errors are analysed based on the time-to-maturity (T) and the moneyness (K/S). The moneyness dimension is further split into OTM, $K/S \in [m_P, 1)$, and deep OTM, $K/S \in (0, m_P)$, where m_P is the median moneyness in each cluster. N is the number of prices in each bucket. Both the Black-Scholes and the compound option pricing errors increases with T and as the option becomes more and more OTM. The pricing error of the simple compound option (CO) generally increases with leverage.

The only available reference to compare the out-of-sample analysis with is Geske et al. (2016). There, the authors implement the Geske (1979) model and compare how a compound option model performs with respect to the Black-Scholes model. My results are in sharp contrast with their findings. On average, I obtain smaller pricing errors for the Black-Scholes than in the case of the compound option model (for those instances in which the samples are comparable). They document the opposite. Even more surprisingly, my errors (both for the *BS* and the *CO*) are significantly smaller than what they report. However, several differences in the approach proposed here are worth mentioning.

Firstly, their sample is formed by American call options only, with at most one year to maturity. I instead focus on both American call and put options with maturity at least equal to six months. Further, they model equity as a 1–fold compound option as they assume that the firms have issued a zero-coupon bond with maturity equal to the duration of the firm's debt. As shown in Section 1.2.1, Figure 1.6, when debt is clustered at one future date only, it would be optimal for shareholders to take on as much debt as possible as the positive sensitivity of equity with respect to business risk increases with leverage. This does not happens in a 3–fold compound option model for equity. Also, their definition of firm debt is much broader than the one used here (as instance, they also include accrued expense and deferred income as well as deferred federal tax in their definition of debt).

Secondly, their calibration methodology is different as they estimate a term structure of asset volatility (embedded in their model) using the three most at-the-money call options and the stock price. In fact, they opt for having two different parameters for the volatility of the assets, one for the duration of the firm's debt and one for the maturity of the option. In order to make a more appropriate comparison with the Black-Scholes model, I instead estimate the asset volatility surface by 'inverting' the compound option pricing model in order to match both the option and stock price (that is, in the same spirit the equity implied volatility is extracted à la Black-Scholes). Also, my estimates are based on both out-of-the-money call and put options.

Finally, they need to have four equations to calibrate the compound option model as they opt for embedding a term structure of the asset volatility within their model. If, instead, the volatility is assumed constant as in a geometric Brownian motion, the implied default barrier (and the implied strike price in the asset space) are implicit functions of the (unique) asset volatility (see Appendix E), which can be retrieved using two equations only, namely (1.9) and (1.13). Also, they do not obtain pseudo-European option prices but consider only those options which, retrospectively, did not pay dividends between the valuation day and the maturity of the option. This information, however, is not usually available when the market

participants trade options. Therefore, the proposed approach seems more parsimonious and makes the comparison with the Black-Scholes model more straightforward.

A second robustness test is based on the comparison of the estimated option-implied asset volatility obtained with and without the additional calibration on the risk-neutral probabilities of default extracted from CDS spreads. Then, the absolute percentage errors $|\sigma_V - \sigma_V'|/\sigma_V$ are computed, where σ_V' and σ_V are the implied asset volatility obtained with and without the CDS calibration for the values of LGD $= \{50, 60, 80\}\%$. This allows to infer the market-implied loss given default consistent with option prices. Table 1.11 reports the results.

The smallest absolute percentage error is observed for LGD $= 60\%$, both for calls and puts, consistently with Collin-Dufresne et al. (2010). The errors are also smaller for put than call options, and they appear to be increasing with leverage.

The robustness section is concluded by re-running the regressions in Sections 1.4.2 and 1.4.4 for alternative values of loss given default (again, 60% and 80%). The results are reported in the tables in Appendix H. The overall conclusions in terms of insensitivity of call options to credit events and the ability of the measure of impact of credit risk to predict the future changes in the negative skew of equity options remain unchanged.

1.5 Conclusions

In this paper I investigate the effect of credit related events on the pricing of equity options. Given a firm which has issued $n \geq 1$ defaultable coupon-bearing bonds, I generalise the results in Merton (1974) and Geske (1977), and price the firm's equity as an n–fold compound option call option on the asset value struck at the face values of the bonds outstanding. Further, I extend the pricing formula in Geske (1979) and show that European vanilla options on the firm's equity are $(n+1)$–fold compound options written on the value of the firm's assets. This frameworks constitutes the most natural environment to study the impact of credit risk on equity options consistently with the structural approach to default.

I further explore the predictions of a compound option model on a sample of 66 US firms from January, 2013 to December, 2017. These are the constituents of the S&P100 which neither issued preferred equity nor engaged into extraordinary financial operations (such as M&As) during the selected sample period.

Given the probabilistic implications of the model, a new measure of impact of credit risk on options is constructed, thus allowing to rank the latter based on how much they are exposed to credit-related events. Consistently with the economic intuition and the results

		LGD					
		Call			Put		
	LEV	50%	60%	80%	50%	60%	80%
AAPL	0.09	0.035	0.010	0.031	0.018	0.007	0.017
ABT	0.11	0.124	0.042	0.106	0.077	0.021	0.075
ACN	0.00	0.000	0.000	0.000	0.000	0.000	0.000
ALL	0.23	0.097	0.089	0.062	0.048	0.037	0.033
AMGN	0.29	0.103	0.091	0.062	0.078	0.045	0.055
AMZN	0.05	0.081	0.068	0.062	0.070	0.044	0.057
BA	0.10	0.025	0.025	0.013	0.027	0.012	0.021
BAC	1.79	1.172	0.570	0.943	0.212	0.272	0.149
BMY	0.08	0.030	0.015	0.023	0.016	0.009	0.012
C	1.63	1.562	0.615	1.284	0.125	0.281	0.311
CAT	0.60	0.390	0.193	0.281	0.261	0.060	0.221
CL	0.10	0.043	0.027	0.032	0.028	0.016	0.020
CMCSA	0.40	0.115	0.102	0.109	0.103	0.064	0.072
COF	1.02	0.499	0.361	0.358	0.380	0.234	0.249
COP	0.37	0.178	0.158	0.113	0.114	0.078	0.072
COST	0.08	0.021	0.020	0.013	0.024	0.010	0.019
CSCO	0.16	0.072	0.045	0.050	0.044	0.023	0.034
CVS	0.21	0.105	0.067	0.075	0.060	0.035	0.043
CVX	0.14	0.130	0.061	0.104	0.048	0.024	0.038
DD	0.21	0.092	0.066	0.063	0.057	0.035	0.042
DIS	0.11	0.081	0.019	0.072	0.054	0.010	0.051
EMR	0.11	0.126	0.049	0.105	0.073	0.020	0.071
EXC	0.81	0.550	0.416	0.389	0.272	0.185	0.165
F	1.99	1.205	0.742	0.926	0.577	0.120	0.483
FDX	0.17	0.085	0.072	0.054	0.053	0.042	0.034
GD	0.08	0.015	0.017	0.008	0.023	0.010	0.018
GE	1.00	0.509	0.293	0.364	0.294	0.108	0.233
HAL	0.22	0.077	0.066	0.048	0.057	0.046	0.035
HD	0.13	0.040	0.034	0.025	0.027	0.017	0.019
IBM	0.24	0.182	0.078	0.146	0.103	0.029	0.087
INTC	0.12	0.047	0.037	0.030	0.035	0.021	0.026
JNJ	0.06	0.022	0.018	0.014	0.009	0.008	0.006
JPM	1.51	0.751	0.658	0.527	0.176	0.141	0.122
KO	0.14	0.063	0.053	0.040	0.029	0.025	0.019
LLY	0.09	0.034	0.029	0.022	0.018	0.015	0.012
LOW	0.21	0.064	0.054	0.041	0.031	0.026	0.019
MCD	0.18	0.076	0.064	0.049	0.039	0.033	0.024
MDT	0.26	0.111	0.093	0.071	0.052	0.043	0.032
MMM	0.09	0.029	0.024	0.018	0.012	0.010	0.007
MO	0.14	0.082	0.069	0.053	0.033	0.028	0.021
MON	0.14	0.068	0.058	0.044	0.033	0.028	0.021
MRK	0.15	0.020	0.017	0.013	0.009	0.008	0.006
MS	2.71	0.786	0.699	0.577	0.554	0.615	0.715
MSFT	0.09	0.027	0.023	0.017	0.015	0.013	0.010
ORCL	0.21	0.070	0.059	0.045	0.041	0.034	0.026
OXY	0.12	0.065	0.055	0.042	0.046	0.039	0.030
PEP	0.22	0.137	0.115	0.088	0.051	0.043	0.032
PFE	0.17	0.065	0.055	0.041	0.033	0.027	0.021
PG	0.10	0.044	0.037	0.028	0.016	0.014	0.010
PM	0.19	0.109	0.092	0.070	0.043	0.036	0.027
RTN	0.14	0.046	0.038	0.029	0.025	0.021	0.016
SLB	0.13	0.050	0.042	0.032	0.028	0.023	0.017
SO	0.68	0.632	0.537	0.417	0.209	0.172	0.127
SPG	0.47	0.451	0.388	0.304	0.207	0.173	0.130
T	0.51	0.506	0.432	0.335	0.208	0.173	0.129
TGT	0.35	0.150	0.127	0.097	0.072	0.060	0.045
TWX	0.36	0.171	0.145	0.111	0.105	0.087	0.065
TXN	0.08	0.033	0.028	0.021	0.015	0.013	0.010
UNH	0.20	0.078	0.066	0.050	0.037	0.031	0.023
UNP	0.16	0.036	0.031	0.025	0.023	0.019	0.014
USB	0.47	0.253	0.214	0.164	0.084	0.069	0.051
UTX	0.23	0.103	0.087	0.066	0.044	0.037	0.028
VZ	0.55	0.476	0.406	0.314	0.211	0.175	0.130
WFC	0.85	0.492	0.422	0.327	0.172	0.138	0.096
WMT	0.20	0.089	0.075	0.057	0.043	0.036	0.027
XOM	0.06	0.020	0.017	0.013	0.008	0.007	0.005
Mean		0.212	0.148	0.153	0.092	0.066	0.073

Table 1.11 Absolute percentage errors between the option-implied asset volatility obtained with and without the CDS spreads calibration for LGD = $\{50, 60, 80\}$%. The average errors are reported at the company level (where the time-average leverage is also reported). The last row display the overall average, thus suggesting a market implied loss given default of 60%.

in Carr and Wu (2011) (who, instead, opt for a reduced-form approach to default), call and put option prices account for the possibility of the company to default very differently. More specifically, call options do not price credit risk, whilst the price of put options does embed it. To the best of my knowledge, this is the first work which explores and rigorously assesses this phenomenon using a large sample of options (both in the cross-section and the time-series dimension).

I finally attempt at predicting the future changes in the negative skew displayed by equity options. I show that the novel measure of credit risk constructed on put prices is able to forecast future movements of the skew for long-maturity equity options. To the best of my knowledge, this is the first work which tries to capture and predict the changes in the option skew with a measure of credit risk. Further work is however required to capture these movements more precisely. Factors based on the channels described in Carr and Wu (2017) could be constructed in order to improve the fit of the proposed regressions.

The implications of this study are multifaceted. Given the importance of default risk for those assets which are more sensitive to events occurring in the left tail of equity distribution (e.g. put options), risk-management implications for those instruments are relevant, especially when the underlying is the equity of either highly-levered or financially-distressed companies.

For example, hedge funds often take highly levered positions in corporate bonds while hedging away interest rate risk by shorting treasuries. As a consequence, their portfolios become extremely sensitive to changes in credit spreads rather than changes in bond yields. If there is a nonnegligible probability of large negative jumps in firm value, then the appropriate hedging tool for corporate debt may not be the firm's equity, but rather deep out-of-the-money puts on the firm's equity. In turn, the writer of these options will need to hedge its short position.

It is trivial to show that the Delta-hedge under the Black-Scholes model, which ignores credit risk, is different than the hedge prescribed by a compound option model. Ignoring dividends for simplicity, the Delta-hedges under the Black-Scholes and a compound option model differ as such

$$\frac{\partial P_\xi^{CO}}{\partial S} = \frac{\partial P_\xi^{CO}/\partial V}{\partial S/\partial V} = \frac{\Delta_{P,\xi}^{(n)}}{\Delta_S^{(n)}} \neq \xi\Phi\left(\xi d_1^{\mathbb{M}}\right) = \frac{\partial P_\xi^{BS}}{\partial S}.$$

Figure 1.14 shows that the Black-Scholes hedge underestimates the number of units of the underlying required to hedge the short option position when the option is out-of-the-money. Conversely, it overestimates the delta-hedged position in the equity when the option is in-the-money. This bias would apply to any other hedging strategy based on the Greeks of
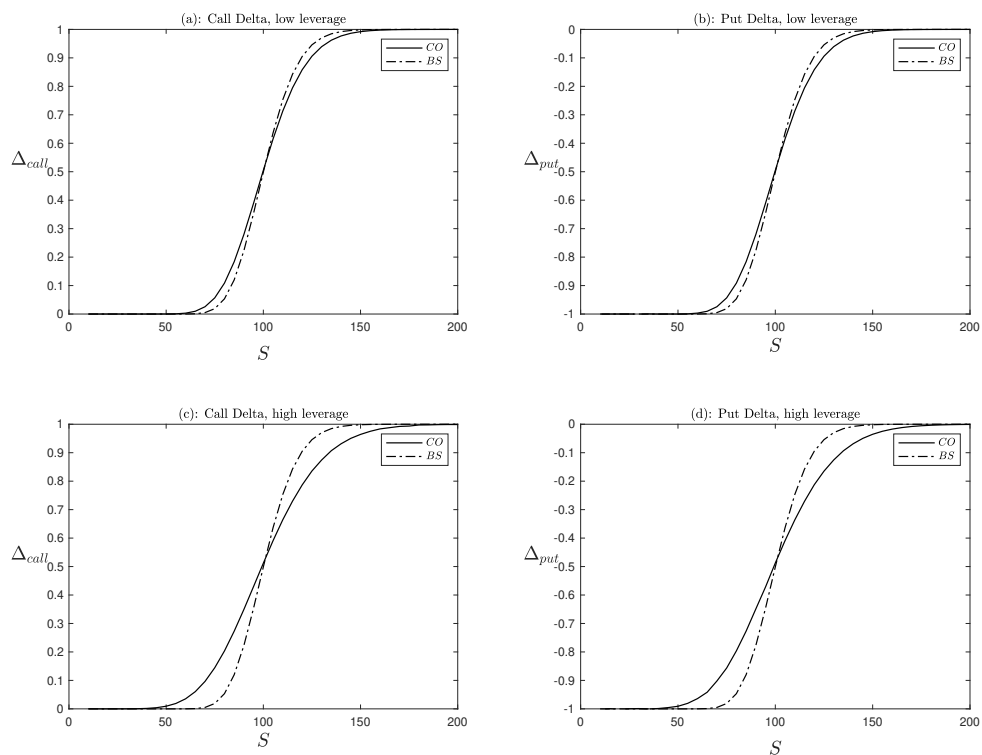
Fig. 1.14 Comparison of the delta of call and put options under the Black-Scholes model and a 3–fold compound option model for the underlying. Pictures (a) and (b) show the effect of ignoring the possibility of default for a low levered firm ($F_1 = F_2 = F_3 = 10$), whilst pictures (c) and (d) show the same comparison for a company which is more levered ($F_1 = F_2 = F_3 = 30$). The optimal hedge ratio is obviously more distorted for the case of highly-levered firms as they are naturally more exposed to credit-related events. Also here $K = 100$, $T = 0.5$, $t_1 = 1, t_2 = 5, t_3 = 10, r = 0.03$ and $\varpi = 0.05$.

the option when credit risk is not modelled. Also, this distortion becomes more and more severe for increasingly levered firms. A more in-depth analysis of this imperfect hedging when default risk is not taken into account is though left for future research.

Furthermore, the countintuitive findings in Carr and Wu (2017) of increasing leverage for increasing diffusive volatility can be easily reconciled with a model in which shareholders maximise the firm value, based on a targeted leverage ratio, and equity is modelled as a compound option. Optimal capital structure policies, however, are not explored in this work and left for future research as well.

Chapter 2

Credit Spreads, Leverage and Volatility: a Cointegration Approach

Abstract

This work documents the existence of a cointegration relationship between credit spreads, leverage and equity volatility for a large set of US companies. It is shown that accounting for the long-run equilibrium dynamic between these variables is essential to correctly explain credit spread changes. Using a novel structural model in which equity is modelled as a compound option on the firm's assets, a new methodology for estimating the unobservable market value of the firm's assets and volatility is developed. The proposed model allows to significantly reduce the pricing errors in predicting credit spreads when compared with several structural models. In terms of correlation analysis, it is shown that not accounting for the long-run equilibrium equation embedded in an Error Correction Mechanism (ECM) results into a misspesification problem when regressing a set of explanatory variables onto the spread changes. Once credit spreads, leverage and volatility are correctly modelled, thus allowing for a long-run equilibrium, the fit of the regressions sensibly increases if compared to the results of previous research. It is further shown that most of the cross-sectional variation of the spreads appears to be more driven by firm-specific characteristics rather than systematic factors.

2.1 Introduction

Structural models of credit risk have faced several difficulties in explaining both the level and changes of bond and CDS spreads observed in the data since its pioneering introduction by Merton (1974). The early empirical work by Jones et al. (1983) shows that the Merton model for callable coupon bonds overprices such bonds. This findings have motivated a variety of extensions, such as allowing for default before the bond maturity, stochastic interest rates, jumps, and strategic default. Despite these extension, the structural approach is still questioned about its ability in explaining credit spreads (Huang and Huang 2012).

Academic research has taken mainly three routes in order to analyse and document this surprising lack of accuracy of structural models. First, attempts to empirically implement models on individual corporate bond spreads have failed (Eom et al. 2004). Mixed evidence supporting the structural approach is instead documented for CDS spreads (Ericsson et al. (2009), Zhang et al. 2009), thus suggesting liquidity and tax arguments for the lack of success in case of bonds (Driessen 2005, Longstaff et al. 2005). Also, Elton et al. (2001) find that expected losses account for a low fraction of spreads for investment grade bonds. Collin-Dufresne et al. (2001) document that proxies for credit risk explain only a small portion of changes in yield spreads and that the unexplained portion is driven mainly by factors that are independent of both credit-risk and standard liquidity measures.

Secondly, efforts to calibrate models to observable moments including historical default rates and Sharpe ratios have been unable to match average credit spreads levels (the so-called credit spread puzzle). Huang and Huang (2012), testing over an extensive class of structural models, show that credit risk accounts for only a small fraction of yield spreads for investment-grade bonds of all maturities, with the fraction lower for bonds of shorter maturities, but it accounts for a much higher fraction of yield spreads for high-yield bonds. They calibrate each of the models on the historical default loss experienced and equity risk premia, and demonstrate that different models (under)predict similar credit risk premia. In partial conflict with these findings is Feldhütter and Schaefer (2018). In their work, the authors argue that the appearance of a credit spread puzzle strongly depends on the period over which historical default rates are measured and how default probabilities are estimated from default rates. Developing a new estimation methodology, they are able to calibrate the Black and Cox (1976) model to historical default rates and the equity risk premium, thus matching the average level of investment grade spreads well. However, model spreads for speculative-grade debt appear still too low and this underpricing is attributed to illiquidity.

Finally, models have been unable to jointly explain dynamics of credit spreads and equity volatilities. Within this framework of research, Campbell and Taksler (2003) find that idiosyncratic volatility can explain one-third of yield spreads for investment grade bonds rated below Aaa. An important recent development which examines potential links between the credit spread puzzle and macroeconomic conditions using consumption-based asset-pricing is Chen et al. (2009). The authors show that the Campbell and Cochrane (1999) pricing kernel combined with some mechanism to match the countercyclical nature of defaults is able to capture the level and time variation of Baa-Aaa spreads. However, they also show that a pricing kernel that explains the equity premium with a constant Sharpe ratio cannot explain the credit spread.

A very recent paper which tries to address all the above-mentioned failures of structural models of default in explaining credit spreads is Du et al. (2019). In their paper, the authors use the framework in Leland (1994) (i.e. the firm has issued a consol bond) in which the unlevered asset process is modelled as in Heston (1993). Thus allowing for stochastic volatility in firm value process and calibrating the variance risk premium consistently with reasonable firm-level Sharpe ratios, they are first able to resolve the credit spread puzzle for medium- to longer-term maturities for representative Baa- and Aa-rated firms. Secondly, introducing jumps in the asset value process allows to fit shorter term credit spreads as well. Moreover, their model succeeds at explaining the joint dynamics of credit spreads and equity volatilities, and allows them to identify economically significant variance risk premia which explain an important part of spread levels.

Based on the evidence that a time-varying volatility of the asset is needed in order to explain the level of credit spread over medium- and long-term maturities, a novel estimation technique of the volatility of the assets is introduced. The proposed model and estimation technique is much simpler than the one in Du et al. (2019). As a matter of fact, their calibration methodology relies on the Fortet's Lemma, maximum likelihood and Chebychev interpolation in the case of stochastic diffusive asset volatility (and, on top of those, on simulated maximum likelihood when jumps are introduced). They have nine parameter, over a total of twelve, to estimate. In this paper, even though the asset value process is assumed to follow a geometric Brownian motion (thus asset volatility is not stochastic), the proposed estimation methodology allows to retrace the time-series of the asset volatility for a given firm. Moreover, the time-series of the equity volatility can be also estimated accordingly.

This work departs from the previous attempts to explain the level and changes of CDS spreads as a new estimation technique is implemented for those variables which structural models of default predict to be the drivers for the spreads. More specifically, a simple

estimation which relies only on the joint calibration on the price of the equity and CDS spreads (and, indirectly, by the book value of the firm's debt) is proposed.

The choice of using CDS instead of bond spreads is motivated by the fact that former constitute a more direct and clean signal for the underlying default risk. In fact, CDS spreads provide relatively pure pricing of the default event of the underlying entity as they are typically traded on standardised terms. In fact, unlike bonds, CDSs have a constant maturity, the underlying instrument is always par valued, they concentrate liquidity in one instrument, and are not affected by different taxation regimes; also, bond spreads are more likely to be affected by differences in contractual arrangements, such as differences in seniority, coupon rates, embedded options, and guarantees. Secondly, many corporate bonds are bought by investors who simply hold them to maturity, and the secondary market liquidity is therefore often poor. Furthermore, shorting bonds is even more difficult in the cash market as the repo market for corporate bond is often illiquid, and the tenor of the agreement is usually very short. CDS contracts instead allow investors to implement trading strategies to hedge credit risk over a longer period of time at a known cost. Moreover, as shown by Blanco et al. (2005), CDS spreads tend to respond more quickly than bond spreads to changes in credit conditions in the short run.

The goodness of estimates of the market value of the asset and volatility of the firm is fist tested as their own ability to predict the one-period ahead CDS spreads. Secondly, an econometric analysis of the determinants of the credit spreads is conducted. Previous works such as Collin-Dufresne et al. (2001), Cremers, Driessen, Meanhout and Weinbaum (2008), Ericsson et al. (2009) and Zhang et al. (2009) investigate the link between credit spreads and their determinants as predicted by structural models of default via regressions. There, a set of variables (usually leverage, equity volatility and characteristics of the term structure of interest rates) is regressed onto bond or CDS spreads in order to explain their level and changes. This paper shows that use of such regressions to explain the level of the spreads (either bonds or CDS) is intrinsically flawed. As shown later in the paper, the level of credit spreads, as well as other variables entering the regressions, display a unit root. Therefore, any regression analysis based on these variables would detect spurious correlations. Hence, the only consistent way to tackle this problem is investigating the presence of a long-run equilibrium equation between these variables using an Error Correction Mechanism (ECM), as introduced by Engle and Granger (1987). If these variables are cointegrated (that is there exists a linear combination of them which is stationary), an ECM can be estimated and the economic relationship between them can be further investigated. If the variables are not cointegrated, only the changes in spreads can be explained by regressing the first differences

those variables onto the former (alternatively, a VAR can be used). The use of an ECM, when possible, is more desirable as it allows to shed light on the economic, and not only statistical, relationship between the variables.

It still appears surprising how previous works fully ignore a possible cointegration, despite Blanco et al. (2005) develop a VECM to investigate the cointegration of bond and CDS spreads. Such analysis is possible only if the time-series component of the spreads is non-stationary. Here, instead, a cointegration analysis is conducted between the CDS spreads and their determinants as predicted by the structural models of default. This leads to a cointegrated system where credit spreads, financial leverage an the firm's riskiness comove adjusting to a long-run equilibrium. Empirical results discussed in this paper support the existence of a cointegrating relationship between these variables

The rest of the paper is organised as follows. Section 2.2 discusses the compound option structural model of default alongside the estimation methodology for the firm's asset value and volatility. Section 2.3 explains how the model is used out-of-sample to reprice the spreads and its performance is compared with the one of other structural models. Section 2.4 models the cointegration relationship between the variables and the short-term adjustment is estimated. Finally, Section 2.5 performs some robustness checks, and Section 2.6 concludes.

2.2 Estimation methodology and Data Description

In order to estimate the volatility of the asset, the following set of variables for each firm are needed: (1) the value of the equity, (2) the term structure of the survival probability and, (3) the face value of its debt as well as the time it due. The model employed is the same as in Maglione (2019) in which equity is seen as a n–fold compound call option written on the firm assets struck at the face value of the n bonds outstanding. Under this framework, default times are defined as

$$\tau := \inf_{i \in I} \left\{ t_i : S_i^\star(V) < F_i \right\}$$

where $I = \{1, \ldots, n\}$ and $S_i^\star(V)$ is the continuation value of equity, which is a function of the firm assets V. That is, the default time occurs the first time at which the value of the equity is lower than the face value of the bond due; by model assumptions, the firm can default only at discrete points in time.

More specifically, it can be shown that the value of the firm's equity can be written as

$$S = e^{-\varpi t_n} V \mathbb{M} \left(\tau \geq t_n \right) - \sum_{i=1}^{n} e^{-rt_i} F_i \mathbb{Q} \left(\tau \geq t_i \right), \tag{2.1}$$

where V is the contemporaneous value of the assets, $(F_i)_{1 \leq i \leq n}$ represent the sequence of the face value of the bond issued due at time t_i, ϖ the payout rate (reflecting both dividends and coupons), r the constant continuously compounded risk-free rate, and $\mathbb{Q}(\tau \geq t_i)$ (respectively $\mathbb{M}(\tau \geq t_i)$) the probability of the firm surviving up to t_i under the risk-neutral measure (respectively the firm-value fund risk measure). If the asset value process follows a geometric Brownian motion with volatility σ_V, the probabilities in (2.1) can be computed in terms of multivariate Gaussian integrals, that is

$$S(V,\sigma_V) = e^{-\varpi t_n} V \Phi_n\left(\mathbf{d}^{\mathbb{M}}; \boldsymbol{\Gamma}_n\right) - \sum_{i=1}^{n} e^{-rt_i} F_i \Phi_i\left(\mathbf{d}_i^{\mathbb{Q}}; \boldsymbol{\Gamma}_i\right) \qquad (2.2)$$

where $\mathbf{d}^{\mathbb{M}} := \left(d_i^{\mathbb{M}}\right)_{1 \leq i \leq n}$ and $\mathbf{d}_i^{\mathbb{Q}} = \left(d_j^{\mathbb{M}} - \sigma_V \sqrt{t_j}\right)_{1 \leq j \leq i}$ with

$$d_i^{\mathbb{M}} = \frac{\ln(V/\bar{V}_i) + \left(r - \varpi + \sigma_V^2/2\right) t_i}{\sigma_V \sqrt{t_i}}, \qquad \boldsymbol{\Gamma}_i = \begin{pmatrix} 1 & \sqrt{\frac{t_1}{t_2}} & \sqrt{\frac{t_1}{t_3}} & \cdots & \sqrt{\frac{t_1}{t_i}} \\ & 1 & \sqrt{\frac{t_2}{t_3}} & \cdots & \sqrt{\frac{t_2}{t_i}} \\ \cdots & \cdots & \cdots & \cdots & \cdots \\ & & & 1 & \sqrt{\frac{t_{i-1}}{t_i}} \\ & & & & 1 \end{pmatrix},$$

and $\Phi_i(\mathbf{z}; \boldsymbol{\Gamma})$ the cumulative distribution function of a i-dimensional normal random vector with zero mean and covariance matrix $\boldsymbol{\Gamma}$ calculated over the set $\times_{j=1}^{i}(-\infty, z_j)$. Also, $(\bar{V}_i)_{1 \leq i \leq n}$ is the latent sequence of default thresholds embedded in the firm's capital structure.

The unobservable parameters of the model are the value of the firm assets, V, and the asset volatility, σ_V. As the sequence of risk-neutral probabilities $\mathbb{Q}(\tau \geq t_i)$ can be estimated from the CDS spreads in a model-free fashion(Brigo 2005), the following system of non-linear equations can be employed to estimate both variables,

$$\begin{cases} S(V,\sigma_V) = S \\ \Phi_i^{\mathbb{Q}}(V,\sigma_V) = \widehat{\Phi}_i^{\mathbb{Q}} \quad \forall i \in I. \end{cases} \qquad (2.3)$$

Here, the functional form of $S(V,\sigma_V)$ and $\Phi_i^{\mathbb{Q}}(V,\sigma_V) = \Phi_i\left(\mathbf{d}_i^{\mathbb{Q}}(V,\sigma_V); \boldsymbol{\Gamma}_i\right)$ are obtained from (2.2). S is the observed stock price, whist $\widehat{\Phi}_i^{\mathbb{Q}}$ are the model-free risk neutral probability of survival (for maturity t_i) estimated from the CDS spread. Notice that, if $i \geq 2$, the system is overdetermined as there are more equations than unknowns; thus, the system can be solved

with nonlinear least squares with Jacobian[1]. More specifically, the Jacobian of the problem is given by an $(i+1) \times 2$ matrix such that

$$\mathbf{J} = \begin{bmatrix} \frac{\partial S}{\partial V} & \frac{\partial S}{\partial \sigma_V} \\ \frac{\partial \Phi_i^Q}{\partial V} & \frac{\partial \Phi_i^Q}{\partial \sigma_V} \end{bmatrix} = \begin{bmatrix} \Delta_S & v_S \\ \frac{\partial \Phi_i^Q}{\partial V} & \frac{\partial \Phi_i^Q}{\partial \sigma_V} \end{bmatrix}$$

where Δ_S and v_S are the Delta and the Vega of the equity respectively. Analytical expressions for the Jacobian are available in Appendix I. Once the estimates of V and σ_V are obtained, the volatility of the equity and the firm's leverage are calculated accordingly, that is

$$\sigma_S = \sigma_V \frac{V}{S} \Delta_S, \qquad \frac{D}{S} = \frac{Ve^{-\varpi t_n} - S}{S}. \tag{2.4}$$

This novel estimation technique is applied to a set of 64 US companies, constituents of the S&P100 during the period January 2013 – December 2017. Companies with either preferred equity or subject to merges or acquisitions are excluded. Also, only companies for which CDS spreads are available are included. Table 2.1 displays the complete name list, alongside the SIC code, credit rating and industry in which the company operates in.

Data on stock prices, number of shares outstanding, dividends and the risk-free yield curve (and other variables used in the next sections) are obtained from Bloomberg. CDS spreads are from Thompson Reuters Datastream. Information relative to the firms' capital structures and cost of debt is gathered from Compustat and the 10-K documents. All the observations are collected at weekly frequency frequency, over a total of 260 week, with the exception of the information on the firm's capital structure which is available at quarterly frequency.

In order to implement the estimation in (2.3), the term-structure of the firm's debt must be known or approximated somehow. I opt for clustering the firm's debt at three fixed point, $t_i = \{1, 5, 10\}$ years, $i = 1, 2, 3$. This clustering mirrors the availability from Compustat of short-term debt which is clustered at one year horizon; then the other fixed future dates are chosen as the most liquid CDS contracts are those with 5– and 10–year maturities.

The face values of the bond due in $t_1 = 1$ represents the company's short-term debt and is computed as the Compustat variable DD1Q (Long-Term Debt Due in One Year), that is $F_1 = \text{DD1Q}$. The remaining two bonds clustered at $t_2 = 5$ and $t_3 = 10$ are obtained from DLTQ (Long-Term Debt Total), such that $F_2 + F_3 = w \cdot \text{DLTQ} + (1-w) \cdot \text{DLTQ}$. Ultimately, the

---

[1]Despite nonlinear least squares can also be implemented without knowing the Jacobian matrix, the use of the latter reduces the number of iterations of about 66%, significantly improving speed and accuracy.

Ticker	SIC	Division	S&P Credit Rating
AAPL	3663	Manufacturing	AA+
ABT	2834	Manufacturing	A+
ALL	6331	Finance, Insurance and Real Estate	A-
AMGN	2836	Manufacturing	A
BA	3721	Manufacturing	A
BAC	6020	Finance, Insurance and Real Estate	A-
BMY	2834	Manufacturing	A+
C	6199	Finance, Insurance and Real Estate	BBB+
CAT	3531	Manufacturing	A
CL	2844	Manufacturing	AA-
CMCSA	4841	Transportation, Communications, Electric, Gas and Sanitary service	A-
COF	6141	Finance, Insurance and Real Estate	BBB
COP	1311	Mining	A
COST	5399	Wholesale Trade	A+
CSCO	3576	Manufacturing	AA-
CVS	5912	Retail Trade	BBB+
CVX	2911	Manufacturing	AA-
DD	2821	Manufacturing	A-
DIS	4888	Transportation, Communications, Electric, Gas and Sanitary service	A
EMR	3823	Manufacturing	A
EXC	4911	Transportation, Communications, Electric, Gas and Sanitary service	BBB
F	3711	Manufacturing	BBB-
FDX	4513	Transportation, Communications, Electric, Gas and Sanitary service	BBB
GD	3721	Manufacturing	A+
GE	4911	Transportation, Communications, Electric, Gas and Sanitary service	AA+
HAL	1389	Mining	A
HD	5211	Wholesale Trade	A
IBM	7370	Services	AA-
INTC	3674	Manufacturing	A+
JNJ	2834	Manufacturing	AAA
JPM	6020	Finance, Insurance and Real Estate	A-
KO	2086	Manufacturing	AA-
LLY	2834	Manufacturing	AA-
LOW	5211	Wholesale Trade	A-
MCD	5812	Retail Trade	A
MDT	3845	Manufacturing	A
MMM	2670	Manufacturing	AA-
MO	2111	Manufacturing	BBB+
MON	5169	Retail Trade	BBB+
MRK	2834	Manufacturing	AA
MS	6211	Finance, Insurance and Real Estate	BBB+
MSFT	7372	Services	AAA
ORCL	7370	Services	AA-
OXY	1311	Mining	A
PEP	2080	Manufacturing	A
PFE	2834	Manufacturing	AA
PG	2840	Manufacturing	AA-
PM	2111	Manufacturing	A
RTN	3812	Manufacturing	A
SLB	1389	Mining	AA-
SO	4911	Transportation, Communications, Electric, Gas and Sanitary service	A-
SPG	6798	Finance, Insurance and Real Estate	A
T	4812	Transportation, Communications, Electric, Gas and Sanitary service	BBB+
TGT	5331	Wholesale Trade	A
TWX	8748	Services	BBB
TXN	3674	Manufacturing	A+
UNH	6324	Finance, Insurance and Real Estate	A+
UNP	4011	Transportation, Communications, Electric, Gas and Sanitary service	A
USB	6020	Finance, Insurance and Real Estate	A+
UTX	3724	Manufacturing	A-
VZ	4812	Transportation, Communications, Electric, Gas and Sanitary service	BBB+
WFC	6020	Finance, Insurance and Real Estate	A
WMT	5331	Retail Trade	AA
XOM	1311	Mining	AAA

Table 2.1 List of the selected companies (ticker) and their SIC code. The sample is further divided into four categories based on the industry/type or business: (a) Financial companies; (b) Mining, Energy and Utilities companies; (c) Manufacturing; (d) Retail, Wholesale and Services. Credit ratings are obtained from Compustat and the mode of the ratings over Jan-2013 to Dec-2017 is reported.

weight is set as $w = 1/3$, as motivated in the next section. This results in an sequence of debt outstanding which is increasing with maturities.

The choice of setting $n = 3$ is considered optimal as it is the smallest number of maturity dates needed in order to match both the level, slope and curvature of the term structure of the survival probabilities extracted from the CDSs. As a matter of fact, an effective calibration of the model should aim at reproducing the aforementioned term structure as accurately as possible. Furthermore, as shown in Appendix J, a 3–fold compound option model displays some desirable properties in terms of leverage.

2.3 Model-implied Spreads and Probabilities of Survival

Consider the payoff of a CDS initiated at $t_0 = 0$ with maturity t_j and intermediate premium payments at $(t_i)_{i=1}^{j}$, $j \in \mathbb{N}$, and notional equal to one (Brigo and Mercurio (2006))

$$\Pi_j(t) = DF(t, \tau)(\tau - \bar{t})s\mathbb{1}_{\{0 < \tau \leq t_j\}} + s\sum_{i=1}^{j} DF(t, t_i)(t_i - t_{i-1})\mathbb{1}_{\{\tau \geq t_i\}} - DF(t, \tau)\text{LGD}\mathbb{1}_{\{0 < \tau \leq t_j\}}$$

with $0 \leq t < t_j$, $\bar{t}$ the last payments date before t, that is $\bar{t} := \sup_{1 \leq i \leq j}\{t_i \leq \tau\}$, s the CDS spread paid by the protection buyer (before default, if it happens), LGD the loss given default, and $DF(t_i, t_j)$ the (stochastic) discount factor between t_i and t_j. The first term is the discounted accrued rate at default and represents the compensation the protection seller receives for the protection provided from the last t_i until default τ. The terms in the summation represent the CDS rate premium payments if there is no default: this is the premium received by the protection seller for the protection being provided. The final term is the payment of protection at default, if this happens before final t_j.

If default is assumed to happen only at reset dates (that is, accrued interests are ignored), the first summand vanishes, and the t_j-maturity CDS price in $t_0 = 0$, according to risk-neutral valuation, is

$$\text{CDS}_j(s, \text{LGD}) = \mathbb{E}^{\mathbb{Q}}\left[\Pi_j(0)\right] = s\sum_{i=1}^{j} P(0, t_i)(t_i - t_{i-1})\mathbb{Q}(\tau \geq t_i) - \text{LGD}\int_0^{t_j} P(0, t)\,d\mathbb{Q}(\tau \geq t)$$

where $P(t_i, t_j)$ is the t_i-value of a zero-coupon bond with maturity $t_j \geq t_i$. Following common market practice, despite being the loss given default a random variable in $(0, 1)$, here it is set as a known parameter. More specifically, the values that are commonly employed by the literature and suggested by the ISDA are $\text{LGD} = \{0.5, 0.6, 0.8\}$.

If the term structure of the risk-free interest rates is also known at inception (and assumed as a deterministic function of the maturity only, $r_t := r_0(t)$), then the previous expression simplifies as

$$\text{CDS}_j(s, \text{LGD}) = s \sum_{i=1}^{j} e^{-r_{t_i} t_i} (t_i - t_{i-1}) \mathbb{Q}(\tau \geq t_i) - \text{LGD} \int_0^{t_j} e^{-r_t t} \, d\mathbb{Q}(\tau \geq t).$$

The CDS spread for maturity t_j is the value of s, say s_j, which makes the price the value of the CDS contract equal to zero when the contract is initiated, that is $s_j := \{s > r_{t_j} : \text{CDS}_j(s, \text{LGD}) = 0\}$. Hence,

$$s_j = \text{LGD} \frac{\int_0^{t_j} e^{-r_t t} \, d\mathbb{Q}(\tau \geq t)}{\sum_{i=1}^{j} e^{-r_{t_i} t_i} (t_i - t_{i-1}) \mathbb{Q}(\tau \geq t_i)} \approx \text{LGD} \frac{\sum_{i=1}^{j} e^{-r_{t_i} t_i} [\mathbb{Q}(\tau \geq t_{i-1}) - \mathbb{Q}(\tau \geq t_i)]}{\sum_{i=1}^{j} e^{-r_{t_i} t_i} (t_i - t_{i-1}) \mathbb{Q}(\tau \geq t_i)}$$

$$(2.5)$$

Equation (2.5) is used to obtain the CDS spread based on the model-implied risk-neutral probabilities of survival calculated via the estimated parameters (V, σ_V) such that (2.3) is met. The estimated asset value and volatility at time t are used to forecast both survival probabilities and CSD spread are at $t + 1$ (one week ahead).

As the probabilities of survival, and therefore the spread, depend on both the loss given default parameter and the aggregation scheme of the firm's capital structure, different combinations are investigated. More specifically, different values of the weight w in $F_2 + F_3 = w \cdot \text{DLTQ} + (1 - w) \cdot \text{DLTQ}$ are tested. These are $w = \{1/2, 1/3, 2/3\}$.

Tables 2.2, 2.3 and 2.4 report the results on the pricing error of the 3–fold compound option model for w equal to 1/2, 1/3 and 2/3 respectively. For each aggregation scheme, the pricing error are obtained for LGD $= \{0.5, 0.6, 0.8\}$. The average CDS spread quoted by the market is reported alongside the one implied by the model for different LGDs. Spreads are expressed in basis points. The signed differences and percentage errors of the average market and the model-implied CDS spreads are reported as well as the percentage error between the model-free and model-implied risk-neutral probabilities of survival. Results are clustered based on contractual maturities (1, 5 and 10 years) and on leverage.

The aggregation scheme in Table 2.2 ($w = 1/2$) underprices short-term spreads of low-levered firms (as extensively documented in the literature for models without jumps) as well as long-term spreads of medium- and high-levered firms. For low- and medium-levered firms, pricing errors are small for short- and long-term CDS contracts (4 bps); the error increases for highly levered firms and in the case of the 5-year spread (46 bps).

		LGD									
		CDS^{model}			CDS^{mrk} − CDS^{model} $(1 - \text{CDS}^{model}/\text{CDS}^{mrk})$			1 − Q^{model}/Q^{mrk}			
LEV	CDS^{mrk}	50%	60%	80%	50%	60%	80%	50%	60%	80%
1-year										
(0, 0.25]	7.68	4.47	4.12	3.80	3.21 (42%)	3.55 (46%)	3.87 (50%)	−0.06%	−0.05%	−0.04%
(0.25, 1]	15.55	20.19	20.02	20.43	−4.64 (−30%)	−4.47 (−29%)	−4.88 (−31%)	0.09%	0.08%	0.06%
(1, ∞)	28.85	91.44	86.25	82.77	−62.59 (−217%)	−57.40 (−199%)	−53.92 (−187%)	1.19%	0.93%	0.66%
5-year										
(0, 0.25]	35.20	43.59	41.51	40.20	−8.39 (−24%)	−6.31 (−18%)	−4.99 (−14%)	0.70%	0.50%	0.31%
(0.25, 1]	60.12	107.84	105.93	106.59	−47.71 (−79%)	−45.80 (−76%)	−46.47 (−77%)	4.30%	3.60%	2.78%
(1, ∞)	89.97	192.52	189.47	189.75	−102.55 (−114%)	−99.50 (−111%)	−99.78 (−111%)	8.69%	7.40%	5.76%
10-year										
(0, 0.25]	62.28	63.28	61.72	61.82	−1.00 (−2%)	0.57 (1%)	0.46 (1%)	−0.25%	−0.16%	−0.09%
(0.25, 1]	93.55	90.40	87.45	86.76	3.15 (3%)	6.10 (7%)	6.79 (7%)	−2.47%	−1.97%	−1.49%
(1, ∞)	134.89	121.84	117.62	115.07	13.05 (10%)	17.27 (13%)	19.82 (15%)	−6.97%	−5.52%	−4.15%

Table 2.2 Pricing error of the CDS spread and risk-neutral probabilities of default for $w = 1/2$. All the model-implied spreads are calculated setting the loss given default equal to either 50%, 60% or 80%. This allows to jointly test for the effect of the aggregation scheme in the firm's capital structure and on the selected value of LGD. The Table reports the market CDS spread alongside those produced by the model (expressed in basis points) based on the estimates of the firm's asset and volatility on the previous week. The results are clustered based on the maturity of the CDS contract (1, 5, and 10 years) and on the firm's average leverage. A positive/negative pricing error CDS^{mrk} − CDS^{model} indicated that the model under/overpredicts the level of the spread. This is reflected into the over/underprediction of the survival probabilities. Errors are also reported as percentages in brackets. For the probabilities of survival, only percentage errors are reported. Based on leverage, the number of companies in each bucket are $N_{low} = 44$, $N_{med} = 15$, $N_{high} = 5$.

| | | CDS^{model} | | | $\left(1-\text{CDS}^{model}/\text{CDS}^{mrk}\right)$ | | | $1-\mathbb{Q}^{model}/\mathbb{Q}^{mrk}$ | | |
| | | LGD | | | | | | | | |
LEV	CDS^{mrk}	50%	60%	80%	50%	60%	80%	50%	60%	80%
1-year										
(0,0.25]	7.68	0.86	0.67	0.50	6.81 (89%)	7.00 (91%)	7.18 (93%)	−0.13%	−0.11%	−0.08%
(0.25,1]	15.55	11.37	10.79	10.39	4.18 (27%)	4.75 (31%)	5.16 (33%)	−0.10%	−0.08%	−0.07%
(1,+∞)	28.85	75.65	70.27	66.58	−46.80 (−162%)	−41.41 (−144%)	−37.73 (−131%)	0.89%	0.67%	0.46%
5-year										
(0,0.25]	35.20	25.22	23.06	21.19	9.98 (28%)	12.14 (34%)	14.01 (40%)	−1.07%	−0.99%	−0.86%
(0.25,1]	60.12	78.66	75.47	74.14	−18.53 (−31%)	−15.35 (−26%)	−14.01 (−23%)	1.45%	1.12%	0.77%
(1,+∞)	89.97	162.23	159.91	162.48	−72.26 (−80%)	−69.94 (−78%)	−72.51 (−81%)	6.15%	5.25%	4.17%
10-year										
(0,0.25]	62.28	64.91	63.27	63.04	−2.62 (−4%)	−0.99 (−2%)	−0.76 (−1%)	0.40%	0.35%	0.27%
(0.25,1]	93.55	95.76	93.09	92.90	−2.21 (−2%)	0.46 (0%)	0.65 (1%)	−0.69%	−0.49%	−0.31%
(1,+∞)	134.89	131.64	127.62	126.99	3.25 (2%)	7.27 (5%)	7.90 (6%)	−4.05%	−3.14%	−2.25%

Table 2.3 Pricing error of the CDS spread and risk-neutral probabilities of default for $w = 1/3$. All the model-implied spreads are calculated setting the loss given default equal to either 50%, 60% or 80%. This allows to jointly test for the effect of the aggregation scheme in the firm's capital structure and on the selected value of LGD. The Table reports the market CDS spread alongside those produced by the model (expressed in basis points) based on the estimates of the firm's asset and volatility on the previous week. The results are clustered based on the maturity of the CDS contract (1, 5, and 10 years) and on the firm's average leverage. A positive/negative pricing error CDS^{mrk} − CDS^{model} indicated that the model under/overpredicts the level of the spread. This is reflected into the over/underprediction of the survival probabilities. Errors are also reported as percentages in brackets. For the probabilities of survival, only percentage errors are reported. Based on leverage, the number of companies in each bucket are $N_{(0,0.25]} = 44$, $N_{(0.25,1]} = 15$, $N_{(1,+∞)} = 5$.

		LGD									
		CDS^{model}			CDS^{mrk} − CDS^{model} (1 − CDS^{model}/CDS^{mrk})			1 − $\mathbb{Q}^{model}$/$\mathbb{Q}^{mrk}$		
LEV	CDS^{mrk}	50%	60%	80%	50%	60%	80%	50%	60%	80%
1-year										
(0, 0.25]	7.68	16.57	16.29	16.53	−8.89 (−116%)	−8.61 (−112%)	−8.85 (−115%)	0.17%	0.14%	0.11%
(0.25, 1]	15.55	26.77	26.60	27.15	−11.22 (−72%)	−11.05 (−71%)	−11.61 (−75%)	0.21%	0.18%	0.14%
(1, +∞)	28.85	94.77	89.07	83.35	−65.92 (−228%)	−60.22 (−209%)	−54.49 (−189%)	1.25%	0.97%	0.67%
5-year										
(0, 0.25]	35.20	63.77	62.07	62.05	−28.57 (−81%)	−26.87 (−76%)	−26.84 (−76%)	2.63%	2.15%	1.63%
(0.25, 1]	60.12	129.01	125.68	125.52	−68.89 (−115%)	−65.55 (−109%)	−65.39 (−109%)	6.17%	5.10%	3.90%
(1, +∞)	89.97	196.16	190.20	186.96	−106.19 (−118%)	−100.23 (−111%)	−96.99 (−108%)	8.92%	7.39%	5.54%
10-year										
(0, 0.25]	62.28	60.77	59.16	58.83	1.51 (2%)	3.12 (5%)	3.45 (6%)	−1.35%	−1.07%	−0.80%
(0.25, 1]	93.55	84.65	81.19	79.41	−22.37 (−24%)	−18.91 (−20%)	−17.13 (−18%)	−4.25%	−3.53%	−2.76%
(1, +∞)	134.89	111.07	106.77	103.77	−48.79 (−36%)	−44.49 (−33%)	−41.49 (−31%)	−9.47%	−7.61%	−5.80%

Table 2.4 Pricing error of the CDS spread and risk-neutral probabilities of default for $w = 2/3$. All the model-implied spreads are calculated setting the loss given default equal to either 50%, 60% or 80%. This allows to jointly test for the effect of the aggregation scheme in the firm's capital structure and on the selected value of LGD. The Table reports the market CDS spread alongside those produced by the model (expressed in basis points) based on the estimates of the firm's asset and volatility on the previous week. The results are clustered based on the maturity of the CDS contract (1, 5, and 10 years) and on the firm's average leverage. A positive/negative pricing error CDS^{mrk} − CDS^{model} indicated that the model under/overpredicts the level of the spread. This is reflected into the over/underprediction of the survival probabilities. Errors are also reported as percentages in brackets. For the probabilities of survival, only percentage errors are reported. Based on leverage, the number of companies in each bucket are $N_{(0,0.25]} = 44$, $N_{(0.25,1]} = 15$, $N_{(1,+\infty)} = 5$.

The second aggregation scheme as in Table 2.3 ($w = 1/3$) further underpredicts short-term spreads of all but highly-levered firms. This is driven by how the default barrier is computed in the compound option model (and common sense): the more debt is due in the distant future, the more likely is the firm to survive at shorter horizons. Seemingly as the previous scheme, it underprices also the long-maturity spread of highly levered firms. The pricing error in the instance of underpricing is around 6 bps; when the model overprices the predicted spreads, the error is about 24 bps.

Finally, the last aggregation scheme in Table 2.4 ($w = 2/3$) consistently overprices short- and medium-term spreads of about 46 bps, whilst underprices long-term spreads of 14 bps. As explained above, this is due by the fact that if $w = 2/3$, the larger fraction of the firm's debt is due at year one and five.

The empirical performance of the compound option model in predicting the one-week-ahead spread based on the selected aggregation scheme and level of loss given default is summarised in Table 2.5. The smallest average absolute mean error (expressed in basis points) is obtained for $w = 1/3$ and LGD = 50%. The same value of loss given default is also employed by Duffie and Singleton (1999) and Huang and Huang (2012). Because most of previous works focus on the 5–years CDS spread as it is the most actively traded in the market, the same average error is checked for that sub-sample. The same conclusion upon the best aggregation scheme is obtained.

In order to compare the ability of the compound option model to price credit spreads, the results reported in Huang and Huang (2012) are used. There, the authors calibrate seven different structural models of default with different desirable features. More specifically, they analyse the performance of the following models: a baseline simple model with and without stochastic interest rates (Longstaff and Schwartz 1995), a model with endogenous default barrier (Leland and Toft 1996), a model with strategic default (Anderson and Sundaresan 1996, Mella-Barral and Perraudin 1997), a model with mean-reverting leverage ratios (Collin-Dufresne and Goldstein 2001), a model with countercyclical market risk premium, and a jump-diffusion model. All the models underpredict credit spreads. Average absolute mean errors are reported in Table 2.6. Similarly, the compound option model ($w = 1/3$ and LGD = 50%) generally underpredicts the spread. However, the extent of the underpricing is much smaller: the proposed model is able to reduce the underpricing to 9.58 bps, whist the pricing errors of other structural models range from 83.19 to 105.67 bps.

Given the extent of the reduction in the pricing error, it is worth stressing further how the model implied spreads were calculated. In terms of market variables, the model spread depends (via the risk-neutral probabilities) on the equity value, the leverage of the company,

the level of interest rates and the asset volatility. The proposed methodology is able to estimate the asset volatility and value at time t using the known capital structure as well as the stock price. Once this volatility is estimated, say $\sigma_{V,t}^{\star}$, it is then used one week ahead to predict the spread. Therefore the spread at time $t + 1$ is essentially a function such as $\widehat{\text{CDS}}_{t+1} = f(S_{t+1}, r_{r+1}, \text{LEV}_{t+1}, \sigma_{V,t}^{\star})$, where the listed variables are the contemporaneous stock price, level of interest rates, leverage and the previous-week asset volatility respectively. As r and LEV are unlikely to vary substantially from week to week, the proposed estimation shows how the equity, alongside the past volatility, is a sufficient statistic for predicting spreads in a compound option model.

However, it may be argued that what is being shown is simply predicting the credit spread at time $t + 1$ with the credit spread at time t. This issue might be very impactful on the analysis as the CDS data do show a significant autoregressive component (which is indeed modelled in the next section). In order to address this concern, the following variables are calculated[2]:

$$X_t = \text{CDS}_t - \text{CDS}_{t-1}, \qquad Y_t = \text{CDS}_t - \widehat{\text{CDS}}_t,$$

where CDS is the observed market spread and $\widehat{\text{CDS}}$ is the spread estimated with the proposed methodology. If this analysis is actually using the past spread to predict the current one, the distributions of X and Y should be, if not identical, relatively similar.

Thus, the two-sample Kolmogorov-Smirnov test is conducted on X and Y for each company in the dataset. Under the null hypothesis X and Y have been drawn from the same distribution. Table 2.7 reports the p-values for each company and for the three tenors (1–, 5– and 10–year). In the case of 1– and 5–year spreads, the null hypothesis is always rejected; for the 10–year spread, there are two companies (namely C and F) for which the test fails to reject the null hypothesis at 5% significance level. Given these results, it can be fairly concluded that the proposed model and estimation technique do not price the contemporaneous spread as the spread realised in the previous period.

To conclude, the sensible reduction in terms of underpricing may suggest that the compound option mechanism is better able at capturing default dynamics that previous models[3]. Better fits are only obtained by Du et al. (2019); however, their model with stochastic asset volatility and jumps is far more complicated to calibrate than the proposed compound option model of default.

---

[2]Given the results discussed in the previous paragraphs, the test is conducted setting LGD = 50% and $w = 1/3$.

[3]Huang and Huang (2012) explicitly decide not to analyse the compound option model in Geske (1977) as "it is not analytically tractable for our calibration approach".

In the next section, the link between credit spreads and the variables which structural models of default predict driving the spreads is investigated. Among these variables, market leverage and equity volatility are used. Given the results of this section, the combination $w = 1/3$ and LGD = 50% is used throughout. Different combinations of the parameters are further tested as a robustness check in Section 2.5.

2.4   Estimating the Cointegration

When regressing credit spread changes on the changes of the variables which structural models of default would predict to influence the spread (as in Collin-Dufresne et al. 2001), if the levels the selected variables are non-stationary and cointegrated, these regressions are misspecified. Moreover, regressions on non-stationary levels (as in Cremers, Driessen, Meanhout and Weinbaum 2008, Ericsson et al. 2009 and Zhang et al. 2009) may lead to spurious correlations. Therefore, it should not be surprising that the regressions on the levels work 'better' than the ones on the changes: despite the OLS estimators being super-consistent, the R^2s and t-statistics are likely to be large even if the underlying variables are not truly correlated. As a consequence, reliable inference cannot be made.

For illustration purposes, Figure 2.1 shows the 5-year CDS spreads, financial leverage and equity volatility (estimated as in (2.4)) for four companies operating in different industries. These variable are evidently non-stationary, also hinting at strong comovemnts. Unit root tests confirm the non-stationarity of all the variables. Identical conclusions are drawn for the other companies in the sample, also if the model-implied market leverage is replaced by book leverage.

Despite the estimation technique for the equity volatility is new, the other variables still display stochastic trends. Hence, if cointegration is present, the appropriate way to model the level of credit spreads is an Error Correction Mechanism. Based on the structural approach of default, the spread is likely to follow upon chances on the firm's financial leverage (D/S) and riskiness (σ_S) and not vice versa. Therefore, the model is implemented à la Engle-Granger instead of using a VECM (that is, only one cointegrating vector is estimated).

Assume the long-run equilibrium equation to be

$$\text{CDS}_{i,t} = \theta_{i,0} + \theta_{i,L}\text{LEV}_{i,t} + \theta_{i,V}\text{VOL}_{i,t} + \varepsilon_{i,t}, \tag{2.6}$$

in which (CDS, LEV, VOL)$_{i,t}$ are, respectively, the CDS spread (for a given maturity), model-implied market leverage (D/S) and equity volatility (σ_S) of firm i at time t. CDS is observed,

All maturities

w	LGD		
	0.50	0.60	0.80
1/2	11.86	24.51	30.00
1/3	9.58	20.14	25.86
2/3	20.99	44.80	55.85

5–year

w	LGD		
	0.50	0.60	0.80
1/2	24.96	49.43	59.25
1/3	16.85	37.66	49.78
2/3	44.08	90.14	110.80

Table 2.5 Average absolute mean errors (expressed in basis points). Considering both all maturities and the 5–year maturity only, which is the most liquid, the error is smallest for the aggregation scheme $w = 1/3$. Also, setting LGD = 0.5 makes the pricing error smallest. As expected, the largest average pricing error is for the scheme $w = 2/3$ which puts a lot of debt expiring in the short-term (which is unlikely to be for most of the companies). Reported figures are weighted averages in which the weights are the number of company in each leverage bucket.

Structural Model	AAME
Baseline	89.49
Baseline plus stochastic interest rates	105.67
Endogenous default barrier	86.27
Strategic default	76.89
Mean-reverting leverage ratios	93.25
Countercyclical market risk premium	83.19
Jump-diffusion	84.78

Table 2.6 Average absolute mean errors (expressed in basis points) based on the results in Huang and Huang (2012). There the authors analyse the ability of structural models of default to reproduce observed credit spreads. They test: a simple baseline model with and without stochastic interest rates (Longstaff and Schwartz 1995), a model with endogenous default barrier (Leland and Toft 1996), a model with strategic default (Anderson and Sundaresan 1996, Mella-Barral and Perraudin 1997), a model with mean-reverting leverage ratios (Collin-Dufresne and Goldstein 2001), a model with countercyclical market risk premium, and a jump-diffusion model. A loss given default parameter of 48.69% is used by the authors for their calibration.

	1–year	5–year	10–year		1–year	5–year	10–year
AAPL	0.0000	0.0000	0.0000	LLY	0.0000	0.0000	0.0000
ABT	0.0000	0.0000	0.0000	LOW	0.0000	0.0000	0.0000
ALL	0.0000	0.0000	0.0000	MCD	0.0000	0.0000	0.0000
AMGN	0.0000	0.0000	0.0000	MDT	0.0000	0.0000	0.0000
BA	0.0000	0.0000	0.0000	MMM	0.0000	0.0000	0.0000
BAC	0.0000	0.0000	0.0003	MO	0.0000	0.0000	0.0000
BMY	0.0000	0.0000	0.0000	MON	0.0000	0.0000	0.0000
C	0.0000	0.0000	0.1693	MRK	0.0000	0.0000	0.0000
CAT	0.0000	0.0000	0.0000	MS	0.0000	0.0000	0.0000
CL	0.0000	0.0000	0.0000	MSFT	0.0000	0.0000	0.0000
CMCSA	0.0000	0.0000	0.0000	ORCL	0.0000	0.0000	0.0000
COF	0.0000	0.0000	0.0002	OXY	0.0000	0.0000	0.0000
COP	0.0000	0.0000	0.0000	PEP	0.0000	0.0000	0.0000
COST	0.0000	0.0000	0.0000	PFE	0.0000	0.0000	0.0000
CSCO	0.0000	0.0000	0.0000	PG	0.0000	0.0000	0.0000
CVS	0.0000	0.0000	0.0000	PM	0.0000	0.0000	0.0000
CVX	0.0000	0.0000	0.0000	RTN	0.0000	0.0000	0.0000
DD	0.0000	0.0000	0.0000	SLB	0.0000	0.0000	0.0000
DIS	0.0000	0.0000	0.0000	SO	0.0000	0.0000	0.0000
EMR	0.0000	0.0000	0.0000	SPG	0.0000	0.0000	0.0000
EXC	0.0000	0.0000	0.0019	T	0.0000	0.0000	0.0000
F	0.0000	0.0000	0.0767	TGT	0.0000	0.0000	0.0000
FDX	0.0000	0.0000	0.0000	TWX	0.0000	0.0000	0.0000
GD	0.0000	0.0000	0.0000	TXN	0.0000	0.0000	0.0000
GE	0.0000	0.0000	0.0000	UNH	0.0000	0.0000	0.0000
HAL	0.0000	0.0000	0.0000	UNP	0.0000	0.0000	0.0000
HD	0.0000	0.0000	0.0000	USB	0.0000	0.0000	0.0000
IBM	0.0000	0.0000	0.0000	UTX	0.0000	0.0000	0.0000
INTC	0.0000	0.0000	0.0000	VZ	0.0000	0.0000	0.0000
JNJ	0.0000	0.0000	0.0000	WFC	0.0000	0.0000	0.0002
JPM	0.0000	0.0000	0.0067	WMT	0.0000	0.0000	0.0000
KO	0.0000	0.0000	0.0000	XOM	0.0000	0.0000	0.0000

Table 2.7 p-values of the two-sample Kolmogorov-Smirnov test on X and Y in order to ascertain that the proposed methodology does not predict CDS_{t+1} as CDS_t. The null hypothesis of X and Y been drawn from the same distribution is rejected for every company and tenor of the CDS, with the exception of two companies for which the test fails to reject the null hypothesis at 5% significance level in the case of the 10-year spread.

whist LEV and VOL are estimated as in (2.4). Unreported results, available upon request, shows that the same conclusions discussed below are obtained using firms' book leverage. As, ultimately, default times are driven by the value of the equity at reimbursement dates, the volatility of the equity is used in the cointegration equation.

These are the variables that structural models of default predict as determinants of default probabilities and, therefore, credit spreads. If the variables are are random walks and cointegrated, then the error term $\varepsilon_{i,t}$ is stationary for all i. Figure 2.2 plots the residuals of the regressions (2.6) for the same four companies taken into consideration in Figure 2.1. Visual inspection, supported by unit root tests, confirms the presence of cointegration between the CDS spreads, leverage, and volatility. This should not come as a surprise as structural model of defaults identify these variables as the drivers of credit spreads. What comes as a surprise is how previous research has never attempted at explaining this link via an Error Correction Mechanism. Same conclusions regarding the existence of a cointegrating vector apply to the whole sample of firms, as well as to CDS spreads for different maturities.

The autoregressive distributive lag, ARDL$(1, 1, 1)$, dynamic panel specification of (2.6) (with exogenous variables) is defined as

$$\text{CDS}_{i,t} = \alpha_i + \phi_i \text{CDS}_{i,t-1} + \beta_{i,0} \text{LEV}_{i,t} + \beta_{i,1} \text{LEV}_{i,t-1} + \gamma_{i,0} \text{VOL}_{i,t} + \gamma_{i,1} \text{VOL}_{i,t-1} + \boldsymbol{\xi}^\top \Delta \mathbf{X}_t + \eta_{i,t},$$

$$(2.7)$$

and the error correction reparameterization of (2.7) is

$$
\begin{aligned}
\Delta \text{CDS}_{i,t} &= \lambda_i \left(\text{CDS}_{i,t-1} - \theta_{i,0} - \theta_{i,L} \text{LEV}_{i,t-1} - \theta_{i,V} \text{VOL}_{i,t-1} \right) + \beta_{i,0} \Delta \text{LEV}_{i,t} + \gamma_{i,0} \Delta \text{VOL}_{i,t} \\
&\quad + \boldsymbol{\xi}^\top \Delta \mathbf{X}_t + \eta_{i,t} \\
&= \lambda_i \varepsilon_{i,t-1} + \beta_{i,0} \Delta \text{LEV}_{i,t} + \gamma_{i,0} \Delta \text{VOL}_{i,t} + \boldsymbol{\xi}^\top \Delta \mathbf{X}_t + \eta_{i,t}
\end{aligned}
$$

$$(2.8)$$

where $\lambda_i = -(1 - \phi_i)$, $\theta_{i,0} = \frac{\alpha_i}{1-\phi_i}$, $\theta_{i,L} = \frac{\beta_{i,0}+\beta_{i,1}}{1-\phi_i}$, and $\theta_{i,V} = \frac{\gamma_{i,0}+\gamma_{i,1}}{1-\phi_i}$. The parameter λ_i is the error-correcting speed of adjustment term. If $\lambda_i = 0$, then there would be no evidence for a long-run relationship. This parameter is expected to be significantly negative under the prior assumption that the variables show a return to a long-run equilibrium. Of particular importance is the vector $\boldsymbol{\theta} = (\theta_L, \theta_V)$, which contains the long-run relationships between the variables driving the spreads.

Following Collin-Dufresne et al. (2001), exogenous variables, in changes ($\Delta \mathbf{X}$), are also added. These are the change in level, slope and curvature of the term structure of interest rates, the log-return on the S&P500, and the change in the CBOE Skew Index.
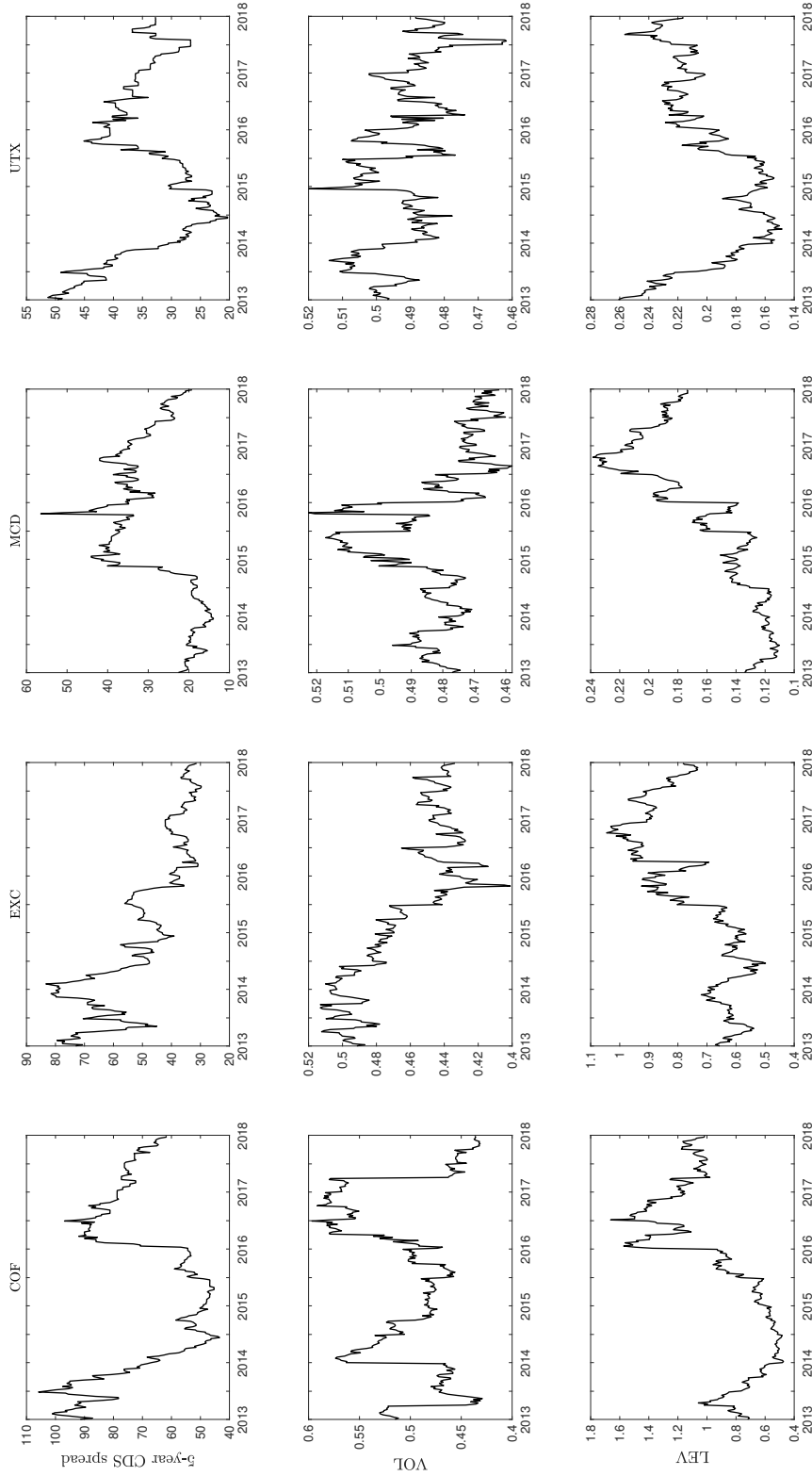
Fig. 2.1 Time-series of the 5-year CDS spreads (top), equity volatility (middle) and financial leverage (bottom) estimated as in (2.4) for four different companies: Capital One Financial (Financials), Exelon (Mining, Energy and Utilities), Mcdonald's (Retail, Wholesale and Services), and United Technologies (Manufacturing). Visual inspection suggest non-stationarity and a strong comovement of the three variables. The non-stationarity of the time-series is confirmed by unit root tests.

(a) Financials

(b) Mining, Energy and Utilities

(c) Retail, Wholesale and Services
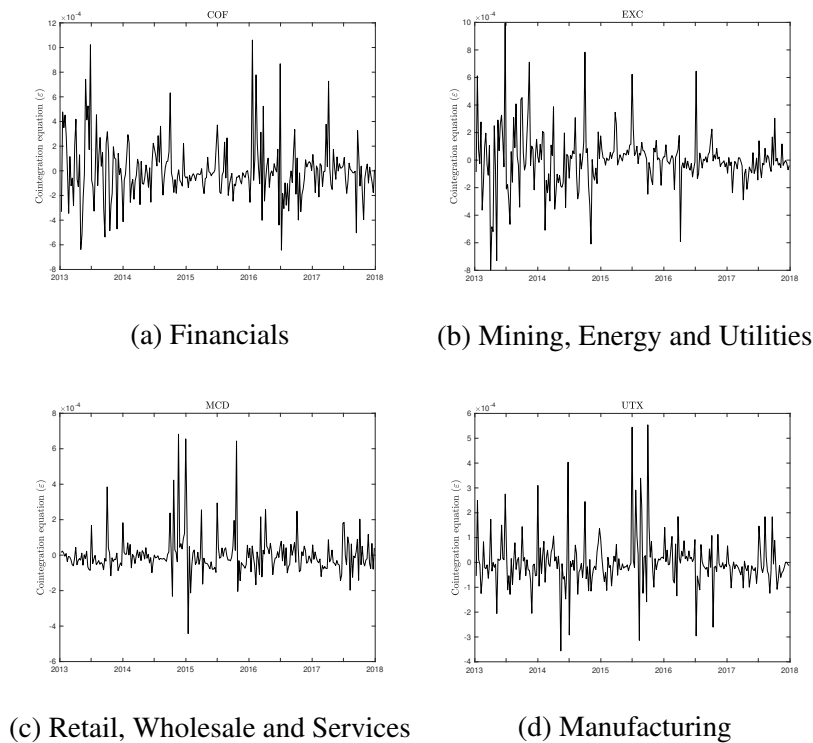
(d) Manufacturing

Fig. 2.2 Cointegration equations (residuals of regression (2.6)) for four different companies: Capital One Financial (Financials), Exelon (Mining, Energy and Utilities), Mcdonald's (Retail, Wholesale and Services), and United Technologies (Manufacturing). Visual inspection suggest stationarity, therefore cointegration of CDS spreads, leverage, volatility and the Treasury yield. Unit root tests confirm the stationarity of the residuals.

The level of interest rates is defined as the Treasury yield for 5 years maturity. The slope of the term structure is defined as the difference between between 5-year and 1-year Treasury yields. Although the spot rate is the only interest-rate-sensitive factor that appears in the firm value process, the spot rate process itself may depend upon other factors as well. For example, Litterman and Scheinkman (1991) find that the two most important factors driving the term structure of interest rates are the level and slope of the term structure. To capture potential nonlinear effects due to convexity, the squared level of the 5-year spot rate is also added as proxy for the curvature.

Similarly, the return on the S&P500 is used to proxy for the state of the economy. In fact, even if the probability of default remains constant for a firm, changes in credit spreads can occur due to changes in the expected recovery rate. The expected recovery rate in turn should be a function of the overall business climate.

Lastly, adding the changes in the CBOE Skew Index aims at capturing the changes in the probability and magnitude of a large negative systematic jump, which ultimately would

affect the firm value. Recent research (Zhou 2001, Zhang et al. 2009, Du et al. 2019) has in fact shown the crucial importance of allowing for jumps in the firm value process in order to explain short-term credit spreads[4].

The choice of the variables (both endogenous and exogenous) mirrors the ones in Collin-Dufresne et al. (2001). However, three major differences need to be highlighted. First, here an ECM is estimated thus adding an additional stationary variable (the long-run equilibrium equation) to the regression in the spread changes. Secondly, the proposed calibration allows to estimate a firm-specific volatility (of both assets and equity), whilst they need to rely on a market-wide measure of volatility, namely the changes in the VIX index. Finally, the proxy for the downward jump risk employed here is different[5].

The linear relationship described in (2.6) serves as a first approximation for the link between the variable mentioned above which, based on (2.2), is highly non-linear. Also, as this analysis is going to be compared with other works in the literature that make use of linear regression for investigating the link between credit spreads and the variables predicted by structural models of default to influence the spread, it seems the most reasonable functional form to implement. Unreported results show however that the same cointegrating mechanism is also present for the several monotonically increasing transformations of the variables (square, logarithm, etc). The purpose of the ECM analysis is to document the cointegration between these variables which has been ignored in the literature so far without necessarily claiming that the link between the variables is exactly linear.

The estimation of the coefficients in (2.8) is carried through using the PMG estimator proposed by Pesaran et al. (1999) which allows for heterogeneous short-run dynamics and common long-run equilibrium. Tables 2.8, 2.9 and 2.10 report the estimates of the long-run equilibrium equation in (2.6) and the short-term adjustment in (2.8). All the coefficients have the predicted sign and are highly statistically significant.

Most of the results are qualitatively identical when 1-, 5- and 10-year spreads are used. For what concerns the long-run equilibrium, both volatility and leverage display a positive and statistically significant loading: an increase in either VOL or LEV lead to a larger level of the spread in the long-run. Focusing on the short-term adjustment, changes in both the firm's equity volatility and its financial leverage increase the change in the spread. In terms of economic significance, an increase of 1% in the firm's volatility increases the CDS spread

---

[4]CBOE Skew Index is a strike independent measure of the slope of the implied volatility curve that increases as this curve tends to steepen. The index is calculated from the price of a tradable portfolio of out-of-the money S&P 500 options, similar to the VIX Index.

[5]They autonomously calculate a measure of skew based on implied volatilities od options on the S&P 5000 futures. Here the CBOE Skew Index is used.

1–year CDS spread

Long-run equilibrium

	Coefficient	t–stat	p–value	
VOL	0.0028	9.88	0.000	***
LEV	0.0024	14.45	0.000	***

Short-term adjustment

	Coefficient	t–stat	p–value	
ε	−0.1005	−11.52	0.000	***
ΔVOL	0.0074	6.29	0.000	***
ΔLEV	0.0036	5.23	0.000	***
ΔLevel	−0.0566	−4.55	0.000	***
ΔSlope	0.0213	4.56	0.000	***
ΔCurvature	1.2409	3.77	0.000	***
$\Delta\ln$(S&P500)	−0.0013	−5.13	0.000	***
ΔSkew	5E-07	2.37	0.018	**
Constant	−0.0001	−9.66	0.000	***

Table 2.8 ECM for 1–year CDS spreads. All the variables which structural models predict to influence the change in spreads are statistically significant and have the predicted signs. The loading on the cointegrating equation (ε) is negative and statistically significant, thus confirming the existence of a long-term equilibrium which spreads, volatility and leverage converge to. This model constrains the long-run coefficient vector to be equal across panels while allowing for group-specific short-run and adjustment coefficients. The averaged short-run parameter estimates are reported.
Number of observations: 16,640; number of groups: 64; observations per group: 260.
Significance levels: 10% (*), 5% (**), 1% (***).

5–year CDS spread

Long-run equilibrium

	Coefficient	t–stat	p–value	
VOL	0.0225	17.13	0.000	***
LEV	0.0159	15.54	0.000	***

Short-term adjustment

	Coefficient	t-stat	p-value	
ε	−0.0293	−9.60	0.000	***
ΔVOL	0.0252	10.39	0.000	***
ΔLEV	0.0114	7.69	0.000	***
ΔLevel	−0.0975	−4.90	0.000	***
ΔSlope	0.0346	3.42	0.001	***
ΔCurvature	1.8381	3.69	0.000	***
$\Delta\ln$(S&P500)	−0.0025	−5.71	0.000	***
ΔSkew	−6E-07	−1.84	0.065	*
Constant	−0.0003	−9.75	0.000	***

Table 2.9 ECM for 5–year CDS spreads. All the variables which structural models predict to influence the change in spreads are statistically significant and have the predicted signs. The loading on the cointegrating equation (ε) is negative and statistically significant, thus confirming the existence of a long-term equilibrium which spreads, volatility and leverage converge to. This model constrains the long-run coefficient vector to be equal across panels while allowing for group-specific short-run and adjustment coefficients. The averaged short-run parameter estimates are reported.
Number of observations: 16,640; number of groups: 64; observations per group: 260.
Significance levels: 10% (*), 5% (**), 1% (***).

10–year CDS spread
Long-run equilibrium

	Coefficient	*t*–stat	*p*–value	
VOL	0.0335	49.94	0.000	***
LEV	0.0335	28.24	0.000	***

Short-term adjustment

	Coefficient	*t*–stat	*p*–value	
ε	−0.0275	−5.18	0.000	***
ΔVOL	0.0399	15.01	0.000	***
ΔLEV	0.0168	7.86	0.000	***
ΔLevel	−0.1129	−4.95	0.000	***
ΔSlope	0.0242	2.31	0.021	**
ΔCurvature	2.2031	3.98	0.000	***
Δln(S&P500)	−0.0027	−5.41	0.000	***
ΔSkew	−9E-07	−2.86	0.004	***
Constant	−0.0004	−5.31	0.000	***

Table 2.10 ECM for 10–year CDS spreads. All the variables which structural models predict to influence the change in spreads are statistically significant and have the predicted signs. The loading on the cointegrating equation (ε) is negative and statistically significant, thus confirming the existence of a long-term equilibrium which spreads, volatility and leverage converge to. This model constrains the long-run coefficient vector to be equal across panels while allowing for group-specific short-run and adjustment coefficients. The averaged short-run parameter estimates are reported.
Number of observations: 16,640; number of groups: 64; observations per group: 260.
Significance levels: 10% (*), 5% (**), 1% (***).

of 0.7, 2.5 and 4 bps for one, five and ten year's maturity respectively. Similarly, an identical change in the firm's financial leverage induces the spread to increase of 0.4, 1.1 and 1.7 bps, *ceteris paribus*. Thus, when considering the short-term adjustment, changes in the variable driving the long-equilibrium have an impact on the spreads which increases with the maturity of the CDS contract.

For what concerns the set of exogenous variables, all the variables display significant coefficients. First, the changes in the level of interest rates have a negative impact on the credit spread: as pointed out by Longstaff and Schwartz (1995), the static effect of a higher spot rate is to increase the risk-neutral drift of the firm value process. A higher drift reduces the probability of default, and in turn, reduces the credit spreads. Duffee (1998) obtain similar results. Likewise, the positive coefficients of the changes on the slope and curvature of the term structure are consistent with the findings of previous studies. As a decrease in yield curve slope may imply a weakening economy, it is reasonable to believe that the expected recovery rate might decrease in times of recession. Therefore, this would further decrease the credit spreads. Also, positive returns in the S&P500 – which accounts for growing economy and therefore an increasing expected recovery rate – have the effect to reduce the spread as suggested by economic intuition.

Finally, the coefficient reflecting the effect of systematic downward jumps (proxied as changes in the CBOE Skew Index) is the only estimate whose sign differs between short- versus medium- and long-term spreads. As shown in Zhou (2001), Zhang et al. (2009) and Du et al. (2019), jumps are necessary to explain the level of short-term spreads: structural models which account only for diffusive shocks in the asset value process imply zero instantaneous probability of default and therefore cannot meet the observed level of 6-month and 1-year spreads. Hence, the coefficient of ΔSkew is positive for 1-year spread changes as expected.

An increase in the probability of a negative systematic jump translates into larger shot-term spreads. However, for longer maturities the the coefficient is negative. This apparently countintuitive result can be easily explained by how systematic negative jumps affect firms. If such event occurs, the ability of firms to repay its debt affects those liabilities expiring in the immediate future. This is what is observed for spreads with 1-year maturity. Conversely, if the firms survives the shot-term shock, it is more likely to be able to survive to futures shocks. Thus medium- and long-term spreads lower. Also, it is worth highlighting that, in the case of 5-year spreads, the impact of negative jumps is only marginally significant.

To conclude, a further analysis of the cointegration mechanism between spreads, volatility and financial leverage is discussed. As expected, the estimated coefficient of the long-run equation (ε) is negative, within the unit circle and statistically significant. The closer the estimate is to zero, the slower is the adjustment[6]. As expected, the size of the coefficient is larger, in absolute value, for shorter maturities: short-term spreads adjust faster to shocks in the firm's volatility and leverage. The associated t–statistic is also larger for 1–year spread changes. Conversely, the degree of cointegration becomes stronger at longer horizons: the t–statistics of the long-run equilibrium equation increase with the maturity of the CDS.

To quantify the speed of convergence towards the long-run equilibrium, half–life statistics can be considered. The estimated negative loading of the cointegrating equation, $\hat{\lambda}$, in (2.8) signifies that $-100 \cdot \hat{\lambda}\%$ of that disequilibrium is dissipated before the next time period and $-100 \cdot (1 - \hat{\lambda})\%$ remains. It is often of interest to estimate how long it will take for an existing disequilibrium to be reduced by 50% (half–life of disequilibrium), that is

$$\text{half–life} = \frac{\ln(0.5)}{\ln(\hat{\lambda} - 1)}.$$

The estimated half–lives are 6.5, 23.3 and 24.9 weeks for the 1–, 5– and 10–year CDS spread respectively. This highlights a significantly different behaviour of the short versus the

---

[6]Symmetrically, the closer to -1 the faster the adjustment. If $\lambda = -1$, there is full correction in 1 period, and if $\lambda < -1$ there is overshooting, that is an oscillatory adjustment dynamic. If $\lambda > 0$, there is not cointegration, that is the disequilibrium expands.

medium and long-term spreads: the short 1-year spreads reacts about four time faster than the 5- and 10-year spreads in order to realign to equilibrium. This finding is not surprising as, given the shorter maturity, the spread should be expected to vary as quickly as possible with the changes in the firm's leverage and volatility.

The cointegrating mechanism is also able to enhance the fit of the regressions on the spreads as compared with Collin-Dufresne et al. (2001) and other studies. For each firm i, the adjusted–R^2s of the short-term adjustment is calculated and reported in Table 2.11. Average adjusted–R^2s of 69%, 45% and 30% are obtained for 1–, 5– and 10–years spread changes. These numbers are significantly larger that the 26% (shot-maturity) and 21% (long-maturity) obtained by Collin-Dufresne et al. (2001). The results in Cremers, Driessen, Meanhout and Weinbaum (2008) are not directly comparable as the authors opt for regressing credit spread levels instead of changes onto similar sets of variables (still in levels)[7]. As the goodness-to-fit of the ECM model is evidently superior to the ones of a simple regression on changes, this provides extra evidence of the importance of a long-run equilibrium dynamic which must be taken into account to correctly identify how credit spreads change.

These promising results could be however driven by over-fitting: as the volatility is obtained using the compound option model so to match the other market variables, the cointegrating mechanism could have been induced by the estimation methodology. In order to remove any doubt, the volatility estimated from the spread and the stock price is replaced by the option-implied volatility. More specifically, for each date the option implied volatility surface is obtained from the most liquid[8] out-of-the-money put options, and its average is used. The rational for focusing on put options is due to the fact part of the option skew displayed by equity option is attributable to the leverage effect (Carr and Wu 2017). Therefore the information conveyed by the implied volatility in the put region may have some relevance for the pricing of credit risk (Carr and Wu 2011, Maglione 2019). Results are reported in Tables 2.12, 2.13 and 2.14.

Even when the implied volatility is used, the triplet spread, leverage, volatility still shows a statistically significant cointegration. However, using the average implied volatility of put options has a significant impact in the short-term adjustment dynamics: changes in the implied volatility are significant (at 10% significance level) only for the 1–year spread. Considering that most of equity options available in the market have maturity less than one year, the loss of significance for the 5– and 10–year spread should not surprise: the changes in

---

[7]Their adjusted–R^2s are 33% (short-maturity) and 52% (long-maturity). However, having regressed non-stationary variables, the goodness to fit is driven by the stochastic trends rather than a real correlation between the variables.

[8]Only out-of-the-money put options with daily trading volume above the annual mean volume are selected.

ticker	1–year	5–year	10–year		Ticker	1–year	5–year	10–year
	adj–R^2					adj–R^2		
AAPL	0.81	0.42	0.01		LLY	0.71	0.44	0.40
ABT	0.86	0.36	0.24		LOW	0.76	0.74	0.07
ALL	0.56	0.22	0.22		MCD	0.32	0.22	0.05
AMGN	0.62	0.38	0.30		MDT	0.92	0.88	0.79
BA	0.58	0.51	0.16		MMM	0.81	0.82	0.57
BAC	0.49	0.26	0.21		MO	0.65	0.41	0.19
BMY	0.71	0.29	0.15		MON	0.87	0.57	0.54
C	0.45	0.27	0.23		MRK	0.81	0.77	0.35
CAT	0.52	0.13	0.08		MS	0.63	0.53	0.50
CL	0.85	0.74	0.20		MSFT	0.90	0.59	0.15
CMCSA	0.57	0.20	0.13		ORCL	0.84	0.60	0.68
COF	0.87	0.72	0.73		OXY	0.71	0.33	0.14
COP	0.34	0.10	0.07		PEP	0.91	0.61	0.36
COST	0.89	0.89	0.87		PFE	0.64	0.43	0.19
CSCO	0.74	0.66	0.62		PG	0.86	0.82	0.20
CVS	0.75	0.57	0.24		PM	0.86	0.74	0.33
CVX	0.80	0.08	0.05		RTN	0.53	0.16	0.04
DD	0.66	0.39	0.43		SLB	0.36	0.12	0.05
DIS	0.77	0.46	0.32		SO	0.39	0.70	0.11
EMR	0.52	0.65	0.36		SPG	0.29	0.10	0.08
EXC	0.94	0.69	0.40		T	0.63	0.18	0.17
F	0.55	0.36	0.31		TGT	0.80	0.70	0.41
FDX	0.71	0.54	0.45		TWX	0.61	0.25	0.19
GD	0.81	0.81	0.76		TXN	0.81	0.40	0.44
GE	0.89	0.91	0.90		UNH	0.67	0.28	0.06
HAL	0.22	0.09	0.10		UNP	0.54	0.18	0.06
HD	0.79	0.55	0.33		USB	0.69	0.28	0.38
IBM	0.59	0.29	0.24		UTX	0.76	0.40	0.17
INTC	0.88	0.07	0.05		VZ	0.62	0.32	0.24
JNJ	0.77	0.50	0.47		WFC	0.62	0.53	0.52
JPM	0.57	0.41	0.39		WMT	0.71	0.33	0.09
KO	0.73	0.80	0.57		XOM	0.83	0.35	0.20

	1–year	5–year	10–year
	adj–R^2		
Mean	0.69	0.45	0.30
Median	0.71	0.41	0.24
Min	0.22	0.07	0.01
Max	0.94	0.91	0.90

Table 2.11 Adjusted R^2s of the firm-specific time-series regressions in (2.8) (short-term adjustments). As shown by both the mean and median adjusted R^2, the explanatory power of the variables which should affect credit spread changes as predicted by structural models diminishes with the maturity of the spread.

1–year CDS spread

Long-run equilibrium

	Coefficient	*t*–stat	*p*–value	
IV	0.0008	3.77	0.000	***
LEV	0.0025	12.18	0.000	***

Short-term adjustment

	Coefficient	*t*–stat	*p*–value	
ε	−0.1063	−9.79	0.000	***
ΔIV	0.0002	1.83	0.067	*
ΔLEV	0.0012	1.42	0.156	
ΔLevel	−0.0390	−1.90	0.057	*
ΔSlope	0.0318	3.17	0.002	***
ΔCurvature	0.5474	1.41	0.157	
Δln(S&P500)	−0.0020	−5.22	0.000	***
ΔSkew	4E-07	1.35	0.176	
Constant	0.0001	2.31	0.000	***

Table 2.12 ECM for 1–year CDS spreads using the average implied volatility of put options instead of σ_S. Similar results are obtained; however, the implied volatility is significant only at the 10% significance level in the short-term adjustment equation. Also ΔLEV, ΔCurvature and ΔSkew have become insignificant, and ΔLevel is significant at the 10% significance level only.
Number of observations: 16,640; number of groups: 64; observations per group: 260.
Significance levels: 10% (*), 5% (**), 1% (***).

5–year CDS spread

Long-run equilibrium

	Coefficient	*t*–stat	*p*–value	
IV	0.0147	8.67	0.000	***
LEV	0.0038	7.18	0.000	***

Short-term adjustment

	Coefficient	*t*-stat	*p*-value	
ε	−0.0360	−10.68	0.000	***
ΔIV	0.0002	0.91	0.361	
ΔLEV	0.0027	1.93	0.053	*
ΔLevel	−0.1099	−2.19	0.028	**
ΔSlope	0.0886	2.71	0.007	***
ΔCurvature	1.1884	1.74	0.081	*
Δln(S&P500)	−0.0045	−5.87	0.000	***
ΔSkew	−1E-06	−1.90	0.057	*
Constant	−6E-06	−0.49	0.623	

Table 2.13 ECM for 5–year CDS spreads using the average implied volatility of put options instead of σ_S. Similar results are obtained; however, the implied volatility is not significant in the short-term adjustment equation. Also ΔLEV, ΔCurvature and ΔSkew are significant at the 10% significance level only, and ΔLevel is significant at the 5% significance level only.
Number of observations: 16,640; number of groups: 64; observations per group: 260.
Significance levels: 10% (*), 5% (**), 1% (***).

10–year CDS spread
Long-run equilibrium

	Coefficient	t–stat	p–value	
IV	0.0312	11.43	0.000	***
LEV	0.0285	17.22	0.000	***

Short-term adjustment

	Coefficient	t–stat	p–value	
ε	−0.0277	−5.82	0.000	***
ΔIV	−2E-05	−0.09	0.931	
ΔLEV	0.0017	1.07	0.283	
ΔLevel	−0.1190	−2.24	0.025	**
ΔSlope	0.0814	2.14	0.032	**
ΔCurvature	1.6594	2.06	0.039	**
$\Delta\ln$(S&P500)	−0.0055	−5.78	0.000	***
ΔSkew	−2E-06	−2.31	0.021	**
Constant	−0.0001	−5.43	0.000	***

Table 2.14 ECM for 10–year CDS spreads using the average implied volatility of put options instead of σ_S. Similar results are obtained; however, neither the implied volatility nor leverage are significant in the short-term adjustment equation. Also ΔLevel, ΔSlope, ΔCurvature and ΔSkew are significant at the 5% significance level only.
Number of observations: 16,640; number of groups: 64; observations per group: 260.
Significance levels: 10% (*), 5% (**), 1% (***).

the (short-term) implied volatility does not explain the reversion to the long-run equilibrium of medium and long term spreads. Nontheless, the cointegration among the variables is still present even though the model-implied volatility is replaced by the option implied volatility.

These results, alongside the good pricing errors obtained via a compound option model of default in Section 2.3, support the importance and ability of structural models in modelling default as well as in explaining the level and changes of credit spreads.

2.5   Robustness Checks

Despite the proposed cointegration displays much larger adjusted R^2s than previous works, the goodness of this approach is further investigated via principal components analysis (PCA), in a similar fashion of Cremers, Driessen, Meanhout and Weinbaum (2008). However, it is worth highlighting that the PCA conducted herein is on the CDS spread changes, whist Cremers, Driessen, Meanhout and Weinbaum (2008) do in on the levels. Based on the same arguments on the non-stationary of credit spreads discussed in the previous section, PCA should always be implemented on i.i.d. data (the changes) and not on random walks

(the levels). Also, they look at raw credit spreads, whilst PCA requires demeaned variables to be used[9].

PCA aims at studying the extent to which the selected set of variables in (2.8) capture systematic credit-spread variations. PCA is in fact an effective tool for analysing the cross-sectional variation of the spread changes, thus searching for common 'factors' (the components) which should affect credit spread changes regardless of firm-specific characteristics.

First, the first ten principal components (PCs) from the demeaned credit spreads changes are extracted for both the 1-, 5-, and 10-year maturities. Figure 2.3 shows the scree plots for the first ten components. The spread changes for different maturities have similar principal components and display the kink around the 3rd/4th component. Overall, the first component explains 25-35% of the total variance of the spread changes; the second component explains around 15%; the third component explains around 10%; the forth component explains less then 10%. That is, in total the first four component explain only about 60% of the total variance of the CDS spread changes. The fact that the first four component explain relatively little of the total variance points towards the possibility that variables influencing spread changes are firm-specific (as leverage and firm's volatility) rather than systematic. This, alongside the successful cointegrating analysis, further support the validity of structural model of default to explain credit spreads.

Secondly, credit spread changes for each company are regressed on an increasing set of PCs. For each set of PCs, the average adjusted–R^2 (and its standard deviation) are reported[10]. Then, the same set of PCs is regressed onto the residuals of (2.8). If the variables used to explain credit spread changes are not capturing systematic variations, large incremental adjusted–R^2 should be found from the regression of the residuals.

In general, average adjusted–R^2s of the regressions of PCs on both the spread changes and on the residual of the short-term adjustment (2.8) are around 10%, thus signalling a very modest impact of systematic factors in explaining the cross-sectional variation of spread changes. The presence of a systematic factor related to the first principal components appears to be slightly more important for the medium- and long-term spreads. This could relate to how jump risk affect CDS spread changes for longer maturities. Perhaps, using the change in the CBOE Skew as a proxy for large jumps in the firms' asset value is appropriate only when considering short-term spreads. This conjecture is based on the fact the average

---

[9]For further details on PCA, see Jolliffe (2002).

[10]Cremers, Driessen, Meanhout and Weinbaum (2008) report simple R^2 instead of its adjusted correction for number of regressor. This is incorrect as adding extra regressor is likely to increase the R^2, but not the adjusted–R^2, even when the variable (here the PC) is not statistically significant.
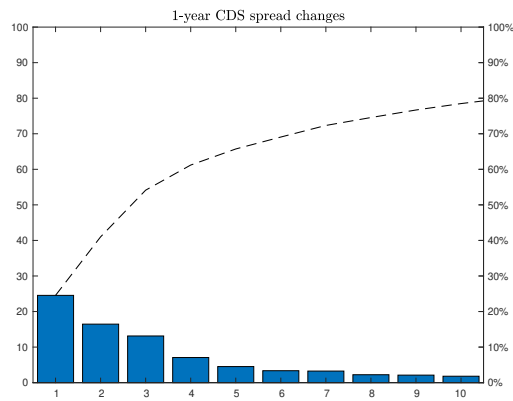
(a) Scree plot for the first 10 PCs of the 1–year spread changes
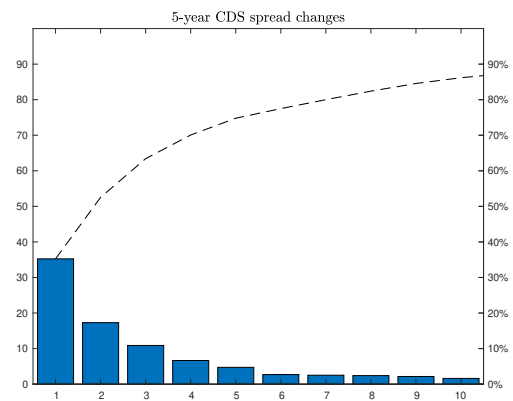
(b) Scree plot for the first 10 PCs of the 5–year spread changes
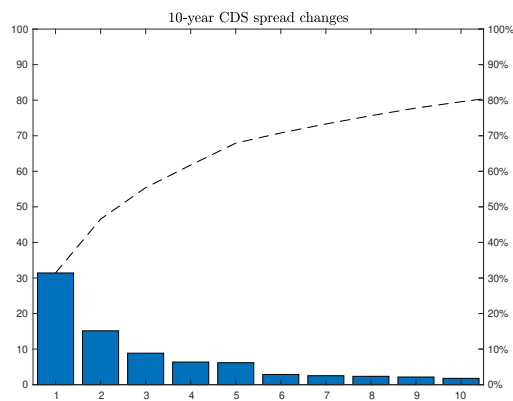
(c) Scree plot for the first 10 PCs of the 10–year spread changes

Fig. 2.3 Scree plots for the first 10 PCs of the demeaned 1–, 5–, and 10–year CDS spread changes. The spread changes for different maturities have similar principal components and display the kink around the 3rd/4th component. Overall, the first component explains 25-35% of the total variance of the spread changes; the second component explains around 15%; the third component explains around 10%; the forth component explains less then 10%. The first 10 PCs are able to explain 80% of the total variance for 1– and 10–year spread changes, and almost 90% of the total variance for the 5–year spread changes. However, the first four are able to explain only about 60% of the total variance.

adjusted R^2 of the regression of the first component onto the 5-year residuals is actually larger than the average adjusted R^2 of the regression on the changes. Somehow, the short-term adjustment regression induces systematic risk in the residuals: the main difference between regression (2.8) estimated on the 5- and 10-year spread changes is the impact of jumps, whose estimated coefficients also display the opposite sign. Alternatively, there is a systematic factor which the model is ignoring[11]; however, it would account only for a very small fraction of the cross-sectional variation of the CDS spread changes of longer maturities.

As last robustness check, the error correction parametrization in (2.8) is re-estimated for different values of the loss given default. Table 2.16 reports the results. All the conclusions obtained in the previous section remain valid.

2.6   Conclusions

This paper develops a new estimation technique for the unobservable firm's asset value and volatility which relies only on the observable equity value, risk-neutral probability of default and the face value of the firm's debt.

The estimated parameters are first used to test the ability of model to reprice CDS spreads out-of-sample. The pricing errors produced by the compound option model of default are then compared with those generated by the structural models in Huang and Huang (2012). The compound option model sensibly outperforms the other models, being able to reduce the pricing error by almost 90%.

Secondly, the estimated parameters are used to investigate the existence of cointegration between credit spreads and those variables which structural models of default predict driving their level. Estimations confirm the presence of an error-correction mechanism which leads to a long-equilibrium between the level of the spreads, financial leverage and the volatility of the firm's equity. Once the cointegration equation is accounted for, the goodness-to-fit of the regressions on the changes improves substantially compared to previous studies.Finally, principal component analysis is employed to study the cross-sectional variation of credit spread changes.

In conclusion, a structural model where equity is modelled as a compound option provides substantial improvement in predicting spreads out-of-sample, thus suggesting its superior ability in capturing firms' default dynamics. Most importantly, this work is the first to document the cointegration between CDS spreads, financial leverage and the firm's risk in a large panel of US firms. Once the cointegration equation is added to the regressions on credit

---

[11]This could be a liquidity factor for the CDS market.

1–year CDS spread

PCs	ΔCDS		η	
	mean adj–R^2	st. dev. adj–R^2	mean adj–R^2	st. dev. adj–R^2
1	0.089	0.202	0.068	0.166
2	0.087	0.211	0.068	0.182
3	0.110	0.261	0.086	0.220
4	0.071	0.189	0.079	0.209
5	0.073	0.200	0.085	0.224
6	0.062	0.189	0.069	0.205
7	0.059	0.179	0.069	0.220
8	0.047	0.165	0.065	0.207
9	0.039	0.153	0.069	0.219
10	0.032	0.141	0.062	0.200

5-year CDS spread

PCs	ΔCDS		η	
	mean adj–R^2	st. dev. adj–R^2	mean adj–R^2	st. dev. adj–R^2
1	0.115	0.239	0.125	0.274
2	0.076	0.218	0.098	0.261
3	0.080	0.227	0.095	0.250
4	0.088	0.232	0.092	0.243
5	0.078	0.217	0.089	0.248
6	0.065	0.180	0.068	0.208
7	0.058	0.176	0.070	0.214
8	0.055	0.178	0.056	0.174
9	0.060	0.194	0.053	0.166
10	0.049	0.167	0.057	0.170

10-year CDS spread

PCs	ΔCDS		η	
	mean adj–R^2	st. dev. adj–R^2	mean adj–R^2	st. dev. adj–R^2
1	0.118	0.248	0.100	0.215
2	0.096	0.243	0.086	0.225
3	0.102	0.263	0.093	0.233
4	0.091	0.243	0.080	0.213
5	0.096	0.252	0.084	0.217
6	0.065	0.208	0.069	0.192
7	0.065	0.207	0.071	0.184
8	0.055	0.199	0.063	0.182
9	0.047	0.178	0.057	0.167
10	0.047	0.176	0.058	0.165

Table 2.15 Regression of both changes in CDS spreads (left columns) and residuals of (2.8) (right columns) onto an increasing set of principal components. Large average adjusted R^2s in the first columns should would translate a significant impact of systematic factors on spread changes. This does not appear to be the case. The pattern of the average adjusted R^2s obtained from regressing the PCs onto the residual of the ECM points should detetect if some systematic factor could have been missed by (2.8). Mixed evidence is found regarding the first PC in the case of 5– and 10–year spreads.

LGD = 60%

1-year CDS spread

Long-run equilibrium

	Coefficient	t-stat	p-value	
VOL	0.0028	8.89	0.000	***
LEV	0.0024	14.30	0.000	***

Short-term adjustment

	Coefficient	t-stat	p-value	
ε	-0.0999	-11.61	0.000	***
ΔVOL	0.0081	6.32	0.000	***
ΔLEV	0.0037	5.27	0.000	***
ΔLevel	-0.0567	-4.50	0.000	***
ΔSlope	0.0206	4.20	0.000	***
ΔCurvature	1.2551	3.69	0.000	***
Δln(S&P500)	-0.0014	-4.93	0.000	***
ΔSkew	5E-07	2.27	0.023	**
Constant	-0.0001	-9.49	0.000	***

5-year CDS spread

Long-run equilibrium

	Coefficient	t-stat	p-value	
VOL	0.0234	16.13	0.000	***
LEV	0.0161	15.36	0.000	***

Short-term adjustment

	Coefficient	t-stat	p-value	
ε	-0.0290	-9.69	0.000	***
ΔVOL	0.0275	10.35	0.000	***
ΔLEV	0.0118	7.65	0.000	***
ΔLevel	-0.0978	-4.69	0.000	***
ΔSlope	0.0333	3.13	0.002	***
ΔCurvature	1.8625	3.48	0.000	***
Δln(S&P500)	-0.0026	-5.47	0.000	***
ΔSkew	-6E-07	-2.08	0.037	**
Constant	-0.0003	-9.87	0.000	***

10-year CDS spread

Long-run equilibrium

	Coefficient	t-stat	p-value	
VOL	0.0356	47.86	0.000	***
LEV	0.0346	27.78	0.000	***

Short-term adjustment

	Coefficient	t-stat	p-value	
ε	-0.0276	-5.23	0.000	***
ΔVOL	0.0434	14.91	0.000	***
ΔLEV	0.0175	7.76	0.000	***
ΔLevel	-0.1128	-4.74	0.000	***
ΔSlope	0.0231	2.10	0.035	**
ΔCurvature	2.1994	3.73	0.000	***
Δln(S&P500)	-0.0028	-5.2	0.000	***
ΔSkew	-1E-06	-3.31	0.001	***
Constant	-0.0004	-5.38	0.000	***

LGD = 80%

1-year CDS spread

Long-run equilibrium

	Coefficient	t-stat	p-value	
VOL	0.0027	7.75	0.000	***
LEV	0.0024	14.01	0.000	***

Short-term adjustment

	Coefficient	t-stat	p-value	
ε	-0.0987	-11.67	0.000	***
ΔVOL	0.0087	6.07	0.000	***
ΔLEV	0.0039	5.44	0.000	***
ΔLevel	-0.0575	-4.63	0.000	***
ΔSlope	0.0214	4.39	0.000	***
ΔCurvature	1.2516	3.78	0.000	***
Δln(S&P500)	-0.0014	-5.02	0.000	***
ΔSkew	4E-07	2.14	0.032	**
Constant	-0.0001	-9.22	0.000	***

5-year CDS spread

Long-run equilibrium

	Coefficient	t-stat	p-value	
VOL	0.0250	15.24	0.000	***
LEV	0.0171	15.48	0.000	***

Short-term adjustment

	Coefficient	t-stat	p-value	
ε	-0.0285	-9.81	0.000	***
ΔVOL	0.0294	9.8	0.000	***
ΔLEV	0.0123	7.71	0.000	***
ΔLevel	-0.0990	-4.69	0.000	***
ΔSlope	0.0350	3.25	0.001	***
ΔCurvature	1.8442	3.51	0.000	***
Δln(S&P500)	-0.0026	-5.59	0.000	***
ΔSkew	-7E-07	-2.34	0.019	**
Constant	-0.0003	-10.01	0.000	***

10-year CDS spread

Long-run equilibrium

	Coefficient	t-stat	p-value	
VOL	0.0385	45.57	0.000	***
LEV	0.0362	27.29	0.000	***

Short-term adjustment

	Coefficient	t-stat	p-value	
ε	-0.0279	-5.21	0.000	***
ΔVOL	0.0463	13.84	0.000	***
ΔLEV	0.0184	7.76	0.000	***
ΔLevel	-0.1148	-4.75	0.000	***
ΔSlope	0.0254	2.27	0.023	**
ΔCurvature	2.1912	3.76	0.000	***
Δln(S&P500)	-0.0028	-5.36	0.000	***
ΔSkew	-1E-06	-3.51	0.000	***
Constant	-0.0005	-5.33	0.000	***

Table 2.16 ECM for 1-, 5- and 10-year CDS spreads in the case LGD either 60% or 80%. All the variables which structural models predict to influence the change in spreads are statistically significant and have the predicted signs. The loading on the cointegrating equation (ε) is negative and statistically significant, thus confirming the existence of a long-term equilibrium which spreads, volatility and leverage converge to. This model constrains the long-run coefficient vector to be equal across panels while allowing for group-specific short-run and adjustment coefficients. The averaged short-run parameter estimates are reported. Number of observations: 16,640; number of groups: 64; observations per group: 260. Significance levels: 10% (*), 5% (**), 1% (***).

spread changes, the selected variables do explain quite well their variation. Consistently with previous findings and the economic intuition, it is shown that short-term spreads react more quickly to shocks to the long-run equilibrium and that jumps affect short- and long-term spreads differently. Also, most of the variation in the cross-section appears to be driven by firm-specific characteristics rather than systematic factors.

Chapter 3

The Option-implied Asset Volatility Surface

Abstract

This paper provides a simple way to obtain an option-implied asset volatility surface. The proposed estimation technique allows to estimate the unobservable asset volatility surface in the same fashion of what is done when equity volatility is extracted from options. Given a sample of 66 US firms, the asset volatility is first estimated at the firm level and then aggregated in order to study the properties of the market-wide asset volatility surface. Principal component analysis (PCA) is conducted on the weekly changes of the volatility surface both across the moneyness and the time-to-maturity dimension, as well as on the overall surface. Both across moneyness and maturity, the first three PCs are able to account for most of the variation and can be identified as level, slope/smirk and curvature factors respectively. When analysed in across the whole surface, the first two PCs account for most of the variation and represent a level and a skew factor. Finally, the joint evolution of the smirk and the slope of the surface is modelled as a Vector Autoregressive model with exogenous variables. Both slope and smirk appear to be jointly autocorrelated and loading of the other market variables display the predicted sign.

91

3.1   Introduction

Since the pioneer works of Black and Scholes (1973) and Merton (1974), contingent claim analysis (CCA) has been successfully and extensively adopted for the valuation of financial contracts. When applied to the modelling of credit risk, CCA is usually referred as structural approach to default risk. Despite its potential and ability to directly link credit events to the company's fundamentals, structural models of default requires as inputs two unobservable parameters: the market value of the assets and the volatility of its returns. On one hand, only if both the company's equity and the whole debt are publicly traded, the market value of the assets is observable; however, the vast majority of listed companies have non-traded debt. On the other hand, asset volatility is always unobservable. This paper develops a new estimation procedure which relies only on the observable value of the firm's equity and the prices of the options written on the former.

One of the first attempt to use CCA to price contracts other than options is found in Ronn and Verma (1986). There, a procedure for computing these two unknown variables is proposed. Their solution is two find two equations (or restrictions) to estimate the two unobservable variables. As the firm's equity is priced as a call option on the value of the assets, and its equity value can be observed, one restriction is placed on the two unknown variables. The second restriction arises from the relationship between the asset and equity volatilities, and the estimates for the asset value and asset volatility are obtained using a numerical procedure to solve a nonlinear two-equation system.

The shortcoming of the Ronn and Verma (1986) is in the second restriction: there, equity volatility is treated as a constant despite it should be stochastic as prescribed by the structural approach. Duan (1994) corrects this drawback introducing a maximum likelihood estimation procedure for asset value and volatility. Given the observable value of the equity (S), the results in Merton (1974) make the latter a function of the asset value (V) and volatility (σ_V), that is $S = f(V, \sigma_V)$. Since this function is invertible at any given asset volatility, $V = f^{-1}(S, \sigma_V)$ follows. Finally, the asset volatility is found as that value which maximises the log-likelihood function of the equity.

Another popular approach for estimating the asset value and volatility is the proprietary KMV model described in Crosbie and Bohn (1993). Despite the full algorithm is not known, it essentially uses a modification of the Merton's model and the unobservable asset value is still estimated via the same numerical inversion. The volatility parameter is though inferred from the time-series of the firm's equity, performing some Bayesian adjustments for country,

industry, and size of the firm[1]. The KMV model is also used by Vassalou and Xing (2004) to assess the effect of default risk on equity returns, and by Bharath and Shumway (2008) to analyse the relative ability of forecasting default by structural versus reduced-form models. In a similar fashion, Bartram et al. (2015) estimate the asset volatility, as implied by the model in Leland and Toft (1996), by minimising the squared deviations of predicted equity volatility from realised volatility.

On a slightly different note, Schaefer and Strebulaev (2008) develop a model-free relationship between asset volatility and the volatility of equity and debt returns. Assuming the firm does not pay dividends nor coupons or interests on its debt, then the return on the assets can be decomposed as follows

$$\frac{\mathrm{d}V}{V} = (1-L)\frac{\mathrm{d}S}{S} + L\frac{\mathrm{d}D}{D},$$

where S and D represent the market value of the equity and debt respectively, and $L := D/V$ is the debt-to-assets ratio. That is, the return on the assets is nothing buy the weighted average of the return on equity and debt having used as weight the relative composition of equity and debt in the firm's capital structure. Further, the variance of asset returns can be decomposed into

$$\sigma_V^2 = (1-L)^2\sigma_S^2 + L^2\sigma_D^2 + 2L(1-L)\rho_{S,D}\sigma_S\sigma_D$$

where and $\rho_{S,D}$ is the correlation between equity and debt returns. However, this decomposition is not operational as the volatility of the debt return is usually unobservable, and assumes that leverage is measured instantaneously[2]. However, this estimation techniques is not fully consistent with the CCA and and any structural model à la Merton[3].

More recently, a couple of works have tried to address the estimation of the asset volatility slightly departing from the usual setup of Merton (1974). Using complete pricing data on equities and corporate debt, Choi and Richardson (2016) are able to estimate the asset volatility and study its cross-sectional and time-series properties. They find that asset volatility decreases with leverage, presumably because firms with low asset volatility exploit the tax advantage of debt while maintaining a low cost of financial distress. Also, they show that asset volatility is significantly less persistent and more symmetric than equity volatility for levered firms.

---

[1]Duan et al. (2005) shows that the maximum-likelihood estimation in Duan (1994) and the KMV algorithm – intended without the Bayesian adjustment – are equivalent.

[2]This decomposition is also used in Feldhütter and Schaefer (2018) to address the credit spread puzzle.

[3]It is easy to show that, as both equity and debt are functions of the value of the assets (and not vice versa), by the virtue of Itô's Lemma $\rho_{S,D}$ must be set equal to one.

Second, the work in Lovreta and Silaghi (2017) is the only attempt at estimating an asset volatility surface rather than providing a point estimate. More specifically, using the structural model in Forte (2011) and the estimation proposed in Forte and Lovreta (2012), they exploit the pricing information in terms of default embedded in credit default swaps (CDS): the term structure of implied firm's asset return volatilities is backed-out from the whole term structure of CDS spreads, however, being the moneyness dimension absent from CDS quotes, they need to proxy it by the ratio of the default threshold to the asset value.

None of these works, however, is able to provide an estimation technique based on observable quantities only. Here, instead, the two unobservable parameters are estimated by solving a (non-linear) system of two equations. The first equation is again of the type

$$S = f(V, \sigma_V) \tag{3.1}$$

The second equation is instead obtained from equity options. In fact, it can be shown that in a compound option model as in Geske (1979) and Maglione (2019), also

$$P = g(V, \sigma_V) \tag{3.2}$$

where P is the price of the option, either call or put, written on the firm's equity. As each option is quoted for a given maturity (T) and moneyness (K/S), the solution this system of equations allows to directly generate an asset volatility surface, $\sigma_V(T, K/S)$. In fact, the asset volatility surface is obtained in the same spirit of what is done when the equity volatility surface is extracted by inverting the Black and Scholes (1973) pricing equation: the only difference is that two, instead of one, equations are used. Furthermore, this approach does not depend on any estimate of the equity volatility and on the 'misused' link between the latter and asset volatility[4].

As shown by Bartram et al. (2015), asset volatility accounts for about 85% of total volatility for the representative nonfinancial US firm, and equity volatility is driven primarily by economic risk factors. The impact of these factors should be reflected into the volatility of the firm's cash-flow, that is σ_V. Thus, having a market-based estimate of the asset volatility

---

[4]Crosbie and Bohn (1993), Vassalou and Xing (2004) Bharath and Shumway (2008), Schaefer and Strebulaev (2008) and others estimate the asset volatility via

$$\sigma_S = \sigma_V \frac{V}{S} \frac{\partial S}{\partial V},$$

as if the equity volatility were deterministic. However, being V the state variable of any structural model, the volatility of the firm's equity is actually stochastic as pointed out by Duan (1994). The approach proposed herein does not need σ_S as an input.

surface appears to be very relevant for asset pricing. Also, Choi and Richardson (2016) argue that more emphasis in research should be put on understanding the cross-sectional and time-series behaviour of firm's asset volatility. This paper tries to fill this gap.

The rest of the paper is organised as follows. In Section 3.2 briefly the pricing model is presented and how the stock price and equity options depend on the unobservable parameters. The dataset is described in Section 3.3. In Section 1.4 principal component analysis (PCA) is performed to disentangle the cross-sectional and time-series variation of the firm-specif and market-wide asset volatility surface. Further, the smirk and slope of the market asset volatility surface are jointly modelled using a Vector Autoregressive (VAR) process. Section 3.5 concludes.

3.2   The model

In order to estimate the volatility of the asset, the following set of variables for each firm are needed: (1) the value of the equity, (2) the face value of its debt as well as the time it due, (3) a set of traded options written on the firm's equity. The model employed is the same as in Maglione (2019) in which equity is seen as a n–fold compound call option written on the firm assets struck at the face value of the n bonds outstanding. Under this framework, default times are defined as

$$\tau := \inf_{i \in I} \{t_i : S_i^\star(V) < F_i\}$$

where $I = \{1, \ldots, n\}$ and $S_i^\star(V)$ is the continuation value of equity, which is a function of the firm assets V. That is, the default time occurs the first time at which the value of the equity is lower than the face value of the bond due; by model assumptions, the firm can default only at discrete points in time.

More specifically, it can be shown that the value of the firm's equity can be written as

$$S = e^{-\varpi t_n} V \mathbb{M}(\tau \geq t_n) - \sum_{i=1}^{n} e^{-r t_i} F_i \mathbb{Q}(\tau \geq t_i), \tag{3.3}$$

where V is the contemporaneous value of the assets, $(F_i)_{1 \leq i \leq n}$ represent the sequence of the face value of the bond issued due at time t_i, ϖ the payout rate (reflecting both dividends and coupons), r the constant continuously compounded risk-free rate, and $\mathbb{Q}(\tau \geq t_i)$ (respectively $\mathbb{M}(\tau \geq t_i)$) the probability of the firm surviving up to t_i under the risk-neutral measure (respectively the firm-value fund risk measure). If the asset value process follows a geometric Brownian motion with volatility σ_V, the probabilities in (3.3) can be computed in terms of

multivariate Gaussian integrals, that is

$$S(V, \sigma_V) = e^{-\varpi t_n} V \Phi_n\left(\mathbf{d}^{\mathbb{M}}; \boldsymbol{\Gamma}_n\right) - \sum_{i=1}^{n} e^{-r t_i} F_i \Phi_i\left(\mathbf{d}_i^{\mathbb{Q}}; \boldsymbol{\Gamma}_i\right) \tag{3.4}$$

where $\mathbf{d}^{\mathbb{M}} := \left(d_i^{\mathbb{M}}\right)_{1 \leq i \leq n}$ and $\mathbf{d}_i^{\mathbb{Q}} = \left(d_j^{\mathbb{M}} - \sigma_V \sqrt{t_j}\right)_{1 \leq j \leq i}$ with

$$d_i^{\mathbb{M}} = \frac{\ln\left(V/\bar{V}_i\right) + \left(r - \varpi + \sigma_V^2/2\right) t_i}{\sigma_V \sqrt{t_i}}, \qquad \boldsymbol{\Gamma}_i = \begin{pmatrix} 1 & \sqrt{\frac{t_1}{t_2}} & \cdots & \sqrt{\frac{t_1}{t_i}} \\ \cdots & \cdots & \cdots & \cdots \\ & & 1 & \sqrt{\frac{t_{i-1}}{t_i}} \\ & & & 1 \end{pmatrix},$$

and $\Phi_i(\mathbf{z}; \boldsymbol{\Gamma})$ the cumulative distribution function of a i-dimensional normal random vector with zero mean and covariance matrix $\boldsymbol{\Gamma}$ calculated over the set $\times_{j=1}^{i}(-\infty, z_j)$. Also, $(\bar{V}_i)_{1 \leq i \leq n}$ is the latent sequence of default thresholds embedded in the firm's capital structure.

Intuitively, as equity is an n–fold compound option, vanilla options are $(n+1)$–fold compound options on the firm's assets. The price of a European option with maturity $T \in (t_i, t_{i+1})$, with $0 \leq t_i < t_{i+1} \leq t_n$, and strike price K written on the firm's equity is computed as

$$P_\xi = \xi \left[e^{-\varpi t_n} V \mathbb{M}\left(\tau \geq t_n \cap \xi S_T \geq \xi K\right) - \sum_{i=1}^{n} e^{-r t_i} F_i \mathbb{Q}\left(\tau \geq t_i \cap \xi S_T \geq \xi K\right) - e^{-rT} K \mathbb{Q}\left(\xi S_T \geq \xi K\right) \right],$$

where $\xi = +1/-1$ if pricing a call/put. If V follows a geometric Brownian motion, the price is computed as

$$P_\xi(V, \sigma_V) = \xi \left[e^{-\varpi t_n} V_0 \Phi_{n+1}\left(\mathbf{d}_\xi^{\mathbb{M}}; \boldsymbol{\Gamma}_{n+1}^\xi\right) - \sum_{k=i+1}^{n} e^{-r t_k} F_k \Phi_{k+1}\left(\mathbf{d}_{\xi, k+1}^{\mathbb{Q}}; \boldsymbol{\Gamma}_{k+1}^\xi\right) - e^{-rT} K \Phi\left(\xi d_T^{\mathbb{Q}}\right) \right]$$
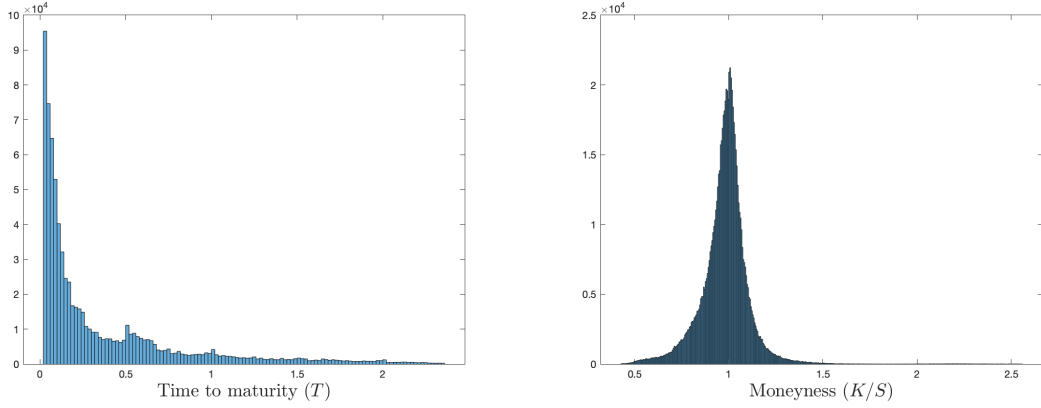
Fig. 3.1 Histograms of time to maturities (left) and moneyness (right) of the options used throughout the analysis. Time to maturity (T) ranges from 6 days to 2.3 years, with vast majority of short-term options. Moneyness (K/S) shows a more symmetric distribution.

	Mean	Median	Mode	IQR	St. Dev.	Skewness	Kurtosis	Min	Max
T (years)	0.3656	0.1587	0.0278	0.4524	0.4565	1.9139	6.3573	0.0238	2.3452
K/S	0.9791	0.9884	1.0204	0.1148	0.1279	0.8192	15.4102	0.4274	2.5565

Table 3.1 Descriptive statistics of the variables time to maturity (T) and moneyness (K/S) in the sample under analysis.

with $\mathbf{d}_\xi^{\mathbb{M}} = \left((d_i^{\mathbb{M}})_{i=1}^k, \xi d_T^{\mathbb{M}}, (d_i^{\mathbb{M}})_{i=k+1}^n \right)$, $\mathbf{d}_{\xi,k+1}^{\mathbb{Q}} = \left(d_{\xi,i}^{\mathbb{M}} - \sigma_V \sqrt{t_i} \right)_{1 \leq i \leq k+1}$, and

$$d_T^{\mathbb{M}} = \frac{\ln\left(V_0/\bar{V}_K\right) + \left(r - \varpi + \sigma_V^2/2\right) T}{\sigma_V \sqrt{T}}, \qquad \mathbf{\Gamma}_{k+1,\xi} = \begin{pmatrix} 1 & \sqrt{\frac{t_1}{t_2}} & \cdots & \xi\sqrt{\frac{t_1}{T}} & \cdots & \sqrt{\frac{t_1}{t_k}} \\ & 1 & \cdots & \xi\sqrt{\frac{t_2}{T}} & \cdots & \sqrt{\frac{t_2}{t_k}} \\ \cdots & \cdots & \cdots & \cdots & \cdots & \cdots \\ & & & & 1 & \sqrt{\frac{t_{k-1}}{t_k}} \\ & & & & & 1 \end{pmatrix}.$$

3.3 Estimation methodology and data description

Given the results in the previous section, observing the stock price $\hat{S}$ as well as an option price $\hat{P}_\xi$, with maturity T and moneyness K/S, allows to estimate the asset implied volatility

$\sigma_V^{IV} = \sigma_V(T, K/S)$ solving the system

$$
\begin{cases}
\hat{S} = S(V, \sigma_V) \\
\hat{P}_\xi = P_\xi(V, \sigma_V).
\end{cases}
\tag{3.5}
$$

This novel estimation technique is applied to a set of 66 US companies, constituents of the S&P100 during the period January 2013 – December 2017. Companies with either preferred equity or subject to merges or acquisitions are excluded.

Data on stock prices, number of shares outstanding, dividends and the risk-free yield curve (and other variables used in the next sections) are obtained from Bloomberg. Information relative to the firms' capital structures and cost of debt is gathered from Compustat and the 10-K documents. All the observations are collected at weekly frequency frequency, over a total of 259 week, with the exception of the information on the firm's capital structure which is available at quarterly frequency. Therefore, it is assumed that the capital structure remains fixed within quarters, having only adjusted the time to maturity of the firm's debt due to the passage of time. It appears a reasonable assumption given the empirical evidence on how often US firms decide to rebalance their capital structures (see Strebulaev and Whited 2012).

In order to implement the estimation in (3.5), the term-structure of the firm's debt must be known or approximated somehow. I opt for clustering the firm's debt at three fixed point, $t_i = \{1, 5, 10\}$ years, $i = 1, 2, 3$. The choice of setting $n = 3$ is considered optimal as it is the smallest number of maturity dates needed in order to match both the level, slope and curvature of the observed term structure of credit spreads.

The face values of the bond due in $t_1 = 1$ represents the company's short-term debt and is computed as the Compustat variable `DD1Q` (Long-Term Debt Due in One Year), that is $F_1 = $ `DD1Q`. The remaining two bonds clustered at $t_2 = 5$ and $t_3 = 10$ are obtained from `DLTQ` (Long-Term Debt Total), such that $F_2 + F_3 = w \cdot$ `DLTQ` $+ (1 - w) \cdot$ `DLTQ`. The empirical findings in Maglione (2020) suggest to set $w = 1/3$ for the model to reproduce a term-structure of credit spread in line with the one observed empirically.

Given the large amount of option data, only the most liquid OTM call and put options traded every Wednesdays with time-to-maturity greater than five days are taken into consideration. To determine the most liquid traded options, those prices whose moneyness is outside the 5th to 95th percentile range are firstly removed. Secondly, only those options with volume above their annual median are kept.

The price of the option is defined as the average of the bid and ask price when both are available; the observation is removed otherwise. Finally, options with zero trading volume

and negative bid-ask spread are also excluded. The final sample counts 338,932 valid call and 428,441 put options observations. Figure 3.1 shows the options' distribution in terms of moneyness and maturity. Table 3.1 summarises the distributional properties of the sample of options.

One of the main disadvantage of working with equity options is that they are usually American-style. This is the case in the analysed dataset and, in order to test and implement the model, European quotes should be used. Hence, the de-Americanization procedure introduced by Carr and Wu (2010) and further tested in Burkovska et al. (2018) is applied. The aim of the de-Americanization is to find the corresponding European price (the so-called pseudo-European price) for a given American price. That is, the price ought to be observed if the contract would not allow to exercise the option before maturity. In a nutshell, a binomial tree is used to price the American option. The volatility parameter such that the squared difference between the market price and the price generated by the tree is minimised is set as the option implied volatility. Once estimated, the pseudo-European price is found by applying the Black-Scholes formula for European options.

The estimation procedure thus produces 259 asset volatility surfaces for each firm in the sample. Once the firm-specific asset volatility surfaces are available, a market-wide asset volatility surface can be constructed. The next section performs PCA on both the cross-section of the firm-specific volatility surfaces as well as on several dimensions of the market-wide asset volatility surface.

It should be noted that solving (3.5) to estimate the asset volatility allows to obtain a surface as each option has different maturity (T) and moneyness (K/S). However, as the equity itself is modelled as a compound call option with (final) maturity t_n, it is assumed that the estimated $\sigma_V(T,K/S)$ is not influenced by t_n. Also being t_n (usually equal to ten years) far in the future with respect to the option maturity, I assume that the estimated surface (and therefore the firm's riskiness) reflects the effect of the (shorter) maturity of the option only.

Furthermore, it should be clear that solving (3.5) for each option produces a different value of the firm's assets $V_0(T,K/S)$. Unreported results, available upon request, show that the estimated asset value is not very sensitive to changes in T and K/S. A possible modification of this methodology could be solving (3.5) to obtain the corresponding asset values $V_{0,j,k} = V_0(T_j,(K/S)_k)$, averaging those estimates to obtain $\bar{V}_0$ and then re-solve the second equation in (3.5) as one equation in one unknown (σ_V) having replaced V_0 as $\bar{V}_0$. However, as ultimately the market-wide asset volatility is studies (which value-averages the obtained volatilities for each company) the change is likely to be negligible.
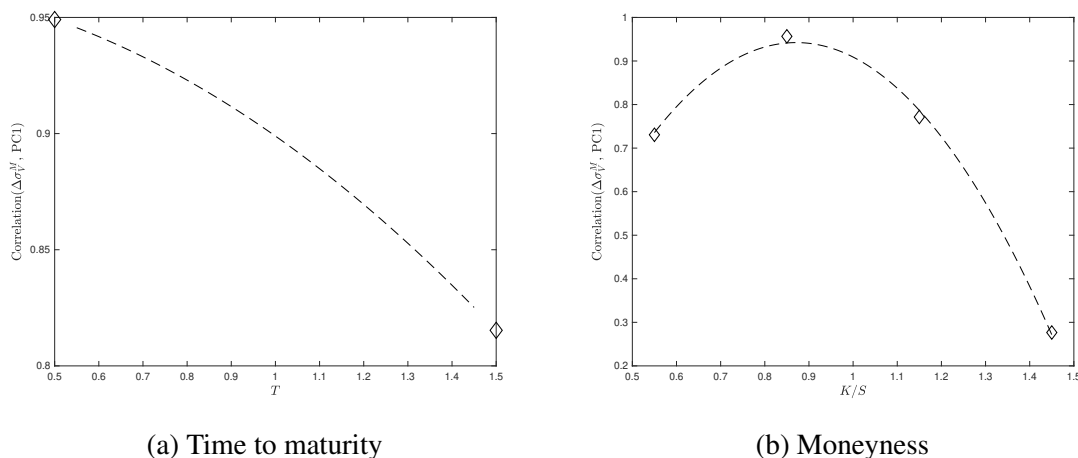
(a) Time to maturity   (b) Moneyness

Fig. 3.2 Behaviour of the correlation between PC1 and the changes in the cross-sectional mean of asset volatility (market volatility) with respect to time to maturity (Panel a) and moneyness (Panel b). Correlation appears overall large and positive being the largest for options close to being at-the-money with short time to maturity.

Maturity	Proportion	Correlation	N
Short term	32.94%	0.9491	687,362
Long term	80.21%	0.8153	80,011

Table 3.2 Systematic variation in firm-level volatility. The proportion of variance explained by the first principal component is shown for PCA on the changes in firm-level implied asset volatilities for the sample of 66 individual firms. This analysis is performed separately for options with maturity less than 1 year (short-term) and with maturity greater than 1 year (long-term). The correlation between changes in the cross-sectional mean of firm-level volatilities and PC1 for changes in firm-level volatility is reported in the third column. The last column reports the number of valid option observations within the relative bucket.

Finally, when naming the estimated $\sigma_V^{IV}(T, K/S)$ as option-implied asset volatility, I mainly refer to the call and put options written on equity (and not the equity as an option itself).

3.4 Empirical results

In this section, first the systematic variation in firm-level implied volatility for the sample of 66 firms is analysed. Then, the market-wide asset volatility surface is constructed as the value-weighted average of the firm-specific surfaces. The asset value is estimated as in (3.5) and averaged across the moneyness and time-to-maturity dimension[5]. Once the market asset

---

[5]Empirical tests show that the variation in V due to different T and K/S is minimal.

Moneyness	Proportion	Correlation	N
$(0, 0.7]$	34.86%	0.7306	19,707
$(0.7, 1]$	23.79%	0.9566	408,734
$(1, 1.3]$	20.94%	0.7714	330,073
$(1.3, \infty)$	78.75%	0.2766	8,859

Table 3.3 Systematic variation in firm-level volatility. The proportion of variance explained by the first principal component is shown for PCA on the changes in firm-level implied asset volatilities for the sample of 66 individual firms. This analysis is performed separately for options in different moneyness buckets (moneyness is defined as K/S). The correlation between changes in the cross-sectional mean of firm-level volatilities and PC1 for changes in firm-level volatility is reported in the third column. The last column reports the number of valid option observations within the relative bucket.

Maturity	Mean	Median	Mode	St. Dev.	Skewness	Kurtosis	Min	Max
Short term	0.1784	0.1382	0.1759	0.0201	1.3591	6.0522	0.1382	0.2666
Long term	0.2045	0.1732	0.2043	0.0139	0.0980	2.1618	0.1732	0.2377

Moneyness	Mean	Median	Mode	St. Dev.	Skewness	Kurtosis	Min	Max
$(0, 0.7]$	0.2828	0.2327	0.2787	0.0235	1.0726	5.5579	0.2327	0.4023
$(0.7, 1]$	0.1954	0.1570	0.1905	0.0232	1.5254	6.1499	0.1570	0.2900
$(1, 1.3]$	0.1477	0.1205	0.1451	0.0167	1.4447	6.1499	0.1205	0.2237
$(1.3, \infty)$	0.2058	0.1508	0.2011	0.0249	0.9505	4.4877	0.1508	0.3117

Table 3.4 Descriptive statistics of the market-wide asset volatility. The majority of the observation are for short-maturity options with moneyness around the the ATM region. The estimates of the asset volatility are in line with previous research in which the volatility is not estimates using options.

volatility surface is obtained, then PCA is conducted across the moneyness (smirk) and time-to-maturity (slope) dimensions as well as across the whole surface.

Given the non-stationarity of the asset volatility[6], changes in implied volatilities are used. Moreover, this is in line with the literature on equity implied volatilities which has mainly applied PCA to changes in equity implied volatility.

3.4.1 PCA on changes of firm-specific asset volatilities

PCA is performed on weekly changes in firm-level implied asset volatilities. The analysis is carried across the time-to-maturity (T) and moneyness (K/S) dimensions. Moneyness is fist split across different buckets: $K/S \in (0, 0.7]$ (deep out-of-the money puts), $K/S \in (0.7, 1]$ (out-of-the money puts), $K/S \in (1, 1.3]$ (out-of-the money calls), $K/S \in (1.3, \infty)$ (deep out-of-the money calls). Second, time-to-maturities are clustered at short term ($T < 1$) and long term ($T \geq 1$).

Tables 3.2 and 3.3 show the explanatory power of the first principal component across maturities and moneyness respectively. Interestingly, the explanatory power increases with maturity and is larger for progressively more out-of-the money options. Secondly, this systematic variation is well captured by the changes in the cross-sectional mean of firm-level volatilities. The third column in Table 3.2 shows that the two variables are almost perfectly correlated when looking at the time to maturity dimension. Across moneyness, the correlation is stronger for options close to being at-the-money. Figure 3.2 shows the decreasing pattern of the correlation based on maturity, and an hump-shaped behaviour with respect to the moneyness dimension.

These findings suggest that the changes in the mean implied volatility for the whole sample of firms is actually capturing the first principal component that drives the variation of individual firm-level volatility. This average volatility is calculated as the value-weighted average of weekly changes in firm-specific asset volatility. Hence, the subsequent analysis focuses on the marked-wide asset volatility.

3.4.2 Market-wide asset volatility

Table 3.4 reports the descriptive statistics of the market-wide asset implied volatility over different maturities and across moneyness. Figure 3.3 dissects the market-wide asset volatility surface into the evolution of its term structure and across moneyness. First, asset volatility is usually smaller in the short term than at longer horizons, being the two highly correlated.

---

[6]Lovreta and Silaghi (2017) document an order of integration ranging from 0.8 to 1.1.

| Maturity	Correlation Matrix		Moneyness	Correlation matrix			
Shot term	1	0.59	$(0, 0.7]$	1	0.78	0.61	0.05
Long term	0.59	1	$(0.7, 1]$	0.78	1	0.91	0.03
			$(1, 1.3]$	0.61	0.91	1	0.08
			$(1.3, \infty)$	0.05	0.03	0.08	1

Table 3.5 Correlation matrix for the asset volatility across different maturities and moneyness. The largest correlation is observed between asset volatilities with moneyness in $(0.7, 1]$ and $(1, 1.3]$. These option constitutes the majority of the observation in the sample.

Second, the evolution of the mean asset volatility across moneyness shows the largest implied asset volatility for deep out-of-the-money options consistent with the well-documented leverage effect. On the other hand, at-the-money asset volatility ranges from 15% to 20% per annum; deep out-of-the money calls display implied volatilities with similar magnitudes.

The only instances in which the short-term asset volatility is larger than the long-term one is during the first months of 2016 when China's stock market fell nearly 18%. Given the interconnection between the US and Chinese markets, China's crush seems to have systematically affected the likelihood of US firms defaulting, especially in the short run. This can be also observed looking at the model-implied default probabilities at different horizons. Using the compound option model in (3.4), given the estimates of the market asset volatility and leverage, the term-structure of default probabilities can be estimated. Figure 3.4 indeed shows that the 1-year default probability is generally smaller than the 5-year ones, and that both increased during the Chinese market crush. However, the largest impact is observed on the short-term default probability, to the point to making default more likely in the short run than for longer horizons. It appears that systematic shock in the Chines market had a stronger impact on the short-term solvency of the US economy.

It is worth noting that lager default probabilities are associated with lower volatilities. This apparently counterintuitive finding is well explained by how volatility works in a compound option model of default. As the asset volatility increases, the option embedded in the firm's equity becomes more in-the-money and its value increases. This pushes the firm away from the default boundary and the default probability decreases.
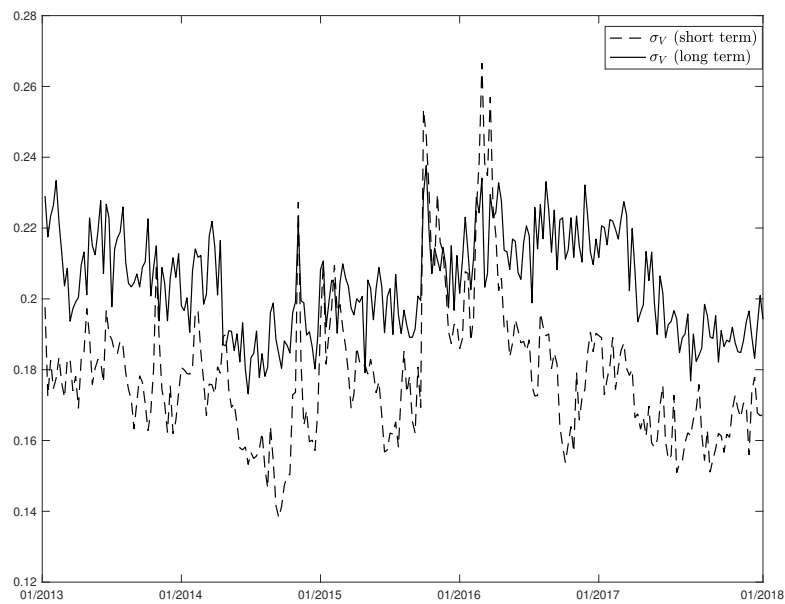
(a) Asset volatility clustered based on time-to-maturity
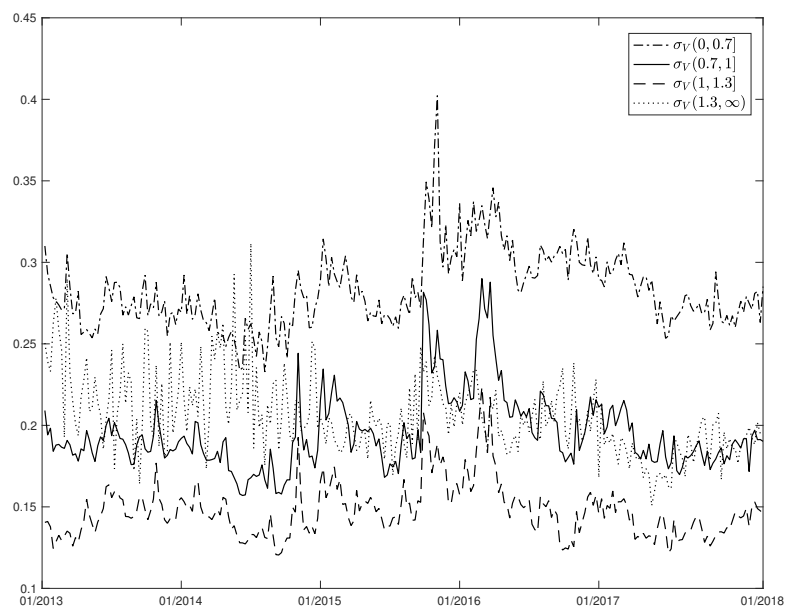
(b) Asset volatility clustered based on moneyness

Fig. 3.3 Time-series evolution of the market-wide asset volatility. Panel (a) represent the evolution of the short-term ($T < 1$) and long-term ($T \geq 1$) asset volatility. Panel (b) display the time-evolution of the asset volatility across the moneyness dimension. In general, short term volatility is smaller than long-term volatility, and deep OTM put options display the largest volatility, consistently with the leverage effect.
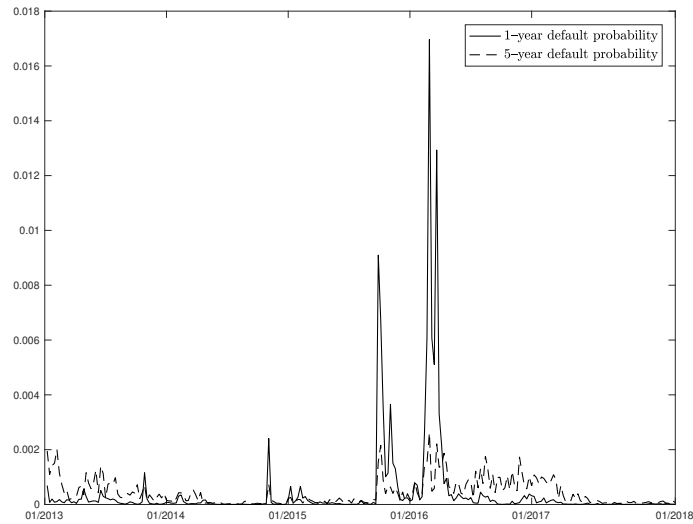
104

Fig. 3.4 Market-wide implied risk-neutral default probabilities based on the average asset volatility across the surface observed every week. Probabilities are obtained from (3.4). The size of 1-year default probability is smaller than the 5-year; however, during the Chinese crush at the beginning of 2016, 1-year default probabilities turned larger than the long-term ones. After the turmoil, the usual ordering is observed.

Maturity	Proportion	Cumulative	Moneyness	Proportion	Cumulative
PC1	78.58%	78.58%	PC1	54.55%	54.55%
PC2	20.34%	98.93%	PC2	31.04%	85.59%
PC3	1.07%	100.00%	PC3	12.99%	98.58%

Table 3.6 PCA on maturity (left table) and moneyness (right table) for changes in the market-wide asset volatility. The first three components are able to account for almost the totality of the variation. They are interpreted as: Level, Slope/Smirk in case of time-to-maturity/moneyness, and Convexity.
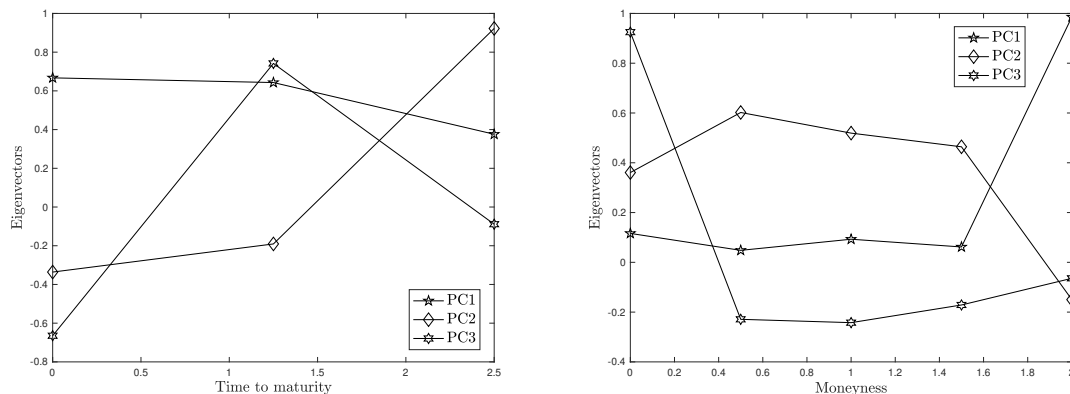
(a) First three eigenvectors PCA on maturity   (b) First three eigenvectors PCA on moneyness

Fig. 3.5 Both across time-to-maturity (panel a) and moneyness (panel b) the first PC is positive and can be interpreted as level. The second PC for the variation of the term structure is a slope fact, whilst the second PC across moneyness is a smirk factor. The convexity component affect more the smirk rather than the term structure of the market-wide asset volatility surface.

3.4.3 PCA on market-wide asset volatility changes

Table 3.5 reports the correlation among implied volatilities at different time horizons and across moneyness. Given the high correlation, this allows to use principal component analysis to find the uncorrelated sources of risk which drive the evolution of asset implied volatilities.

I proceed as follows: PCA is firstly applied on the maturity dimension, analyzing the term structure of asset implied volatilities. I then perform PCA on the second dimension, moneyness. Finally, PCA is applied on the entire implied volatility surface, analyzing both dimensions simultaneously.

PCA on time-to-maturity

The results of the PCA performed on the correlation matrices in Table 3.5 are shown in Table 3.6. Both over the moneyness and the maturity dimensions, the first three principal components are enough to account for the whole variability exhibited by the changes of the market-wide asset volatility. In order to identify the effect of each component on the asset volatility surface, the first three eigenvectors corresponding to the three largest eigenvalues are computed. Figure 3.5, panel (a), displays the elements of each eigenvector.

Alongside the maturity dimension, all of the components of the first eigenvector are positive. Thus a positive shock in the first principal component (an upward shift) induces a roughly parallel shift in the term structure of the implied volatility, resulting in a global

increase of all the implied volatilities. Therefore, the first principal component can be interpreted as a 'level' or a 'trend' component of the implied volatility term structure. For the overall sample period, 78.58% of the total variation in the term structure can be attributed to (roughly) parallel shifts.

The factor weights on the second principal component change sign, increasing monotonically with maturity. Therefore, a positive shock in the second principal component leads to a change in the slope of the term structure of implied volatilities, with short maturities moving down and long ones moving up. Thus, the second principal component can be interpreted as a 'slope' or 'tilt' component which explains 20.34% of the total variation. To confirm that the second PC does represent the slope of the surface, the correlation between the former and the latter can be computed. Defining the slope across the maturity dimension as the difference between short and long-term asset implied volatility. I find a very strong correlation of 0.91.

The third eigenvector has a negative weight for the shortest maturity, with increasing and positive weights for the medium-term volatilities, and negative and decreasing weights for the longer maturities. Thus, the third principal component is interpreted as 'convexity' and accounts for 1.07% of the total variation.

PCA on moneyness

Table 3.6 also report the explained variance of the PCs obtained through the moneyness dimension. An upward shift in the first principal component leads to a near parallel shift in the smirk of the implied volatility, being the volatility of deep OTM call options the most sensitive to those changes. That is, parallel shifts tend to accentuate the smirk observed in that region. Therefore, the first component can be interpreted as a 'level' component and account for 54.55% of the variation in the smirk of the implied volatility.

The factor weights on the second principal component is positive except, again, for deep OTM call options where it turns negative. The second component corresponds then to a change in the slope of the asset volatility smirk, with volatilities corresponding to low moneyness bins increasing and those corresponding to high ones moving down. That is, an increase in the slope tend to reduce the smirk observed in the deep OTM call region. The second component accounts for 31.04% of the total variation of the smirk. According to the leverage effect, the slope of the smirk should be connected with increase in credit risk. Hence, similar to the maturity dimension, the correlation between the second PC and change in market leverage is computed. This correlation equals 0.58.

The third eigenvector however show a different impact over deep OTM put options. It has a positive weight for the smallest moneyness, with increasing and negative weights for

Surface	Proportion	Cumulative
PC1	87.16%	87.16%
PC2	11.47%	98.63%
PC3	0.95%	99.58%
PC4	0.42%	100.00%

Table 3.7 PCA on the whole surface for changes in the market-wide asset volatility. The first two components are able to account for the almost the totality of the variation.

the medium and high levels of moneyness. Thus, the third principal component is interpreted as a 'convexity'. An increase in the convexity affects the most deep OTM put options with their volatility being the one which increases the most. This last component account for the remaining 12.99% of the variation in the smirk. It is worth highlighting that the convexity component affect more the smirk rather than the term structure of the market-wide asset volatility surface. Figure 3.6 shows the 'typical' shape of the asset volatility surface, displaying the most curvature across the moneyness dimension.

Overall, the comparative PCAs documents a larger impact of the first two PCs on the maturity dimension rather than on the moneyness. That is, the level and slope have a larger impact at governing the term-structure of the market-wide asset volatility than they have in affecting the volatility smirk. Conversely, the convexity factor have a larger impact on the moneyness rather than the time-to-maturity dimension.

PCA on the whole surface

To complete this analysis, PCA is performed on the dynamics of the entire volatility surface. Figure 3.6 plots the asset implied volatility surface as a function of moneyness and maturity. The surface shows that asset implied volatilty decreases both across the moneyness bins and across maturity. Since more indebted firms are more likely to be in a high moneyness bin, the negative skew obtained could be explained by the negative relationship between asset volatility and leverage. As Choi and Richardson (2016) suggest, firm's asset volatility decreases with leverage (and thus with moneyness) since firms with lower asset volatility can probably better exploit the tax advantage of debt while maintaining a relatively low cost of financial distress.

Alternatively, the shape of the asset implied volatility surface could be related to investors' preference for lottery-like assets. In particular, Boyer and Vorkink (2014) find that options trading out-of-the money offer substantially more skewness (a proxy for lottery-like
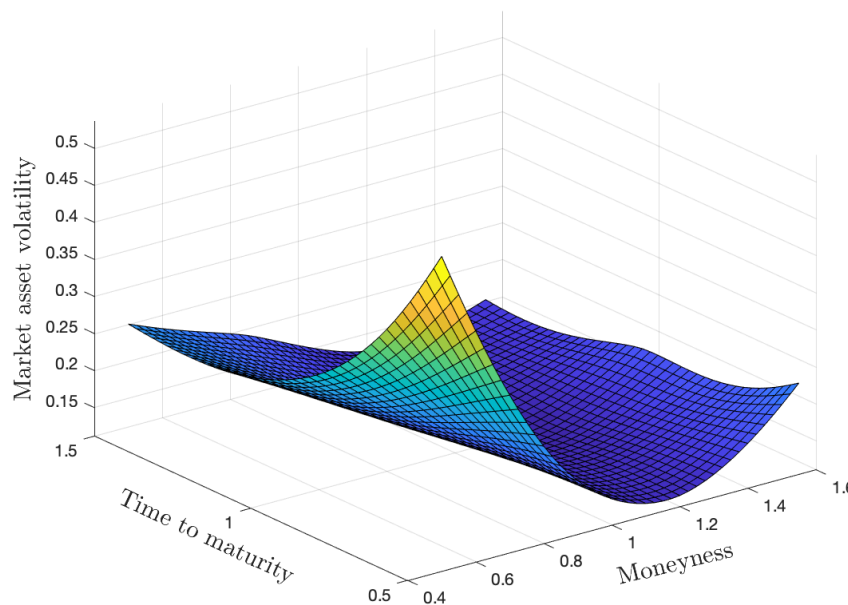
Fig. 3.6 Typical shape of the option-implied market-wide asset volatility surface. Consistently with the leverage effect, the largest volatilities are observed in the default region, i.e. for short-maturity deep OTM put options. The convexity is more pronounced across the moneyness dimension rather than the term structure, despite displaying a decreasing trend. Outside the default region, the asset volatility appears quite constant. This surface was observed on October 11th 2017.

characteristics) than in-the-money options, especially as maturity decreases. This would, in contrast, translate into higher buying pressure for option contracts at shorter maturities and for lower moneyness bins (which are deeper out-of-the- money). However, both effects would produce a downward sloping term structure and moneyness smirk, in line with our shape of the asset volatility surface.

Comparing to the findings on equity volatility, a similar negative skew is found for equity implied volatility (Cont and da Fonseca 2002, Andersen et al. 2015). However, a downward sloping term structure of equity implied volatility is not common, especially during tranquil periods.

In order to perform PCA on the entire data set, e maturity levels are pooled together. The results of the PCA on the volatility surface are presented in Figure 3.7 and Table 3.7. The factor loadings of the first principal component (PC1) of Figure 3.7 show an almost constant effect on the entire volatility surface. That is, the first PC can be interpreted as 'level' and it explains 87.16% of the surface total variation.
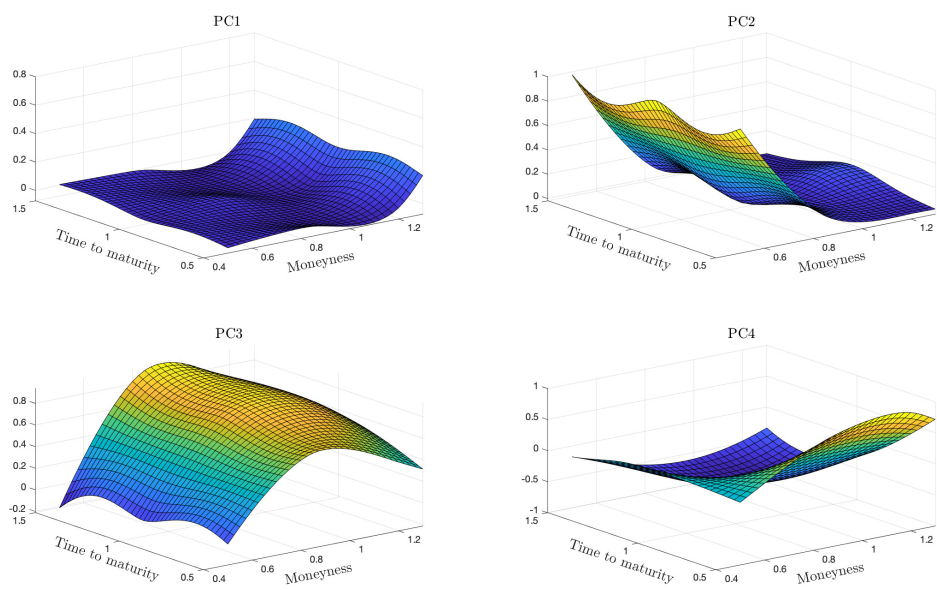
Fig. 3.7 Principal components (modes) of the whole surface. PC1 explains 87.16% of the variance in the changes in the surface, and appears to be a Level factor. PC2 is a skew factor as it affects the moneyness dimension only and explains 11.47% of the variance. PC3 is a convexity factor which affects moneyness, and PC4 appears to be a term factor as it acts in the time-to-maturity dimension. PC3 and PC4 explain together less than 2% of the variation.

The factor loadings of the second principal component (PC2) indicate that this is a skew factor, with volatilities in low moneyness bins moving in the opposite direction from those in higher moneyness bins, with little variation across maturity. This factor explains 11.47% of the surface variation and exhibit positive correlation with changes in leverage. The correlation with the second PC and changes in market leverage is equal to 0.14 when short-term options are considered, but increase to 0.26 when long-term options are taken into account. This result is consistent with Maglione (2019) in which credit risk factors are shown to affect mostly long-maturity options rather than options with shorter maturities. The correlation is however relatively small, thus suggesting that the second PC is only partially linked to credit risk (also in line with the findings in Carr and Wu 2017 and Maglione 2019).

The factor loadings for the third principal component (PC3) appears to be a convexity factor affecting the moneyness dimension. Finally, the fourth factor (PC4) plotted in Figure 3.7 appears to be a curvature mode related to the term structure. Together, the first two principal components explain 98.58% of the surface variation, thus showing that the convexity effects are only marginally important in the evolution of the surface.

### 3.4.4   Time-series dynamics of Slope and Smirk

Given the results in the previous section, the dynamics of the asset implied volatility surface is further investigated. As the second principal components for both the maturity and moneyness analyses are highly correlated with changes in the slope of the empirical term structure and moneyness smirk, respectively, the latter are used to study the evolution of the surface across time. The variables Slope and Smirk are defined as follows[7]

$$\text{Slope}_t = \sigma_{V,t}(\text{long term}) - \sigma_{V,t}(\text{short term})$$
$$\text{Smirk}_t = \sigma_{V,t}(\text{DOOM call}) - \sigma_{V,t}(\text{DOOM put}).$$

Figure 3.8, panel (a), shows the evolution of the term structure Slope. The term structure is downward sloping during most the whole sample period. In panel (b) the Smirk is plotted and is also mostly negative during the sample period. A downward sloping term structure is also found by Lovreta and Silaghi (2017). This may come as a surprise as, in equity markets, an upward sloping term structure is usually observed. This inversion in the slope is easily explained by how default is driven in the compound option model. As previously stated, lager default probabilities are associated with lower volatilities as increasing volatilities increase the value of the firm's equity, thus pushing the latter away from the default barrier. Observing

---

[7]DOOM stands for deep out-of-the-money.
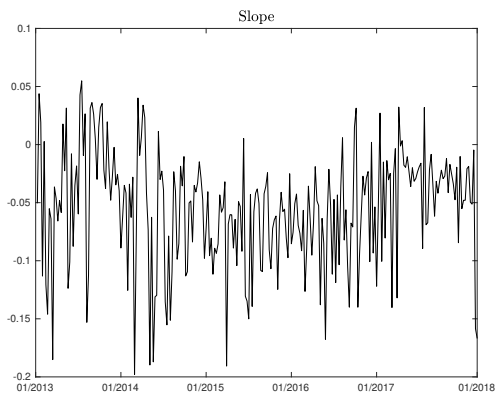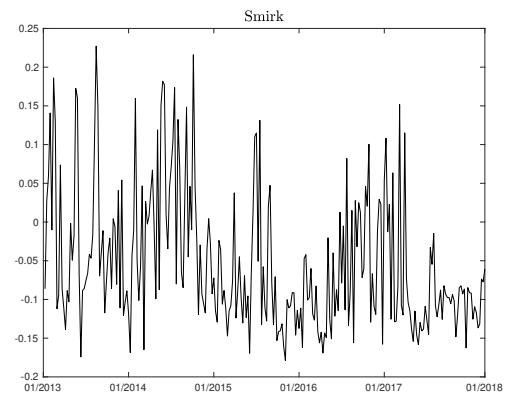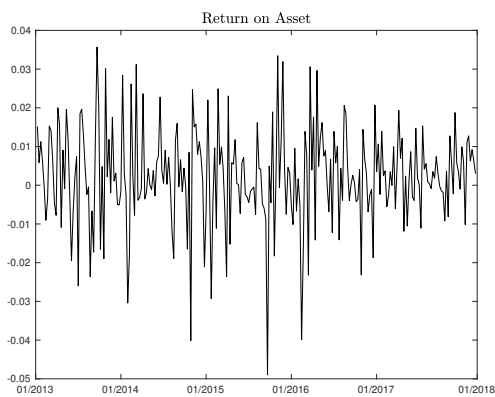
(a) Slope

(b) Smirk

(c) Return on Asset
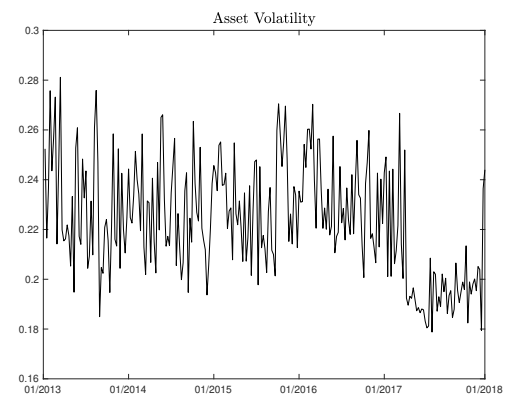
(d) Average Asset Volatility
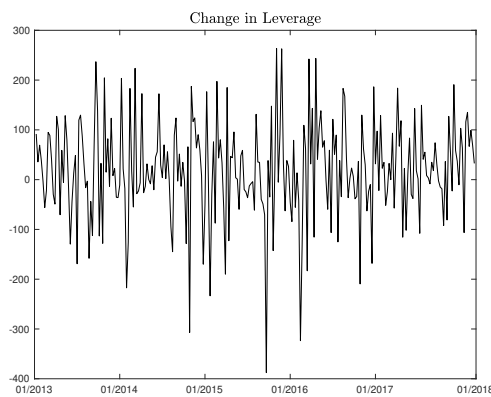
(e) Changes in Market Leverage

Fig. 3.8 Time-series variation of slope, smirk, market asset return (r_V^M), average volatility level ($\bar{\sigma}_V^M$), and change in market leverage (ΔLEV^M). All the signals are stationary according to the ADF test; therefore $\mathbf{X}_t = (X_1, X_2)_t = (\text{Slope}, \text{Smirk})_t$ can be modelled as a Vector Autoregressive process. $\mathbf{Z}_t = (Z_1, Z_2, Z_3)_t = (r_V^M, \bar{\sigma}_V^M, \Delta \text{LEV}^M)_t$ is added to the autoregressive structure as set of exogenous variables.

| Included observations: 259 | | | | | |
Autocorrelation	Partial Correlation		AC	PAC	Q-Stat	Prob
		1	0.226	0.226	13.434	0.000
		2	0.121	0.073	17.270	0.000
		3	0.128	0.092	21.617	0.000
		4	0.048	-0.006	22.223	0.000
		5	0.036	0.011	22.577	0.000
		6	0.063	0.042	23.637	0.001
		7	0.064	0.039	24.745	0.001
		8	0.117	0.091	28.406	0.000
		9	0.213	0.167	40.632	0.000
		10	0.119	0.025	44.446	0.000

| Included observations: 259 | | | | | |
Autocorrelation	Partial Correlation		AC	PAC	Q-Stat	Prob
		1	0.399	0.399	41.754	0.000
		2	0.313	0.183	67.518	0.000
		3	0.263	0.108	85.806	0.000
		4	0.262	0.114	103.99	0.000
		5	0.142	-0.048	109.34	0.000
		6	0.134	0.018	114.15	0.000
		7	0.207	0.131	125.60	0.000
		8	0.191	0.058	135.42	0.000
		9	0.232	0.118	149.92	0.000
		10	0.184	0.008	159.14	0.000

(a) Slope   (b) Smirk

Fig. 3.9 Correlograms of the variables Slope (left) and Smirk (right). Slope display a significant autocorrelation of the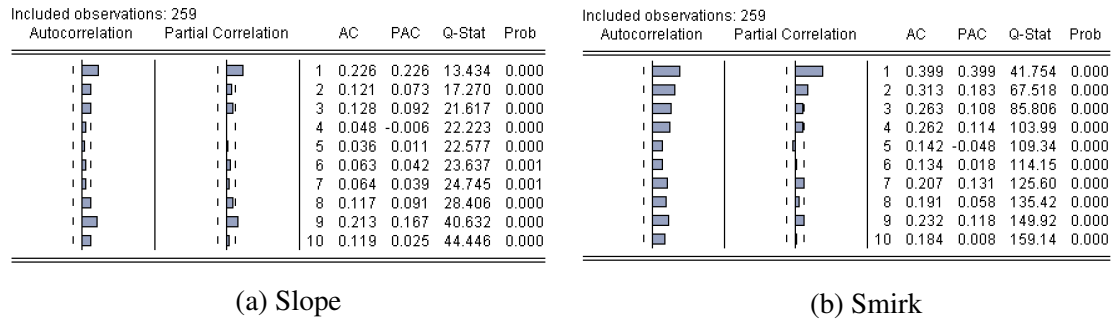 first order, whilst Smirk shows an autocorrelation structure up to the second lag. Given these findings, the bivariate process $\mathbf{X}_t$ is modelled as a vector autoregressive process of order two, VAR(2).

a downward sloping term structure is what should be normally expected when a compound option model is used to estimate the asset volatility from the data.

In order to model the joint evolution of the slope and smirk of the market-wide asset volatility, a Vector Autoregressive (VAR) model is used. Let $\mathbf{X}_t = (X_1, X_2)_t = (\text{Slope}, \text{Smirk})_t$ and a set of exogenous variables $\mathbf{Z}_t = (Z_1, Z_2, Z_3)_t = (r_V^M, \bar{\sigma}_V^M, \Delta\text{LEV}^M)_t$. The exogenous variable $r_{V,t}^M = \ln(V_t^M) - \ln(V_{t-1}^M)$, where V^M is the value-weighted market value of the assets, is the market return on asset. The other two exogenous variables are the average level of asset volatility and the change in market leverage respectively.

From the correlograms of $\mathbf{X}_t$ in Figure 3.9, the slope of the surface exhibit some autocorrelation of the first order, whilst its smirk appears to have an autoregressive structure up to the second lag. Based on these findings, a VAR(2) with exogenous variables is modelled, that is

$$\mathbf{X}_t = \boldsymbol{\alpha} + \mathbf{A}_1\mathbf{X}_{t-1} + \mathbf{A}_2\mathbf{X}_{t-2} + \mathbf{B}\mathbf{Z}_t + \boldsymbol{\varepsilon}_t \tag{3.6}$$

where $\boldsymbol{\alpha}$ is the vector of intercepts, $\mathbf{A}_1, \mathbf{A}_2$ and $\mathbf{B}$ are matrices of loadings and $\boldsymbol{\varepsilon}_t$ is a zero mean white noise vector process.

Table 3.8, left panel, reports the estimated parameters of the VAR. Confirming the graphical pattern displayed by the correlograms, the slope of the surface observed at time t is positively correlated with the surface observed the previous week. Lovreta and Silaghi (2017) document also a similar autoregressive behaviour. The lagged slope affects also the present smirk, being the two positively correlated. The slope lagged of two weeks does not have any impact on either the present slope or smirk. On the contrary, the smirk lagged up to two weeks display is positively correlated with both the present slope and smirk. The variable Smirk_{t-2} does affect the present smirk only. Overall, the evolution of the asset volatility

surface display a strong autoregressive component both in term of the variation across the time-to-maturity and moneyness dimension.

The set of exogenous variables have also some explanatory power in describing the time-series evolution of the surface. Consistently with the PCA conducted in the previous section, the average level of the surface does explain both the slope and the smirk of the surface. An increase in the average volatility reduces the slope thus becoming more negative. This implies that the surface becomes steeper, suggesting that short term volatilities experience a larger increase than the volatilities at longer horizons. On the other hand, a positive shock to the average volatility translates into an increase of the smirk. Being the smirk mostly negative across the sample, the positive loading on average volatility signals that, after a positive shock, the surface flattens across the moneyness dimension. The volatilities of out-of-the money calls appear to increase more than out-of-the-money puts, thus reducing the spread between the two.

The second exogenous variable is represented by the contemporaneous asset return on the market. This variable is positively correlated with both the slope and the smirk of the surface. Being both Slope and Smirk mostly negative, this implies that an increasing market is associated with a flatter surface. Conversely, negative market shocks make the surface both steeper and more skewed. Therefore, option market participants adjust option prices to negative shocks as theory would predict, demanding a larger risk-premium for those contracts which are mostly affected. These are most likely short-term deep OTM put options. If the market participants fear a negative temporary market shock, put prices increase more than call prices and, then, surface becomes steeper and more skewed.

Finally, consistently with the leverage effect, changes in market leverage affects only the evolution of the surface across moneyness. As the loading on ΔLEV is negative, an increase in the market leverage, and therefore in the market-wide probability of defaults, reduce the smirk making it more negative. This reduction is induced by the increase in the volatility of DOOM puts which indeed are the contracts mostly affected by credit risk factors (Maglione 2019). Overall, the unrestricted VAR(2) is able to explain almost half of the variation of both the slope and the smirk of the surface.

For completeness, a restricted VAR(2) is also estimated in Table 3.8, right panel. The restricted VAR is obtained by setting to zero the coefficients of those loadings on variables which are statistically insignificant. The restricted VAR does not significantly improve the fit of the model. However, the F-test for restrictions has a p-value of 0.09, thus making the restricted VAR more informative than the unrestricted at 10% significance level.

	Slope$_t$		Smirk$_t$			Slope$_t$		Smirk$_t$	
Slope$_{t-1}$	0.143 (0.008)	***	0.352 (0.000)	***	Slope$_{t-1}$	0.160 (0.001)	***	0.379 (0.000)	***
Slope$_{t-2}$	0.056 (0.295)		0.087 (0.369)		Slope$_{t-2}$	0 -		0 -	
Smirk$_{t-1}$	0.068 (0.034)	**	0.367 (0.000)	***	Smirk$_{t-1}$	0.075 (0.006)	**	0.383 (0.000)	***
Smirk$_{t-2}$	0.166 (0.604)		0.184 (0.002)	***	Smirk$_{t-2}$	0 -		0.162 (0.001)	***
$\sigma^M_{V,t}$	-1.413 (0.000)	***	1.876 (0.000)	***	$\sigma^M_{V,t}$	-1.417 (0.000)	***	1.87 (0.000)	***
$r^M_{V,t}$	0.218 (0.333)		0.679 (0.098)	**	$r^M_{V,t}$	0 -		0.773 (0.051)	**
ΔLEV^M_t	0.396 (0.364)		-1.899 (0.018)	**	ΔLEV^M_t	0 -		-1.724 (0.026)	**
α	0.276 (0.000)	***	-0.422 (0.000)	***	α	0.274 (0.000)	***	-0.424 (0.000)	***
R^2	0.48		0.46		R^2	0.48		0.46	

Table 3.8 Unrestricted VAR(2) (left) and restricted VAR(2) (right). The results show an autoregressive structure of the first order for Slope and of the second order for Smirk. The set of exogenous variable affect the surface as expected by the compound option model. The process of adding restrictions is conducted 'step-by-step', that is the coefficients are set to zero one at a time and the VAR is then re-estimated. Then, the next most insignificant coefficient is set to zero and so on, until the model on the left panel of Figure 3.8 is obtained. F-test for restricted vs unrestricted has p-value 0.09, thus making the restricted model more informative than the unrestricted at 10% significance level.
Significance levels: 10% (*), 5% (**), 1% (***).

3.5   Conclusions

In this paper the surface of asset implied volatility is estimated and analysed, as a function of maturity and moneyness. The firm's asset volatility is estimated using a compound option structural model of default on a sample of 66 US companies that belong to the S&P100 and spans over the 2013–2017 period. As both the stock and option prices are modelled as function of the underlying asset value and volatility, a joint calibration allows to estimate these two unobservable parameters. Because options are used, the estimated asset volatility depends both on the option time-to-maturity and moneyness, thus generating a surface. To the best of my knowledge, this is the first work which provides an option-implied asset volatility surface. Only Lovreta and Silaghi (2017) develop an methodology for estimating the asset volatility for CDSs which, however, require some extra assumptions for estimating the volatility across moneyness. Here instead, both the maturity and moneyness dimensions are naturally embedded in the estimation procedure.

Once the firm-specific surface is obtained, then the market-wide asset volatility surface can be constructed. Principal component analysis on the changes in asset volatility over the cross-section of firms shows that market-wide asset volatility is able to to explain most of the cross-sectional variation. Therefore, PCA is conducted on the changes of the market volatility surface across the time-to-maturity and moneyness dimension as well as across the surface as whole. In terms of maturity, the first three PCs are able to explain all the variability and are ascribed as a level, slope and curvature factors affecting the term structure. Regarding the moneyness dimension, the first three PCs also explain the whole variation and are associated to level, smirk and curvature. When analysed as a whole, the first two PC (modes), interpreted as level and smirk are able to account almost the totality of the variation. The third and fouth components together accounts to less than 2% of the variance and are associated to a convexity related to the moneyness and to the term structure respectively.

The analysis also finds a downward sloping term structure of asset implied volatilities. With respect to to moneyness, a negative skew is documented, in line with evidence on equity implied volatility. In order to jointly model the slope and the smirk of the implied volatility surface a Vector Autoregressive with exogenous variables is used. The proposed statistical model is able to account for almost half of the variation exhibited by the asset volatility surface, and document an autoregressive component for both the slope and the smirk of the surface, being the smirk more persistent. The estimated parameters suggest that the term structure gets steeper during crises and flatter in tranquil periods; also the skew gets steeper during crises and is flatter for longer-term maturities.

References

Andersen, T. G., Fusari, N. and Todorov, V. (2015), 'The risk premia embedded in index options', *Journal of Financial Economics* **117**(3), 558–584.

Anderson, R. W. and Sundaresan, S. (1996), 'Design and valuation of debt contracts', *Review of Financial Studies* **9**(1), 37–68.

Bartram, S. M., Brown, G. W. and Waller, W. (2015), 'How important is financial risk?', *Journal of Financial and Quantitative Analysis* **50**(4), 801–824.

Bharath, S. T. and Shumway, T. (2008), 'Forecasting default with the merton distance to default model', *Review of Financial Studies* **21**(3), 1339–1369.

Black, F. (1976), 'Studies of stock price volatility changes', *Proceedings of the 1976 Meeting of the Business and Economic Statistics Section* pp. 177–181. American Statistical Association.

Black, F. and Cox, J. C. (1976), 'Valuing corporate securities: Some effects of bond indenture provisions', *Journal of Finance* **31**(2), 351–367.

Black, F. and Scholes, M. (1973), 'The pricing of options and corporate liabilities', *Journal of Political Economy* **81**(3), 637–654.

Blanco, R., Brennan, S. and Marsh, I. W. (2005), 'An empirical analysis of the dynamic relation between investment-grade bonds and credit default swaps', *Journal of Finance* **60**(5), 2255–2281.

Boyer, B. H. and Vorkink, K. (2014), 'Stock options as lotteries', *Journal of Finance* **69**(4), 1485–1527.

Brigo, D. (2005), 'Market models for cds options and callable floaters', *Risk Magazine* .

Brigo, D. and Mercurio, F. (2006), *Interest Rate Models: Theory and Practice*, Springer Finance.

Burkovska, O., Gass, M., Glau, K., Mahlstedt, M., Schoutens, W. and Wohlmuth, B. (2018), 'Calibration to american options: numerical investigation of the de-americanization method', *Quantitative Finance* **18**(7), 1091–1113.

Campbell, J. Y. and Cochrane, J. H. (1999), 'By force of habit: A consumption-based explanation of aggregate stock market behavior', *Journal of Political Economy* **107**(2), 205–251.

References

Campbell, J. Y. and Taksler, G. B. (2003), 'Equity volatility and corporate bond yields', *Journal of Finance* **58**(6), 2321–2349.

Cao, C., Yu, F. and Zhong, Z. (2010), 'The information content of option-implied volatility for credit default swap valuation', *Journal of Financial Markets* **13**(3), 321–343.

Carr, P. and Linetsky, V. (2006), 'A jump to default extended CEV model: An application of Bessel processes', *Finance and Stochastics* **10**(3), 303–330.

Carr, P., Mendoza-Arriga, R. and Linetsky, V. (2010), 'Time-changed Markov processes in unified credit-equity modeling', *Mathematical Finance* **20**(4), 527–569.

Carr, P. and Wu, L. (2007), 'Theory and evidence on the dynamic interactions between sovereign credit default swaps and currency options', *Journal of Banking and Finance* **31**(8), 2383–2403.

Carr, P. and Wu, L. (2010), 'Stock options and credit default swaps: A joint framework for valuation and estimation', *Journal of Financial Econometrics* **8**(4), 409–449.

Carr, P. and Wu, L. (2011), 'A simple robust link between american puts and credit protection', *Review of Financial Studies* **24**(2), 473–505.

Carr, P. and Wu, L. (2017), 'Leverage effect, volatility feedback, and self-exciting market disruptions', *Journal of Financial and Quantitative Analysis* **52**(5), 2119–2156.

Chen, L., Collin-Dufresne, P. and Goldstein, R. S. (2009), 'On the relation between the credit spread puzzle and the equity premium puzzle', *Review of Financial Studies* **22**(9), 3367–3409.

Chen, R.-R. (2013), 'On the geske compound option model when interest rates change randomly - with an application to credit risk modeling', *Working paper* .

Choi, J. and Richardson, M. (2016), 'The volatility of a firm's assets and the leverage effect', *Journal of Financial Economics* **121**(2), 254–277.

Christie, A. A. (1982), 'The stochastic behavior of common stock variances: Value, leverage and interest rate effects', *Journal of Financial Economics* **10**(4), 407–432.

Collin-Dufresne, P. and Goldstein, R. S. (2001), 'Do credit spreads reflect stationary leverage ratios?', *Journal of Finance* **56**(5), 1929–1957.

Collin-Dufresne, P., Goldstein, R. S. and Helwege, J. (2010), 'Is credit event risk priced? modeling contagion via the updating of beliefs', *NBER Working Paper* (15733), 1–46.

Collin-Dufresne, P., Goldstein, R. S. and Martin, J. S. (2001), 'The determinants of credit spread changes', *Journal of Finance* **56**(6), 2177–2207.

Collin-Dufresne, P., Goldstein, R. S. and Yang, F. (2012), 'On the relative pricing of long-maturity index options and collateralized debt obligations', *Journal of Finance* **67**(6), 1983–2014.

Cont, R. and da Fonseca, J. (2002), 'Dynamics of implied volatility surfaces', *Quantitative Finance* **2**(1), 45–60.

Cover, T. M. and Thomas, J. A. (2006), *Elements of Information Theory*, Wiley-Blackwell.

Cox, J. C. (1996), 'The constant elasticity of variance option pricing model', *Journal of Portfolio Management* **23**(4), 15–17.

Cremers, K. J. M., Driessen, J. and Meanhout, P. (2008), 'Explaining the level of credit spreads: Option-implied jump risk premia in a firm value model', *Review of Financial Studies* **21**(5), 2209–2242.

Cremers, K. J. M., Driessen, J., Meanhout, P. and Weinbaum, D. (2008), 'Individual stock-option prices and credit spreads', *Journal of Banking and Finance* **32**(12), 2706–2715.

Crosbie, P. J. and Bohn, J. R. (1993), 'Modeling default risk', *Unpublished* .

Driessen, J. (2005), 'Is default event risk priced in corporate bonds?', *Review of Financial Studies* **18**(1), 165–195.

Du, D., Elkamhi, R. and Ericsson, J. (2019), 'Time-varying asset volatility and the credit-spread puzzle', *Journal of Finance* **74**(4), 1841–1885.

Duan, J. (1994), 'Maximul likelihood estimation using price data of the derivative contract', *Mathematical Finance* **4**(2), 155–167.

Duan, J., Gauthier, G. and Simonato, J. (2005), 'On the equivalence of the kmv and maximum likelihood methods for structural credit risk models', *Unpublished* .

Duffee, G. R. (1998), 'The relation between treasury yields and corporate bond yield spreads', *Journal of Finance* **53**(6), 2225–2241.

Duffie, D. and Singleton, K. J. (1999), 'Modeling term structures of defaultable bonds', *Review of Financial Studies* **12**(4), 687–720.

Dupire, B. (1994), 'Pricing with a smile', *Risk* .

Elton, E. J., Gruber, M. J., Agrawal, D. and Mann, C. (2001), 'Explaining the rate spread on corporate bonds', *Journal of Finance* **56**(1), 247–277.

Engle, R. F. and Granger, C. W. J. (1987), 'Co-integration and error correction: Representation, estimation, and testing', *Econometrica* **55**(2), 251–276.

Eom, Y. H., Helwege, J. and Huang, J.-Z. (2004), 'Structural models of corporate bond pricing: An empirical analysis', *Review of Financial Studies* **17**(2), 499–544.

Ericsson, J., Jacobs, K. and Ovied, R. (2009), 'The determinants of credit default swap premia', *Journal of Financial and Quantitative Analysis* **44**(1), 109–132.

Ericsson, J. and Reneby, J. (2002), 'A note on contingent claims pricing with non-traded assets', *SSE/EFI Working Paper Series in Economics and Finance* (314), 1–9.

Ericsson, J., Reneby, J. and Wang, H. (2015), 'Can structural models price default risk? evidence from bond and credit derivative markets', *Quartely Journal of Finance* **5**(3).

References

Feldhütter, P. and Schaefer, S. M. (2018), 'The myth of the credit spread puzzle', *Review of Financial Studies* **3**(8), 2897–2942.

Forte, S. (2011), 'Calibrating structural models: a new methodology based on stock and credit default swap data', *Quantitative Finance* **11**(12), 1745–1746.

Forte, S. and Lovreta, L. (2012), 'Endogenizing exogenous default barrier models: The *MM* algorithm', *Journal of Banking and Finance* **36**(6), 1639–1652.

Frey, R. and Sommer, D. (1998), 'The generalization of the geske-formula for compound options to stochastic interestrates is not trivial - a note', *Journal of Applied Probability* **35**(2), 501–509.

Gatheral, J. (2006), *The Volatility Surface: A Practitioner's Guide*, John Wiley & Sons.

Geman, H., Karoui, N. E. and Rochet, J.-C. (1995), 'Change of numéraire, change of probability measure and option pricing', *Journal of Applied Probability* **32**(2), 443–458.

Genz, A. (2004), 'Numerical computation of rectangular bivariate and trivariate normal and t probabilities', *Statistics and Computing* **14**(3), 251–260.

Genz, A. and Bretz, F. (1999), 'Numerical computation of multivariate t probabilities with application to power calculation of multiple contrasts', *Journal of Statistical Computation and Simulation* **63**, 361–378.

Genz, A. and Bretz, F. (2002), 'Comparison of methods for the computation of multivariate t probabilities', *Journal of Computational and Graphical Statistics* **11**(4), 950–971.

Geske, R. (1977), 'The valuation of corporate liabilities as compound options', *Journal of Financial and Quantitative Analysis* **12**(4), 541–552.

Geske, R. (1979), 'The valuation of compound options', *Journal of Financial Economics* **7**(1), 63–81.

Geske, R., Subrahmanyam, A. and Zhou, Y. (2016), 'Capital structure effects on the prices of equity call options', *Journal of Financial Economics* **36**(6), 1639–1652.

Greene, W. H. (2008), *Econometric Analysis*, 6 edn, Pearson Prentice Hall.

Henry-Labordère, P. (2009), 'Calibration of local stochastic volatility models to market smiles: A monte-carlo approach', *Risk Magazine* .

Heston, S. L. (1993), 'A closed-form solution for options with stochastic volatility with applications to bond and currency options', *Review of Financial Studies* **6**(2), 327–343.

Huang, J.-Z. and Huang, M. (2012), 'How much of the corporate-treasury yield spread is due to credit risk?', *Review of Asset Pricing Studies* **2**(2), 153–202.

Hull, J. C., Nelken, I. and White, A. D. (2004), 'Merton's model, credit risk and volatility skews', *Journal of Credit Risk* **1**(1), 3–28.

Jolliffe, I. T. (2002), *Principal Component Analysis*, Spinger.

Jones, E. P., Mason, S. P. and Rosenfeld, E. (1983), 'Contingent claims analysis of corporate capital structures: An empirical investigation', *Journal of Finance* **39**(3), 611–625.

Leland, H. E. (1994), 'Corporate debt value, bond covenants, and optimal capital structure', *Journal of Finance* **49**(4), 1213–1252.

Leland, H. E. and Toft, K. B. (1996), 'Optimal capital structure, endogenous bankruptcy, and the termstructure of credit spreads', *Journal of Finance* **51**(3), 987–1019.

Litterman, R. and Scheinkman, J. (1991), 'Common factors affecting bond returns', *Journal of Fixed Income* **1**(1), 54–61.

Longstaff, F. A., Mithal, S. and Neis, E. (2005), 'Corporate yield spreads: Default risk or liquidity? new evidence from the credit default swap market', *Journal of Finance* **60**(5), 2213–2253.

Longstaff, F. A. and Schwartz, E. (1995), 'A simple approach to valuing risky fixed and floating rate debt', *Journal of Finance* **50**(3), 789–821.

Lovreta, L. and Silaghi, F. (2017), 'The surface of implied firm's asset volatility', *Journal of Banking and Finance* **000**, 1–18.

Maglione, F. (2019), The impact of credit risk on equity options.

Maglione, F. (2020), Credit spreads, leverage and volatility: A cointegration approach.

Mella-Barral, P. and Perraudin, W. (1997), 'Strategic debt service', *Journal of Finance* **52**(2), 531–556.

Merton, R. C. (1974), 'On the pricing of corporate debt: The risk structure of interest rates', *Journal of Finance* **29**(3), 449–470.

Merton, R. C. (1977), 'On the pricing of contingent claims and the Modigliani-Miller theorem', *Journal of Financial Economics* **5**(2), 241–249.

Miller, M. H. and Modigliani, F. (1961), 'Dividend policy, growth, and the valuation of shares', *Journal of Business* **34**(4), 411–433.

Pesaran, M. H., Y., S. and P., S. R. (1999), 'Pooled mean group estimation of dynamic heterogeneous panels', *Pooled mean group estimation of dynamic heterogeneous panels* **94**, 621–634.

Ronn, E. I. and Verma, A. K. (1986), 'Pricing risk-adjusted deposit insurance: An option-based model', *Journal of Finance* **41**(4), 871–895.

Schaefer, S. M. and Strebulaev, I. A. (2008), 'Structural models of credit risk are useful: Evidence from hedge ratios on corporate bonds', *Journal of Financial Economics* **90**(1), 1–19.

Strebulaev, I. A. and Whited, T. M. (2012), *Dynamic Models and Structural Estimation in Corporate Finance*, Now Publishers Inc.

References

Toft, K. B. and Prucyk, B. (1997), 'Options on leveraged equity: Theory and empirical tests', *Journal of Finance* **53**(3), 1151–1180.

Vassalou, M. and Xing, Y. (2004), 'Default risk in equity returns', *Journal of Finance* **59**(2), 831–868.

Zhang, B. Y., Zhou, H. and Zhu, H. (2009), 'Explaining credit default swap spreads with the equity volatility and jump risks ofindividual firms', *Review of Financial Studies* **22**(12), 5099–5131.

Zhou, C. (2001), 'The term structure of credit spreads with jump risk', *Journal of Banking and Finance* **25**(11), 2015–2040.

Appendix A

Notation and Abbreviation

If not differently specified, sets as well as univariate random variables are indicated as upper case letters (X), scalars as lower case letters (x), vectors as lower case bold letters ($\mathbf{x}$), matrices as well as multivariate random vectors as upper case bold letters ($\mathbf{X}$).

$\mathbb{N} = \{1, 2, \dots\}$	set of natural number
$\mathbb{R} = (-\infty, +\infty)$	set of real number
$\mathbb{R}_+ = [0, +\infty)$	set of non-negative real number
$\mathbb{R}^n$	Euclidean n-dimensional space
$\mathscr{M}_+^n$	space of positive definite matrices
$\circ$	composition of function (operator)
$f \in o(g)$ as $x \to a$	$\lim_{x \to a} f/g = 0$
$f \in O(g)$ as $x \to a$	$\limsup_{x \to a} \lvert f/g \rvert < \infty$
$f \sim g$ as $x \to a$	$\lim_{x \to a} f/g = 1$
$\mathbb{1}_A : X \to [0, 1]$	indicator function of a subset A of a set X
$(\Omega, \mathscr{F}, \mathbb{F}, \mathbb{P})$	filtered probability space, with $\mathbb{F} := (\mathscr{F}_t)_{t \in [0,T]}$
$\mathscr{S}(\mathbb{F}, \mathbb{P})$	vector space of semimartingales on $(\Omega, \mathscr{F}, \mathbb{F}, \mathbb{P})$
$\mathbb{E}^{\mathbb{P}}$	expectation under $\mathbb{P}$
$\mathbb{E}_t^{\mathbb{P}}$ (or $\mathbb{E}_k^{\mathbb{P}}$)	conditional expectation under $\mathbb{P}$ given $\mathscr{F}_t$ (or $\mathscr{F}_{t_k}$)
$\mathbb{V}$	variance
$\mathbb{C}\mathrm{ov}$	covariance
$\mathbb{C}\mathrm{orr}$	correlation
$\mathbb{Q}^n$	t_n-forward measure
$\mathbb{Q}$	risk-neutral measure
$\mathbb{Q} \sim \mathbb{P}$	$\mathbb{Q}$ is equivalent with respect to $\mathbb{P}$

Notation and Abbreviation

PDF	probability density function
CDF	cumulative distribution function
$X \sim \ldots$	X is distributed as $\ldots$
$n(\cdot; \mu, \sigma)$	PDF of $X \sim \mathcal{N}(\mu, \sigma)$
$n_m(\cdot; \boldsymbol{\mu}, \boldsymbol{\Sigma})$	PDF of $\mathbf{X} \sim \mathcal{N}_m(\boldsymbol{\mu}, \boldsymbol{\Sigma})$
$N(\cdot; \mu, \sigma)$	CDF of $X \sim \mathcal{N}(\mu, \sigma)$
$N_m(\cdot; \boldsymbol{\mu}, \boldsymbol{\Sigma})$	CDF of $\mathbf{X} \sim \mathcal{N}_m(\boldsymbol{\mu}, \boldsymbol{\Sigma})$
$\phi(\cdot)$	PDF of $X \sim \mathcal{N}(0, 1)$
$\phi_m(\cdot; \boldsymbol{\Gamma})$	PDF of $\mathbf{X} \sim \mathcal{N}_m(\mathbf{0}, \boldsymbol{\Gamma})$ with $\gamma_{ii} = 1, \forall i \leq m$
$\Phi(\cdot)$	CDF of $X \sim \mathcal{N}(0, 1)$
$\Phi_n(\cdot; \boldsymbol{\Gamma})$	CDF of $\mathbf{X} \sim \mathcal{N}_m(\mathbf{0}, \boldsymbol{\Gamma})$ with $\gamma_{ii} = 1, \forall i \leq m$
$\Phi_n(\cdot)$	CDF of $\mathbf{X} \sim \mathcal{N}_m(\mathbf{0}, \mathbf{I})$ with $\mathbf{I}$ the $m \times m$ identity matrix
X_{t-} (or X_{i-})	$\lim_{s \uparrow t} X_s$ (or $\lim_{s \uparrow t_i} X_s$)
r_t	instantaneous spot rate at time t
$B_t = \exp\left(\int_0^t r_s \, \mathrm{d}s\right)$	value of a bank account at time t
$DF(t, T) = \frac{B_t}{B_T}$	discount factor between time t and T
τ	default time
LGD	loss given default
V_t	market value of the firm at time t
S_t	market value of the firm's equity at time t
$D_{t,T}$	market value of the firm's debt with maturity T at time t
$\mathrm{El}_x(y)$	elasticity of y with respect to x

Appendix B

Further Description of the Data and Construction of the Variables

In order implement the calibration described in Section 1.3, one of the most crucial aspects is to effectively and efficiently represent the firms' capital structures. In particular, every firm can actually have $n \geq 0$ bonds outstanding; however, it is virtually impossible to solve for the unobservable (V_0, σ_V) if n is very large, as the calibration involves the solution of an n-dimentional integral equation. Moreover, the estimation of the asset value and its volatility involes the inversion of the multivariate normal CDF, which is implemented in Matlab via the function `mvncdf`. For bivariate and trivariate distributions, `mvncdf` uses adaptive quadrature on a transformation of the t density, based on methods developed in Genz (2004). For four or more dimensions, `mvncdf` uses a quasi-Monte Carlo integration algorithm based on methods developed by Genz and Bretz (1999) and Genz and Bretz (2002). As a matter of fact, for $n \geq 4$, the algorithm becomes much slower due to the quasi-Monte Carlo integration.

In addition, as each company have a different n, it is extremely impractical not to have a 'standard framework' of valuation. Also, for US firms detailed data about individual bonds outstanding is available only at yearly frequency in the 10-K document (and the face value of the bonds are to be collected manually). On the other hand, in order to homogenise different capital structures and construct a standard framework for the implementation, the number of bond outstanding is set such that $n \leq 3$ as described below.

From Compustat, the variables `DLTTQ` (Long-Term Debt – Total) and `DD1Q` (Long-Term Debt Due in One Year) are downloaded every quarter. `DLTTQ` represents debt obligations due more than one year from the company's Balance Sheet date or due after the current operating cycle, whilst `DD1Q` represents the current portion of long-term debt. They proxy as long-term

and short-term debt respectively. Finally, the three synthetic bonds are defined as

$$F_1 = \frac{\texttt{DD1Q}}{\texttt{CSHO}}, \qquad F_2 = F_3 = 0.5 \cdot \frac{\texttt{DLTTQ}}{\texttt{CSHO}},$$

with $\{t_1, t_2, t_3\} = \{1, 5, 10\}$ and $\texttt{CSHO}$ the number of common share outstanding. Those are reset at each quarter, and the time to maturity is adjusted accordingly for the effect of passage of time when the estimates of the implied volatility of the assets are carried out.

The choice of $t_1 = 1$ is trivial and given by the definition of the variables; $t_2 = 5$ is chosen as it is well-documented that the most actively traded CDS is the 5-year contract (which is used for the calibration). Also t_3 is set at 10 years in order not to rely on CDS with very long maturities (such as 20 or 30-years contracts) as they could be very illiquid.

Unfortunately, the variable $\texttt{DD1Q}$ can either be not available at quarterly frequency or is not reported at all (the latter is usually observed for banks and energy companies). Under these cases, the variable is estimated using the quarterly variable Debt in Current Liabilities ($\texttt{DLCQ}$) which is always available. Notice that $\texttt{DD1Q}$ (when available) is a fraction of $\texttt{DLCQ}$. Therefore, in case of missing observation, the last available $\texttt{DD1Q/DLCQ}$ ratio is used to determine the contemporaneous $\texttt{DD1Q}$. Finally, if $\texttt{DD1Q}$ is never reported, the average $\texttt{DD1Q/DLCQ}$ of comparable companies based on Division/Sub-division (see Table B.1) is estimated and $\texttt{DD1Q}$ is projected accordingly.

Moreover, I believe that the choice of setting $n = 3$[1] constitutes the optimal number of bonds such that both *level*, *slope* and *curvature* of the term structure of the survival probabilities extracted from CDS are matched by the model. As a matter of fact, the calibration procedure to be effective relies on the ability of the structural model of default to reproduce the aforementioned term structure.

For completeness, I report the composition of $\texttt{DD1Q}$ and $\texttt{DLTTQ}$.

$\texttt{DD1Q}$ includes:

1. Current portion of any item defined as long-term debt (for example, the current portion of a long-term lease obligation);

2. Instalments on a loan;

3. Sinking fund payments.

This item excludes:

---

[1]There are instances where $n < 3$ as the company does not have either short-term or long-term debt; however the most frequent capital structures have $n = 3$.

1. Current portions of debt that do not reflect discounts on long term debt;

2. Debt that includes interest payments due;

3. Demand notes;

4. Debt in default if there is no associated long term debt reported as part of the long term liabilities;

5. Estimated claims and other liabilities under Chapter XI or other bankruptcy proceedings;

6. Interest on capitalized lease obligations.

`DLTTQ` includes:

1. Advances to finance construction;

2. Bonds, mortgages, and similar debt;

3. ESOP loan guarantees;

4. Extractive industries' advances for exploration and development;

5. Forestry and paper companies' timber contracts;

6. Gold and bullion loans;

7. Guaranteed Preferred Beneficial Interests in Corporation's Junior Subordinated Deferred Interest Debentures;

8. Indebtedness to affiliates;

9. Industrial revenue bonds;

10. Instalment Obligations – nonrecourse;

11. Line of credit, when reclassified as a non-current liability;

12. Loans;

13. Loans on insurance policies;

14. Long-term lease obligations (capitalized lease obligations);

Further Description of the Data and Construction of the Variables

15. Mandatorily Redeemable Capital Securities of Subsidiary Trust;

16. Notes payable, due within one year to be refunded by long-term debt when carried as noncurrent liability;

17. Obligations called "note" or "deb" whether or not they are interest-bearing;

18. Obligations requiring interest payment that are not specified by type;

19. Production payments and advances for exploration and development;

20. Publishing companies' royalty contracts payable;

21. Purchase obligations and payments to officers (when listed as long-term liabilities);

22. Unamortized debt discount.

This item excludes:

1. Accounts payable due after one year (included in Liabilities – Other);

2. Accrued interest on long-term debt (included in Liabilities – Other);

3. Chapter XI bankruptcy terms;

4. Current portion of long-term debt (included in Current Liabilities);

5. Customers' deposits on bottles, kegs, and cases (included in Liabilities – Other);

6. Deferred compensation;

7. Subsidiary preferred stock (included in Minority Interest).

Finally, the payout ratio is calculated as the weighted average cost of capital for the company. The cost of equity (i.e. dividend yield, q) is estimated as the average dividend yield over the previous year. These data are downloaded from Bloomberg. The cost of debt is calculated as

$$c = \min\left\{ \frac{\sum_{i=1}^{n} c_i F_i}{F}, \ln\left(1 + \frac{\texttt{XINT}}{F}\right) \right\},$$

where $F = \sum_{i=1}^{n} F_i$ and c_i the continuously compounded debt payout rate. $\texttt{XINT}$ is the Compustat variable Interest and Related Expense – Total. The individual rates c_i are observed

at yearly frequency and manually collected from the 10-K documents. Eventually, the payout rate is estimated every year as

$$\varpi = \frac{cF + qS}{F + S},$$

where S is the value of the equity at the beginning of the year and q the dividend yield estimated as described above.

Further Description of the Data and Construction of the Variables

Table B.1 List of the selected companies and their SIC code.

Ticker	SIC	Division
AAPL	3663	Manufacturing
ABT	2834	Manufacturing
ACN	8742	Services
ALL	6331	Finance, Insurance and Real Estate
AMGN	2836	Manufacturing
AMZN	5961	Wholesale Trade
BA	3721	Manufacturing
BAC	6020	Finance, Insurance and Real Estate
BMY	2834	Manufacturing
C	6199	Finance, Insurance and Real Estate
CAT	3531	Manufacturing
CL	2844	Manufacturing
CMCSA	4841	Transportation, Communications, Electric, Gas and Sanitary service
COF	6141	Finance, Insurance and Real Estate
COP	1311	Mining
COST	5399	Wholesale Trade
CSCO	3576	Manufacturing
CVS	5912	Retail Trade
CVX	2911	Manufacturing
DD	2821	Manufacturing
DIS	4888	Transportation, Communications, Electric, Gas and Sanitary service
EMR	3823	Manufacturing
EXC	4911	Transportation, Communications, Electric, Gas and Sanitary service
F	3711	Manufacturing
FDX	4513	Transportation, Communications, Electric, Gas and Sanitary service
GD	3721	Manufacturing
GE	4911	Transportation, Communications, Electric, Gas and Sanitary service
HAL	1389	Mining
HD	5211	Wholesale Trade
IBM	7370	Services
INTC	3674	Manufacturing
JNJ	2834	Manufacturing
JPM	6020	Finance, Insurance and Real Estate
KO	2086	Manufacturing
LLY	2834	Manufacturing
LOW	5211	Wholesale Trade
MCD	5812	Retail Trade
MDT	3845	Manufacturing
MMM	2670	Manufacturing
MO	2111	Manufacturing
MON	5169	Retail Trade
MRK	2834	Manufacturing
MS	6211	Finance, Insurance and Real Estate
MSFT	7372	Services
ORCL	7370	Services
OXY	1311	Mining
PEP	2080	Manufacturing
PFE	2834	Manufacturing
PG	2840	Manufacturing
PM	2111	Manufacturing
RTN	3812	Manufacturing
SLB	1389	Mining
SO	4911	Transportation, Communications, Electric, Gas and Sanitary service
SPG	6798	Finance, Insurance and Real Estate
T	4812	Transportation, Communications, Electric, Gas and Sanitary service
TGT	5331	Wholesale Trade
TWX	8748	Services
TXN	3674	Manufacturing
UNH	6324	Finance, Insurance and Real Estate
UNP	4011	Transportation, Communications, Electric, Gas and Sanitary service
USB	6020	Finance, Insurance and Real Estate
UTX	3724	Manufacturing
VZ	4812	Transportation, Communications, Electric, Gas and Sanitary service
WFC	6020	Finance, Insurance and Real Estate
WMT	5331	Retail Trade
XOM	1311	Mining

Appendix C

Gaussian Integrals

Theorem 1. *Given a binary variables ξ taking values ± 1, $a \in \mathbb{R}$, and $\mathbf{b}, \mathbf{c} \in \mathbb{R}^m$ then*

$$\xi \int_a^{\xi\infty} n(x; \mu, \sigma) \Phi_m\left(\mathbf{b}x + \mathbf{c}; \tilde{\boldsymbol{\Gamma}}\right) dx = \Phi_{m+1}\left(\xi \frac{\mu - a}{\sigma}, \mathbf{d}; \boldsymbol{\Gamma}_\xi\right), \qquad \text{(C.1)}$$

for $\mathbf{d} \in \mathbb{R}^m : d_i = \frac{b_i\mu + c_i}{\sqrt{1 + b_i^2\sigma^2}}$,

$$\boldsymbol{\Gamma}_\xi = \begin{pmatrix} \tilde{\boldsymbol{\Gamma}} & \boldsymbol{\gamma}_\xi \\ \boldsymbol{\gamma}_\xi^\top & 1 \end{pmatrix},$$

and $\boldsymbol{\gamma}_\xi \in \mathbb{R}^m : \gamma_{i,\xi} = \xi \frac{b_i\sigma}{\sqrt{1 + b_i^2\sigma^2}}$.

Proof. For notational convenience, define

$$I_\xi := \xi \int_a^{\xi\infty} n(x; \mu, \sigma) \Phi_m\left(\mathbf{b}x + \mathbf{c}; \tilde{\boldsymbol{\Gamma}}\right) dx.$$

I distinguish the two cases $\xi = 1$ and $\xi = -1$ (for convenience of notation the dependence on the distributions' parameters such as μ, σ and $\tilde{\boldsymbol{\Gamma}}$ is omitted).

1. Consider first $\xi = 1$, that is

$$I_1 = \int_a^\infty n(x) \left[\int_{-\infty}^{b_1 x + c_1} \cdots \int_{-\infty}^{b_m x + c_m} \frac{1}{\sqrt{(2\pi)^m \det\tilde{\boldsymbol{\Gamma}}}} \exp\left(-\frac{\mathbf{y}^\top \tilde{\boldsymbol{\Gamma}}^{-1} \mathbf{y}}{2}\right) d^m\mathbf{y}\right] dx$$

$$= \int_{D_0} \frac{1}{\sqrt{2\pi}\sigma} \exp\left(-\frac{1}{2}\left(\frac{x - \mu}{\sigma}\right)^2\right) \frac{1}{\sqrt{(2\pi)^m \det\tilde{\boldsymbol{\Gamma}}}} \exp\left(-\frac{\mathbf{y}^\top \tilde{\boldsymbol{\Gamma}}^{-1} \mathbf{y}}{2}\right) d^m\mathbf{y}\, dx$$

where $D_0 := \{x \in \mathbb{R}, \mathbf{y} \in \mathbb{R}^m : x \geq a, \bigcap_{i=1}^{m} \{y_i \leq b_i x + c_i\}\}$.

Consider the transformation $\mathbf{T_1} : \mathbb{R}^{m+1} \to \mathbb{R}^{m+1}$

$$\mathbf{T_1} := \begin{cases} x = \mu - \sigma w \\ \mathbf{y} = \mathbf{y} \end{cases}$$

with Jacobian

$$\mathbf{J_1} = \begin{pmatrix} -\sigma & 0 & \dots & 0 \\ 0 & 1 & \dots & 0 \\ \dots & \dots & \dots & \dots \\ 0 & 0 & \dots & 1 \end{pmatrix} = \begin{pmatrix} -\sigma & \mathbf{0}^\top \\ \mathbf{0} & \mathbf{I} \end{pmatrix}$$

where $\mathbf{0}$ is the null column vector in $\mathbb{R}^m$ and $\mathbf{I}$ the $m \times m$ identity matrix.

Furthermore, $D_1 := D_0(\mathbf{T_1}) = \left\{ w \in \mathbb{R}, \mathbf{y} \in \mathbb{R}^m : w \leq \frac{\mu - a}{\sigma}, \bigcap_{i=1}^{m} \{y_i \leq -b_i \sigma w + b_i \mu + c_i\} \right\}$.
Hence the integral becomes

$$I_1 = \int_{D_1} n\left(\mu - \sigma w\right) \frac{1}{\sqrt{(2\pi)^m \det \tilde{\mathbf{\Gamma}}}} \exp\left(-\frac{\mathbf{y}^\top \tilde{\mathbf{\Gamma}}^{-1} \mathbf{y}}{2}\right) |\det \mathbf{J_1}| \, \mathrm{d}^m \mathbf{y} \, \mathrm{d}w$$

$$= \int_{D_1} \phi\left(w\right) \frac{1}{\sqrt{(2\pi)^m \det \tilde{\mathbf{\Gamma}}}} \exp\left(-\frac{\mathbf{y}^\top \tilde{\mathbf{\Gamma}}^{-1} \mathbf{y}}{2}\right) \mathrm{d}^m \mathbf{y} \, \mathrm{d}w.$$

Consider another transformation $\mathbf{T_2} : \mathbb{R}^{m+1} \to \mathbb{R}^{m+1}$

$$\mathbf{T_2} := \begin{cases} w = w \\ \mathbf{y} = \mathbf{\Lambda}\left(\mathbf{z} - \boldsymbol{\gamma} w\right) \end{cases}$$

with

$$\mathbf{\Lambda} := \begin{pmatrix} \frac{1}{\sqrt{1 - \gamma_1^2}} & 0 & \dots & 0 \\ 0 & \frac{1}{\sqrt{1 - \gamma_2^2}} & \dots & 0 \\ \dots & \dots & \dots & \dots \\ 0 & 0 & \dots & \frac{1}{\sqrt{1 - \gamma_m^2}} \end{pmatrix}, \quad \boldsymbol{\gamma} := \begin{pmatrix} \gamma_1 \\ \gamma_2 \\ \dots \\ \gamma_m \end{pmatrix},$$

where $\gamma_i \in (-1, 1)$, for all $i \leq m$, are parameters that will be determined later. The corresponding Jacobian is

$$\mathbf{J_2} = \begin{pmatrix} 1 & 0 & \ldots & 0 \\ -\dfrac{\gamma_1}{\sqrt{1-\gamma_1^2}} & \dfrac{1}{\sqrt{1-\gamma_1^2}} & \ldots & 0 \\ \ldots & \ldots & \ldots & \ldots \\ -\dfrac{\gamma_m}{\sqrt{1-\gamma_m^2}} & 0 & \ldots & \dfrac{1}{\sqrt{1-\gamma_m^2}} \end{pmatrix}.$$

Furthermore,

$$D_2 := D_1(\mathbf{T_2}) = \left\{ w \in \mathbb{R}, \mathbf{z} \in \mathbb{R}^m : w \leq \frac{\mu - a}{\sigma}, \right.$$

$$\left. \bigcap_{i=1}^m \left\{ z_i \leq \left(\gamma_i - b_i \sigma \sqrt{1-\gamma_i^2} \right) w + (b_i \mu + c_i) \sqrt{1-\gamma_i^2} \right\} \right\}.$$

Hence

$$I_1 = \int_{D_2} \phi(w) \frac{1}{\sqrt{(2\pi)^m \det \tilde{\mathbf{\Gamma}}}} \exp\left(-\frac{(\mathbf{\Lambda}(\mathbf{z}-\boldsymbol{\gamma}w))^\top \tilde{\mathbf{\Gamma}}^{-1} (\mathbf{\Lambda}(\mathbf{z}-\boldsymbol{\gamma}w))}{2} \right) |\det \mathbf{J_2}| \, d^m \mathbf{z} \, dw$$

$$= \int_{D_2} \phi(w) \frac{1}{\sqrt{(2\pi)^m \prod_{i=1}^m (1-\gamma_i^2) \det \tilde{\mathbf{\Gamma}}}} \exp\left(-\frac{(\mathbf{z}-\boldsymbol{\gamma}w)^\top \mathbf{\Lambda}^\top \tilde{\mathbf{\Gamma}}^{-1} \mathbf{\Lambda}(\mathbf{z}-\boldsymbol{\gamma}w)}{2} \right) d^m \mathbf{z} \, dw.$$

Noticing that $\prod_{i=1}^m (1-\gamma_i^2) = \det\left(\mathbf{\Lambda}^{-1} \right)^2$, then

$$I_1 = \int_{D_2} \phi(w) \frac{1}{\sqrt{(2\pi)^m \det \hat{\mathbf{\Gamma}}}} \exp\left(-\frac{(\mathbf{z}-\boldsymbol{\gamma}w)^\top \hat{\mathbf{\Gamma}}^{-1} (\mathbf{z}-\boldsymbol{\gamma}w)}{2} \right) d^m \mathbf{z} \, dw$$

$$= \int_{D_2} \phi(w) \, n_m(\mathbf{z}|W) \, d^m \mathbf{z} \, dw$$

with $\hat{\mathbf{\Gamma}}^{-1} := \mathbf{\Lambda}^\top \tilde{\mathbf{\Gamma}}^{-1} \mathbf{\Lambda}$, and $\mathbf{Z}|W \sim \mathcal{N}_m\left(\boldsymbol{\gamma}W, \hat{\mathbf{\Gamma}} \right)$. This means that ij-element of the covariance matrix $\hat{\mathbf{\Gamma}}$ is given by

$$\hat{\gamma}_{ij} = \tilde{\gamma}_{ij} \sqrt{\left(1-\gamma_i^2\right)\left(1-\gamma_j^2\right)}$$

with $\tilde{\gamma}_{ii} = 1$.

Furthermore, by setting $\gamma_i - b_i \sigma \sqrt{1 - \gamma_i^2} = 0$, that corresponds to $\gamma_i = \frac{b_i \sigma}{\sqrt{1 + b_i^2 \sigma^2}}$, the region of integration reduces to $D_2 = \left\{ w \in \mathbb{R}, \mathbf{z} \in \mathbb{R}^m : w \le \frac{\mu - a}{\sigma}, \bigcap_{i=1}^m \left\{ z_i \le \frac{b_i \mu + c_i}{\sqrt{1 + b_i^2 \sigma^2}} \right\} \right\}$, and the expression for the generic element of $\hat{\boldsymbol{\Gamma}}$ reduces to

$$\hat{\gamma}_{ij} = \frac{\tilde{\gamma}_{ij}}{\sqrt{\left(1 + b_i^2 \sigma^2\right)\left(1 + b_j^2 \sigma^2\right)}}.$$

Finally, using the result in Greene (2008) (pag. 1013), I_1 can be written as

$$I_1 = \int_{D_2} n\left(\tilde{\mathbf{z}}\right) d^{m+1}\tilde{\mathbf{z}} = \Phi_{m+1}\left(\frac{\mu - a}{\sigma}, \frac{b_1 \mu + c_1}{\sqrt{1 + b_1^2 \sigma^2}}, \ldots, \frac{b_m \mu + c_m}{\sqrt{1 + b_m^2 \sigma^2}}; \boldsymbol{\Gamma}_1\right)$$

with $\tilde{\mathbf{Z}}^\top := \begin{pmatrix} \mathbf{Z} & W \end{pmatrix} \sim \mathcal{N}_{m+1}\left(\mathbf{0}, \boldsymbol{\Gamma}_1\right)$; the correlation matrix $\boldsymbol{\Gamma}_1$ after proving the case $\xi = -1$.

2. Consider $\xi = -1$, that is

$$I_{-1} = \int_{-\infty}^a n\left(x\right) \left[\int_{-\infty}^{b_1 x + c_1} \cdots \int_{-\infty}^{b_m x + c_m} \frac{1}{\sqrt{(2\pi)^m \det \tilde{\boldsymbol{\Gamma}}}} \exp\left(-\frac{\mathbf{y}^\top \tilde{\boldsymbol{\Gamma}}^{-1} \mathbf{y}}{2}\right) d^m \mathbf{y} \right] dx$$

$$= \int_{D_0} \frac{1}{\sqrt{2\pi}\sigma} \exp\left(-\frac{1}{2}\left(\frac{x - \mu}{\sigma}\right)^2\right) \frac{1}{\sqrt{(2\pi)^m \det \tilde{\boldsymbol{\Gamma}}}} \exp\left(-\frac{\mathbf{y}^\top \tilde{\boldsymbol{\Gamma}}^{-1} \mathbf{y}}{2}\right) d^m \mathbf{y}\, dx$$

where $D_0 := \left\{ x \in \mathbb{R}, \mathbf{y} \in \mathbb{R}^m : x \le a, \bigcap_{i=1}^m \{ y_i \le b_i x + c_i \} \right\}$. The derivation follows the same steps as in the previous case, with the only difference that in the transformation $\mathbf{T_1}$ the change of variable is $x = \mu + \sigma w$. Consequently

$$I_{-1} = \int_{D_2} n\left(\tilde{\mathbf{z}}\right) d^{m+1}\tilde{\mathbf{z}} = \Phi_{m+1}\left(\frac{a - \mu}{\sigma}, \frac{b_1 \mu + c_1}{\sqrt{1 + b_1^2 \sigma^2}}, \ldots, \frac{b_m \mu + c_m}{\sqrt{1 + b_m^2 \sigma^2}}; \boldsymbol{\Gamma}_{-1}\right)$$

where $D_2 = \left\{ w \in \mathbb{R}, \mathbf{z} \in \mathbb{R}^m : w \le \frac{a - \mu}{\sigma}, \bigcap_{i=1}^m \left\{ z_i \le \frac{b_i \mu + c_i}{\sqrt{1 + b_i^2 \sigma^2}} \right\} \right\}$, and $\tilde{\mathbf{Z}}^\top := \begin{pmatrix} \mathbf{Z} & W \end{pmatrix} \sim \mathcal{N}_{m+1}\left(\mathbf{0}, \boldsymbol{\Gamma}_{-1}\right)$.

Finally the general solution of the integral can be written in compact way as

$$\xi \int_a^{\xi\infty} n(x) \Phi_m \left(\mathbf{b}x + \mathbf{c}; \tilde{\boldsymbol{\Gamma}} \right) dx = \Phi_{m+1} \left(\xi \frac{\mu - a}{\sigma}, \mathbf{d}; \boldsymbol{\Gamma}_\xi \right).$$

where $\mathbf{d} \in \mathbb{R}^m : d_i = \frac{b_i \mu + c_i}{\sqrt{1 + b_i^2 \sigma^2}}$.

In order to determine the covariance matrix of $\tilde{\mathbf{Z}}$, the relationship between $\hat{\boldsymbol{\Gamma}}$ and $\tilde{\boldsymbol{\Gamma}}$ provided in Greene (2008) (pag. 1013) can be used, that is

$$\hat{\boldsymbol{\Gamma}} = \tilde{\boldsymbol{\Gamma}} - \boldsymbol{\gamma}_\xi \boldsymbol{\gamma}_\xi^\top, \tag{C.2}$$

where $\boldsymbol{\gamma}_\xi \in \mathbb{R}^m$ is a vector which needs to be determined. Having constructed the correlation matrix $\boldsymbol{\Gamma}_\xi$ as

$$\boldsymbol{\Gamma}_\xi = \begin{pmatrix} \tilde{\boldsymbol{\Gamma}} & \boldsymbol{\gamma}_\xi \\ \boldsymbol{\gamma}_\xi^\top & 1 \end{pmatrix},$$

(C.2) can be solved as

$$\frac{\tilde{\gamma}_{ij}}{\sqrt{\left(1 + b_i^2 \sigma^2\right)\left(1 + b_j^2 \sigma^2\right)}} = \tilde{\gamma}_{ij} - \gamma_{i,\xi} \gamma_{j,\xi},$$

$$\gamma_{i,\xi} \gamma_{j,\xi} = \tilde{\gamma}_{ij} \left(1 - \frac{1}{\sqrt{\left(1 + b_i^2 \sigma^2\right)\left(1 + b_j^2 \sigma^2\right)}} \right),$$

if $i = j$, then

$$\gamma_{i,\xi} = \xi \frac{b_i \sigma}{\sqrt{1 + b_i^2 \sigma^2}}.$$

$\square$

Theorem 2. *Given a binary variables ξ taking values ± 1, $a \in \mathbb{R}$, and $\mathbf{b}, \mathbf{c} \in \mathbb{R}^m$ then*

$$\xi \int_a^{\xi\infty} e^x n(x; \mu, \sigma) \Phi_m \left(\mathbf{b}x + \mathbf{c}; \tilde{\boldsymbol{\Gamma}} \right) dx = e^{\mu + \frac{\sigma^2}{2}} \Phi_{m+1} \left(\xi \frac{\mu + \sigma^2 - a}{\sigma}, \mathbf{f}; \boldsymbol{\Gamma}_\xi \right), \tag{C.3}$$

for $\mathbf{f} \in \mathbb{R}^m : f_i = \dfrac{b_i(\mu+\sigma^2)+c_i}{\sqrt{1+b_i^2\sigma^2}}$,

$$\mathbf{\Gamma}_\xi = \begin{pmatrix} \tilde{\mathbf{\Gamma}} & \boldsymbol{\gamma}_\xi \\ \boldsymbol{\gamma}_\xi^\top & 1 \end{pmatrix},$$

and $\boldsymbol{\gamma}_\xi \in \mathbb{R}^m : \gamma_{i,\xi} = \xi\dfrac{b_i\sigma}{\sqrt{1+b_i^2\sigma^2}}$.

Proof. For notational convenience, define

$$J_\xi := \xi \int_a^{\xi\infty} e^x n\,(x;\mu,\sigma)\,\Phi_m\left(\mathbf{b}x+\mathbf{c};\tilde{\mathbf{\Gamma}}\right)\,\mathrm{d}x.$$

I distinguish the two cases $\xi = 1$ and $\xi = -1$ (for convenience of notation the dependence on the distributions' parameters such as μ, σ and $\tilde{\mathbf{\Gamma}}$ is omitted).

1. Consider first $\xi = 1$, that is

$$J_1 = \int_a^\infty e^x n\,(x) \left[\int_{-\infty}^{b_1x+c_1}\cdots\int_{-\infty}^{b_mx+c_m} \frac{1}{\sqrt{(2\pi)^m \det\tilde{\mathbf{\Gamma}}}}\exp\left(-\frac{\mathbf{y}^\top\tilde{\mathbf{\Gamma}}^{-1}\mathbf{y}}{2}\right)\mathrm{d}^m\mathbf{y}\right]\mathrm{d}x$$

$$= \int_{D_0} e^x \frac{1}{\sqrt{2\pi}\sigma}\exp\left(-\frac{1}{2}\left(\frac{x-\mu}{\sigma}\right)^2\right)\frac{1}{\sqrt{(2\pi)^m \det\tilde{\mathbf{\Gamma}}}}\exp\left(-\frac{\mathbf{y}^\top\tilde{\mathbf{\Gamma}}^{-1}\mathbf{y}}{2}\right)\mathrm{d}^m\mathbf{y}\,\mathrm{d}x$$

where $D_0 := \{x \in \mathbb{R}, \mathbf{y} \in \mathbb{R}^m : x \geq a, \bigcap_{i=1}^m \{y_i \leq b_ix+c_i\}\}$.

Consider the transformation $\mathbf{T_1} : \mathbb{R}^{m+1} \to \mathbb{R}^{m+1}$

$$\mathbf{T_1} := \begin{cases} x = \mu + \sigma w \\ \mathbf{y} = \mathbf{y} \end{cases}$$

with Jacobian

$$\mathbf{J_1} = \begin{pmatrix} \sigma & 0 & \ldots & 0 \\ 0 & 1 & \ldots & 0 \\ \ldots & \ldots & \ldots & \ldots \\ 0 & 0 & \ldots & 1 \end{pmatrix} = \begin{pmatrix} \sigma & \mathbf{0}^\top \\ \mathbf{0} & \mathbf{I} \end{pmatrix}$$

where $\mathbf{0}$ is the null column vector in $\mathbb{R}^m$ and $\mathbf{I}$ the $m \times m$ identity matrix. Furthermore, $D_1 := D_0(\mathbf{T_1}) = \left\{w \in \mathbb{R}, \mathbf{y} \in \mathbb{R}^m : w \geq \frac{a-\mu}{\sigma}, \bigcap_{i=1}^m \{y_i \leq -b_i\sigma w + b_i\mu + c_i\}\right\}$. Hence

the integral becomes

$$J_1 = \int_{D_1} e^{\mu + \sigma w} n \left(\mu + \sigma w \right) \frac{1}{\sqrt{(2\pi)^m \det \tilde{\Gamma}}} \exp \left(-\frac{\mathbf{y}^\top \tilde{\Gamma}^{-1} \mathbf{y}}{2} \right) |\det \mathbf{J_1}| \, d^m \mathbf{y} \, dw$$

$$= e^{\mu + \frac{\sigma^2}{2}} \int_{D_1} \frac{1}{\sqrt{2\pi}} e^{-\frac{(w-\sigma)^2}{2}} \frac{1}{\sqrt{(2\pi)^m \det \tilde{\Gamma}}} \exp \left(-\frac{\mathbf{y}^\top \tilde{\Gamma}^{-1} \mathbf{y}}{2} \right) d^m \mathbf{y} \, dw.$$

Consider another transformation $\mathbf{T_2} : \mathbb{R}^{m+1} \to \mathbb{R}^{m+1}$

$$\mathbf{T_2} := \begin{cases} w = -v + \sigma \\ \mathbf{y} = \mathbf{\Lambda} \left(\mathbf{z} - \boldsymbol{\gamma} v \right) \end{cases}$$

with

$$\mathbf{\Lambda} := \begin{pmatrix} \frac{1}{\sqrt{1-\gamma_1^2}} & 0 & \dots & 0 \\ 0 & \frac{1}{\sqrt{1-\gamma_2^2}} & \dots & 0 \\ \dots & \dots & \dots & \dots \\ 0 & 0 & \dots & \frac{1}{\sqrt{1-\gamma_m^2}} \end{pmatrix}, \qquad \boldsymbol{\gamma} := \begin{pmatrix} \gamma_1 \\ \gamma_2 \\ \dots \\ \gamma_m \end{pmatrix},$$

where $\gamma_i \in (-1, 1)$, for all $i \le m$, are parameters that will be determined later. The corresponding Jacobian is

$$\mathbf{J_2} = \begin{pmatrix} -1 & 0 & \dots & 0 \\ -\frac{\gamma_1}{\sqrt{1-\gamma_1^2}} & \frac{1}{\sqrt{1-\gamma_1^2}} & \dots & 0 \\ \dots & \dots & \dots & \dots \\ -\frac{\gamma_m}{\sqrt{1-\gamma_m^2}} & 0 & \dots & \frac{1}{\sqrt{1-\gamma_m^2}} \end{pmatrix}.$$

and

$$D_2 := D_1 \left(\mathbf{T_2} \right)$$

$$= \left\{ v \in \mathbb{R}, \mathbf{z} \in \mathbb{R}^m : v \le \frac{\mu + \sigma^2 - a}{\sigma}, \right.$$

$$\left. \bigcap_{i=1}^m \left\{ z_i \le \left(\gamma_i - b_i \sigma \sqrt{1-\gamma_i^2} \right) v + \left[b_i \left(\mu + \sigma^2 \right) + c_i \right] \sqrt{1-\gamma_i^2} \right\} \right\}.$$

Hence

$$
\begin{aligned}
J_1 &= e^{\mu + \frac{\sigma^2}{2}} \int_{D_2} \phi\left(v\right) \frac{1}{\sqrt{(2\pi)^m \det \tilde{\boldsymbol{\Gamma}}}} \exp\left(-\frac{\left(\boldsymbol{\Lambda}\left(\mathbf{z} - \boldsymbol{\gamma}v\right)\right)^\top \tilde{\boldsymbol{\Gamma}}^{-1} \left(\boldsymbol{\Lambda}\left(\mathbf{z} - \boldsymbol{\gamma}v\right)\right)}{2}\right) \left|\det \mathbf{J}_2\right| \mathrm{d}^m \mathbf{z}\,\mathrm{d}v \\
&= e^{\mu + \frac{\sigma^2}{2}} \int_{D_2} \phi\left(v\right) \frac{1}{\sqrt{(2\pi)^m \prod_{i=1}^m \left(1 - \gamma_i^2\right) \det \tilde{\boldsymbol{\Gamma}}}} \exp\left(-\frac{\left(\mathbf{z} - \boldsymbol{\gamma}v\right)^\top \boldsymbol{\Lambda}^\top \tilde{\boldsymbol{\Gamma}}^{-1} \boldsymbol{\Lambda} \left(\mathbf{z} - \boldsymbol{\gamma}v\right)}{2}\right) \mathrm{d}^m \mathbf{z}\,\mathrm{d}v.
\end{aligned}
$$

Noticing that $\prod_{i=1}^m \left(1 - \gamma_i^2\right) = \det\left(\boldsymbol{\Lambda}^{-1}\right)^2$, then

$$
\begin{aligned}
J_1 &= e^{\mu + \frac{\sigma^2}{2}} \int_{D_2} n\left(v\right) \frac{1}{\sqrt{(2\pi)^m \det \hat{\boldsymbol{\Gamma}}}} \exp\left(-\frac{\left(\mathbf{z} - \boldsymbol{\gamma}v\right)^\top \hat{\boldsymbol{\Gamma}}^{-1} \left(\mathbf{z} - \boldsymbol{\gamma}v\right)}{2}\right) \mathrm{d}^m \mathbf{z}\,\mathrm{d}v \\
&= e^{\mu + \frac{\sigma^2}{2}} \int_{D_2} n\left(v\right) n_m(\mathbf{z}|V)\,\mathrm{d}^m \mathbf{z}\,\mathrm{d}v
\end{aligned}
$$

with $\hat{\boldsymbol{\Gamma}}^{-1} := \boldsymbol{\Lambda}^\top \tilde{\boldsymbol{\Gamma}}^{-1} \boldsymbol{\Lambda}$, and $\mathbf{Z}|V \sim \mathcal{N}_m\left(\boldsymbol{\gamma}V, \hat{\boldsymbol{\Gamma}}\right)$. This means that the ij-element of the covariance matrix $\hat{\boldsymbol{\Gamma}}$ is given by

$$
\hat{\gamma}_{ij} = \tilde{\gamma}_{ij} \sqrt{\left(1 - \gamma_i^2\right)\left(1 - \gamma_j^2\right)}
$$

with $\tilde{\gamma}_{ii} = 1$.

Furthermore, by setting $\gamma_i - b_i \sigma \sqrt{1 - \gamma_i^2} = 0$, that corresponds to $\gamma_i = \frac{b_i \sigma}{\sqrt{1 + b_i^2 \sigma^2}}$, the region of integration reduces to $D_2 = \left\{v \in \mathbb{R}, \mathbf{z} \in \mathbb{R}^m : v \le \frac{\mu + \sigma^2 - a}{\sigma}, \bigcap_{i=1}^m \left\{z_i \le \frac{b_i\left(\mu + \sigma^2\right) + c_i}{\sqrt{1 + b_i^2 \sigma^2}}\right\}\right\}$, and the expression for the generic element of $\hat{\boldsymbol{\Gamma}}$ reduces to

$$
\hat{\gamma}_{ij} = \frac{\tilde{\gamma}}{\sqrt{\left(1 + b_i^2 \sigma^2\right)\left(1 + b_j^2 \sigma^2\right)}}.
$$

Finally, using the result in Greene (2008) (pag. 1013), J_1 can be written as

$$
\begin{aligned}
J_1 &= e^{\mu + \frac{\sigma^2}{2}} \int_{D_2} n\left(\tilde{\mathbf{z}}\right) \mathrm{d}^{m+1} \tilde{\mathbf{z}} \\
&= e^{\mu + \frac{\sigma^2}{2}} \Phi_{m+1}\left(\frac{\mu + \sigma^2 - a}{\sigma}, \frac{b_1\left(\mu + \sigma^2\right) + c_1}{\sqrt{1 + b_1^2 \sigma^2}}, \dots, \frac{b_m\left(\mu + \sigma^2\right) + c_m}{\sqrt{1 + b_m^2 \sigma^2}}; \boldsymbol{\Gamma}_1\right)
\end{aligned}
$$

with $\tilde{\mathbf{Z}}^\top := \begin{pmatrix} \mathbf{Z} & W \end{pmatrix} \sim \mathcal{N}_{m+1}(\mathbf{0}, \boldsymbol{\Gamma}_1)$; the correlation matrix $\boldsymbol{\Gamma}_1$ after proving the case $\xi = -1$.

2. Consider $\xi = -1$, that is

$$
J_{-1} = \int_{-\infty}^{a} e^x n(x) \left[\int_{-\infty}^{b_1 x + c_1} \cdots \int_{-\infty}^{b_m x + c_m} \frac{1}{\sqrt{(2\pi)^m \det \tilde{\boldsymbol{\Gamma}}}} \exp\left(-\frac{\mathbf{y}^\top \tilde{\boldsymbol{\Gamma}}^{-1} \mathbf{y}}{2} \right) d^m \mathbf{y} \right] dx
$$

$$
= \int_{D_0} e^x \frac{1}{\sqrt{2\pi}\sigma} \exp\left(-\frac{1}{2}\left(\frac{x-\mu}{\sigma}\right)^2 \right) \frac{1}{\sqrt{(2\pi)^m \det \tilde{\boldsymbol{\Gamma}}}} \exp\left(-\frac{\mathbf{y}^\top \tilde{\boldsymbol{\Gamma}}^{-1} \mathbf{y}}{2} \right) d^m \mathbf{y}\, dx
$$

where $D_0 := \{x \in \mathbb{R}, \mathbf{y} \in \mathbb{R}^m : x \leq a, \bigcap_{i=1}^m \{y_i \leq b_i x + c_i\}\}$. The derivation follows the same steps as in the previous case, with the only difference that in the transformation $\mathbf{T_1}$ the change of variable is $x = \mu + \sigma w$. Consequently

$$
J_{-1} = e^{\mu + \frac{\sigma^2}{2}} \Phi_{m+1}\left(\frac{a - \mu - \sigma^2}{\sigma}, \frac{b_1\left(\mu + \sigma^2\right) + c_1}{\sqrt{1 + b_1^2 \sigma^2}}, \ldots, \frac{b_m\left(\mu + \sigma^2\right) + c_m}{\sqrt{1 + b_m^2 \sigma^2}}; \boldsymbol{\Gamma}_{-1} \right)
$$

where $D_2 = \left\{ v \in \mathbb{R}, \mathbf{z} \in \mathbb{R}^m : v \leq \frac{a - \mu - \sigma^2}{\sigma}, \bigcap_{i=1}^m \left\{ z_i \leq \frac{b_i\left(\mu + \sigma^2\right) + c_i}{\sqrt{1 + b_i^2 \sigma^2}} \right\} \right\}$, and $\tilde{\mathbf{Z}}^\top := \begin{pmatrix} \mathbf{Z} & W \end{pmatrix} \sim \mathcal{N}_{m+1}(\mathbf{0}, \boldsymbol{\Gamma}_{-1})$.

Thus the general solution of the integral can be written in compact way as

$$
\xi \int_a^{\xi \infty} e^x n(x) \Phi_m\left(\mathbf{b}x + \mathbf{c}; \tilde{\boldsymbol{\Gamma}} \right) dx = e^{\mu + \frac{\sigma^2}{2}} \Phi_{m+1}\left(\xi \frac{\mu + \sigma^2 - a}{\sigma}, \mathbf{f}; \boldsymbol{\Gamma}_\xi \right),
$$

where $\mathbf{f} \in \mathbb{R}^m : f_i = \frac{b_i\left(\mu + \sigma^2\right) + c_i}{\sqrt{1 + b_i^2 \sigma^2}}$.

The correlation coefficients of $\boldsymbol{\Gamma}_\xi$ are the same of Theorem 1. $\qquad\square$

Appendix D

Estimating the Model-Free Risk Neutral Probability of Survival

The estimation of risk-neutral probabilities of survival from CDS spreads presented herein is based on Brigo (2005) and Brigo and Mercurio (2006). This constitute a model-free technique to estimate those quantities.

The t-payoff of a CDS initiated at $t_0 = 0$ with maturity t_j and intermediate premium payments at $(t_i)_{i=1}^{j}$, $j \in \mathbb{N}$, and notional set to one is given by

$$\Pi_j(t) = DF(t,\tau)(\tau - \bar{t})s\mathbb{1}_{\left\{0 < \tau \leq t_j\right\}} + s \sum_{i=1}^{j} DF(t,t_i)\alpha_i \mathbb{1}_{\{\tau \geq t_i\}} - DF(t,\tau)\mathrm{LGD}\mathbb{1}_{\left\{0 < \tau \leq t_j\right\}}$$

with $0 \leq t < t_j$, $\bar{t}$ the last payments date before t, that is $\bar{t} := \sup_{1 \leq i \leq j}\{t_i \leq \tau\}$, α_i the year fraction between t_{i-1} and t_i, s the CDS spread paid by the protection buyer (before default, if it happens), and LGD the loss given default. The first term is the discounted accrued rate at default and represents the compensation the protection seller receives for the protection provided from the last t_i until default τ. The terms in the summation represent the CDS rate premium payments if there is no default: this is the premium received by the protection seller for the protection being provided. The final term is the payment of protection at default, if this happens before final t_j.

The t_j-maturity CDS price in $t_0 = 0$ according to risk-neutral valuation is

$$\mathrm{CDS}_j(s, \mathrm{LGD}) = \mathbb{E}^{\mathbb{Q}}\left[\Pi_j(0)\right].$$

For computing the expectation is more convenient to separate the payments made by the protection buyer from the ones made by the protection seller. Also, it is assumed that default

can occur at reset dates only, that is the first summand can be ignored (there are no accrued interests). Following Brigo and Mercurio (2006), the expected value of premium leg is equal to

$$\text{PremiumLeg}_j(s) = \mathbb{E}^{\mathbb{Q}}\left[s\sum_{i=1}^{j}DF(0,t_i)\alpha_i\mathbb{1}_{\{\tau \geq t_i\}}\right] = s\left[\sum_{i=1}^{j}P(0,t_i)\alpha_i\mathbb{Q}(\tau \geq t_i)\right],$$

where $P(t_i,t_j)$ is the t_i-value of a zero-coupon bond with maturity $t_j \geq t_i$, under the assumption of independence between the discount factor and the default time. From the perspective of the protection seller,

$$\text{ProtecLeg}_j(\text{LGD}) = \mathbb{E}^{\mathbb{Q}}\left[DF(0,\tau)\text{LGD}\mathbb{1}_{\{0<\tau\leq t_j\}}\right] = \text{LGD}\int_0^{t_j}P(0,t)\,d\mathbb{Q}(\tau \geq t)$$

Hence the value of the CDS in $t_0 = 0$ is given by

$$\begin{aligned}\text{CDS}_j(s,\text{LGD}) &= \text{PremiumLeg}_j(s) - \text{ProtecLeg}_j(\text{LGD})\\ &= s\left[\sum_{i=1}^{j}P(0,t_i)\alpha_i\mathbb{Q}(\tau \geq t_i)\right] - \text{LGD}\int_0^{t_j}P(0,t)\,d\mathbb{Q}(\tau \geq t)\end{aligned}$$

If we assume that in t_0 the term structure of the risk-free interest rates is known and a deterministic function of the maturity only, $r_0(t)$, then the previous expression simplifies as

$$\text{CDS}_j(s,\text{LGD}) = s\left[\sum_{i=1}^{j}e^{-r_0(t_i)t_i}\alpha_i\mathbb{Q}(\tau \geq t_i)\right] - \text{LGD}\int_0^{t_j}e^{-r_0(t)t}\,d\mathbb{Q}(\tau \geq t).$$

At time t_0, provided that default has not occurred yet, the market sets the spread s to a value, s_j^{MID}, which makes the CDS fair at time t_0 that is

$$s_j^{\text{MID}} := \left\{s > r_0(t_j) : \text{CDS}_j(s,\text{LGD}) = 0\right\}$$

for different maturities t_j. Having assigned a level of loss given default (usually $\text{LGD} = \{0.5, 0.6, 0.8\}$), the set of equations

$$\text{PremiumLeg}_j\left(s_j^{\text{MID}},\mathbb{Q}(\tau \geq t)\right) = \text{ProtecLeg}_j(\text{LGD},\mathbb{Q}(\tau \geq t))$$

can be solved in $\mathbb{Q}$, starting from the CDS quotation with shortest tenor, and recursively solving for the spread with longer maturities. Therefore, the market implied risk-neutral
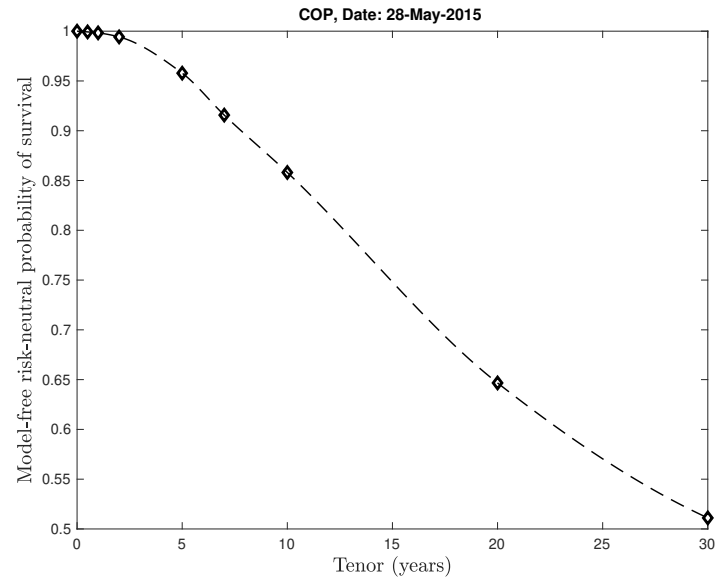
Fig. D.1 Term-structure of risk-neutral survival probabilities for COP on 28/05/2015, LGD = 60%.

survival probabilities $\mathbb{Q}(\tau \geq t)$,with $t \in (t_j, t_{j+1}]$, can be found. Figure D.1 displays the term-structure of the risk neutral probability of survival for ConocoPhillips (COP) observed on May, 28th 2015.

The data on corporate CDS spreads are usually available for maturities $t_j \in \{6m, 1y, 2y, 5y, 7y, 10y, 20y, 30y\}$. The extraction of the risk-neutral probability of surviving is therefore conducted as follows:

- start from $t_j = 6m$ and estimate the market implied survival probability $\mathbb{Q}(\tau \geq t)$, with $t \in (0, 0.5]$ years;

- insert the estimated value into CDS legs formulas for $t_j = 1y$, and solve the same type of equation with $t_j = 1y$ to find the market implied survival probability $\mathbb{Q}(\tau \geq t)$, with $t \in (0.5, 1]$ years;

- repeat the same recursive procedure for all the tenors up to $t_j = 30$ years.

For further details see Brigo (2005).

Appendix E

Estimating the Endogenous Default Barrier

The implied default barrier pays a crucial role in the compound option model dynamics and its value ultimately defines the default region in the asset value space. Given the risk-free and payout rates as well as the firm's capital structure, the values of the default thresholds are functions of the (unknown) volatility of the assets only. They are defined as

$$\bar{V}_i(\sigma_V) := \{v \in \mathbb{R}_+ : S_i^\star(v, \sigma_V) = F_i\}. \tag{E.1}$$

with $i \in I = \{1, \dots n\}$ where n is the number of bonds outstanding. That is, the implied barrier at t_i is defined as the value of the asset such that the continuation value of the equity, $S_i^\star$, is at least as large as the bond due, F_i. In order to determine the values of the sequence $(\bar{V}_i)_{i \in I}$, the problem must be solved starting from the latest maturity t_n and backwardly to the first payment date t_1.

As the most common instance for the given data is a company with three bond outstanding, I are going to present the estimation for the case $n = 3$. Trivially

$$\bar{V}_3 = F_3,$$

as in Merton (1974). This is the only default threshold that does not depend on the asset volatility (or any other model parameter). According to (E.1), as the continuation value of

the equity is also a compound call option, the previous default point is defined as

$$\bar{V}_2(\sigma_V) = \{v \in \mathbb{R}_+ : S_2^\star(v, \sigma_V) = F_2\}$$
$$= \left\{v \in \mathbb{R}_+ : e^{-\varpi(t_3-t_2)}v\Phi\left(d_{3,2}^{\mathbb{M}}\right) - e^{-r(t_3-t_2)}F_3\Phi(d_{3,2}^{\mathbb{Q}}) = F_2\right\}$$

with

$$d_{3,2}^{\mathbb{M}} = \frac{\ln(v/F_3) + (r - \varpi + \sigma_V^2/2)(t_3 - t_2)}{\sigma_V\sqrt{t_3 - t_2}} \qquad d_{3,2}^{\mathbb{Q}} = d_{3,2}^{\mathbb{M}} - \sigma_V\sqrt{t_3 - t_2}.$$

This notation should make clear that different values of $\bar{V}_2$ are obtained for different values of σ_V[1]. Ultimately, if σ_V is known, estimating the barrier is equivalent to just solving a nonlinear integral equation[2].

Similarly, the value of the barrier at the first reimbursement date is

$$\bar{V}_1(\sigma_V) = \{v \in \mathbb{R}_+ : S_1^\star(v, \sigma_V) = F_1\}$$
$$= \left\{v \in \mathbb{R}_+ : e^{-\varpi(t_3-t_1)}v\Phi_2\left(d_{2,1}^{\mathbb{M}}, d_{3,1}^{\mathbb{M}}; \boldsymbol{\Gamma}\right)\right.$$
$$\left. - e^{-r(t_3-t_1)}F_3\Phi_2\left(d_{2,1}^{\mathbb{Q}}, d_{3,1}^{\mathbb{Q}}; \boldsymbol{\Gamma}\right) - e^{-r(t_2-t_1)}F_2\Phi(d_{2,1}^{\mathbb{Q}}) = F_1\right\}$$

with

$$d_{2,1}^{\mathbb{M}} = \frac{\ln(v/\bar{V}_2) + (r - \varpi + \sigma_V^2/2)(t_2 - t_1)}{\sigma_V\sqrt{t_2 - t_1}} \qquad d_{2,1}^{\mathbb{Q}} = d_{2,1}^{\mathbb{M}} - \sigma_V\sqrt{t_2 - t_1}.$$

$$d_{3,1}^{\mathbb{M}} = \frac{\ln(v/F_3) + (r - \varpi + \sigma_V^2/2)(t_3 - t_1)}{\sigma_V\sqrt{t_3 - t_1}} \qquad d_{3,1}^{\mathbb{Q}} = d_{3,1}^{\mathbb{M}} - \sigma_V\sqrt{t_3 - t_1}.$$

and

$$\boldsymbol{\Gamma} = \begin{pmatrix} 1 & \sqrt{\frac{t_2-t_1}{t_3-t_1}} \\ \sqrt{\frac{t_2-t_1}{t_3-t_1}} & 1 \end{pmatrix}.$$

Again, $\bar{V}_1$ is found as the solution of a nonlinear equation which involves double integrals. The same procedure can be applied for $n > 3$; however, the computational cost becomes progressively more severe with increasing the number of bond outstanding[3].

---

[1]The same is true for different values of r, ϖ, ... However those parameters are assumed to be known and estimated with no error.

[2]I refer it as integral equation as the integration interval/hyperrectangular depends on v.

[3]The main reason being that the function Φ_n is calculated relying on Monte Carlo simulation for $n \geq 4$.

If the value of σ_V were known, the entire default barrier could be easily computed and the today-value of the assets could be easily found calibrating on the today-value of the equity,

$$S_0 = e^{-\varpi t_n} V_0 \Phi_n \left(\mathbf{d}^{\mathbb{M}}(V_0, \sigma_V); \mathbf{\Gamma}_n \right) - \sum_{k=1}^{n} e^{-rt_k} F_k \Phi_k \left(\mathbf{d}_k^{\mathbb{Q}}(V_0, \sigma_V); \mathbf{\Gamma}_k \right). \qquad \text{(E.2)}$$

However, as both asset volatility and value are not observable, (E.2) can be seen as an equation in the two unknowns σ_V and V_0. In order to solve for those values, the dependence of the barrier on σ_V is reversely engineered in order to determine the implied asset volatility. Similarly to the computation of the Black-Scholes implied volatility, the observable option price

$$P_{0,\xi} = \xi \left[e^{-\varpi t_n} V_0 \Phi_{n+1} \left(\mathbf{d}_\xi^{\mathbb{M}}(V_0, \sigma_V); \mathbf{\Gamma}_{n+1,\xi} \right) - \sum_{k=i+1}^{n} e^{-rt_k} F_k \Phi_{k+1} \left(\mathbf{d}_{\xi,k+1}^{\mathbb{Q}}(V_0, \sigma_V); \mathbf{\Gamma}_{k+1,\xi} \right) \right.$$
$$\left. - e^{-rT} K \Phi \left(\xi d_T^{\mathbb{Q}}(V_0, \sigma_V) \right) \right]$$

$$\text{(E.3)}$$

is used as second equation in order to determine the asset implied volatility and the corresponding asset value. Notably, only the value of the option and the equity are needed to determine the implied volatility of the assets $\sigma_V = \sigma_V(K, T)$ and construct the term-structure of the asset volatility's surface.

In addition, in order to make computations more efficient, (E.2) can be replaced by

$$S_0 = e^{-\varpi t_n} V_0 \Phi_n \left(\mathbf{d}^{\mathbb{M}}(V_0, \sigma_V); \mathbf{\Gamma}_n \right) - \sum_{k=1}^{n} e^{-rt_k} F_k \hat{\mathbb{Q}} \left(\tau > t_k \right), \qquad \text{(E.4)}$$

where $\hat{\mathbb{Q}}(\tau > t_k)$ are the estimates of the risk-neutral probability of survival extracted from the CDS written on the same reference entity. These are estimated as in Appendix D, in which a simple model-free estimation procedure is provided.

Using (E.4) instead of (E.2) speeds up computation and serves as an indirect test on the integration of the CDS and option markets. If the two estimates of the implied volatility of the asset – obtained with and without the calibration on the CDS – are consistent, it can be inferred that options market participants incorporate information on default-related events into option prices consistently with the price of default quoted by CDS market participants.

At first glance, deriving the sensitivity of the default barrier with respect to volatility is not trivial for $n \geq 2$, as $V_i(\sigma_V)$ is implicitly defined via the integral equation (E.1). For

illustrative purposes, consider the case of $n = 2$, where $\bar{V}_2 = F_2$ and

$$\bar{V}_1(\sigma_V) = \left\{ v \in \mathbb{R}_+ : e^{-\varpi(t_2 - t_1)} v \Phi\left(d_{2,1}^+\right) - e^{-r(t_2 - t_1)} F_2 \Phi\left(d_{2,1}^-\right) = F_1 \right\}$$

with

$$d_{2,1}^+ = \frac{\ln(v/F_2) + \left(r - \varpi + \sigma_V^2/2\right)(t_2 - t_1)}{\sigma_V \sqrt{t_2 - t_1}} \qquad d_{2,1}^- = d_{2,1}^+ - \sigma_V \sqrt{t_2 - t_1}.$$

Let $\sigma_V = x$ and $\bar{V}_1 = y$. In order to determine $y'(x)$, the Implicit Function Theorem can be used. Associating the curve

$$\Xi(x,y) = e^{-\varpi(t_2 - t_1)} y \Phi\left(d_{2,1}^+(x,y)\right) - e^{-r(t_2 - t_1)} F_2 \Phi\left(d_{2,1}^-(x,y)\right) - F_1 = 0$$

the derivative of the implicit function is

$$y'(x) = -\frac{\Xi_x}{\Xi_y}(x, y(x)).$$

Notice that the numerator is nothing but the Vega (see Appendix G) of the continuation value of the equity $S_1^\star$ (as a function of the asset volatility and the barrier) whilst the denominator is its Delta with respect the default threshold $\bar{V}_1$ (see Appendix F). That is

$$\bar{V}_1' = -\frac{v_{S^\star}^{(1)}}{\Delta_{S^\star}^{(1)}} = -\frac{\phi\left(d_{2,1}^+\right)}{\Phi\left(d_{2,1}^+\right)} \bar{V}_1 \sqrt{t_2 - t_1}.$$

The same reasoning applies to any $n \geq 2$, and in general[4]

$$\bar{V}_i' = \begin{cases} -v_{S^\star}^{(i)}/\Delta_{S^\star}^{(i)} & \text{if } i < n \\ 0 & \text{if } i = n. \end{cases}$$

---

[4]It can be also shown that

$$V'' = -\frac{\text{Delta}^2 \cdot \text{Volga} - 2 \cdot \text{Delta} \cdot \text{Vega} \cdot \text{Vanna} + \text{Vega}^2 \cdot \text{Gamma}}{\text{Delta}^3}.$$

Notice that $v_{S^\star}$ is obtained as the Vega of the equity in Appendix F having set the sensitivity of the barrier to zero.

It can be shown numerically that, provided a reasonable set of parameters[5], the function $\bar{V}(\sigma_V)$ is positive and decreasing, displaying an inflation point. See Figure E.1 and E.2 for graphical inspection. The reason why the barrier lowers as σ_V increases can be intuitively explained as follows. As equity is a compound call option, by standard option pricing arguments, an increase in the volatility leads to an increase of the option premium, i.e. the equity value, which ultimately makes the firm 'safer'. As default events are measured based on the distance between the continuation value of the equity and the face value of the bond expiring, an increase in volatility lowers the default threshold as the equity has increased accordingly. This is a structural property of using a geometric Brownian motion for the dynamics of the assets and the equity as a compound call option on the value of the assets. The model in Merton (1974) displays similar features.
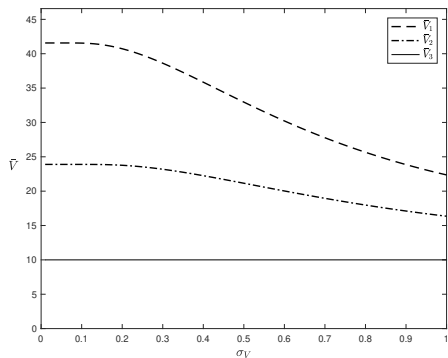
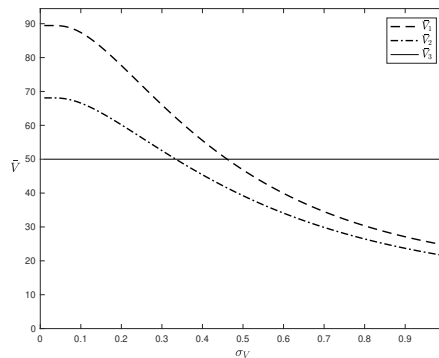Additional references are Geske (1977) and Geske et al. (2016).

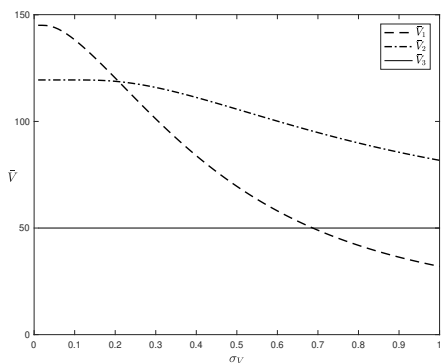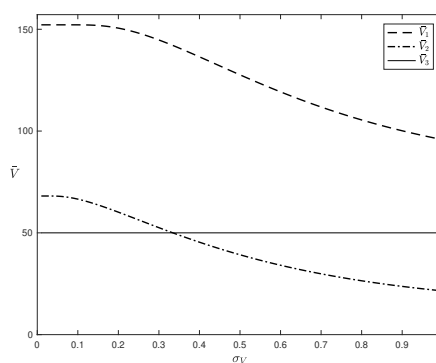[5] That is for $\sigma_V \in (0,1)$ and $F_2 < 10 \cdot F_1$.
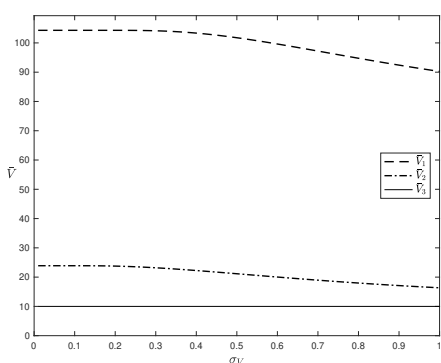
(a) $F_1 = F_2 = F_3 = 10$

(b) $F_1 = F_2 = 10, F_3 = 50$

(c) $F_1 = 10, F_2 = F_3 = 50$

(d) $F_1 = F_3 = 50, F_2 = 10$

(e) $F_1 = 50, F_2 = F_3 = 10$

(f) $F_1 = F_3 = 10, F_2 = 50$

Fig. E.1 $\bar{V}_i(\sigma_V)$, $i = \{1, 2, 3\}$, for $t_1 = 1, t_2 = 5, t_3 = 10$, $r = 0.03$ and $\varpi = 0.05$.

150

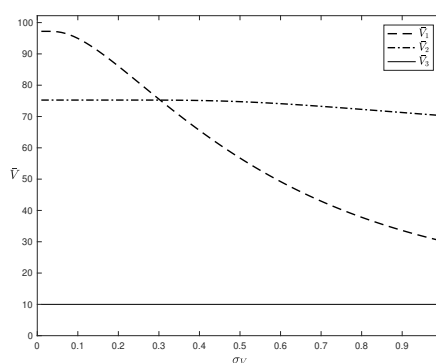(a) $F_1 = F_2 = F_3 = 10$

(b) $F_1 = F_2 = 10, F_3 = 50$

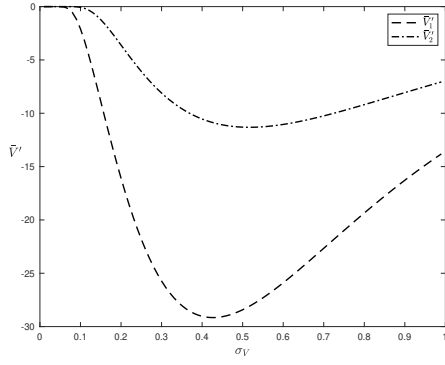(c) $F_1 = 10, F_2 = F_3 = 50$

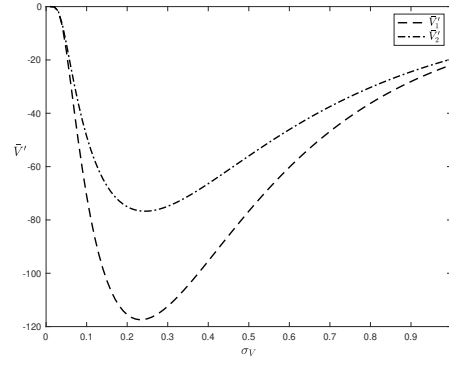(d) $F_1 = F_3 = 50, F_2 = 10$

(e) $F_1 = 50, F_2 = F_3 = 10$

(f) $F_1 = F_3 = 10, F_2 = 50$

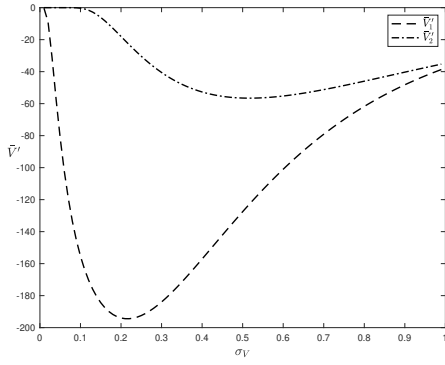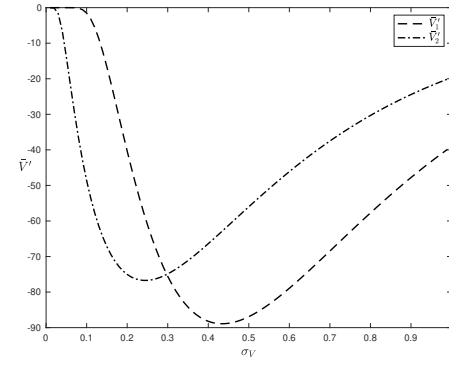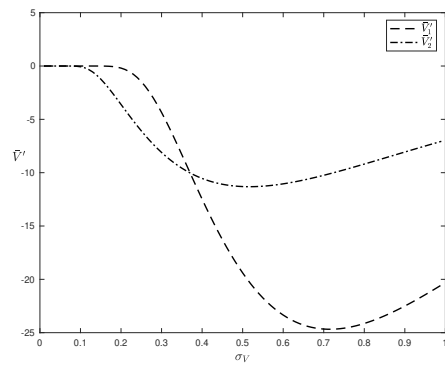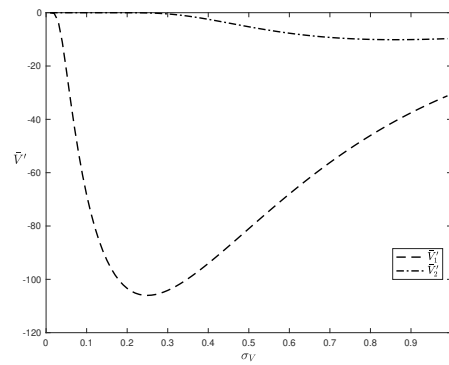Fig. E.2 $\bar{V}_i'(\sigma_V)$, $i = \{1, 2, 3\}$, for $t_1 = 1, t_2 = 5, t_3 = 10$, $r = 0.03$ and $\varpi = 0.05$.

151

Appendix F

The Delta of the Equity

In order to compute the sensitivity of the equity with respect to changes in the asset value (herein, delta of the equity), the following result is needed.

Theorem 3. *Let*

$$\Phi_k\left(\mathbf{d}(x);\mathbf{\Gamma}\right) = \int_{\Upsilon(x)} \phi_k(y_1,\ldots,y_i,\ldots,y_k;\mathbf{\Gamma})\mathrm{d}y_1\ldots\mathrm{d}y_i\ldots\mathrm{d}y_k$$

with $\mathbf{\Gamma} \in \mathscr{M}_+^k$ *and* $\Upsilon(x) = \cap_{i=1}^k\{y_i \in \mathbb{R} : y_i \le d_i(x)\}$, *with* $\mathbf{d}(x) : \mathbb{R}_+ \to \mathbb{R}^k$, $d_i(x) = \frac{\ln x + a_i}{b_i}$ *with* $a_i \in \mathbb{R}$ *and* $b_i \in \mathbb{R}_+$. *Then*

$$\frac{\partial \Phi_k\left(\mathbf{d}(x);\mathbf{\Gamma}\right)}{\partial x} = \frac{1}{x}\sum_{i=1}^k \frac{1}{b_i}\int_{\bar{\Upsilon}_i(x)} \phi_k(y_1,\ldots,d_i(x),\ldots,y_k;\mathbf{\Gamma})\mathrm{d}y_1\ldots\mathrm{d}y_k,$$

where $\bar{\Upsilon}_i(x) = \Upsilon(x) \setminus \{y_i \le d_i(x)\}$.

Proof. Let $z_i = d_i(x)$, with $i = \{1,\ldots,k\}$. Applying the chain rule, it follows

$$\frac{\partial \Phi_k(z_1,\ldots,z_k)}{\partial x} = \sum_{i=1}^k \frac{\partial \Phi_k}{\partial z_i}\frac{\partial z_i}{\partial x}$$

and by the virtue of the fundamental theorem of calculus

$$\frac{\partial \Phi_k}{\partial z_i} = \int_{-\infty}^{z_1}\cdots\int_{-\infty}^{z_{i-1}}\int_{-\infty}^{z_{i+1}}\cdots\int_{-\infty}^{z_k} \phi_k(y_1,\ldots,y_{i-1},z_i,y_{i+1},\ldots,y_k;\mathbf{\Gamma})\mathrm{d}y_1\ldots\mathrm{d}y_{i-1}\mathrm{d}y_{i+1}\ldots\mathrm{d}y_k.$$

As
$$\frac{\partial z_i}{\partial x} = \frac{1}{b_i x},$$

153

the result follows. □

Given n bond outstanding, the value of the equity $s = S(v)$ is given by (1.9), that is

$$s = e^{-\varpi t_n} v \Phi_n\left(\mathbf{d}^{\mathbb{M}}(v); \mathbf{\Gamma}_n\right) - \sum_{k=1}^{n} e^{-r t_k} F_k \Phi_k\left(\mathbf{d}_k^{\mathbb{Q}}(v); \mathbf{\Gamma}_k\right)$$

where $\mathbf{d}^{\mathbb{M}}(v) := \left(d_i^{\mathbb{M}}(v)\right)_{1 \le i \le n}$ and $\mathbf{d}_k^{\mathbb{Q}}(v) = \left(d_i^{\mathbb{M}}(v) - \sigma_V \sqrt{t_i}\right)_{1 \le i \le k}$ with

$$d_i^{\mathbb{M}} = \frac{\ln\left(v/\bar{V}_i\right) + \left(r - \varpi + \sigma_V^2/2\right) t_i}{\sigma_V \sqrt{t_i}} \qquad \text{and} \qquad \mathbf{\Gamma}_k = \begin{pmatrix} 1 & \sqrt{\frac{t_1}{t_2}} & \sqrt{\frac{t_1}{t_3}} & \cdots & \sqrt{\frac{t_1}{t_k}} \\ & 1 & \sqrt{\frac{t_2}{t_3}} & \cdots & \sqrt{\frac{t_2}{t_k}} \\ \cdots & \cdots & \cdots & \cdots & \cdots \\ & & & 1 & \sqrt{\frac{t_{k-1}}{t_k}} \\ & & & & 1 \end{pmatrix}.$$

Therefore, the delta of the equity is generally defined as

$$\Delta_S^{(n)} := \frac{\partial s}{\partial v} = e^{-\varpi t_n}\left(\Phi_n\left(\mathbf{d}^{\mathbb{M}}(v); \mathbf{\Gamma}_n\right) + v\frac{\partial \Phi_n\left(\mathbf{d}^{\mathbb{M}}(v); \mathbf{\Gamma}_n\right)}{\partial v}\right) - \sum_{k=1}^{n} e^{-r t_k} F_k \frac{\partial \Phi_k\left(\mathbf{d}_k^{\mathbb{Q}}(v); \mathbf{\Gamma}_k\right)}{\partial v}.$$

The derivation of a semi-closed formula for the computation of the delta for a generic n is not straightforward. However, I explicitly develop analytical expressions for $n = \{1, 2, 3\}$ (which suffice for the actual calculations present in the paper). Also, despite $\Delta_S^{(n)} : \mathbb{R}_+ \to (0, 1)$, for all $n \in \mathbb{N}$, its numerical computation becomes progressively more intensive (as n grows).

For convenience of notation, the dependence on v in the integration intervals (the d's and related expressions) is omitted.

If $n = 1$ (also, let $t_1 = t$ and $F_1 = F$)

$$s = e^{-\varpi t} v \Phi(d^{\mathbb{M}}) - e^{-r t} F \Phi(d^{\mathbb{Q}})$$

with

$$d^{\mathbb{M}} = \frac{\ln\left(v/F\right) + \left(r - \varpi + \sigma_V^2/2\right) t}{\sigma_V \sqrt{t}} \qquad d^{\mathbb{Q}} = d^{\mathbb{M}} - \sigma_V \sqrt{t}.$$

Obviously, the delta is the same of Black and Scholes (1973). In fact

$$\frac{\partial s}{\partial v} = e^{-\varpi t}\left(\Phi(d^{\mathbb{M}}) + v\frac{\partial \Phi(d^{\mathbb{M}})}{\partial v}\right) - e^{-rt}F\frac{\partial \Phi(d^{\mathbb{Q}})}{\partial v}$$

$$= e^{-\varpi t}\left(\Phi(d^{\mathbb{M}}) + v\phi(d^{\mathbb{M}})\frac{1}{v\sigma_V\sqrt{t}}\right) - e^{-rt}F\phi(d^{\mathbb{Q}})\frac{1}{v\sigma_V\sqrt{t}}$$

as

$$\phi(d^{\mathbb{Q}}) = \phi(d^{\mathbb{M}} - \sigma_V\sqrt{t}) = \frac{ve^{-\varpi t}}{Fe^{-rt}}\phi(d^{\mathbb{M}}).$$

it follows

$$\boxed{\Delta_S^{(1)} = e^{-\varpi t}\Phi(d^{\mathbb{M}})}.$$

See Figures F.1a and F.1b for a graphical analysis of the delta in the case of one bond outstanding.

For $n = 2$

$$s = e^{-\varpi t_2}v\Phi_2\left(\mathbf{d}^{\mathbb{M}};\mathbf{\Gamma}\right) - e^{-rt_1}F_1\Phi(d_1^{\mathbb{Q}}) - e^{-rt_2}F_2\Phi_2\left(\mathbf{d}_2^{\mathbb{Q}};\mathbf{\Gamma}\right)$$

with

$$\mathbf{\Gamma} = \begin{pmatrix} 1 & \gamma \\ \gamma & 1 \end{pmatrix} \qquad \text{and} \qquad \gamma = \sqrt{\frac{t_1}{t_2}}$$

$$\mathbf{d}^{\mathbb{M}} = \left(d_1^{\mathbb{M}} \quad d_2^{\mathbb{M}}\right) = \left(\frac{\ln\frac{v}{V_1} + \left(r-\varpi+\frac{\sigma_V^2}{2}\right)t_1}{\sigma_V\sqrt{t_1}} \quad \frac{\ln\frac{v}{F_2} + \left(r-\varpi+\frac{\sigma_V^2}{2}\right)t_2}{\sigma_V\sqrt{t_2}}\right)$$

$$\mathbf{d}_2^{\mathbb{Q}} = \left(d_1^{\mathbb{Q}} \quad d_2^{\mathbb{Q}}\right) = \left(\frac{\ln\frac{v}{V_1} + \left(r-\varpi-\frac{\sigma_V^2}{2}\right)t_1}{\sigma_V\sqrt{t_1}} \quad \frac{\ln\frac{v}{F_2} + \left(r-\varpi-\frac{\sigma_V^2}{2}\right)t_2}{\sigma_V\sqrt{t_2}}\right).$$

Here the delta is

$$\frac{\partial s}{\partial v} = e^{-\varpi t_2}\left(\Phi_2\left(\mathbf{d}^{\mathbb{M}};\mathbf{\Gamma}\right) + v\frac{\partial \Phi_2\left(\mathbf{d}^{\mathbb{M}};\mathbf{\Gamma}\right)}{\partial v}\right) - e^{-rt_1}F_1\frac{\partial \Phi(d_1^{\mathbb{Q}})}{\partial v} - e^{-rt_2}F_2\frac{\partial \Phi_2(\mathbf{d}_2^{\mathbb{Q}};\mathbf{\Gamma})}{\partial v}.$$

In order to effectively compute the delta of the equity for $n = 2$, I need to find an expression for the partial derivative of the bivariate CDF. Based on Theorem 3 (for convenience of

notation the dependence on the measure is also omitted), it follows

$$\frac{\partial \Phi_2 (\mathbf{d};\Gamma)}{\partial v} = \frac{\partial \Phi_2 (\mathbf{d};\Gamma)}{\partial d_1} \frac{\partial d_1}{\partial v} + \frac{\partial \Phi_2 (\mathbf{d};\Gamma)}{\partial d_2} \frac{\partial d_2}{\partial v}$$

$$= \frac{1}{v} \left(\frac{1}{\sigma_V \sqrt{t_1}} \int_{-\infty}^{d_2} \frac{1}{2\pi \sqrt{1-\gamma^2}} \exp \left(-\frac{1}{2} \frac{x^2 - 2\gamma d_1 x + d_1^2}{1-\gamma^2} \right) dx \right.$$

$$\left. + \frac{1}{\sigma_V \sqrt{t_2}} \int_{-\infty}^{d_1} \frac{1}{2\pi \sqrt{1-\gamma^2}} \exp \left(-\frac{1}{2} \frac{d_2^2 - 2\gamma d_2 y + y^2}{1-\gamma^2} \right) dy \right)$$

$$= \frac{1}{v} \left(\frac{1}{\sigma_V \sqrt{t_1}} \frac{\exp \left(-\frac{d_1^2}{2} \right)}{\sqrt{2\pi}} \int_{-\infty}^{d_2} \frac{1}{\sqrt{2\pi(1-\gamma^2)}} \exp \left(-\frac{1}{2} \frac{(x - \gamma d_1)^2}{1-\gamma^2} \right) dx \right.$$

$$\left. + \frac{1}{\sigma_V \sqrt{t_2}} \frac{\exp \left(-\frac{d_2^2}{2} \right)}{\sqrt{2\pi}} \int_{-\infty}^{d_1} \frac{1}{\sqrt{2\pi(1-\gamma^2)}} \exp \left(-\frac{1}{2} \frac{(y - \gamma d_2)^2}{1-\gamma^2} \right) dy \right)$$

$$= \frac{1}{v} \left(\frac{\phi(d_1)}{\sigma_V \sqrt{t_1}} \Phi \left(\frac{d_2 - \gamma d_1}{\sqrt{1-\gamma^2}} \right) + \frac{\phi(d_2)}{\sigma_V \sqrt{t_2}} \Phi \left(\frac{d_1 - \gamma d_2}{\sqrt{1-\gamma^2}} \right) \right).$$

Setting

$$\mathfrak{d}_2^{\mathbb{M}} := \frac{d_2^{\mathbb{M}} - \gamma d_1^{\mathbb{M}}}{\sqrt{1-\gamma^2}} = \frac{\ln \frac{\bar{V}_1}{F_2} + \left(r - \varpi + \frac{\sigma_V^2}{2} \right)(t_2 - t_1)}{\sigma_V \sqrt{t_2 - t_1}}$$

$$\mathfrak{d}_2^{\mathbb{Q}} := \frac{d_2^{\mathbb{Q}} - \gamma d_1^{\mathbb{Q}}}{\sqrt{1-\gamma^2}} = \mathfrak{d}_2^{\mathbb{M}} - \sigma_V \sqrt{t_2 - t_1}$$

(F.1)

and[1]

$$\mathfrak{d}_1^{\mathbb{M}} := \frac{d_1^{\mathbb{M}} - \gamma d_2^{\mathbb{M}}}{\sqrt{1-\gamma^2}} = \frac{\ln \left(\frac{v}{\bar{V}_1} \right) t_2 - \ln \left(\frac{v}{F_2} \right) t_1}{\sigma_V \sqrt{t_1 t_2 (t_2 - t_1)}} = \frac{d_1^{\mathbb{Q}} - \gamma d_2^{\mathbb{Q}}}{\sqrt{1-\gamma^2}} := \mathfrak{d}_1^{\mathbb{Q}}$$

(F.2)

---

[1] Just notice that

$$\frac{d_1^{\mathbb{Q}} - \gamma d_2^{\mathbb{Q}}}{\sqrt{1-\gamma^2}} = \frac{d_1^{\mathbb{M}} - \gamma d_2^{\mathbb{M}}}{\sqrt{1-\gamma^2}}$$

as

$$d_1^{\mathbb{M}} - d_1^{\mathbb{Q}} = \gamma \left(d_2^{\mathbb{M}} - d_2^{\mathbb{Q}} \right)$$

$$\sigma_V \sqrt{t_1} = \sqrt{\frac{t_1}{t_2}} \sigma_V \sqrt{t_2}.$$

it follows

$$\frac{\partial s}{\partial v} = e^{-\varpi t_2} \left(\Phi_2\left(\mathbf{d}^{\mathbb{M}}; \mathbf{\Gamma}\right) + \frac{\phi(d_1^{\mathbb{M}})}{\sigma_V \sqrt{t_1}} \Phi\left(\eth_2^{\mathbb{M}}\right) + \frac{\phi(d_2^{\mathbb{M}})}{\sigma_V \sqrt{t_2}} \Phi\left(\eth_1^{\mathbb{M}}\right) \right)$$
$$- e^{-rt_1} \frac{F_1}{v\sigma_V \sqrt{t_1}} \phi(d_1^{\mathbb{Q}}) - e^{-rt_2} \frac{F_2}{v} \left(\frac{\phi(d_1^{\mathbb{Q}})}{\sigma_V \sqrt{t_1}} \Phi(\eth_2^{\mathbb{Q}}) + \frac{\phi(d_2^{\mathbb{Q}})}{\sigma_V \sqrt{t_2}} \Phi(\eth_1^{\mathbb{Q}}) \right).$$

Finally, using

$$\phi(d_1^{\mathbb{Q}}) = \phi(d_1^{\mathbb{M}} - \sigma_V\sqrt{t_1}) = \frac{ve^{-\varpi t_1}}{\bar{V}_1 e^{-rt_1}} \phi(d_1^{\mathbb{M}}) \quad \text{and} \quad \phi(d_2^{\mathbb{Q}}) = \phi(d_2^{\mathbb{M}} - \sigma_V\sqrt{t_2}) = \frac{ve^{-\varpi t_2}}{F_2 e^{-rt_2}} \phi(d_2^{\mathbb{M}})$$

and (F.2), the previous expression can be written as

$$\boxed{\Delta_S^{(2)} = e^{-\varpi t_2} \left[\Phi_2\left(\mathbf{d}^{\mathbb{M}}; \mathbf{\Gamma}\right) + \frac{\phi(d_1^{\mathbb{M}})}{\sigma_V \sqrt{t_1}} \left(\Phi\left(\eth_2^{\mathbb{M}}\right) - \frac{F_2 e^{-r(t_2-t_1)}}{\bar{V}_1 e^{-\varpi(t_2-t_1)}} \Phi(\eth_2^{\mathbb{Q}}) \right) \right] - e^{-rt_1} \frac{F_1}{v\sigma_V \sqrt{t_1}} \phi(d_1^{\mathbb{Q}})}$$

See Figures F.1c and F.1d for a graphical analysis of the delta in the case of two bonds outstanding.

Finally, if $n = 3$

$$s = e^{-\varpi t_3} v\Phi_3\left(\mathbf{d}^{\mathbb{M}}; \mathbf{\Gamma_3}\right) - e^{-rt_1} F_1 \Phi(d_1^{\mathbb{Q}}) - e^{-rt_2} F_2 \Phi_2(\mathbf{d}_2^{\mathbb{Q}}; \mathbf{\Gamma_2}) - e^{-rt_3} F_3 \Phi_3(\mathbf{d}_3^{\mathbb{Q}}; \mathbf{\Gamma_3})$$

with

$$\mathbf{\Gamma_3} = \begin{pmatrix} 1 & \gamma_{12} & \gamma_{13} \\ \gamma_{12} & 1 & \gamma_{23} \\ \gamma_{13} & \gamma_{23} & 1 \end{pmatrix}, \qquad \mathbf{\Gamma_2} = \begin{pmatrix} 1 & \gamma_{12} \\ \gamma_{12} & 1 \end{pmatrix} \qquad \text{and} \qquad \gamma_{ij} = \sqrt{\frac{t_i}{t_j}}, \text{ with } i \leq j$$

$$\mathbf{d}^{\mathbb{M}} = \begin{pmatrix} d_1^{\mathbb{M}} & d_2^{\mathbb{M}} & d_3^{\mathbb{M}} \end{pmatrix} = \begin{pmatrix} \frac{\ln \frac{v}{\bar{V}_1} + \left(r - \varpi + \frac{\sigma_V^2}{2}\right) t_1}{\sigma_V \sqrt{t_1}} & \frac{\ln \frac{v}{\bar{V}_2} + \left(r - \varpi + \frac{\sigma_V^2}{2}\right) t_2}{\sigma_V \sqrt{t_2}} & \frac{\ln \frac{v}{F_3} + \left(r - \varpi + \frac{\sigma_V^2}{2}\right) t_3}{\sigma_V \sqrt{t_3}} \end{pmatrix}$$

and

$$\mathbf{d}_3^{\mathbb{Q}} = \begin{pmatrix} \mathbf{d}_2^{\mathbb{Q}} & d_3^{\mathbb{Q}} \end{pmatrix} = \begin{pmatrix} d_1^{\mathbb{Q}} & d_2^{\mathbb{Q}} & d_3^{\mathbb{Q}} \end{pmatrix} = \begin{pmatrix} \frac{\ln \frac{v}{\bar{V}_1} + \left(r - \varpi - \frac{\sigma_V^2}{2}\right) t_1}{\sigma_V \sqrt{t_1}} & \frac{\ln \frac{v}{\bar{V}_2} + \left(r - \varpi - \frac{\sigma_V^2}{2}\right) t_2}{\sigma_V \sqrt{t_2}} & \frac{\ln \frac{v}{F_3} + \left(r - \varpi - \frac{\sigma_V^2}{2}\right) t_3}{\sigma_V \sqrt{t_3}} \end{pmatrix}.$$

Here the delta is equal to

$$
\frac{\partial s}{\partial v} = e^{-\varpi t_3} \left(\Phi_3 \left(\mathbf{d}^{\mathbb{M}}; \mathbf{\Gamma_3} \right) + v \frac{\partial \Phi_3 \left(\mathbf{d}^{\mathbb{M}}; \mathbf{\Gamma_3} \right)}{\partial v} \right) - e^{-rt_1} F_1 \frac{\partial \Phi \left(d_1^{\mathbb{Q}} \right)}{\partial v} - e^{-rt_2} F_2 \frac{\partial \Phi_2 \left(\mathbf{d}_2^{\mathbb{Q}}; \mathbf{\Gamma_2} \right)}{\partial v}
$$

$$
- e^{-rt_3} F_3 \frac{\partial \Phi_3 \left(\mathbf{d}_3^{\mathbb{Q}}; \mathbf{\Gamma_3} \right)}{\partial v}.
$$

Again, to compute the delta of the equity for $n = 3$, I need to find an expression for the partial derivative of the trivariate CDF. Using Theorem 3, it follows

$$
\frac{\partial \Phi_3 \left(\mathbf{d}; \mathbf{\Gamma} \right)}{\partial v} = \frac{\partial \Phi_3 \left(\mathbf{d}; \mathbf{\Gamma} \right)}{\partial d_1} \frac{\partial d_1}{\partial v} + \frac{\partial \Phi_3 \left(\mathbf{d}; \mathbf{\Gamma} \right)}{\partial d_2} \frac{\partial d_2}{\partial v} + \frac{\partial \Phi_3 \left(\mathbf{d}; \mathbf{\Gamma} \right)}{\partial d_3} \frac{\partial d_3}{\partial v}
$$

$$
= \frac{1}{v} \left(\frac{1}{\sigma_V \sqrt{t_1}} \int_{-\infty}^{d_2} \int_{-\infty}^{d_3} \frac{1}{\sqrt{(2\pi)^3 \det \mathbf{\Gamma}}} \exp \left(-\frac{\tau_1 x^2 + \tau_4 y^2 + \tau_9 d_1^2 + 2\tau_2 xy + 2\tau_6 d_1 y}{2} \right) dx\,dy \right.
$$

$$
+ \frac{1}{\sigma_V \sqrt{t_2}} \int_{-\infty}^{d_1} \int_{-\infty}^{d_3} \frac{1}{\sqrt{(2\pi)^3 \det \mathbf{\Gamma}}} \exp \left(-\frac{\tau_1 x^2 + \tau_4 d_2^2 + \tau_9 z^2 + 2\tau_2 d_2 x + 2\tau_6 d_2 z}{2} \right) dx\,dz
$$

$$
+ \frac{1}{\sigma_V \sqrt{t_3}} \int_{-\infty}^{d_1} \int_{-\infty}^{d_2} \frac{1}{\sqrt{(2\pi)^3 \det \mathbf{\Gamma}}} \exp \left(-\frac{\tau_1 d_3^2 + \tau_4 y^2 + \tau_9 z^2 + 2\tau_2 d_3 y + 2\tau_6 yz}{2} \right) dy\,dz \left. \right)
$$

$$
= \frac{1}{v} \left(\frac{I_1}{\sigma_V \sqrt{t_1}} + \frac{I_2}{\sigma_V \sqrt{t_2}} + \frac{I_3}{\sigma_V \sqrt{t_3}} \right)
$$

where $\det \mathbf{\Gamma} = \frac{(t_2 - t_1)(t_3 - t_2)}{t_2 t_3}$ and

$$
\mathbf{\Gamma}^{-1} = \begin{pmatrix} \frac{t_2}{t_2 - t_1} & -\frac{\sqrt{t_1 t_2}}{t_2 - t_1} & 0 \\ -\frac{\sqrt{t_1 t_2}}{t_2 - t_1} & \frac{t_2 (t_3 - t_1)}{(t_2 - t_1)(t_3 - t_2)} & -\frac{\sqrt{t_2 t_3}}{t_3 - t_2} \\ 0 & -\frac{\sqrt{t_2 t_3}}{t_3 - t_2} & \frac{t_3}{t_3 - t_2} \end{pmatrix} = \begin{pmatrix} \tau_1 & \tau_2 & 0 \\ \tau_2 & \tau_4 & \tau_6 \\ 0 & \tau_6 & \tau_9 \end{pmatrix}.
$$

All the double integrals can be computed recognising appropriate bivariate Gaussian random vector and re-expressing the integrals as an appropriate bivariate normal CDF, i.e.

$$
\int_{-\infty}^{a} \int_{-\infty}^{b} \frac{1}{2\pi \sigma_1 \sigma_2 \sqrt{1 - \rho^2}} \exp \left(-\frac{\left(\frac{w_1 - \mu_1}{\sigma_1} \right)^2 + \left(\frac{w_2 - \mu_2}{\sigma_2} \right)^2 - 2\rho \left(\frac{w_1 - \mu_1}{\sigma_1} \right) \left(\frac{w_2 - \mu_2}{\sigma_2} \right)}{2 (1 - \rho^2)} \right) dw_1\,dw_2.
$$

<u>Solution of I_1</u>

In order to find the appropriate random vector $\mathbf{W_1} \sim \mathcal{N}(\boldsymbol{\mu_1}, \boldsymbol{\Sigma_1})$, I need to determine $\Theta_1 = \{\boldsymbol{\mu_1}, \boldsymbol{\Sigma_1}\} = \{\mu_1, \mu_2, \sigma_1, \sigma_2, \rho\}$ such that

$$\frac{\left(\frac{w_1-\mu_1}{\sigma_1}\right)^2 + \left(\frac{w_2-\mu_2}{\sigma_2}\right)^2 - 2\rho\left(\frac{w_1-\mu_1}{\sigma_1}\right)\left(\frac{w_2-\mu_2}{\sigma_2}\right)}{1-\rho^2} = \tau_1 w_1^2 + \tau_4 w_2^2 + 2\tau_2 w_1 w_2 + 2\tau_6 d_1 w_2 + \tilde{a}_1$$

(F.3)

and re-express the density as normalised based on its covariance matrix (notice that $\tilde{a}_1$ is a free parameter). Expanding the left-hand side of (F.3)

$$\frac{1}{1-\rho^2}\left[\frac{w_1^2}{\sigma_1^2} + \frac{w_2^2}{\sigma_2^2} - 2\frac{\rho}{\sigma_1\sigma_2}w_1 w_2 + \frac{2}{\sigma_1}\left(\rho\frac{\mu_2}{\sigma_2} - \frac{\mu_1}{\sigma_1}\right)w_1 + \frac{2}{\sigma_2}\left(\rho\frac{\mu_1}{\sigma_1} - \frac{\mu_2}{\sigma_2}\right)w_2 \right.$$
$$\left. + \left(\frac{\mu_1}{\sigma_1}\right)^2 + \left(\frac{\mu_2}{\sigma_2}\right)^2 - 2\rho\frac{\mu_1\mu_2}{\sigma_1\sigma_2}\right]$$

the following conditions must be met

$$\frac{1}{(1-\rho^2)\sigma_1^2} = \tau_1$$

$$\frac{1}{(1-\rho^2)\sigma_2^2} = \tau_4$$

$$-\frac{\rho}{(1-\rho^2)\sigma_1\sigma_2} = \tau_2$$

$$\frac{1}{(1-\rho^2)\sigma_1}\left(\rho\frac{\mu_2}{\sigma_2} - \frac{\mu_1}{\sigma_1}\right) = 0$$

$$\frac{1}{(1-\rho^2)\sigma_2}\left(\rho\frac{\mu_1}{\sigma_1} - \frac{\mu_2}{\sigma_2}\right) = \tau_6 d_1$$

$$\frac{1}{1-\rho^2}\left[\left(\frac{\mu_1}{\sigma_1}\right)^2 + \left(\frac{\mu_2}{\sigma_2}\right)^2 - 2\rho\frac{\mu_1\mu_2}{\sigma_1\sigma_2}\right] = \tilde{a}_1.$$

The first three conditions allow to find σ_1, σ_2 and ρ as

$$\rho = -\frac{\tau_2}{\sqrt{\tau_1\tau_4}} \qquad \sigma_1^2 = \frac{1}{\tau_1(1-\rho^2)} = \frac{\tau_4}{\tau_1\tau_4 - \tau_2^2} \qquad \sigma_2^2 = \frac{1}{\tau_4(1-\rho^2)} = \frac{\tau_1}{\tau_1\tau_4 - \tau_2^2}.$$

The forth condition, imposes

$$\frac{\mu_1}{\sigma_1} = \rho\frac{\mu_2}{\sigma_2}$$

which can be substituted into the fifth condition to find μ_2 as

$$\mu_2 = -\tau_6 \sigma_2^2 d_1 = -\frac{\tau_6}{\tau_4 \left(1-\rho^2\right)} d_1 = -\frac{\tau_1 \tau_6}{\tau_1 \tau_4 - \tau_2^2} d_1.$$

Finally, μ_1 is found as

$$\mu_1 = \rho \frac{\mu_2 \sigma_1}{\sigma_2} = \frac{\tau_2 \tau_6}{\tau_1 \tau_4 (1-\rho^2)} d_1 = \frac{\tau_2 \tau_6}{\tau_1 \tau_4 - \tau_2^2} d_1,$$

and

$$\tilde{a}_1 = \frac{\tau_1 \tau_6^2}{\tau_1 \tau_4 - \tau_2^2} d_1^2.$$

Therefore

$$I_1 = \sqrt{\frac{\det \Sigma_1}{\det \Gamma}} \frac{\exp\left(-\frac{\tau_9 d_1^2 - \tilde{a}_1}{2}\right)}{\sqrt{2\pi}} \int_{-\infty}^{d_2} \int_{-\infty}^{d_3} \frac{1}{2\pi\sqrt{\det \Sigma_1}} \exp\left(-\frac{(\mathbf{w_1} - \boldsymbol{\mu_1})^\top \Sigma_1^{-1} (\mathbf{w_1} - \boldsymbol{\mu_1})}{2}\right) d\mathbf{w_1}$$

$$= \sqrt{\frac{\det \Sigma_1}{\det \Gamma}} \phi\left(\sqrt{a_1} d_1\right) N_2\left(d_2, d_3; \boldsymbol{\mu_1}, \Sigma_1\right)$$

with

$$a_1 = \tau_9 - \frac{\tau_1 \tau_6^2}{\tau_1 \tau_4 - \tau_2^2}$$

and

$$\det \Sigma_1 = \sigma_1^2 \sigma_2^2 \left(1 - \rho^2\right) = \frac{1}{\tau_1 \tau_4 - \tau_2^2}.$$

Solution of I_2

The second integral is simpler to solve as there is no xz term. In fact, it can be expressed as the CDFs of two univariate Gaussian (independent) random variables as

$$I_2 = \int_{-\infty}^{d_1} \int_{-\infty}^{d_3} \frac{1}{\sqrt{(2\pi)^3 \det \Gamma}} \exp\left(-\frac{\tau_1 x^2 + \tau_4 d_2^2 + \tau_9 z^2 + 2\tau_2 d_2 x + 2\tau_6 d_2 z}{2}\right) dx\,dz$$

$$= \frac{\sigma_x \sigma_z}{\sqrt{\det \Gamma}} \frac{\exp\left(-\frac{a_2 d_2^2}{2}\right)}{\sqrt{2\pi}} \int_{-\infty}^{d_1} \frac{1}{\sqrt{2\pi}\sigma_x} \exp\left(-\frac{1}{2}\left(\frac{x-\mu_x}{\sigma_x}\right)^2\right) dx \int_{-\infty}^{d_3} \frac{1}{\sqrt{2\pi}\sigma_z} \exp\left(-\frac{1}{2}\left(\frac{z-\mu_z}{\sigma_z}\right)^2\right) dz$$

with

$$\mu_x = -\frac{\tau_2 d_2}{\tau_1}, \qquad \sigma_x^2 = \frac{1}{\tau_1},$$

$$\mu_z = -\frac{\tau_6 d_2}{\tau_9}, \qquad \sigma_z^2 = \frac{1}{\tau_9},$$

$$a_2 = \tau_4 - \frac{\tau_2^2}{\tau_1} - \frac{\tau_6^2}{\tau_9}, \qquad \mathbf{\Sigma_2} = \begin{pmatrix} \sigma_x^2 & 0 \\ 0 & \sigma_z^2 \end{pmatrix}.$$

Therefore

$$I_2 = \sqrt{\frac{\det \mathbf{\Sigma_2}}{\det \mathbf{\Gamma}}} \phi\left(\sqrt{a_2}d_2\right) \Phi\left(\frac{\tau_1 d_1 + \tau_2 d_2}{\sqrt{\tau_1}}\right) \Phi\left(\frac{\tau_9 d_3 + \tau_6 d_2}{\sqrt{\tau_9}}\right)$$

with

$$\det \mathbf{\Sigma_2} = \sigma_x^2 \sigma_z^2 = \frac{1}{\tau_1 \tau_9}.$$

Alternatively, the integral can also be expressed as

$$I_2 = \sqrt{\frac{\det \mathbf{\Sigma_2}}{\det \mathbf{\Gamma}}} \phi\left(\sqrt{a_2}d_2\right) N_2\left(d_1, d_3; \mathbf{\mu_2}, \mathbf{\Sigma_2}\right),$$

where $\mathbf{\mu_2} = \begin{pmatrix} \mu_x & \mu_y \end{pmatrix}^{\top}$.

Solution of I_3

The procedure to solve the last integral is the same used for I_1. Consider the random vector $\mathbf{W_3} \sim \mathcal{N}\left(\mathbf{\mu_3}, \mathbf{\Sigma_3}\right)$. Again, I need to determine $\Theta_3 = \{\mathbf{\mu_3}, \mathbf{\Sigma_3}\} = \{\mu_1, \mu_2, \sigma_1, \sigma_2, \rho\}$ such that

$$\frac{\left(\frac{w_1 - \mu_1}{\sigma_1}\right)^2 + \left(\frac{w_2 - \mu_2}{\sigma_2}\right)^2 - 2\rho\left(\frac{w_1 - \mu_1}{\sigma_1}\right)\left(\frac{w_2 - \mu_2}{\sigma_2}\right)}{1 - \rho^2} = \tau_4 w_1^2 + \tau_9 w_2^2 + 2\tau_2 d_3 w_1 + 2\tau_6 w_1 w_2 + \tilde{a}_3.$$

Thus, the following conditions must be met

$$\frac{1}{(1 - \rho^2)\sigma_1^2} = \tau_4$$

$$\frac{1}{(1 - \rho^2)\sigma_2^2} = \tau_9$$

$$-\frac{\rho}{(1 - \rho^2)\sigma_1 \sigma_2} = \tau_6$$

$$\frac{1}{(1 - \rho^2)\sigma_1}\left(\rho\frac{\mu_2}{\sigma_2} - \frac{\mu_1}{\sigma_1}\right) = \tau_2 d_3$$

$$\frac{1}{(1 - \rho^2)\sigma_2}\left(\rho\frac{\mu_1}{\sigma_1} - \frac{\mu_2}{\sigma_2}\right) = 0$$

$$\frac{1}{1 - \rho^2}\left[\left(\frac{\mu_1}{\sigma_1}\right)^2 + \left(\frac{\mu_2}{\sigma_2}\right)^2 - 2\rho\frac{\mu_1 \mu_2}{\sigma_1 \sigma_2}\right] = \tilde{a}_3.$$

161

The Delta of the Equity

The first three conditions allow to find σ_1, σ_2 and ρ as

$$\rho = -\frac{\tau_6}{\sqrt{\tau_4\tau_9}} \qquad \sigma_1^2 = \frac{1}{\tau_4\left(1-\rho^2\right)} = \frac{\tau_9}{\tau_4\tau_9 - \tau_6^2} \qquad \sigma_2^2 = \frac{1}{\tau_9\left(1-\rho^2\right)} = \frac{\tau_4}{\tau_4\tau_9 - \tau_6^2}.$$

The fifth condition, imposes

$$\frac{\mu_2}{\sigma_2} = \rho\frac{\mu_1}{\sigma_1}$$

which can be substituted into the forth condition to find μ_1 as

$$\mu_1 = -\tau_2\sigma_1^2 d_3 = -\frac{\tau_2}{\tau_4\left(1-\rho^2\right)}d_3 = -\frac{\tau_2\tau_9}{\tau_4\tau_9 - \tau_6^2}d_3.$$

Finally, μ_2 is found as

$$\mu_2 = \rho\frac{\mu_1\sigma_2}{\sigma_1} = \frac{\tau_2\tau_6}{\tau_4\tau_9\left(1-\rho^2\right)}d_3 = \frac{\tau_2\tau_6}{\tau_4\tau_9 - \tau_6^2}d_3,$$

and

$$\tilde{a}_3 = \frac{\tau_9\tau_2^2}{\tau_4\tau_9 - \tau_6^2}d_3^2.$$

Therefore

$$I_3 = \sqrt{\frac{\det\boldsymbol{\Sigma_3}}{\det\boldsymbol{\Gamma}}}\frac{\exp\left(-\frac{\tau_1 d_3^2 - \tilde{a}_3}{2}\right)}{\sqrt{2\pi}}\int_{-\infty}^{d_1}\int_{-\infty}^{d_2}\frac{1}{2\pi\sqrt{\det\boldsymbol{\Sigma_3}}}\exp\left(-\frac{(\mathbf{w_3}-\boldsymbol{\mu_3})^\top\boldsymbol{\Sigma_3}^{-1}(\mathbf{w_3}-\boldsymbol{\mu_3})}{2}\right)\mathrm{d}\mathbf{w_3}$$

$$= \sqrt{\frac{\det\boldsymbol{\Sigma_3}}{\det\boldsymbol{\Gamma}}}\phi\left(\sqrt{a_3}d_3\right)N_2\left(d_1,d_2;\boldsymbol{\mu_3},\boldsymbol{\Sigma_3}\right)$$

with

$$a_3 = \tau_1 - \frac{\tau_9\tau_2^2}{\tau_4\tau_9 - \tau_6^2}$$

and

$$\det\boldsymbol{\Sigma_3} = \sigma_1^2\sigma_2^2\left(1-\rho^2\right) = \frac{1}{\tau_4\tau_9 - \tau_6^2}.$$

Hence, the delta of the equity in the case $n=3$ is

$$\frac{\partial s}{\partial v} = e^{-\varpi t_3}\left(\Phi_3\left(\mathbf{d}^{\mathbb{M}};\boldsymbol{\Gamma_3}\right) + \frac{I_1^{\mathbb{M}}}{\sigma_V\sqrt{t_1}} + \frac{I_2^{\mathbb{M}}}{\sigma_V\sqrt{t_2}} + \frac{I_3^{\mathbb{M}}}{\sigma_V\sqrt{t_3}}\right) - e^{-rt_3}\frac{F_3}{v}\left(\frac{I_1^{\mathbb{Q}}}{\sigma_V\sqrt{t_1}} + \frac{I_2^{\mathbb{Q}}}{\sigma_V\sqrt{t_2}} + \frac{I_3^{\mathbb{Q}}}{\sigma_V\sqrt{t_3}}\right)$$

$$- e^{-rt_2}\frac{F_2}{v}\left(\frac{\phi(d_1^{\mathbb{Q}})}{\sigma_V\sqrt{t_1}}\Phi(\eth_2^{\mathbb{Q}}) + \frac{\phi(d_2^{\mathbb{Q}})}{\sigma_V\sqrt{t_2}}\Phi(\eth_1^{\mathbb{Q}})\right) - e^{-rt_1}\frac{F_1}{v\sigma_V\sqrt{t_1}}\phi(d_1^{\mathbb{Q}})$$

Writing the three integrals explicitly, it follows

$$
\begin{aligned}
\Delta_S^{(3)} = {}& e^{-\varpi t_3} \left(\Phi_3 \left(\mathbf{d}^{\mathbb{M}}; \boldsymbol{\Gamma_3} \right) + \frac{1}{\sigma_V \sqrt{\det \boldsymbol{\Gamma_3}}} \sum_{i=1}^{3} \sqrt{\frac{\det \boldsymbol{\Sigma_i}}{t_i}} \phi \left(\sqrt{a_i} d_i^{\mathbb{M}} \right) N_2 \left(\mathbf{d}^{\mathbb{M}} \setminus d_i^{\mathbb{M}}; \boldsymbol{\mu_i^{\mathbb{M}}}, \boldsymbol{\Sigma_i} \right) \right) \\
& - e^{-r t_3} \frac{F_3}{v} \frac{1}{\sigma_V \sqrt{\det \boldsymbol{\Gamma_3}}} \sum_{i=1}^{3} \sqrt{\frac{\det \boldsymbol{\Sigma_i}}{t_i}} \phi \left(\sqrt{a_i} d_i^{\mathbb{Q}} \right) N_2 \left(\mathbf{d}_3^{\mathbb{Q}} \setminus d_i^{\mathbb{Q}}; \boldsymbol{\mu_i^{\mathbb{Q}}}, \boldsymbol{\Sigma_i} \right) \\
& - e^{-r t_2} \frac{F_2}{v} \left(\frac{\phi(d_1^{\mathbb{Q}})}{\sigma_V \sqrt{t_1}} \Phi(\mathfrak{d}_2^{\mathbb{Q}}) + \frac{\phi(d_2^{\mathbb{Q}})}{\sigma_V \sqrt{t_2}} \Phi(\mathfrak{d}_1^{\mathbb{Q}}) \right) - e^{-r t_1} \frac{F_1}{v \sigma_V \sqrt{t_1}} \phi(d_1^{\mathbb{Q}}),
\end{aligned}
$$

where $\mathbf{d} \setminus d_i$ must be intended as the vector obtained from $\mathbf{d}$ by removing the element d_i (and keeping the order of the other elements unchanged). See Figures F.1e and F.1f for a graphical analysis of the delta in the case of three bonds outstanding.
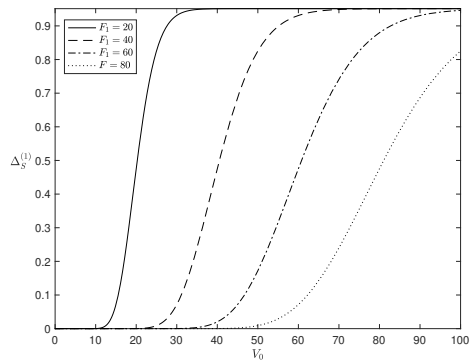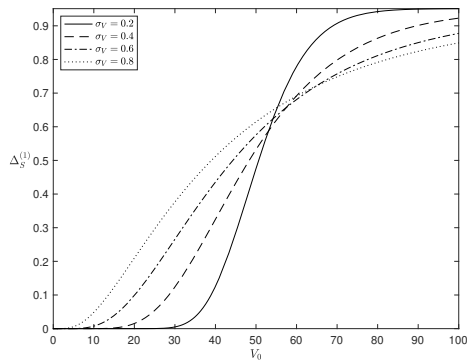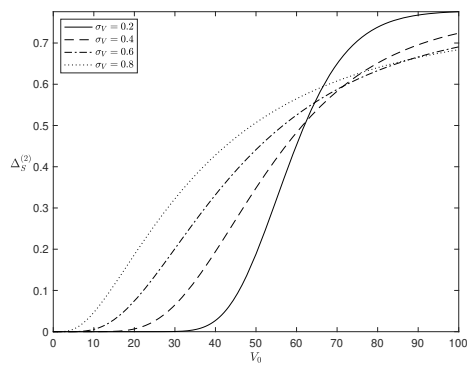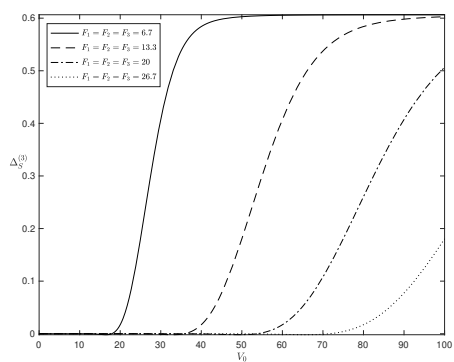
(a) $\sigma_V = 0.2, t_1 = 1$

(b) $F_1 = 50, t_1 = 1$
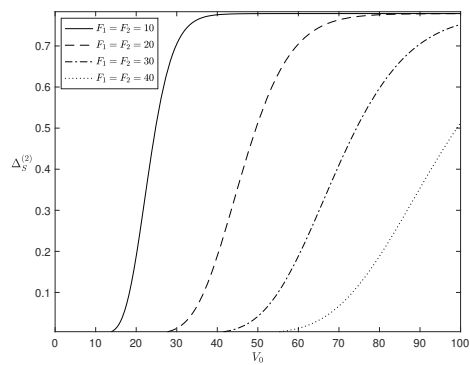
(c) $\sigma_V = 0.2, t_1 = 1, t_2 = 5$

(d) $F_1 = F_2 = 25, t_1 = 1, t_2 = 5$

(e) $\sigma_V = 0.2, t_1 = 1, t_2 = 5, t_3 = 10$
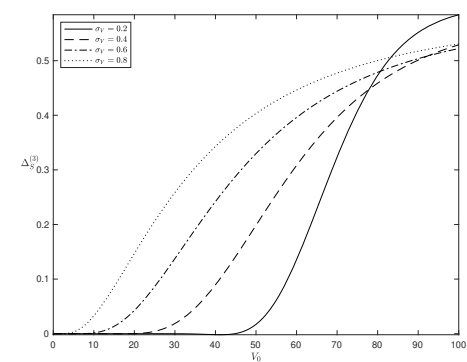
(f) $F_1 = F_2 = F_3 = 50/3, t_1 = 1, t_2 = 5, t_3 = 10$

Fig. F.1 Sensitivity of equity with respect to financial leverage (left) and asset volatility (right). $r = 0.03$, $\varpi = 0.05$ throughout.

Appendix G

The Vega of the Equity

In order to study the vega of the equity, the following result is needed.

Theorem 4. *Let*

$$\Phi_k\left(\mathbf{d}(x);\boldsymbol{\Gamma}\right) = \int_{\Upsilon(x)} \phi_k(y_1,\ldots,y_i,\ldots,y_k;\boldsymbol{\Gamma})\mathrm{d}y_1\ldots\mathrm{d}y_i\ldots\mathrm{d}y_k$$

with $\boldsymbol{\Gamma} \in \mathcal{M}_+^k$ *and* $\Upsilon(x) = \bigcap_{i=1}^k \{y_i \in \mathbb{R} : y_i \le d_i(x)\}$, *with* $\mathbf{d}(x) : \mathbb{R}_+ \to \mathbb{R}^k$, $d_i(x) = b_i x \pm \frac{a_i}{x}$ *with* $a_i : \mathbb{R}_+ \to \mathbb{R}$ *and* $b_i \in \mathbb{R}_+$. *Then*

$$\frac{\partial \Phi_k\left(\mathbf{d}(x);\boldsymbol{\Gamma}\right)}{\partial x} = \sum_{i=1}^k \left(b_i \mp \frac{a_i(x)}{x^2}\right) \int_{\bar{\Upsilon}_i(x)} \phi_k(y_1,\ldots,d_i(x),\ldots,y_k;\boldsymbol{\Gamma})\mathrm{d}y_1\ldots\mathrm{d}y_k,$$

where $\bar{\Upsilon}_i(x) = \Upsilon(x) \setminus \{y_i \le d_i(x)\}$.

Proof. It follows by the same arguments of Theorem 3 with

$$\frac{\partial d_i}{\partial x} = b_i \mp \frac{a_i(x)}{x^2}.$$

□

Given n bond outstanding, the value of the equity $s = S(\sigma_V)$ is given by (1.9), that is

$$s = e^{-\varpi t_n} V_0 \Phi_n\left(\mathbf{d}^{\mathbb{M}}(\sigma_V);\boldsymbol{\Gamma}_n\right) - \sum_{k=1}^n e^{-r t_k} F_k \Phi_k\left(\mathbf{d}_k^{\mathbb{Q}}(\sigma_V);\boldsymbol{\Gamma}_k\right)$$

where $\mathbf{d}^{\mathbb{M}}(\sigma_V) := \left(d_i^{\mathbb{M}}(\sigma_V) \right)_{1 \le i \le n}$ and $\mathbf{d}_k^{\mathbb{Q}}(\sigma_V) = \left(d_i^{\mathbb{M}}(\sigma_V) - \sigma_V \sqrt{t_i} \right)_{1 \le i \le k}$ with

$$
d_i^{\mathbb{M}} = \frac{\ln\left(V_0/\bar{V}_i\right) + \left(r - \varpi + \sigma_V^2/2\right) t_i}{\sigma_V \sqrt{t_i}} \qquad \text{and} \qquad \mathbf{\Gamma}_k = \begin{pmatrix} 1 & \sqrt{\frac{t_1}{t_2}} & \sqrt{\frac{t_1}{t_3}} & \cdots & \sqrt{\frac{t_1}{t_k}} \\ & 1 & \sqrt{\frac{t_2}{t_3}} & \cdots & \sqrt{\frac{t_2}{t_k}} \\ \cdots & \cdots & \cdots & \cdots & \cdots \\ & & & 1 & \sqrt{\frac{t_{k-1}}{t_k}} \\ & & & & 1 \end{pmatrix},
$$

and

$$
\bar{V}_i := \left\{ v \in \mathbb{R}_+ : S_i^{\star}(v) = F_i \right\}.
$$

The vega of the equity is defined in genaral as

$$
v_S^{(n)} := \frac{\partial s}{\partial \sigma_V} = e^{-\varpi t_n} V_0 \frac{\partial \Phi_n \left(\mathbf{d}^{\mathbb{M}}(\sigma_V); \mathbf{\Gamma}_n \right)}{\partial \sigma_V} - \sum_{k=1}^{n} e^{-r t_k} F_k \frac{\partial \Phi_k \left(\mathbf{d}_k^{\mathbb{Q}}(\sigma_V); \mathbf{\Gamma}_k \right)}{\partial \sigma_V}.
$$

In the same fashion of Appendix F, I calculate the vega of the equity for $n = \{1, 2, 3\}$. For convenience of notation, the dependence on σ_V in the integration intervals (the d's and related expressions) is omitted.

If $n = 1$ (also, let $t_1 = t$ and $F_1 = F$)

$$
s = e^{-\varpi t} V_0 \Phi(d^{\mathbb{M}}) - e^{-rt} F \Phi(d^{\mathbb{Q}})
$$

with

$$
d^{\mathbb{M}} = \frac{\ln\left(V_0/F\right) + \left(r - \varpi + \sigma_V^2/2\right) t}{\sigma_V \sqrt{t}} \qquad d^{\mathbb{Q}} = d^{\mathbb{M}} - \sigma_V \sqrt{t}.
$$

Obviously, the vega is the same of Black and Scholes (1973). In fact

$$
\begin{aligned}
\frac{\partial s}{\partial \sigma_V} &= e^{-\varpi t} V_0 \frac{\partial \Phi(d^{\mathbb{M}})}{\partial \sigma_V} - e^{-rt} F \frac{\partial \Phi(d^{\mathbb{Q}})}{\partial \sigma_V} \\
&= e^{-rt} V_0 \phi\left(d^{\mathbb{M}}\right) \left(-\frac{d^{\mathbb{Q}}}{\sigma_V} \right) - e^{-\varpi t} F \phi\left(d^{\mathbb{Q}}\right) \left(-\frac{d^{\mathbb{M}}}{\sigma_V} \right) \\
&= e^{-\varpi t} V_0 \phi\left(d^{\mathbb{M}}\right) \frac{\sigma_V \sqrt{t} - d^{\mathbb{M}}}{\sigma_V} + e^{-rt} F \phi\left(d^{\mathbb{Q}}\right) \frac{d^{\mathbb{M}}}{\sigma_V}
\end{aligned}
$$

as

$$
\phi(d^{\mathbb{Q}}) = \phi(d^{\mathbb{M}} - \sigma_V \sqrt{t}) = \frac{V_0 e^{-\varpi t}}{F e^{-rt}} \phi(d^{\mathbb{M}}).
$$

it follows

$$\boxed{v_S^{(1)} = e^{-\varpi t}\phi(d^{\mathbb{M}})V_0\sqrt{t}}.$$

See Figures G.1a and G.1b for a graphical analysis of the vega in the case of one bond outstanding.

For $n = 2$

$$s = e^{-\varpi t_2}V_0\Phi_2\left(\mathbf{d}^{\mathbb{M}};\mathbf{\Gamma}\right) - e^{-rt_1}F_1\Phi(d_1^{\mathbb{Q}}) - e^{-rt_2}F_2\Phi_2\left(\mathbf{d}_2^{\mathbb{Q}};\mathbf{\Gamma}\right)$$

with

$$\mathbf{\Gamma} = \begin{pmatrix} 1 & \gamma \\ \gamma & 1 \end{pmatrix} \qquad \text{and} \qquad \gamma = \sqrt{\frac{t_1}{t_2}}$$

$$\mathbf{d}^{\mathbb{M}} = \begin{pmatrix} d_1^{\mathbb{M}} & d_2^{\mathbb{M}} \end{pmatrix} = \begin{pmatrix} \dfrac{\ln\frac{V_0}{\bar{V}_1} + \left(r - \varpi + \frac{\sigma_V^2}{2}\right)t_1}{\sigma_V\sqrt{t_1}} & \dfrac{\ln\frac{V_0}{F_2} + \left(r - \varpi + \frac{\sigma_V^2}{2}\right)t_2}{\sigma_V\sqrt{t_2}} \end{pmatrix}$$

$$\mathbf{d}_2^{\mathbb{Q}} = \begin{pmatrix} d_1^{\mathbb{Q}} & d_2^{\mathbb{Q}} \end{pmatrix} = \begin{pmatrix} \dfrac{\ln\frac{V_0}{\bar{V}_1} + \left(r - \varpi - \frac{\sigma_V^2}{2}\right)t_1}{\sigma_V\sqrt{t_1}} & \dfrac{\ln\frac{V_0}{F_2} + \left(r - \varpi - \frac{\sigma_V^2}{2}\right)t_2}{\sigma_V\sqrt{t_2}} \end{pmatrix}.$$

Here the delta is

$$\frac{\partial s}{\partial \sigma_V} = e^{-\varpi t_2}V_0\frac{\partial\Phi_2\left(\mathbf{d}^{\mathbb{M}};\mathbf{\Gamma}\right)}{\partial \sigma_V} - e^{-rt_1}F_1\frac{\partial\Phi(d_1^{\mathbb{Q}})}{\partial \sigma_V} - e^{-rt_2}F_2\frac{\partial\Phi_2\left(\mathbf{d}_2^{\mathbb{Q}};\mathbf{\Gamma}\right)}{\partial \sigma_V}.$$

In order to effectively compute the vega of the equity for $n = 2$, I need to find an expression for the partial derivative of the bivariate CDF. Furthermore, notice that $\bar{V}_1$ is an implicit function of σ_V. Analytical expression for $\partial\bar{V}_1/\partial\sigma_V = \bar{V}_1'$ are available in Appendix E. Based on Theorem 4 (for convenience of notation the dependence on the measure is written as

$\{\mathbb{M}, \mathbb{Q}\} = \{+, -\}$), it follows

$$\frac{\partial \Phi_2\left(\mathbf{d}^{\pm}; \boldsymbol{\Gamma}\right)}{\partial \sigma_V} = \frac{\partial \Phi_2\left(\mathbf{d}^{\pm}; \boldsymbol{\Gamma}\right)}{\partial d_1^{\pm}} \frac{\partial d_1^{\pm}}{\partial \sigma_V} + \frac{\partial \Phi_2\left(\mathbf{d}^{\pm}; \boldsymbol{\Gamma}\right)}{\partial d_2^{\pm}} \frac{\partial d_2^{\pm}}{\partial \sigma_V}$$

$$= -\frac{1}{\sigma_V}\left[\left(d_1^{\mp} + \frac{\bar{V}_1'}{\bar{V}_1\sqrt{t_1}}\right)\int_{-\infty}^{d_2^{\pm}} \frac{1}{2\pi\sqrt{1-\gamma^2}} \exp\left(-\frac{1}{2}\frac{x^2 - 2\gamma d_1^{\pm} x + d_1^{\pm 2}}{1-\gamma^2}\right) \mathrm{d}x\right.$$

$$\left. + d_2^{\mp}\int_{-\infty}^{d_1^{\pm}} \frac{1}{2\pi\sqrt{1-\gamma^2}} \exp\left(-\frac{1}{2}\frac{d_2^{\pm 2} - 2\gamma d_2^{\pm} y + y^2}{1-\gamma^2}\right) \mathrm{d}y\right]$$

$$= -\frac{1}{\sigma_V}\left[\left(d_1^{\mp} + \frac{\bar{V}_1'}{\bar{V}_1\sqrt{t_1}}\right)\frac{\exp\left(-\frac{d_1^{\pm 2}}{2}\right)}{\sqrt{2\pi}}\int_{-\infty}^{d_2^{\pm}} \frac{1}{\sqrt{2\pi(1-\gamma^2)}} \exp\left(-\frac{1}{2}\frac{(x-\gamma d_1^{\pm})^2}{1-\gamma^2}\right) \mathrm{d}x\right.$$

$$\left. + d_2^{\mp}\frac{\exp\left(-\frac{d_2^{\pm 2}}{2}\right)}{\sqrt{2\pi}}\int_{-\infty}^{d_1^{\pm}} \frac{1}{\sqrt{2\pi(1-\gamma^2)}} \exp\left(-\frac{1}{2}\frac{(y-\gamma d_2^{\pm})^2}{1-\gamma^2}\right) \mathrm{d}y\right]$$

$$= -\frac{1}{\sigma_V}\left[\left(d_1^{\mp} + \frac{\bar{V}_1'}{\bar{V}_1\sqrt{t_1}}\right)\phi\left(d_1^{\pm}\right)\Phi\left(\frac{d_2^{\pm} - \gamma d_1^{\pm}}{\sqrt{1-\gamma^2}}\right) + d_2^{\mp}\phi\left(d_2^{\pm}\right)\Phi\left(\frac{d_1^{\pm} - \gamma d_2^{\pm}}{\sqrt{1-\gamma^2}}\right)\right].$$

Using (F.1) and (F.2), and rearranging, it follows

$$\boxed{\begin{aligned}
v_S^{(2)} = \frac{1}{\sigma_V}&\left[e^{-rt_2}F_2\left(\left(d_1^{\mathbb{M}} + \frac{\bar{V}_1'}{\bar{V}_1\sqrt{t_1}}\right)\phi\left(d_1^{\mathbb{Q}}\right)\Phi\left(\eth_2^{\mathbb{Q}}\right) + d_2^{\mathbb{M}}\phi\left(d_2^{\mathbb{Q}}\right)\Phi\left(\eth_1^{\mathbb{Q}}\right)\right)\right.\\
&- e^{-\varpi t_2}V_0\left(\left(d_1^{\mathbb{Q}} + \frac{\bar{V}_1'}{\bar{V}_1\sqrt{t_1}}\right)\phi\left(d_1^{\mathbb{M}}\right)\Phi\left(\eth_2^{\mathbb{M}}\right) + d_2^{\mathbb{Q}}\phi\left(d_2^{\mathbb{M}}\right)\Phi\left(\eth_1^{\mathbb{M}}\right)\right)\\
&\left.+ e^{-rt_1}F_1\left(d_1^{\mathbb{M}} + \frac{\bar{V}_1'}{\bar{V}_1\sqrt{t_1}}\right)\phi\left(d_1^{\mathbb{Q}}\right)\right]
\end{aligned}}$$

See Figures G.1c and G.1d for a graphical analysis of the delta in the case of two bonds outstanding.

Finally, if $n = 3$

$$s = e^{-\varpi t_3}V_0\Phi_3\left(\mathbf{d}^{\mathbb{M}}; \boldsymbol{\Gamma}_3\right) - e^{-rt_1}F_1\Phi\left(d_1^{\mathbb{Q}}\right) - e^{-rt_2}F_2\Phi_2\left(\mathbf{d}_2^{\mathbb{Q}}; \boldsymbol{\Gamma}_2\right) - e^{-rt_3}F_3\Phi_3\left(\mathbf{d}_3^{\mathbb{Q}}; \boldsymbol{\Gamma}_3\right)$$

with

$$\mathbf{\Gamma_3} = \begin{pmatrix} 1 & \gamma_{12} & \gamma_{13} \\ \gamma_{12} & 1 & \gamma_{23} \\ \gamma_{13} & \gamma_{23} & 1 \end{pmatrix}, \qquad \mathbf{\Gamma_2} = \begin{pmatrix} 1 & \gamma_{12} \\ \gamma_{12} & 1 \end{pmatrix} \qquad \text{and} \qquad \gamma_{ij} = \sqrt{\frac{t_i}{t_j}}, \text{ with } i \leq j$$

$$\mathbf{d}^{\mathbb{M}} = \begin{pmatrix} d_1^{\mathbb{M}} & d_2^{\mathbb{M}} & d_3^{\mathbb{M}} \end{pmatrix} = \begin{pmatrix} \dfrac{\ln\frac{V_0}{\bar{V}_1} + \left(r - \varpi + \frac{\sigma_V^2}{2}\right)t_1}{\sigma_V\sqrt{t_1}} & \dfrac{\ln\frac{V_0}{\bar{V}_2} + \left(r - \varpi + \frac{\sigma_V^2}{2}\right)t_2}{\sigma_V\sqrt{t_2}} & \dfrac{\ln\frac{V_0}{F_3} + \left(r - \varpi + \frac{\sigma_V^2}{2}\right)t_3}{\sigma_V\sqrt{t_3}} \end{pmatrix}$$

and

$$\mathbf{d}_3^{\mathbb{Q}} = \begin{pmatrix} \mathbf{d}_2^{\mathbb{Q}} & d_3^{\mathbb{Q}} \end{pmatrix} = \begin{pmatrix} d_1^{\mathbb{Q}} & d_2^{\mathbb{Q}} & d_3^{\mathbb{Q}} \end{pmatrix} = \begin{pmatrix} \dfrac{\ln\frac{V_0}{\bar{V}_1} + \left(r - \varpi - \frac{\sigma_V^2}{2}\right)t_1}{\sigma_V\sqrt{t_1}} & \dfrac{\ln\frac{V_0}{\bar{V}_2} + \left(r - \varpi - \frac{\sigma_V^2}{2}\right)t_2}{\sigma_V\sqrt{t_2}} & \dfrac{\ln\frac{V_0}{F_3} + \left(r - \varpi - \frac{\sigma_V^2}{2}\right)t_3}{\sigma_V\sqrt{t_3}} \end{pmatrix}.$$

Here the vega is equal to

$$\frac{\partial s}{\partial \sigma_V} = e^{-\varpi t_3} V_0 \frac{\partial \Phi_3\left(\mathbf{d}^{\mathbb{M}}; \mathbf{\Gamma_3}\right)}{\partial \sigma_V} - e^{-rt_1} F_1 \frac{\partial \Phi\left(d_1^{\mathbb{Q}}\right)}{\partial \sigma_V} - e^{-rt_2} F_2 \frac{\partial \Phi_2\left(\mathbf{d}_2^{\mathbb{Q}}; \mathbf{\Gamma_2}\right)}{\partial \sigma_V} - e^{-rt_3} F_3 \frac{\partial \Phi_3\left(\mathbf{d}_3^{\mathbb{Q}}; \mathbf{\Gamma_3}\right)}{\partial \sigma_V}.$$

Again, to compute the delta of the equity for $n = 3$, I need to find an expression for the partial derivative of the trivariate CDF. Using Theorem 4 (for convenience of notation the dependence on the measure is written as $\{\mathbb{M}, \mathbb{Q}\} = \{+, -\}$), it follows

$$\frac{\partial \Phi_3\left(\mathbf{d}^{\pm}; \mathbf{\Gamma}\right)}{\partial \sigma_V} = \frac{\partial \Phi_3\left(\mathbf{d}^{\pm}; \mathbf{\Gamma}\right)}{\partial d_1^{\pm}} \frac{\partial d_1^{\pm}}{\partial \sigma_V} + \frac{\partial \Phi_3\left(\mathbf{d}^{\pm}; \mathbf{\Gamma}\right)}{\partial d_2^{\pm}} \frac{\partial d_2^{\pm}}{\partial \sigma_V} + \frac{\partial \Phi_3\left(\mathbf{d}^{\pm}; \mathbf{\Gamma}\right)}{\partial d_3^{\pm}} \frac{\partial d_3^{\pm}}{\partial \sigma_V}$$

$$= -\frac{1}{\sigma_V}\left[\left(d_1^{\mp} + \frac{\bar{V}_1'}{\bar{V}_1\sqrt{t_1}}\right) \int_{-\infty}^{d_2^{\pm}} \int_{-\infty}^{d_3^{\pm}} \frac{1}{\sqrt{(2\pi)^3 \det\mathbf{\Gamma}}} \exp\left(-\frac{\tau_1 x^2 + \tau_4 y^2 + \tau_9 d_1^{\pm 2} + 2\tau_2 xy + 2\tau_6 d_1^{\pm} y}{2}\right) dx\,dy \right.$$

$$+ \left(d_2^{\mp} + \frac{\bar{V}_2'}{\bar{V}_2\sqrt{t_2}}\right) \int_{-\infty}^{d_1^{\pm}} \int_{-\infty}^{d_3^{\pm}} \frac{1}{\sqrt{(2\pi)^3 \det\mathbf{\Gamma}}} \exp\left(-\frac{\tau_1 x^2 + \tau_4 d_2^{\pm 2} + \tau_9 z^2 + 2\tau_2 d_2^{\pm} x + 2\tau_6 d_2^{\pm} z}{2}\right) dx\,dz$$

$$\left. + d_3^{\mp} \int_{-\infty}^{d_1^{\pm}} \int_{-\infty}^{d_2^{\pm}} \frac{1}{\sqrt{(2\pi)^3 \det\mathbf{\Gamma}}} \exp\left(-\frac{\tau_1 d_3^{\pm 2} + \tau_4 y^2 + \tau_9 z^2 + 2\tau_2 d_3^{\pm} y + 2\tau_6 yz}{2}\right) dy\,dz \right]$$

$$= -\frac{1}{\sigma_V}\left[\left(d_1^{\mp} + \frac{\bar{V}_1'}{\bar{V}_1\sqrt{t_1}}\right) I_1 + \left(d_2^{\mp} + \frac{\bar{V}_2'}{\bar{V}_2\sqrt{t_2}}\right) I_2 + d_3^{\mp} I_3 \right]$$

where $\det\mathbf{\Gamma} = \frac{(t_2 - t_1)(t_3 - t_2)}{t_2 t_3}$ and

$$\mathbf{\Gamma}^{-1} = \begin{pmatrix} \dfrac{t_2}{t_2 - t_1} & -\dfrac{\sqrt{t_1 t_2}}{t_2 - t_1} & 0 \\ -\dfrac{\sqrt{t_1 t_2}}{t_2 - t_1} & \dfrac{t_2(t_3 - t_1)}{(t_2 - t_1)(t_3 - t_2)} & -\dfrac{\sqrt{t_2 t_3}}{t_3 - t_2} \\ 0 & -\dfrac{\sqrt{t_2 t_3}}{t_3 - t_2} & \dfrac{t_3}{t_3 - t_2} \end{pmatrix} = \begin{pmatrix} \tau_1 & \tau_2 & 0 \\ \tau_2 & \tau_4 & \tau_6 \\ 0 & \tau_6 & \tau_9 \end{pmatrix}.$$

The Vega of the Equity

All the double integrals can computed in the same fashion described in Appendix F.

Solution of I_1

$$I_1 = \sqrt{\frac{\det \mathbf{\Sigma_1}}{\det \mathbf{\Gamma}}} \phi \left(\sqrt{a_1} d_1^{\pm} \right) N_2 \left(d_2^{\pm}, d_3^{\pm}; \boldsymbol{\mu_1^{\pm}}, \mathbf{\Sigma_1} \right)$$

with

$$\mathbf{\Sigma_1} = \frac{1}{\tau_1 \tau_4 - \tau_2^2} \begin{pmatrix} \tau_4 & -\tau_2 \\ -\tau_2 & \tau_1 \end{pmatrix}, \quad \boldsymbol{\mu_1^{\pm}} = -\det \mathbf{\Sigma_1} \begin{pmatrix} -\tau_2 \tau_6 \\ \tau_1 \tau_6 \end{pmatrix} d_1^{\pm} \quad \text{and} \quad a_1 = \tau_9 - \det \mathbf{\Sigma_1} \tau_1 \tau_6^2$$

Solution of I_2

$$I_2 = \sqrt{\frac{\det \mathbf{\Sigma_2}}{\det \mathbf{\Gamma}}} \phi \left(\sqrt{a_2} d_2^{\pm} \right) N_2 \left(d_1^{\pm}, d_3^{\pm}; \boldsymbol{\mu_2^{\pm}}, \mathbf{\Sigma_2} \right) = \sqrt{\frac{\det \mathbf{\Sigma_2}}{\det \mathbf{\Gamma}}} \phi \left(\sqrt{a_2} d_2^{\pm} \right) \Phi \left(\frac{\tau_1 d_1^{\pm} + \tau_2 d_2^{\pm}}{\sqrt{\tau_1}} \right) \Phi \left(\frac{\tau_9 d_3^{\pm} + \tau_6 d_2^{\pm}}{\sqrt{\tau_9}} \right).$$

with

$$\mathbf{\Sigma_2} = \frac{1}{\tau_1 \tau_9} \begin{pmatrix} \tau_9 & 0 \\ 0 & \tau_1 \end{pmatrix}, \quad \boldsymbol{\mu_2^{\pm}} = -\det \mathbf{\Sigma_2} \begin{pmatrix} \tau_2 \tau_9 \\ \tau_1 \tau_6 \end{pmatrix} d_2^{\pm} \quad \text{and} \quad a_2 = \tau_4 - \det \mathbf{\Sigma_2} \left(\tau_2^2 \tau_9 + \tau_1 \tau_6^2 \right).$$

Solution of I_3

$$I_1 = \sqrt{\frac{\det \mathbf{\Sigma_3}}{\det \mathbf{\Gamma}}} \phi \left(\sqrt{a_3} d_3^{\pm} \right) N_2 \left(d_1^{\pm}, d_2^{\pm}; \boldsymbol{\mu_3^{\pm}}, \mathbf{\Sigma_3} \right)$$

with

$$\mathbf{\Sigma_3} = \frac{1}{\tau_4 \tau_9 - \tau_6^2} \begin{pmatrix} \tau_9 & -\tau_6 \\ -\tau_6 & \tau_4 \end{pmatrix}, \quad \boldsymbol{\mu_3^{\pm}} = -\det \mathbf{\Sigma_3} \begin{pmatrix} \tau_2 \tau_9 \\ -\tau_2 \tau_6 \end{pmatrix} d_1^{\pm} \quad \text{and} \quad a_3 = \tau_1 - \det \mathbf{\Sigma_3} \tau_2^2 \tau_9.$$

Hence, the vega of the equity in the case $n = 3$ is

$$\frac{\partial s}{\partial \sigma_V} = \frac{1}{\sigma_V} \left[e^{-rt_3} F_3 \left(\left(d_1^{\mathbb{M}} + \frac{\bar{V}_1'}{\bar{V}_1 \sqrt{t_1}} \right) I_1^{\mathbb{Q}} + \left(d_2^{\mathbb{M}} + \frac{\bar{V}_2'}{\bar{V}_2 \sqrt{t_2}} \right) I_2^{\mathbb{Q}} + d_3^{\mathbb{M}} I_3^{\mathbb{Q}} \right) \right.$$

$$- e^{-\varpi t_3} V_0 \left(\left(d_1^{\mathbb{Q}} + \frac{\bar{V}_1'}{\bar{V}_1 \sqrt{t_1}} \right) I_1^{\mathbb{M}} + \left(d_2^{\mathbb{Q}} + \frac{\bar{V}_2'}{\bar{V}_2 \sqrt{t_2}} \right) I_2^{\mathbb{M}} + d_3^{\mathbb{Q}} I_3^{\mathbb{M}} \right)$$

$$+ e^{-rt_2} F_2 \left(\left(d_1^{\mathbb{M}} + \frac{\bar{V}_1'}{\bar{V}_1 \sqrt{t_1}} \right) \phi(d_1^{\mathbb{Q}}) \Phi(\partial_2^{\mathbb{Q}}) + \left(d_2^{\mathbb{M}} + \frac{\bar{V}_2'}{\bar{V}_2 \sqrt{t_2}} \right) \phi(d_2^{\mathbb{Q}}) \Phi(\partial_1^{\mathbb{Q}}) \right)$$

$$\left. + e^{-rt_1} F_1 \left(d_1^{\mathbb{M}} + \frac{\bar{V}_1'}{\bar{V}_1 \sqrt{t_1}} \right) \phi(d_1^{\mathbb{Q}}) \right]$$

Writing the three integrals explicitly, it follows

$$
\begin{aligned}
v_S^{(3)} = \frac{1}{\sigma_V} \Bigg[& e^{-rt_3} F_3 \frac{1}{\sqrt{\det \mathbf{\Gamma_3}}} \sum_{i=1}^{3} \left(d_i^{\mathbb{M}} + \frac{\bar{V}_i'}{\bar{V}_i \sqrt{t_i}} \right) \sqrt{\det \mathbf{\Sigma_i}} \phi \left(\sqrt{a_i} d_i^{\mathbb{Q}} \right) N_2 \left(\mathbf{d}_3^{\mathbb{Q}} \setminus d_i^{\mathbb{Q}}; \boldsymbol{\mu_i^{\mathbb{Q}}}, \mathbf{\Sigma_i} \right) \\
& - e^{-\varpi t_3} V_0 \frac{1}{\sqrt{\det \mathbf{\Gamma_3}}} \sum_{i=1}^{3} \left(d_i^{\mathbb{Q}} + \frac{\bar{V}_i'}{\bar{V}_i \sqrt{t_i}} \right) \sqrt{\det \mathbf{\Sigma_i}} \phi \left(\sqrt{a_i} d_i^{\mathbb{M}} \right) N_2 \left(\mathbf{d}^{\mathbb{M}} \setminus d_i^{\mathbb{M}}; \boldsymbol{\mu_i^{\mathbb{M}}}, \mathbf{\Sigma_i} \right) \\
& + e^{-rt_2} F_2 \left(\left(d_1^{\mathbb{M}} + \frac{\bar{V}_1'}{\bar{V}_1 \sqrt{t_1}} \right) \phi \left(d_1^{\mathbb{Q}} \right) \Phi \left(\eth_2^{\mathbb{Q}} \right) + \left(d_2^{\mathbb{M}} + \frac{\bar{V}_2'}{\bar{V}_2 \sqrt{t_2}} \right) \phi \left(d_2^{\mathbb{Q}} \right) \Phi \left(\eth_1^{\mathbb{Q}} \right) \right) \\
& + e^{-rt_1} F_1 \left(d_1^{\mathbb{M}} + \frac{\bar{V}_1'}{\bar{V}_1 \sqrt{t_1}} \right) \phi \left(d_1^{\mathbb{Q}} \right) \Bigg] ,
\end{aligned}
$$

where $\mathbf{d} \setminus d_i$ must be intended as the vector obtained from $\mathbf{d}$ by removing the element d_i (and keeping the order of the other elements unchanged) and $\bar{V}_3' = 0$ (by construction). See Figures G.1e and G.1f for a graphical analysis of the delta in the case of three bonds outstanding.
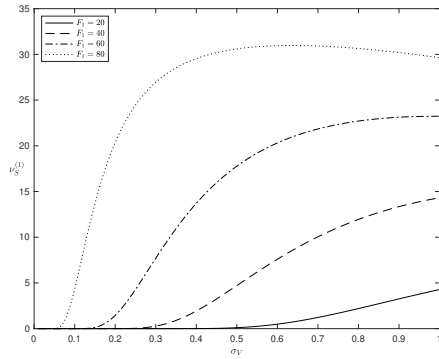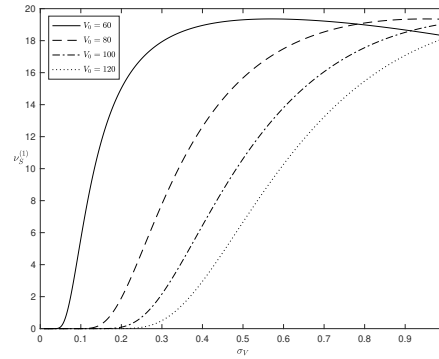
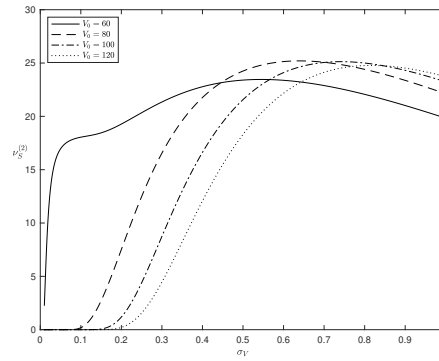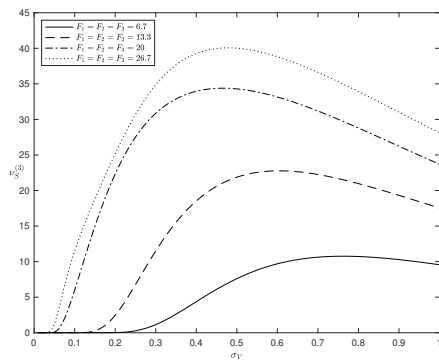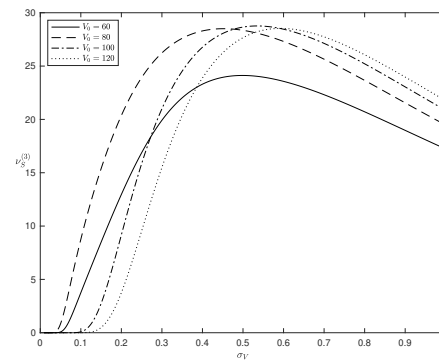(a) $V_0 = 100, t = 1$

(b) $F = 50, t = 1$
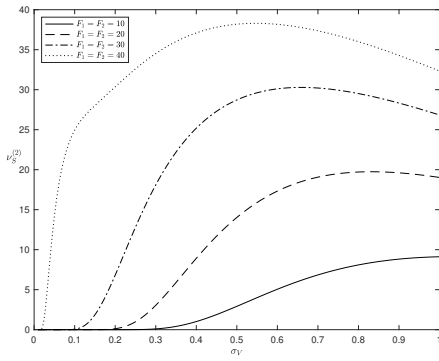
(c) $V_0 = 100, t_1 = 1, t_2 = 5$

(d) $F_1 = F_2 = 25, t_1 = 1, t_2 = 5$

(e) $V_0 = 100, t_1 = 1, t_2 = 5, t_3 = 10$

(f) $F_1 = F_2 = F_3 = 50/3, t_1 = 1, t_2 = 5, t_3 = 10$

Fig. G.1 Sensitivity of equity with respect to asset volatility under different aggregation schemes for debt (left) and leverage (right). $r = 0.03$, $\varpi = 0.05$ throughout.

Appendix H

Robustness checks

Regressand				Adj–R^2:	0.9433
$\overline{AICR}'_1$					
Regressors	Coefficient	Robust Standard Error	t–stat	p–value	
$\overline{AICR}_1$	0.7748793	0.0052173	148.52	0.000	***
α_1	0.0007165	0.0000297	24.13	0.000	***

(a): LGD = 60%

Regressand				Adj–R^2:	0.8788
$\overline{AICR}'_{-1}$					
Regressors	Coefficient	Robust Standard Error	t–stat	p–value	
$\overline{AICR}_{-1}$	0.9196883	0.0242480	37.93	0.000	***
α_{-1}	0.0001626	0.0000705	2.31	0.021	**

(b): LGD = 60%

Regressand				Adj–R^2:	0.9484
$\overline{AICR}'_1$					
Regressors	Coefficient	Robust Standard Error	t–stat	p–value	
$\overline{AICR}_1$	0.7647910	0.0056719	134.84	0.000	***
α_1	0.0008249	0.0000275	29.99	0.000	***

(c): LGD = 80%

Regressand				Adj–R^2:	0.5552
$\overline{AICR}'_{-1}$					
Regressors	Coefficient	Robust Standard Error	t–stat	p–value	
$\overline{AICR}_{-1}$	0.6130806	0.0379853	16.14	0.000	***
α_{-1}	0.0005543	0.0001077	5.15	0.000	***

(d): LGD = 80%

Table H.1 Estimation of regression (1.18) for different values of LGD.
(a): Estimates of the pooled panel regression of average *AICR* obtained from call options ($\xi = 1$) and CDS regressed onto average *AICR* obtained from call options only. Number of observations: 15,470. F–stat: 22,058.80 (p–value: 0.0000).
(b): Estimates of the pooled panel regression of average *AICR* obtained from put options ($\xi = -1$) and CDS regressed onto average *AICR* obtained from put options only. Number of observations: 15,027. F–stat: 1,438.57 (p–value: 0.0000).
(c): Estimates of the pooled panel regression of average *AICR* obtained from call options ($\xi = 1$) and CDS regressed onto average *AICR* obtained from call options only. Number of observations: 15,470. F–stat: 18,181.34 (p–value: 0.0000).
(d): Estimates of the pooled panel regression of average *AICR* obtained from put options ($\xi = -1$) and CDS regressed onto average *AICR* obtained from put options only. Number of observations: 15,027. F–stat: 260.50 (p–value: 0.0000).
A sandwich estimator for panel data is used to obtain robust standard errors. Significance levels: 10% (*), 5% (**), 1% (***).

Robustness checks

Regressand				Adj–R^2:	0.0590
$\overline{AICR}'_1$					

Regressors	Coefficient	Robust Standard Error	t–stat	p–value	
LEV	0.0075571	0.0032449	2.33	0.102	
α_1	-0.001002	0.0019052	-0.53	0.635	
Industry-FE	✓				
Year-FE	✓				

(a): LGD = 60%

Regressand				Adj–R^2:	0.5676
$\overline{AICR}'_{-1}$					

Regressors	Coefficient	Robust Standard Error	t–stat	p–value	
LEV	0.0365895	0.0057882	6.32	0.008	***
α_{-1}	-0.0112664	0.0051351	-2.19	0.116	
Industry-FE	✓		-	0.379	
Year-FE	✓	-	-	-	-

(b): LGD = 60%

Regressand				Adj–R^2:	0.0622
$\overline{AICR}'_1$					

Regressors	Coefficient	Robust Standard Error	t–stat	p–value	
LEV	0.0076758	0.002566	2.99	0.058	*
α_1	-0.0011136	0.0013743	-0.81	0.477	
Industry-FE	✓				
Year-FE	✓				

(c): LGD = 80%

Regressand				Adj–R^2:	0.5980
$\overline{AICR}'_{-1}$					

Regressors	Coefficient	Robust Standard Error	t–stat	p–value	
LEV	0.0303678	0.0093729	3.24	0.048	**
α_{-1}	-0.0086424	0.0082499	-1.05	0.372	
Industry-FE	✓				
Year-FE	✓				

(d): LGD = 80%

Table H.2 Estimation of regression (1.19) for different values of LGD.
(a): Estimates of the fixed-effects panel regression of market model-implied leverage *LEV* onto average *AICR* calculated over call options and CDSs, with LGD = 60%. Number of observations: 15,470.
(b): Estimates of the fixed-effects panel regression of market model-implied leverage *LEV* onto average *AICR* calculated over put options and CDSs, with LGD = 60%. Number of observations: 15,027.
(c): Estimates of the fixed-effects panel regression of market model-implied leverage *LEV* onto average *AICR* calculated over call options and CDSs, with LGD = 80%. Number of observations: 15,470.
(d): Estimates of the fixed-effects panel regression of market model-implied leverage *LEV* onto average *AICR* calculated over put options and CDSs, with LGD = 80%. Number of observations: 15,027.
Standard errors are adjusted for four clusters based on industry. Significance levels: 10% (*), 5% (**), 1% (***).

Regressand					Adj–R^2:	0.3653
η_1						

Regressors	Coefficient	Robust Standard Error	t–stat	p–value	
LEV	0.0051749	0.0025327	2.04	0.134	
α_1	-0.0012296	0.0020341	-0.60	0.588	
Industry-FE	✓				
Year-FE	✓		-		

(a): LGD = 60%

Regressand					Adj–R^2:	0.0923
η_{-1}						

Regressors	Coefficient	Robust Standard Error	t–stat	p–value
LEV	0.0054215	0.0026694	2.03	0.135
α_{-1}	-0.0028967	0.0023997	-1.21	0.314
Industry-FE	✓			
Year-FE	✓			

(b): LGD = 60%

Regressand					Adj–R^2:	0.4673
η_1						

Regressors	Coefficient	Robust Standard Error	t–stat	p–value	
LEV	0.0054288	0.001427	3.80	0.032	**
α_1	-0.0014958	0.0010836	-1.38	0.261	
Industry-FE	✓				
Year-FE	✓		-		

(c): LGD = 80%

Regressand					Adj–R^2:	0.1645
η_{-1}						

Regressors	Coefficient	Robust Standard Error	t–stat	p–value
LEV	0.0105748	0.0075426	1.40	0.255
α_{-1}	-0.0040323	0.0067281	-0.60	0.591
Industry-FE	✓			
Year-FE	✓			

(d): LGD = 80%

Table H.3 Estimation of regression (1.20) for different values of LGD.
(a): Estimates of the fixed-effects panel regression of market model-implied leverage *LEV* onto the residuals obtain from regression (1.18) (calls), for LGD = 60%. Number of observations: 15,470.
(b): Estimates of the fixed-effects panel regression of market model-implied leverage *LEV* onto the residuals obtain from regression (1.18) (puts), for LGD = 60%. Number of observations: 15,027.
(c): Estimates of the fixed-effects panel regression of market model-implied leverage *LEV* onto the residuals obtain from regression (1.18) (calls), for LGD = 80%. Number of observations: 15,470.
(d): Estimates of the fixed-effects panel regression of market model-implied leverage *LEV* onto the residuals obtain from regression (1.18) (puts), for LGD = 80%. Number of observations: 15,027.
Standard errors are adjusted for four clusters based on industry. Significance levels: 10% (*), 5% (**), 1% (***).

Robustness checks

Regressand			Adj–R^2:	0.6608
$\overline{AICR}'_{-1}$				

Regressors	Coefficient	Robust Standard Error	t–stat	p–value	
LEV	0.0391051	0.0012387	31.57	0.000	***
α_{-1}	-0.0145449	0.0011321	-12.85	0.000	***
Year-FE	✓				

(a): Financials, LGD = 60%

Regressand			Adj–R^2:	0.2128
$\overline{AICR}'_{-1}$				

Regressors	Coefficient	Robust Standard Error	t–stat	p–value	
LEV	0.0069186	0.0004261	16.24	0.000	***
α_{-1}	-0.0007640	0.0001489	-5.13	0.000	***
Year-FE	✓				

(b): Mining, Energy and Utilities, LGD = 60%

Regressand			Adj–R^2:	0.1173
$\overline{AICR}'_{-1}$				

Regressors	Coefficient	Robust Standard Error	t–stat	p–value	
LEV	0.0014455	0.0000861	16.78	0.000	***
α_{-1}	-0.0000211	0.0000163	-1.29	0.197	
Year-FE	✓				

(c): Manufacturing, LGD = 60%

Regressand			Adj–R^2:	0.2450
$\overline{AICR}'_{-1}$				

Regressors	Coefficient	Robust Standard Error	t–stat	p–value	
LEV	0.0075047	0.0009004	8.34	0.000	***
α_{-1}	-0.0007342	0.0001427	-5.14	0.000	***
Year-FE	✓				

(d): Retail, Wholesale and Services, LGD = 60%

Table H.4 Estimation of regression (1.19) over the four sub-samples for LGD = 60%.
(a): Estimates of the year-fixed effect panel regression of market model-implied leverage *LEV* onto average *AICR* calculated over put options and CDSs of Financials. Number of observations: 1,938. F–stat = 199.90 (p–value = 0.000).
(b): Estimates of the year-fixed effect panel regression of market model-implied leverage *LEV* onto average *AICR* calculated over put options and CDSs of Mining, Energy and Utilities. Number of observations: 1,916. F–stat = 73.60 (p–value = 0.000).
(c): Estimates of the year-fixed effect panel regression of market model-implied leverage *LEV* onto average *AICR* calculated over put options and CDSs of Manufacturing. Number of observations: 6,515. F–stat = 80.21 (p–value = 0.000).
(d): Estimates of the year-fixed effect panel regression of market model-implied leverage *LEV* onto average *AICR* calculated over put options and CDSs of Retail, Wholesale and Services. Number of observations: 4,658. F–stat = 20.63 (p–value = 0.000).
A sandwich estimator for panel data is used in order to obtain robust standard errors. Significance levels: 10% (*), 5% (**), 1% (***).

Regressand				Adj–R^2:	0.6608
$\overline{AICR}'_{-1}$					

Regressors	Coefficient	Robust Standard Error	t–stat	p–value	
LEV	0.0391051	0.0012387	31.57	0.000	***
α_{-1}	-0.0145449	0.0011321	-12.85	0.000	***
Year-FE	✓				

(a): Financials, LGD = 80%

Regressand				Adj–R^2:	0.2128
$\overline{AICR}'_{-1}$					

Regressors	Coefficient	Robust Standard Error	t–stat	p–value	
LEV	0.0069186	0.0004261	16.24	0.000	***
α_{-1}	-0.0007640	0.0001489	-5.13	0.000	***
Year-FE	✓				

(b): Mining, Energy and Utilities, LGD = 80%

Regressand				Adj–R^2:	0.1173
$\overline{AICR}'_{-1}$					

Regressors	Coefficient	Robust Standard Error	t–stat	p–value	
LEV	0.0014455	0.0000861	16.78	0.000	***
α_{-1}	-0.0000211	0.0000163	-1.29	0.197	
Year-FE	✓				

(c): Manufacturing, LGD = 80%

Regressand				Adj–R^2:	0.2450
$\overline{AICR}'_{-1}$					

Regressors	Coefficient	Robust Standard Error	t–stat	p–value	
LEV	0.0075047	0.0009004	8.34	0.000	***
α_{-1}	-0.0007342	0.0001427	-5.14	0.000	***
Year-FE	✓				

(d): Retail, Wholesale and Services, LGD = 80%

Table H.5 Estimation of regression (1.19) over the four sub-samples for LGD = 80%.
(a): Estimates of the year-fixed effect panel regression of market model-implied leverage *LEV* onto average *AICR* calculated over put options and CDSs of Financials. Number of observations: 1,938. F–stat = 199.90 (p–value = 0.000).
(b): Estimates of the year-fixed effect panel regression of market model-implied leverage *LEV* onto average *AICR* calculated over put options and CDSs of Mining, Energy and Utilities. Number of observations: 1,916. F–stat = 73.60 (p–value = 0.000).
(c): Estimates of the year-fixed effect panel regression of market model-implied leverage *LEV* onto average *AICR* calculated over put options and CDSs of Manufacturing. Number of observations: 6,515. F–stat = 80.21 (p–value = 0.000).
(d): Estimates of the year-fixed effect panel regression of market model-implied leverage *LEV* onto average *AICR* calculated over put options and CDSs of Retail, Wholesale and Services. Number of observations: 4,658. F–stat = 20.63 (p–value = 0.000).
A sandwich estimator for panel data is used in order to obtain robust standard errors. Significance levels: 10% (*), 5% (**), 1% (***).

Robustness checks

Regressand				Adj–R^2:	0.0005
$\Delta\mathrm{Skew}_{T<1}$					

Regressors	Coefficient	Robust Standard Error	t–stat	p–value	
$\overline{AICR}'_{-1,T<1}$	1.479315	0.9954766	1.49	0.142	
$\alpha_{T<1}$	-0.0038017	0.0009416	-4.04	0.000	***
firm-FE	✓				
year-FE	✓				

(a): Predictive regression for short-term skew, LGD = 60%

Regressand				Adj–R^2:	0.0004
$\Delta\mathrm{Skew}_{T>1}$					

Regressors	Coefficient	Robust Standard Error	t–stat	p–value	
$\overline{AICR}'_{-1,T>1}$	0.3945692	0.1372269	2.88	0.005	***
$\alpha_{T>1}$	-0.0106972	0.0017378	-6.16	0.000	***
firm-FE	✓				
year-FE	✓				

(b): Predictive regression for long-term skew, LGD = 60%

Regressand				Adj–R^2:	0.0007
$\Delta\mathrm{Skew}_{T<1}$					

Regressors	Coefficient	Robust Standard Error	t–stat	p–value	
$\overline{AICR}'_{-1,T<1}$	1.567852	1.051431	1.49	0.141	
$\alpha_{T<1}$	-0.0038733	0.000953	-4.06	0.000	***
firm-FE	✓				
year-FE	✓				

(c): Predictive regression for short-term skew, LGD = 80%

Regressand				Adj–R^2:	0.0005
$\Delta\mathrm{Skew}_{T>1}$					

Regressors	Coefficient	Robust Standard Error	t–stat	p–value	
$\overline{AICR}'_{-1,T>1}$	0.4403912	0.1533718	2.87	0.006	***
$\alpha_{T>1}$	-0.011145	0.0018258	-6.10	0.000	***
firm-FE	✓				
year-FE	✓				

(d): Predictive regression for long-term skew, LGD = 80%

Table H.6 Estimation of regression (1.22) for different values of LGD.
(a): Predictive regression for short-term skew based on the average *AICR* calculated over short-term put options and CDSs (LGD = 60%). Number of observations: 7,656. F–stat = 8.72 (p–value = 0.000).
(b): Predictive regression for long-term skew based on the average *AICR* calculated over long-term put options and CDSs (LGD = 60%). Number of observations: 6,818. F–stat = 11.47 (p–value = 0.000).
(c): Predictive regression for long-term skew based on the average *AICR* calculated over short-term put options and CDSs (LGD = 80%). Number of observations: 7,656. F–stat = 8.73 (p–value = 0.000).
(d): Predictive regression for long-term skew based on the average *AICR* calculated over long-term put options and CDSs (LGD = 80%). Number of observations: 6,818 F–stat = 11.54 (p–value = 0.000).
A sandwich estimator for panel data is used to obtain robust standard errors. Significance levels: 10% (*), 5% (**), 1% (***).

Regressand					Adj–R^2:	0.0018
$\Delta\text{Skew}_{T>1}$						

Regressors	Coefficient	Robust Standard Error	t–stat	p–value	
$\overline{AICR}'_{-1,T>1}$	0.3746640	0.1414883	2.65	0.029	**
$\alpha_{T>1}$	-0.0116986	0.0109631	-1.07	0.317	
firm-FE	✓				
year-FE	✓				

(a): Long-term skew of Financials, LGD = 60%

Regressand					Adj–R^2:	0.0014
$\Delta\text{Skew}_{T>1}$						

Regressors	Coefficient	Robust Standard Error	t–stat	p–value	
$\overline{AICR}'_{-1,T>1}$	0.5889985	0.6279188	0.94	0.379	
$\alpha_{T>1}$	-0.0164705	0.0029668	-5.55	0.001	***
firm-FE	✓				
year-FE	✓				

(b): Long-term skew of Mining, Energy and Utilities, LGD = 60%

Regressand					Adj–R^2:	0.0007
$\Delta\text{Skew}_{T>1}$						

Regressors	Coefficient	Robust Standard Error	t–stat	p–value	
$\overline{AICR}'_{-1,T>1}$	-4.338104	3.015046	-1.44	0.166	
$\alpha_{T>1}$	-0.0073019	0.0022992	-3.18	0.005	***
firm-FE	✓				
year-FE	✓				

(c): Long-term skew of Manufacturing, LGD = 60%

Regressand					Adj–R^2:	0.0006
$\Delta\text{Skew}_{T>1}$						

Regressors	Coefficient	Robust Standard Error	t–stat	p–value	
$\overline{ICR}'_{-1,T>1}$	1.2258928	0.8286194	1.48	0.151	
$\alpha_{T>1}$	-0.0107916	0.0027597	-3.91	0.001	***
firm-FE	✓				
year-FE	✓				

(d):Long-term skew of Retail, Wholesale and Services, LGD = 60%

Table H.7 Estimation of regression (1.22) over the four sub-samples for LGD = 60%.
(a): Predictive regression for short-term skew based on the average *AICR* calculated over long-term put options and CDSs of Financials. Number of observations: 810. F–stat = 10.99 (p–value = 0.002).
(b): Predictive regression for short-term skew based on the average *AICR* calculated over long-term put options and CDSs of Mining, Energy and Utilities. Number of observations: 791. F–stat = 24.87 (p–value = 0.000).
(c): Table 5b: Predictive regression for short-term skew based on the average *AICR* calculated over long-term put options and CDSs of Manufacturing. Number of observations: 2,305 F–stat = 4.17 (p–value = 0.010).
(d): Predictive regression for short-term skew based on the average *AICR* calculated over long-term put options and CDSs of Retail, Wholesale and Services. Number of observations: 2,912 F–stat = 5.78 (p–value = 0.001). A sandwich estimator for panel data is used to obtain robust standard errors. Significance levels: 10% (*), 5% (**), 1% (***).

Robustness checks

Regressand			Adj–R^2:	0.0022
$\Delta\text{Skew}_{T>1}$				

Regressors	Coefficient	Robust Standard Error	t–stat	p–value	
$\overline{AICR}'_{-1,T>1}$	0.4297893	0.1668369	2.58	0.033	**
$\alpha_{T>1}$	-0.0145834	0.0121469	-1.20	0.264	
firm-FE	✓				
year-FE	✓				

(a): Predictive regression for long-term skew of Financials, LGD = 80%

Regressand			Adj–R^2:	0.0017
$\Delta\text{Skew}_{T>1}$				

Regressors	Coefficient	Robust Standard Error	t–stat	p–value	
$\overline{AICR}'_{-1,T>1}$	0.2832847	0.0658556	4.30	0.004	***
$\alpha_{T>1}$	-0.0194797	0.002694	-7.23	0.000	***
firm-FE	✓				
year-FE	✓				

(b): Long-term skew of Mining, Energy and Utilities, LGD = 80%

Regressand			Adj–R^2:	0.0006
$\Delta\text{Skew}_{T>1}$				

Regressors	Coefficient	Robust Standard Error	t–stat	p–value	
$\overline{ICR}'_{-1,T>1}$	-2.560192	2.574604	-0.99	0.333	
$\alpha_{T>1}$	-0.0078215	0.0022739	-3.44	0.003	***
firm-FE	✓				
year-FE	✓				

(c): Long-term skew of Manufacturing, LGD = 80%

Regressand			Adj–R^2:	0.0006
$\Delta\text{Skew}_{T>1}$				

Regressors	Coefficient	Robust Standard Error	t–stat	p–value	
$\overline{ICR}'_{-1,T>1}$	1.310575	0.6199556	2.11	0.044	**
$\alpha_{T>1}$	-0.0110623	0.0027377	-4.04	0.000	***
firm-FE	✓				
year-FE	✓				

(d): Long-term skew of Retail, Wholesale and Services, LGD = 80%

Table H.8 Estimation of regression (1.22) over the four sub-samples for LGD =80%.
(a): Predictive regression for short-term skew based on the average *AICR* calculated over long-term put options and CDSs of Financials. Number of observations: 810. F–stat = 7.63 (p–value = 0.007).
(b): Predictive regression for short-term skew based on the average *AICR* calculated over long-term put options and CDSs of Mining, Energy and Utilities. Number of observations: 791. F–stat = 32.75 (p–value = 0.000).
(c): Table 5b: Predictive regression for short-term skew based on the average *AICR* calculated over long-term put options and CDSs of Manufacturing. Number of observations: 2,305 F–stat = 4.04 (p–value = 0.011).
(d): Predictive regression for short-term skew based on the average *AICR* calculated over long-term put options and CDSs of Retail, Wholesale and Services. Number of observations: 2,912 F–stat = 6.77 (p–value = 0.000).
A sandwich estimator for panel data is used to obtain robust standard errors. Significance levels: 10% (*), 5% (**), 1% (***).

Appendix I

Jacobian in the Non-Linear Least Squares Algorithm

Here, the formulas for the Jacobian of the optimization problem in (2.3) are listed. All the results are obtained from Maglione (2019).

If $n = 1$, that is F_1 due at $t_1 > 0$, the Jacobian is given by

$$\mathbf{J}(V, \sigma_V) = \begin{bmatrix} \Delta_S^{(1)} & v_S^{(1)} \\ \partial \Phi_1^{\mathbb{Q}}/\partial V & \partial \Phi_1^{\mathbb{Q}}/\partial \sigma_V \end{bmatrix}$$

with

$$\Delta_S^{(1)} = e^{-pt_1} \Phi(d_1^{\mathbb{M}})$$

$$v_S^{(1)} = e^{-pt_1} V \phi(d_1^{\mathbb{M}}) \sqrt{t_1}$$

$$\frac{\partial \Phi_1^{\mathbb{Q}}}{\partial V} = \frac{\phi(d_1^{\mathbb{Q}})}{V \sigma_V \sqrt{t_1}}$$

$$\frac{\partial \Phi_1^{\mathbb{Q}}}{\partial \sigma_V} = -\frac{d_1^{\mathbb{M}} \phi(d_1^{\mathbb{Q}})}{\sigma_V}$$

and

$$d_1^{\mathbb{M}} = \frac{\ln \frac{V}{F_1} + \left(r - p + \sigma_V^2/2 \right) t_1}{\sigma_V \sqrt{t_1}}, \quad d_1^{\mathbb{Q}} = d_1^{\mathbb{M}} - \sigma_V \sqrt{t_1}$$

If $n = 2$, that is (F_1, F_2) due at (t_1, t_2) (with $0 < t_1 < t_2$), the Jacobian is given by

$$\mathbf{J}(V, \sigma_V) = \begin{bmatrix} \Delta_S^{(2)} & v_S^{(2)} \\ \partial \Phi_1^{\mathbb{Q}}/\partial V & \partial \Phi_1^{\mathbb{Q}}/\partial \sigma_V \\ \partial \Phi_2^{\mathbb{Q}}/\partial V & \partial \Phi_2^{\mathbb{Q}}/\partial \sigma_V \end{bmatrix}$$

with

$$\Delta_S^{(2)} = e^{-pt_2}\left[\Phi_2\left(\mathbf{d}_2^{\mathbb{M}};\Gamma_2\right) + \frac{\phi(d_1^{\mathbb{M}})}{\sigma_V\sqrt{t_1}}\left(\Phi\left(\eth_2^{\mathbb{M}}(\gamma_{12})\right) - \frac{F_2 e^{-r(t_2-t_1)}}{\bar{V}_1 e^{-p(t_2-t_1)}}\Phi(\eth_2^{\mathbb{Q}}(\gamma_{12}))\right)\right]$$

$$- e^{-rt_1}\frac{F_1}{V}\frac{\phi(d_1^{\mathbb{Q}})}{\sigma_V\sqrt{t_1}}$$

$$v_S^{(2)} = \frac{1}{\sigma_V}\left[e^{-rt_2}F_2\left(\left(d_1^{\mathbb{M}} + \frac{\bar{V}_1'}{\bar{V}_1\sqrt{t_1}}\right)\phi(d_1^{\mathbb{Q}})\Phi(\eth_2^{\mathbb{Q}}(\gamma_{12})) + d_2^{\mathbb{M}}\phi(d_2^{\mathbb{Q}})\Phi(\eth_1^{\mathbb{Q}}(\gamma_{12}))\right)\right.$$

$$- e^{-pt_2}V_0\left(\left(d_1^{\mathbb{Q}} + \frac{\bar{V}_1'}{\bar{V}_1\sqrt{t_1}}\right)\phi\left(d_1^{\mathbb{M}}\right)\Phi\left(\eth_2^{\mathbb{M}}(\gamma_{12})\right) + d_2^{\mathbb{Q}}\phi\left(d_2^{\mathbb{M}}\right)\Phi\left(\eth_1^{\mathbb{M}}(\gamma_{12})\right)\right)$$

$$\left.+ e^{-rt_1}F_1\left(d_1^{\mathbb{M}} + \frac{\bar{V}_1'}{\bar{V}_1\sqrt{t_1}}\right)\phi(d_1^{\mathbb{Q}})\right]$$

$$\frac{\partial\Phi_1^{\mathbb{Q}}}{\partial V} = \frac{1}{V}\frac{\phi(d_1^{\mathbb{Q}})}{\sigma_V\sqrt{t_1}}$$

$$\frac{\partial\Phi_1^{\mathbb{Q}}}{\partial\sigma_V} = -\frac{1}{\sigma_V}\left(d_1^{\mathbb{M}} + \frac{\bar{V}_1'}{\bar{V}_1\sqrt{t_1}}\right)\phi(d_1^{\mathbb{Q}})$$

$$\frac{\partial\Phi_2^{\mathbb{Q}}}{\partial V} = \frac{1}{V}\left(\frac{\phi(d_1^{\mathbb{Q}})}{\sigma_V\sqrt{t_1}}\Phi(\eth_2^{\mathbb{Q}}(\gamma_{12})) + \frac{\phi(d_2^{\mathbb{Q}})}{\sigma_V\sqrt{t_2}}\Phi(\eth_1^{\mathbb{Q}}(\gamma_{12}))\right)$$

$$\frac{\partial\Phi_2^{\mathbb{Q}}}{\partial\sigma_V} = -\frac{1}{\sigma_V}\left(\left(d_1^{\mathbb{M}} + \frac{\bar{V}_1'}{\bar{V}_1\sqrt{t_1}}\right)\phi(d_1^{\mathbb{Q}})\Phi(\eth_2^{\mathbb{Q}}(\gamma_{12})) + d_2^{\mathbb{M}}\phi(d_2^{\mathbb{Q}})\Phi(\eth_1^{\mathbb{Q}}(\gamma_{12}))\right)$$

and

$$d_1^{\mathbb{M}} = \frac{\ln\frac{V}{\bar{V}_1} + (r - p + \sigma_V^2/2)\,t_1}{\sigma_V\sqrt{t_1}}, \quad d_2^{\mathbb{M}} = \frac{\ln\frac{V}{F_2} + (r - p + \sigma_V^2/2)\,t_2}{\sigma_V\sqrt{t_2}},$$

$$d_1^{\mathbb{Q}} = d_1^{\mathbb{M}} - \sigma_V\sqrt{t_1}, \quad d_2^{\mathbb{Q}} = d_2^{\mathbb{M}} - \sigma_V\sqrt{t_2}$$

$$\mathbf{d}_2^{\mathbb{M}} = \begin{pmatrix} d_1^{\mathbb{M}} & d_2^{\mathbb{M}} \end{pmatrix}, \quad \Gamma_2 = \begin{pmatrix} 1 & \gamma_{12} \\ \gamma_{12} & 1 \end{pmatrix} = \begin{pmatrix} 1 & \sqrt{t_1/t_2} \\ \sqrt{t_1/t_2} & 1 \end{pmatrix}$$

$$\eth_1^{\mathbb{M}}(\gamma_{12}) = \frac{d_1^{\mathbb{M}} - \gamma_{12}d_2^{\mathbb{M}}}{\sqrt{1 - \gamma_{12}^2}}, \quad \eth_1^{\mathbb{Q}}(\gamma_{12}) = \frac{d_1^{\mathbb{Q}} - \gamma_{12}d_2^{\mathbb{Q}}}{\sqrt{1 - \gamma_{12}^2}}, \quad \eth_2^{\mathbb{M}}(\gamma_{12}) = \frac{d_2^{\mathbb{M}} - \gamma_{12}d_1^{\mathbb{M}}}{\sqrt{1 - \gamma_{12}^2}}, \quad \eth_2^{\mathbb{Q}}(\gamma_{12}) = \frac{d_2^{\mathbb{Q}} - \gamma_{12}d_1^{\mathbb{Q}}}{\sqrt{1 - \gamma_{12}^2}}$$

If $n = 3$, that is (F_1, F_2, F_3) due at (t_1, t_2, t_3) (with $0 < t_1 < t_2 < t_3$), the Jacobian in given by

$$\mathbf{J}(V, \sigma_V) = \begin{bmatrix} \Delta_S^{(2)} & v_S^{(2)} \\ \partial\Phi_1^{\mathbb{Q}}/\partial V & \partial\Phi_1^{\mathbb{Q}}/\partial\sigma_V \\ \partial\Phi_2^{\mathbb{Q}}/\partial V & \partial\Phi_2^{\mathbb{Q}}/\partial\sigma_V \\ \partial\Phi_3^{\mathbb{Q}}/\partial V & \partial\Phi_3^{\mathbb{Q}}/\partial\sigma_V \end{bmatrix}$$

with

$$\Delta_S^{(3)} = e^{-pt_3}\left(\Phi_3\left(\mathbf{d}_3^{\mathbb{M}};\boldsymbol{\Gamma_3}\right) + \frac{I_1^{\mathbb{M}}}{\sigma_V\sqrt{t_1}} + \frac{I_2^{\mathbb{M}}}{\sigma_V\sqrt{t_2}} + \frac{I_3^{\mathbb{M}}}{\sigma_V\sqrt{t_3}}\right) - e^{-rt_3}\frac{F_3}{v}\left(\frac{I_1^{\mathbb{Q}}}{\sigma_V\sqrt{t_1}} + \frac{I_2^{\mathbb{Q}}}{\sigma_V\sqrt{t_2}} + \frac{I_3^{\mathbb{Q}}}{\sigma_V\sqrt{t_3}}\right)$$

$$- e^{-rt_2}\frac{F_2}{v}\left(\frac{\phi(d_1^{\mathbb{Q}})}{\sigma_V\sqrt{t_1}}\Phi\left(\mathfrak{d}_2^{\mathbb{Q}}(\gamma_{12})\right) + \frac{\phi(d_2^{\mathbb{Q}})}{\sigma_V\sqrt{t_2}}\Phi\left(\mathfrak{d}_1^{\mathbb{Q}}(\gamma_{12})\right)\right) - e^{-rt_1}\frac{F_1}{v\sigma_V\sqrt{t_1}}\phi(d_1^{\mathbb{Q}})$$

$$v_S^{(3)} = \frac{1}{\sigma_V}\left[e^{-rt_3}F_3\left(\left(d_1^{\mathbb{M}} + \frac{\bar{V}_1'}{\bar{V}_1\sqrt{t_1}}\right)I_1^{\mathbb{Q}} + \left(d_2^{\mathbb{M}} + \frac{\bar{V}_2'}{\bar{V}_2\sqrt{t_2}}\right)I_2^{\mathbb{Q}} + d_3^{\mathbb{M}}I_3^{\mathbb{Q}}\right)\right.$$

$$- e^{-pt_3}V_0\left(\left(d_1^{\mathbb{Q}} + \frac{\bar{V}_1'}{\bar{V}_1\sqrt{t_1}}\right)I_1^{\mathbb{M}} + \left(d_2^{\mathbb{Q}} + \frac{\bar{V}_2'}{\bar{V}_2\sqrt{t_2}}\right)I_2^{\mathbb{M}} + d_3^{\mathbb{Q}}I_3^{\mathbb{M}}\right)$$

$$+ e^{-rt_2}F_2\left(\left(d_1^{\mathbb{M}} + \frac{\bar{V}_1'}{\bar{V}_1\sqrt{t_1}}\right)\phi(d_1^{\mathbb{Q}})\Phi(\mathfrak{d}_2^{\mathbb{Q}}(\gamma_{12})) + \left(d_2^{\mathbb{M}} + \frac{\bar{V}_2'}{\bar{V}_2\sqrt{t_2}}\right)\phi(d_2^{\mathbb{Q}})\Phi(\mathfrak{d}_1^{\mathbb{Q}}(\gamma_{12}))\right)$$

$$\left.+ e^{-rt_1}F_1\left(d_1^{\mathbb{M}} + \frac{\bar{V}_1'}{\bar{V}_1\sqrt{t_1}}\right)\phi(d_1^{\mathbb{Q}})\right]$$

$$\frac{\partial\Phi_1^{\mathbb{Q}}}{\partial V} = \frac{1}{V}\frac{\phi(d_1^{\mathbb{Q}})}{\sigma_V\sqrt{t_1}}$$

$$\frac{\partial\Phi_1^{\mathbb{Q}}}{\partial\sigma_V} = -\frac{1}{\sigma_V}\left(d_1^{\mathbb{M}} + \frac{\bar{V}_1'}{\bar{V}_1\sqrt{t_1}}\right)\phi(d_1^{\mathbb{Q}})$$

$$\frac{\partial\Phi_2^{\mathbb{Q}}}{\partial V} = \frac{1}{V}\left(\frac{\phi(d_1^{\mathbb{Q}})}{\sigma_V\sqrt{t_1}}\Phi(\mathfrak{d}_2^{\mathbb{Q}}(\gamma_{12})) + \frac{\phi(d_2^{\mathbb{Q}})}{\sigma_V\sqrt{t_2}}\Phi(\mathfrak{d}_1^{\mathbb{Q}}(\gamma_{12}))\right)$$

$$\frac{\partial\Phi_2^{\mathbb{Q}}}{\partial\sigma_V} = -\frac{1}{\sigma_V}\left(\left(d_1^{\mathbb{M}} + \frac{\bar{V}_1'}{\bar{V}_1\sqrt{t_1}}\right)\phi(d_1^{\mathbb{Q}})\Phi(\mathfrak{d}_2^{\mathbb{Q}}(\gamma_{12})) + \left(d_2^{\mathbb{M}} + \frac{\bar{V}_2'}{\bar{V}_2\sqrt{t_2}}\right)\phi(d_2^{\mathbb{Q}})\Phi(\mathfrak{d}_1^{\mathbb{Q}}(\gamma_{12}))\right)$$

$$\frac{\partial\Phi_3^{\mathbb{Q}}}{\partial V} = \frac{1}{V}\left(\frac{I_1^{\mathbb{Q}}}{\sigma_V\sqrt{t_1}} + \frac{I_2^{\mathbb{Q}}}{\sigma_V\sqrt{t_2}} + \frac{I_3^{\mathbb{Q}}}{\sigma_V\sqrt{t_3}}\right)$$

$$\frac{\partial\Phi_3^{\mathbb{Q}}}{\partial\sigma_V} = -\frac{1}{\sigma_V}\left[\left(d_1^{\mathbb{M}} + \frac{\bar{V}_1'}{\bar{V}_1\sqrt{t_1}}\right)I_1^{\mathbb{Q}} + \left(d_2^{\mathbb{M}} + \frac{\bar{V}_2'}{\bar{V}_2\sqrt{t_2}}\right)I_2^{\mathbb{Q}} + d_3^{\mathbb{M}}I_3^{\mathbb{Q}}\right]$$

and

$$d_1^{\mathbb{M}} = \frac{\ln\frac{V}{\bar{V}_1} + (r - p + \sigma_V^2/2)t_1}{\sigma_V\sqrt{t_1}}, \quad d_2^{\mathbb{M}} = \frac{\ln\frac{V}{\bar{V}_2} + (r - p + \sigma_V^2/2)t_2}{\sigma_V\sqrt{t_2}}, \quad d_3^{\mathbb{M}} = \frac{\ln\frac{V}{F_3} + (r - p + \sigma_V^2/2)t_3}{\sigma_V\sqrt{t_3}}$$

$$d_1^{\mathbb{Q}} = d_1^{\mathbb{M}} - \sigma_V\sqrt{t_1}, \quad d_2^{\mathbb{Q}} = d_2^{\mathbb{M}} - \sigma_V\sqrt{t_2}, \quad d_3^{\mathbb{Q}} = d_3^{\mathbb{M}} - \sigma_V\sqrt{t_3}, \quad \mathbf{d}_3^{\mathbb{M}} = \begin{pmatrix} d_1^{\mathbb{M}} & d_2^{\mathbb{M}} & d_3^{\mathbb{M}} \end{pmatrix}$$

Jacobian in the Non-Linear Least Squares Algorithm

$$\mathbf{\Gamma_3} = \begin{pmatrix} 1 & \gamma_{12} & \gamma_{13} \\ \gamma_{12} & 1 & \gamma_{23} \\ \gamma_{13} & \gamma_{23} & 1 \end{pmatrix} = \begin{pmatrix} 1 & \sqrt{t_1/t_2} & \sqrt{t_1/t_3} \\ \sqrt{t_1/t_2} & 1 & \sqrt{t_2/t_3} \\ \sqrt{t_1/t_3} & \sqrt{t_2/t_3} & 1 \end{pmatrix}, \quad \mathbf{\Gamma_2} = \begin{pmatrix} 1 & \gamma_{12} \\ \gamma_{12} & 1 \end{pmatrix} = \begin{pmatrix} 1 & \sqrt{t_1/t_2} \\ \sqrt{t_1/t_2} & 1 \end{pmatrix}$$

$$\mathfrak{d}_1^{\mathbb{M}}(\gamma_{12}) = \frac{d_1^{\mathbb{M}} - \gamma_{12} d_2^{\mathbb{M}}}{\sqrt{1 - \gamma_{12}^2}}, \quad \mathfrak{d}_1^{\mathbb{Q}}(\gamma_{12}) = \frac{d_1^{\mathbb{Q}} - \gamma_{12} d_2^{\mathbb{Q}}}{\sqrt{1 - \gamma_{12}^2}}, \quad \mathfrak{d}_2^{\mathbb{M}}(\gamma_{12}) = \frac{d_2^{\mathbb{M}} - \gamma_{12} d_1^{\mathbb{M}}}{\sqrt{1 - \gamma_{12}^2}}, \quad \mathfrak{d}_2^{\mathbb{Q}}(\gamma_{12}) = \frac{d_2^{\mathbb{Q}} - \gamma_{12} d_1^{\mathbb{Q}}}{\sqrt{1 - \gamma_{12}^2}}$$

$$\mathbf{\Gamma_3}^{-1} = \begin{pmatrix} \frac{t_2}{t_2-t_1} & -\frac{\sqrt{t_1 t_2}}{t_2-t_1} & 0 \\ -\frac{\sqrt{t_1 t_2}}{t_2-t_1} & \frac{t_2(t_3-t_1)}{(t_2-t_1)(t_3-t_2)} & -\frac{\sqrt{t_2 t_3}}{t_3-t_2} \\ 0 & -\frac{\sqrt{t_2 t_3}}{t_3-t_2} & \frac{t_3}{t_3-t_2} \end{pmatrix} = \begin{pmatrix} \tau_1 & \tau_2 & 0 \\ \tau_2 & \tau_4 & \tau_6 \\ 0 & \tau_6 & \tau_9 \end{pmatrix}.$$

$$\boldsymbol{\mu}_1^{\mathbb{Q}/\mathbb{M}} = \frac{\tau_6 d_1^{\mathbb{Q}/\mathbb{M}}}{\tau_1 \tau_4 - \tau_2^2} \begin{pmatrix} \tau_2 \\ -\tau_1 \end{pmatrix}, \quad \boldsymbol{\mu}_2^{\mathbb{Q}/\mathbb{M}} = -d_2^{\mathbb{Q}/\mathbb{M}} \begin{pmatrix} \tau_2/\tau_1 \\ \tau_6/\tau_9 \end{pmatrix}, \quad \boldsymbol{\mu}_3^{\mathbb{Q}/\mathbb{M}} = \frac{\tau_2 d_3^{\mathbb{Q}/\mathbb{M}}}{\tau_4 \tau_9 - \tau_6^2} \begin{pmatrix} -\tau_9 \\ \tau_6 \end{pmatrix}$$

$$\mathbf{\Sigma_1} = \frac{1}{\tau_1 \tau_4 - \tau_2^2} \begin{pmatrix} \tau_4 & -\tau_2 \\ -\tau_2 & \tau_1 \end{pmatrix}, \quad \mathbf{\Sigma_2} = \begin{pmatrix} 1/\tau_1 & 0 \\ 0 & 1/\tau_9 \end{pmatrix}, \quad \mathbf{\Sigma_3} = \frac{1}{\tau_4 \tau_9 - \tau_6^2} \begin{pmatrix} \tau_9 & -\tau_6 \\ -\tau_6 & \tau_4 \end{pmatrix}$$

$$a_1 = \tau_9 - \frac{\tau_1 \tau_6^2}{\tau_1 \tau_4 - \tau_2^2}, \quad a_2 = \tau_4 - \frac{\tau_2^2}{\tau_1} - \frac{\tau_6^2}{\tau_9}, \quad a_3 = \tau_1 - \frac{\tau_9 \tau_2^2}{\tau_4 \tau_9 - \tau_6^2}$$

$$I_1^{\mathbb{Q}/\mathbb{M}} = \sqrt{\frac{\det \mathbf{\Sigma_1}}{\det \mathbf{\Gamma_3}}} \phi\left(\sqrt{a_1} d_1^{\mathbb{Q}/\mathbb{M}}\right) N_2\left(d_2^{\mathbb{Q}/\mathbb{M}}, d_3^{\mathbb{Q}/\mathbb{M}}; \boldsymbol{\mu}_1^{\mathbb{Q}/\mathbb{M}}, \mathbf{\Sigma_1}\right)$$

$$I_2^{\mathbb{Q}/\mathbb{M}} = \sqrt{\frac{\det \mathbf{\Sigma_2}}{\det \mathbf{\Gamma_3}}} \phi\left(\sqrt{a_2} d_2^{\mathbb{Q}/\mathbb{M}}\right) \Phi\left(\frac{\tau_1 d_1^{\mathbb{Q}/\mathbb{M}} + \tau_2 d_2^{\mathbb{Q}/\mathbb{M}}}{\sqrt{\tau_1}}\right) \Phi\left(\frac{\tau_9 d_3^{\mathbb{Q}/\mathbb{M}} + \tau_6 d_2^{\mathbb{Q}/\mathbb{M}}}{\sqrt{\tau_9}}\right)$$

$$I_3^{\mathbb{Q}/\mathbb{M}} = \sqrt{\frac{\det \mathbf{\Sigma_3}}{\det \mathbf{\Gamma_3}}} \phi\left(\sqrt{a_3} d_3^{\mathbb{Q}/\mathbb{M}}\right) N_2\left(d_1^{\mathbb{Q}/\mathbb{M}}, d_2^{\mathbb{Q}/\mathbb{M}}; \boldsymbol{\mu}_3^{\mathbb{Q}/\mathbb{M}}, \mathbf{\Sigma_3}\right)$$

Appendix J

The leverage and volatility effect in a compound option model of default

As credit events are dictated by the level of the equity, it is crucial to have a clear vision on how equity reacts to changes in the value of the assets and its riskiness in order to understand what drives default in the model. Also, understanding the properties of the market value of debt adds extra insight to the implications of the model.

Assume the asset value process follows a geometric Brownian motion

$$dV_t = (r - \varpi) V_t \, dt + \sigma_V V_t \, dW_t^{\mathbb{Q}}, \tag{J.1}$$

where ϖ is the continuously compounded payout rate (reflecting both dividends and coupon payments), σ_V the instantaneous volatility of the assets, and $W_t^{\mathbb{Q}}$ a $\mathbb{Q}$-standard Brownian motion.

Let $\Lambda \in \{S, D\}$, where S the market value of the equity and D the market value of debt. As both equity and debt are functions of the firm value and time only, Itô's Lemma can be used to determine their risk-neutral dynamics. Under (J.1), the residual claim Λ evolves as

$$d\Lambda_t = \alpha_\Lambda^{\mathbb{Q}}(V_t, t)\Lambda_t \, dt + \sigma_\Lambda(V_t, t)\Lambda_t \, dW_t^{\mathbb{Q}}, \tag{J.2}$$

with

$$\alpha_\Lambda^{\mathbb{Q}}(V_t, t) := \frac{1}{\Lambda_t}\left(\frac{\partial \Lambda}{\partial t} + \frac{\partial \Lambda}{\partial V}(r - \varpi)V_t + \frac{1}{2}\frac{\partial^2 \Lambda}{\partial V^2}\sigma_V^2 V_t^2\right) \quad \text{and} \quad \sigma_\Lambda(V_t, t) := \sigma_V \frac{V_t}{\Lambda_t}\frac{\partial \Lambda}{\partial V}.$$

Therefore, neither the dynamics of the equity nor the ones of the market value of debt are log-normal (no matter what is the distribution of V_t), displaying both stochastic drift and volatility.

Focusing on the firm's equity, it is worth highlighting that the process does not only have stochastic volatility, but it is also a model of local volatility in the sense of Dupire (1994). In fact,

$$\sigma_S = \sigma_S(S_t, t).$$

Remarkably, the equity process is also able to combine both the dependence of the equity volatility on its level, S, (and its sensitivities), and on the model state variable, V. Local volatility models where the volatility depends also on other variables than S are usually referred as hybrid local stochastic volatility models. These are widely-used in the industry to estimate the implied volatility surface extracted from options, the most common being the model in Heston (1993) plus local volatility. In fact, it is well known that a stochastic volatility model with time-homogeneous parameters only (as Heston) cannot fit market prices. For a more comprehensive discussion on pros and cons of stochastic volatility models, see Gatheral (2006). Thus, the proposed model appears to be the most natural way to construct an hybrid local volatility model consistent with the structural approach to default.

For convenience of notation, let $t = 0$ and the time subscripts be omitted. By model assumptions, the accounting identity

$$e^{-\varpi t_n} V = S + D \tag{J.3}$$

holds, where the left-hand side can be thought as the net asset value[1]. Based on it, some identities regarding the sensitivity of equity and debt with respect to the state variables can be derived as well. In particular, I can link the Delta (i.e. partial derivative with respect to the asset value) and Vega (i.e. partial derivative with respect to the asset volatility) of equity and debt via (J.3). Setting $\Delta_\Lambda := \partial \Lambda / \partial V$ and $\nu_\Lambda := \partial \Lambda / \partial \sigma_V$, it follows

$$\Delta_D = e^{-\varpi t_n} - \Delta_S \qquad \text{and} \qquad \nu_D = -\nu_S.$$

Notice that these sensitivities depends on the number of bond outstanding n. The analytical expression for $\Delta_S^{(n)}$ and $\nu_S^{(n)}$ are available in Maglione (2019). The analogous counterparts for debt can be found using the expressions above. Also, as $\sigma_\Lambda = \sigma_V \frac{V}{\Lambda} \Delta_\Lambda$, the following

---

[1]Net of all the future payments to either shareholders and bondholders.

accounting relationship holds for volatilities,

$$e^{-\varpi t_n}\sigma_V = \frac{S\sigma_S + D\sigma_D}{S+D},$$

where σ_S and σ_D are obviously stochastic and time-varying. Also, by applying Itô's Lemma,

$$\sigma_S = \sigma_V \frac{V}{S}\Delta_S \qquad \text{and} \qquad \sigma_D = \sigma_V \frac{V}{D}\Delta_D. \qquad (J.4)$$

Therefore, the model allows to interpret the volatility of the firm's claims (equity or debt) in terms of the riskiness of the firm (σ_V), its (inverse) debt-to-equity ratio in case of equity (debt), and the sensitivity of the claim with respect to changes in the asset value (Delta).

Figure J.1 shows how equity, debt, and their respective volatilities react when either the leverage decreases (that is V increases) or the firm's riskiness changes. Whereas the Black and Scholes (1973) model assumes that the variance of the stock return is not a function of the stock price, here the variance of the return on the equity is inversely related to the stock price. As the asset value falls (rises), the value of the equity falls (rises) too, the firm's debt-equity ratio rises (falls), and this increased (decreased) risk is reflected by a rise (fall) in the variance of the returns on the stock. Also, if the riskiness of the whole firm increases, the volatility of the equity increases too. Furthermore, it can be shown that if V and σ_V simultaneously increases, the overall effect result in an increase of the equity volatility. Similar dynamics are observed for debt despite the impact is much smaller, consistently with the empirical evidence that publicly traded debt is much less volatile than equity.

Furthermore, the volatility of the equity can also be written as

$$\sigma_S = \sigma_V \left(\frac{\partial S}{S} / \frac{\partial V}{V} \right) = \sigma_V \, \mathrm{El}_S(V,t)$$

where $\mathrm{El}_S(V_t,t)$ is the elasticity of the equity with respect to changes in the asset value. Evidently, the elasticity of variance is not constant but a stochastic function of the state variable V. Moreover, the elasticity is always greater than one (being one for $v \uparrow \infty$ or in the trivial case $V = S$). That is, a $x\%$ change in the value of the assets induces the equity to change more than $x\%$ (i.e. equity is elastic with respect to asset value). See Figure J.2 for a graphical analysis of the elasticity.

A well-known process where the elasticity of equity drives its volatility is the Cox (1996) Constant Elasticity of Variance (CEV). The dynamics in (J.2) can be seen as a possible generalisation of it. In fact, without loss of generality, setting $\mathrm{El}_S(V_t,t) = S^{-\gamma(V_t,t)}$, and
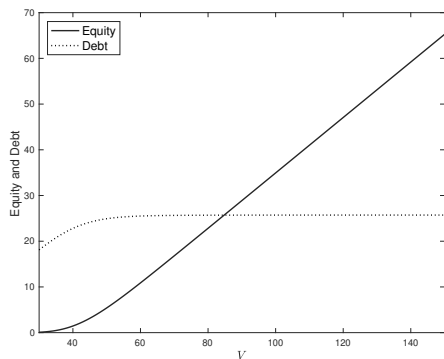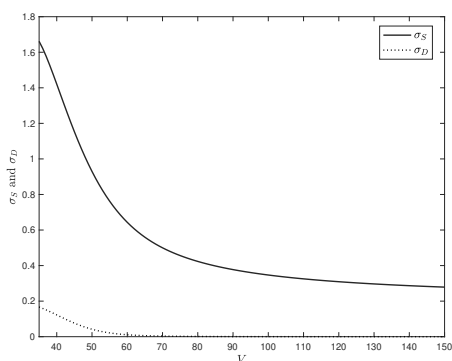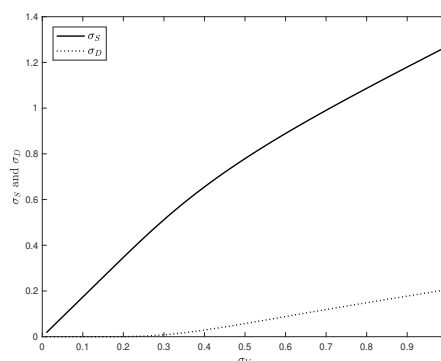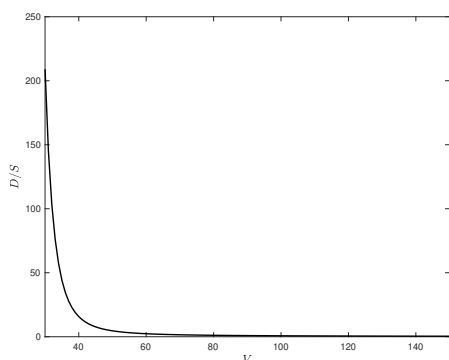
(a) S and D as functions of V
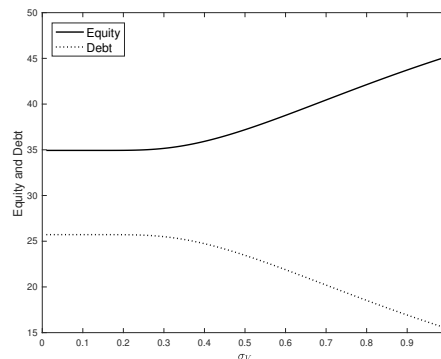
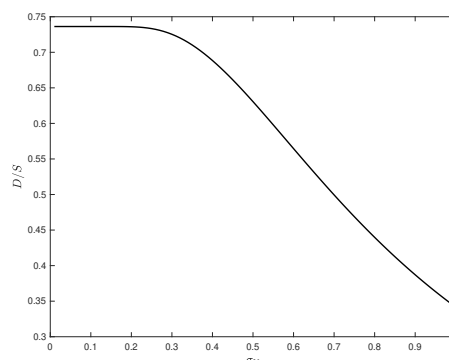(b) S and D as functions of σ_V

(c) σ_S and σ_D as functions of V

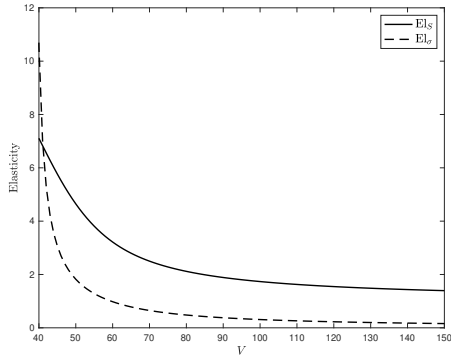(d) σ_S and σ_D as functions of σ_V
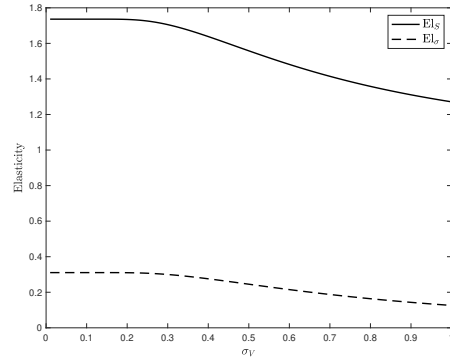

(e) D/S as function of V

(f) D/S as function of σ_V

Fig. J.1 $F_i = 10$, $t_i = \{1, 5, 10\}$, $r = 0.03$, $p = 0.05$. When leverage is fixed (left column), $\sigma_V = 0.2$; when the firm's riskiness is fixed (right column), $V = 100$.

(a) El_S and $\mathrm{El}_{\sigma_{\mathrm{d}S/S}^2}$ as functions of V (b) El_S and $\mathrm{El}_{\sigma_{\mathrm{d}S/S}^2}$ as functions of σ_V

Fig. J.2 $F_i = 10$, $t_i = \{1, 5, 10\}$, $r = 0.03$, $p = 0.05$. When leverage is fixed (left), $\sigma_V = 0.2$; when the firm's riskiness is fixed (right), $V = 100$.

defining

$$\beta(V,t) := 1 - \gamma(V,t) = 1 + \frac{\ln \mathrm{El}_S(V,t)}{\ln S}$$

then the dynamic of the equity reads as

$$\mathrm{d}S_t = \alpha_S^{\mathbb{Q}}(V_t,t)S_t\,\mathrm{d}t + \sigma_V S_t^{\beta(V_t,t)}\,\mathrm{d}W_t^{\mathbb{Q}}, \tag{J.5}$$

thus resembling the equation governing the CEV[2]. Being the elasticity stochastic, the process will be referred as Stochastic Elasticity of Variance (SEV).

Furthermore, a closer inspection to (J.5) reveals that the stochastic function $\beta(V_t,t)$ is indeed related to the elasticity of the quadratic variation of the stock returns[3] with respect to the stock price by

$$\mathrm{El}_{\sigma_{\mathrm{d}S/S}^2}(V,t) = \frac{\partial \sigma_{\mathrm{d}S/S}^2}{\sigma_{\mathrm{d}S/S}^2}\bigg/\frac{\partial S}{S} = 2\left(\beta(V,t) - 1\right).$$

Figure J.2 shows that the elasticity of the instantaneous variance of the stock returns behaves similarly to El_S, tending to infinity as the value of the asset drops (that is as financial leverage increases). Increasing the riskiness of the firm lowers both El_S and $\mathrm{El}_{\sigma_{\mathrm{d}S/S}^2}$, despite the effect being modest. Overall, this dynamic allows to explain many stylised facts observed in equity markets, namely the increase of the return variance as the stock price drops and relatively

---

[2]In the CEV both the drift and β are constant parameters.

[3]More formally, the quadratic variation of the stochastic logarithm of S.

stable riskiness for mature companies. In fact, (1.10) is able to account for increases in the instantaneous variance (as well as in the elasticity of the instantaneous variance) when the stock price falls. On the other hand, when the firm is mature and 'safe' company, the elasticity of the instantaneous variance approaches zero, thus making the value of the stock insensitive to changes in the firm value. In the first case (bankruptcy) the equity become progressively more and more sensitive to changes in the value of the assets; in the second case (safety) the firm is so far from default that changes in the firm value do not affect the value of the equity.

To some extent this process produces similar trajectories to the reduced-form default-extended CEV process in Carr and Linetsky (2006). The main difference between the two approaches is that their process is only able to statistically reproduce the patterns caused by the leverage effect, while here the the statistical properties of the SEV are directly attributable to the firm's capital structure.

On a different note, a compound option default model is able to explain some of the 'puzzling' findings in Carr and Wu (2017). They document that, contrary to conventional wisdom, financial leverage does not always decline with increased business risk. Instead, the financial leverage can increase with increasing business risk if the risk increase is due to small, diffusive market movements[4]. Surprisingly, their finding is what our model predicts. In order to understand how equity, and thus leverage, reacts to increase in business risk (that is, σ_V), the sensitivity of the equity with respect to asset volatility can be looked at.

If the volatility of the company increases, every structural model à la Merton would predict that the value of its equity increases too as displayed in Figure J.1 (b). Also, in line with common sense, Figure J.1 (a), (c) and (e) shows that the firm equity and debt are increasing in the asset value (but they display opposite concavity), and that the volatility of equity and debt both tend to decline as the firm becomes safer due to a larger asset value. The same applies for the debt to equity ratio. On the other hand, panels (d) and (f) can help shedding some light on the counter-intuitive findings in Carr and Wu (2017). If the choice of rebalancing the capital structure to hit a targeted leverage ratio is not modelled (i.e. the capital structure is insensitive to changes in the business risk), the company's financial leverage drops (panel (f)). Instead, in a model where the firm can react to changes in its business risk and adjust its capital structure accordingly, as the riskiness of the firm increases, it would be optimal to take on more debt given the rise in equity so that the leverage ratio remains constant. Also, it would make sense to take in a larger fraction of debt than the

---

[4]Only when the 'self-exciting' downside jump risk increases do companies become concerned and start the deleveraging process.
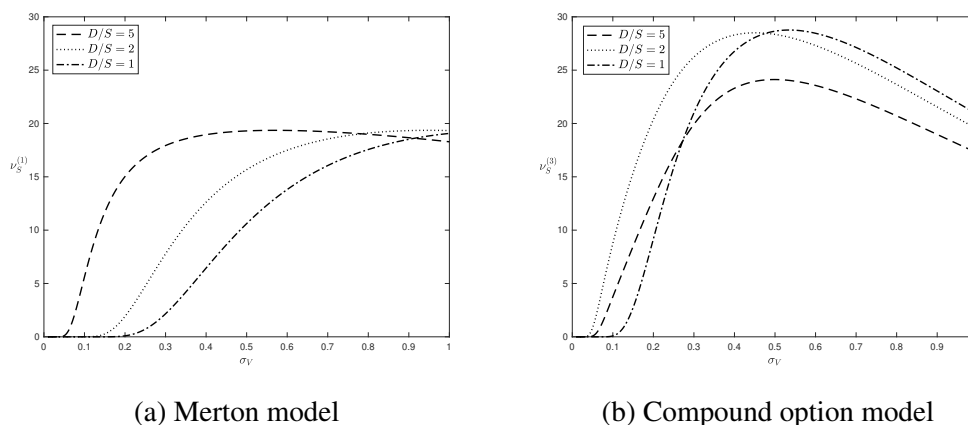
(a) Merton model   (b) Compound option model

Fig. J.3 Sensitivity of equity with respect to asset volatility under the Merton (panel (a)) and a compound option model (panel (b)) ($r = 0.03$, $p = 0.05$). In panel (a): $F_1 = 50$, $t_1 = 1$; in panel (b): $F_1 = F_2 = F_3 = 50/3$; $t_1 = 1$, $t_2 = 5$, $t_3 = 10$. Panel (a) shows how $v_S^{(1)}$ reacts to changes in the riskiness of the firm: it is optima for equity holders to increase leverage, as this makes equity more sensitive to further changes in volatility. Panel (b) shows how $v_S^{(3)}$ reacts to increasing business risk: pushing leverage is optimal as long as the sensitivity of equity starts decreasing. The sensitivity of a highly-levered (dashed) company falls between the sensitivities of the medium-levered (dotted) and low-levered (dotted-dashed) companies for plausible value of $\sigma_V \in (0, 0.3)$ p.a..

percentage increase of the value of equity, being debt less volatile than equity (panel (d)). Thus, the findings in Carr and Wu (2017) of increasing leverage for increasing diffusive volatility can be easily reconciled with a model in which shareholders maximise the firm value, based on a targeted leverage ratio, and where equity is seen as a compound option.

Furthermore, in order to understand how equity, and thus leverage, reacts to increase in business risk (that is, σ_V), the sensitivity of the equity with respect to asset volatility, $v_S^{(n)}$ (i.e. the 'Vega' of the equity), can be looked at. Figure J.3 shows how equity reacts to volatility changes over different capital structures and aggregation schemes. It also provides a valid motivation for preferring a compound option model with respect to the Merton model. Panel (a) shows the sensitivity of the equity under the Merton model (where the whole firm's debt is clustered at unique date in the future); panel (b) shows how the same sensitivity displays a different behaviour by having allowed for a more realistic aggregation scheme of the company's capital structure (debt is clustered at three future dates).

Comparing the two panels, it is evident that the effect of leverage is exacerbated in a compound option model: the equity of moderately-levered firms changes more severely in panel (b). For reasonable combinations of asset volatility and leverage, there is an incentive by the shareholders to increase the leverage. Considering plausible values of the asset volatility (say between 5% and 40% p.a.), panel (b) in Figure J.3 shows that equityholders of the 'dashed company' would be better off increasing leverage to become the 'dotted

company'. However, increasing leverage further, that is turning into the 'dotted-dashed company', would reflect into a reduction on the sensitivity of the equity. Notice that the Merton model is not able to reproduce this pattern: it is always optimal for shareholders to increase leverage further.